http://researchcommons.waikato.ac.nz/

Research Commons at the University of Waikato

Copyright Statement:

The digital copy of this thesis is protected by the Copyright Act 1994 (New Zealand).

The thesis may be consulted by you, provided you comply with the provisions of the Act and the following conditions of use:

- Any use you make of these documents or images must be for research or private study purposes only, and you may not make them available to any other person.
- Authors control the copyright of their thesis. You will recognise the author's right to be identified as the author of the thesis, and due acknowledgement will be made to the author where appropriate.
- You will obtain the author's permission before publishing any material from the thesis.

Identifying the signalling pathway of a novel Myostatin Splice Variant (MSV)

A thesis

submitted in fulfilment

of the requirements for the degree

of

Doctor of Philosophy in Biological Sciences

at

The University of Waikato

by

Alex Hennebry

THE UNIVERSITY OF
WAIKATO
Te Whare Wānanga o Waikato

2014

Abstract

Myostatin (Mstn), a member of the transforming growth factor-β super family, is a potent negative regulator of skeletal muscle mass. Studies delineating the function of Mstn have identified multiple signal transduction pathways that convey the Mstn signal. Mstn has been shown to influence canonical TGF-β, mitogen activated protein kinase (MAPK) and the PI3K/AKT signal transduction cascades. The discovery in our laboratory of a novel splice variant of Mstn (MSV) that opposes Mstn and stimulates the proliferation of myoblasts provided the impetus for the investigations in this thesis. The splicing of MSV was restricted to the Cetartiodactyl clade of mammals, and MSV may represent an intragenic regulator of Mstn. Thus, the studies undertaken in this thesis were to delineate the signalling pathways used by Mstn and MSV in order to understand how their opposing roles in myoblasts regulate myogenesis.

Initially, microarray analysis was used to investigate the transcriptional responses of ovine myoblasts following exposure to recombinant Mstn (eukaryotic) and MSV (prokaryotic) protein. Mstn treatment induced changes in number of transcripts, with changes consistent with previous investigations, for example increased interlukin-6 (IL6) and decreased MyoD. In addition, a novel transcriptional target of Mstn, the β1 subunit of the Na^+-K^+-ATPase was discovered. Treatment of ovine myoblasts with recombinant MSV induced a plethora of transcriptional responses. IPA analysis suggested a number of these were due to LPS (endotoxin) contamination, which could be attributed to the production of this protein in *E. coli*. This was confirmed using the Limulus amebocyte lysate assay. Phase separation using Triton-X 114 proved an effective method for the removal of LPS from the MSV preparation.

Western blot analysis was performed following the treatment of ovine myoblasts with Mstn and purified MSV. Consistent with previous myoblast studies Mstn stimulated canonical TGF-β (Smad) signalling and the p38 and ERK components of the MAPK signalling cascade. In contrast to previous studies, Mstn also stimulated AKT signalling, with specific phosphorylation of serine 473 (AKT^{S473}). In addition, Mstn altered the abundance of multiple myogenic transcription factors (MyoD, Myf5, MRF4, Pax7 and Mef2) and the abundance

and/or the phosphorylation of targets that have a metabolic role in skeletal muscle (rps6, 4EBP1 and p70S6K). Treatment with MSV increased the abundance of Smad 3, Myf5, 4EBP1 and stimulated AKT^{S473} and 4EBP1 phosphorylation. These data provided the foundation for confirmation of these pathways targeted by MSV in C_2C_{12} myoblasts that stably expressed MSV.

C_2C_{12} cells expressing MSV had an increased proliferative capacity and showed increased mitochondrial activity (EZ4U assay) as compared to controls. These cells showed an increased abundance of the MRFs MyoD, MRF4 and Myogenin and an increased abundance or phosphorylation of signalling targets involved in canonical TGF-β, MAPK and PI3K/AKT signalling cascades. In addition, cells expressing MSV had an increased abundance and phosphorylation of acetyl co-enzyme A carboxylase (ACC) and 4EBP1, which have established roles in regulating metabolism and the synthesis of protein

The significant overlap of processes influenced by the Na^+, K^+ ATPase complex and Mstn prompted an investigation on how Mstn regulates the β1 subunit of the Na^+, K^+ ATPase. This transcriptional response was found to be dependent on the Smad pathway. In addition, these studies also show that Na^+ K^+ ATPase activity plays a role in proliferation and differentiation of ovine myoblasts and suggest that Mstn inhibits ion flow controlled through the function of this enzyme complex.

In conclusion, these studies show that Mstn and MSV share a number of common signalling targets. In contrast to previous studies of Mstn, the stable expression MSV increases the activation of AKT signalling and increases the abundance of key myogenic transcription factors. In addition, MSV increases the abundance and phosphorylation of ACC and 4EBP1, molecules involved regulating the synthesis of protein and fatty acids. In addition, the β1 subunit of the Na^+ K^+ ATPase, was identified as a novel transcriptional target of Mstn, with this regulation controlled through a Smad dependant mechanism. These data confirm the postulate that Mstn and MSV have divergent signalling functions and suggest a role for MSV in the control of oxidative metabolism.

Acknowledgements

First and foremost I would like to acknowledge my supervisors, Dr Chris McMahon and Professor Vic Arcus. Chris, I could not have made this journey without your guidance and support. Thank you for your time, passing on your knowledge, your leadership, your sense of humour and your patience. I have very much enjoyed my time spent working with you. Vic, your support over the last five years has been outstanding. Thank you for welcoming me in to your group, providing perspective and for the continued encouragement.

A special mention for the AgResearch/former AgResearch crew, Carole Berry, Gina Nicholas, Mônica Senna Salerno de Moura, Jenny Oldham, Shelly Falconer, Frank Jeanplong, Mark Thomas, Trevor Watson, Grant Smolenski, Jeremy Bracegirdle and Ken Matthews. Thank you for all the knowledge, skills, laughter, fantastic conversations, tears, compassion, cross-dressing, pranks, barbeques, work, friendship and other things that we have shared during the last decade and a bit at Ruakura. Without you my journey would have been far more difficult, and a lot less fun!. It has being a privilege to work with you all. I would also like to acknowledge the various support staff at Ruakura, who have made our jobs that bit easier. I would also like to acknowledge the structural biology team at the University of Waikato. Thank you for sharing your fantastic science and making me feel like part of the crew.

Thank you to all my friends for your support, the fishing trips, cricket games and karate trainings that have helped me keep it together during my studies. A special thank you to Ryan Paul, for sharing an office, the great discussions, your humour and the dinners away from the families. Cheers mate and all the best for the completion of your studies.

To my family, firstly, my wife Miranda. Thank you for putting up with the late nights, the piles of paper and me. What else can I say, other than I love you. My two gorgeous children Cody and Jasmine, you keep me grounded, and so often after a long day helped me laugh and appreciate what life is all really about, and that's you guys! I love you both dearly. Mum, thank you for always being there. My brothers Dan, Ben and Dion, cheers boys. To the rest of the family and extended families, there are too many to mention, thank you all for your love and

support during this journey and for providing inspiration. Thank you to my grandfather Dan, who passed away at the start of my studies, he was the main man in my life. Rest easy old son.

Table of Contents

List of Figures

List of Tables

List of Abbreviations

3'	3 Prime
5'	5 Prime
4EBP1	4E-binding protein 1
A	Adenine
A	Alanine
A	Ampere
α	Alpha
ACC	Acetyl co-enzyme A carboxylase
ADP	Adenosine diphosphate
AKT	V-akt murine thymoma viral oncogene homolog/protein kinase B
ALK	Activin receptor-like kinase
AMP	Adenosine monophosphate
AMPK	Adenosine monophosphate activated kinase
ANOVA	Analysis of variance
ATCC	American type culture collection
ATP	Adenosine Triphosphate
ATP1B1	Na+, K+ ATPase β1 subunit
β	Beta
bp	Base pair
BDNF	Brain-derived neurotrophic factor
bHLH	basic helix loop helix
BHLH40	Basic helix loop helix family member e40
BMP	Bone morphogenic protein

C	Cysteine
C	Cytosine
C_2C_{12}	Immortalised murine myoblast cell line
Ca^{2+}	Calcium ion
$[Ca^{2+}]_i$	Intracellular calcium concentration
CCL2	Chemokine (C-C motif) ligand 2
CCL20	Chemokine (C-C motif) ligand 20
CDK	Cyclin dependent kinase
CHO	Chinese hamster ovary
cDNA	Complementary deoxyribonucleic acid
CEBPα	CCAAT/Enhancer binding protein alpha
CKI	Cyclin dependent kinase inhibitor
cm	Centimetre
CTNND2	Catenin, delta2
CTS	Cardiotonic steroid
D	Aspartate
DAPI	4',6-Diamidino-2-phenylindole
DMEM	Dulbecco's modified eagle medium
DMSO	Dimethyl sulfoxide
DNA	Deoxyribonucleic acid
E	Glutamic acid (Glutamate)
E.coli	Escherichia coli
EDTA	Ethylenediaminetetraacetic acid
EGTA	Ethylene glycol tetraacetic acid

ERK	Extracellular regulated kinase
EU	Endotoxin units
F	Phenylalanine
FAD	Flavin adenine dinucleotide
FAO	Fatty acid oxidation
FBS	Foetal bovine serum
FGF	Fibroblast growth factor
FGFR	Fibroblast growth factor receptor 4
FXYD	FXYD domain containing ion transport regulator
γ	Gamma
g	Gram
g	Gravity
G	Glycine
G	Guanine
GAPDH	Glyceraldehyde 3-phosphate dehydrogenase
Grb2	Growth factor receptor-bound 2
H	Histidine
H	Hydrogen
HEK	Human embryonic kidney
H/S	Horse serum
HRP	Horseradish peroxidase
I	Isoleucine
IGF-1	Insulin-like growth factor 1
IgG	Immunoglobin G

IL-1A	Interlukin-1A
IL-6	Interleukin-6
IL-8	Interleukin-8
IPA	Ingenuity pathways analysis
IRS1	Insulin receptor substrate 1
K	Lysine
K^+	Potassium ion
$[K^+]_i$	Intracellular potassium concentration
kb	Kilobase
kDa	Kilodalton
L	Litre
L	Leucine
λ	Lambda
LAP	latency-associated peptide
LAL	Limulus amebocyte lysate
LDLRAD4	Low density lipoprotein receptor class A dominant containing 4
LPS	Lipopolysaccharide
LTBP3	Latent transforming growth factor beta binding protein-3
μ	Micro ($x10^{-6}$)
m	metre
m	Milli ($x10^{-3}$)
M	Molar, moles per litre
M	Methionine
MAPK	Mitogen-activated protein kinase

MAPKAPK2	Mitogen activated protein kinase activated protein kinase 2
MAPKK	Mitogen activated protein kinase kinase
Mef2	Myocyte enhancer factor-2
MEK1	Mitogen activated protein kinase ERK kinase
MHC	Myosin heavy chain
min	Minute
MOPS	3-(N-morpholino) propanesulfonic acid
MRF	Myogenic regulatory factor
MRF4	Muscle regulatory factor 4
mRNA	Messenger ribonucleic acid
Mstn/GDF8	Myostatin
MSV	Myostatin splice variant
mTOR	Mammalian target of rapamycin
mTORC1/TORC1	Mammalian target of rapamycin complex 1
mTORC2/TORC2	Mammalian target of rapamycin complex 2
Myf5	Myogenic factor 5
MyoD	Myogenic differentiation antigen
n	Nano ($x10^{-9}$)
N	Asparagine
Na^+	Sodium ion
$[Na^+]_i$	Intracellular sodium concentration
NAD	Nicotinamide adenine dinucleotide
NSS	Normal sheep serum
OD	Optical density

ORF	Open reading frame
OSR2	Odd-skipped related 2
p	pico ($x10^{-12}$)
P	Probability
P	Proline
p38	Protein 38 kDa mitogen activated protein kinase
p53	Protein 53
p70S6K	Phospho protein 70 ribosomal protein S6 kinase
PAGE	Poly acrylamide gel electrophoresis
Pax3	Paired box 3
Pax7	Paired box 7
PBS	Phosphate buffered saline
PCR	Polymerase chain reaction
PDK1	Phosphoinositide-dependant kinase 1
PDK3	Pyruvate dehydrogenase kinase 3
PEG	Polyethylene glycol
pH	Hydrogen ion concentration
PI3K	Phosphatidylinositol-3-kinase
PIP2	Phosphatidylinositol 3,4,5-bisphosphate
PIP3	Phosphatidylinositol 4,5-bisphosphate
PTX3	Pentraxin 3
PVP	Poly vinyl pyrrolidone
Q	Glutamine
qPCR	Quantitative reverse transcriptase polymerase chain reaction

R	Arginine
Raf	Rapidly accelerated fibrosarcoma
Ras	Rat sarcoma
Rb	Retinoblastoma protein
RNA	Ribonucleic acid
rpm	Revolutions per minute
RPS6	Ribosomal protein S6
RTK	Receptor Tyrosine Kinase
s	Second
S	Serine
SDS	Sodium dodecyl sulphate
SEM	Standard error of the mean
siRNA	Small interfering RNA
Smad	Small mothers against decapentaplegic
T	Threonine
T	Thymine
TAE	Tris, acetate and ethylenediaminetetraacetic acid
TAK1	Transforming growth factor beta activated kinase 1
TBST	Tris buffered saline and tween 20
TCA	Tricarboxylic acid
TGF-β	Transforming growth factor beta
Tris	2-Amino-2-hydroxymethyl-propane-1,3-diol
U	Units of enzyme
V	Valine

W	Tryptophan
Wnt	Intergration/Wingless family
WT	Wild type
X	Stop codon
Y	Tyrosine

Chapter One

1 Review of Literature

This thesis investigates the signalling pathway(s) of a novel splice variant of myostatin (MSV), discovered in this laboratory. The following chapter will review the current literature on the structure of skeletal muscle in mammals, the process of myogenesis, and signal transduction in skeletal muscle. A detailed review of myostatin (Mstn) will follow, covering the discovery of the Mstn gene and its splice variant, the structure of the gene, signal transduction events associated with Mstn, and the function of Mstn in myogenesis and metabolism. A section covering the basic intermediary metabolism of skeletal muscle is also included. The chapter concludes with the aims to be addressed in this thesis.

1.1 Skeletal muscle

1.1.1 Structure

The myofibril is the basic contractile structure responsible for the contraction of muscle fibres. The smallest functional unit of a myofibril is the sarcomere, which occur in repetitive units. Approximately 10,000 sarcomeres linked end to end constitute a single myofibril. Each muscle fibre can contain hundreds or thousands of myofibrils, which span the length of the fibre and are physically attached to the outer membrane (sarcolemma) of the muscle fibre (Martini 2001). Myofibrils are composed of protein filaments, predominantly actin (thin filaments) and myosin (thick filaments), and a dynamic interaction between these two proteins provides the mechanical basis for muscle contraction (Martini 2001) (discussed later). The sarcoplasmic reticulum (analogous to the endoplasmic reticulum in undifferentiated myoblasts) surrounds each myofibril, and in conjunction with the network of transverse-tubules (t-tubules), is responsible for the propagation of an action potential and the subsequent release of Ca^{2+} required to initiate the contraction of skeletal muscle (see 1.1.2). The t-tubules are contiguous with the surface of the sarcolemma and provide the structural framework required to evenly distribute an action potential for the co-ordinated contraction of skeletal muscle (Martini 2001). The membrane network provided by the t-tubule and sarcolemma contains numerous specialised membrane micro-domains such as caveolae (Lapidos, Kakkar et al. 2004) the

dystrophin sarcoglycan complex (Murphy, Mollica et al. 2009), and the neuromuscular junction (Hezel, de Groat et al. 2010). These domains are important for the innervation and structural integrity of skeletal muscle. In addition, these domains play a role in the regulation of numerous proteins and protein complexes critical for signal transduction, the regulation of ion flow and the control of metabolite entry into skeletal muscle fibres (Clausen 2003; Fecchi, Volonte et al. 2006; Hezel, de Groat et al. 2010).

In individual muscles, multiple fibres are grouped into bundles, termed fascicles. The sarcolemma encases each fibre, which, in turn, is surrounded by a delicate layer of connective tissue called the endomysium that ties adjacent fibres together. The perimysium surrounds the muscle fascicles and contains collagen and elastic fibres. The perimysium provides structural support for the fascicles, in addition it supports the blood vessels and nerves required to fuel and innervate the muscle fibres. The final layer is the epimysium, which is composed of a dense layer of collagen fibres that encapsulate the muscle and separate it from surrounding tissues. The tendon connecting the muscle to bone is a blend of connective tissue fibres from the endo-, peri- and epimysium layers. Tendon fibres are interwoven with bone periosteum and continue into the bone matrix, providing the firm attachment required for muscle contraction to move the bone(s) (Martini 2001). Figure 1.1 shows a pictorial representation of skeletal muscle and an individual muscle fibre.

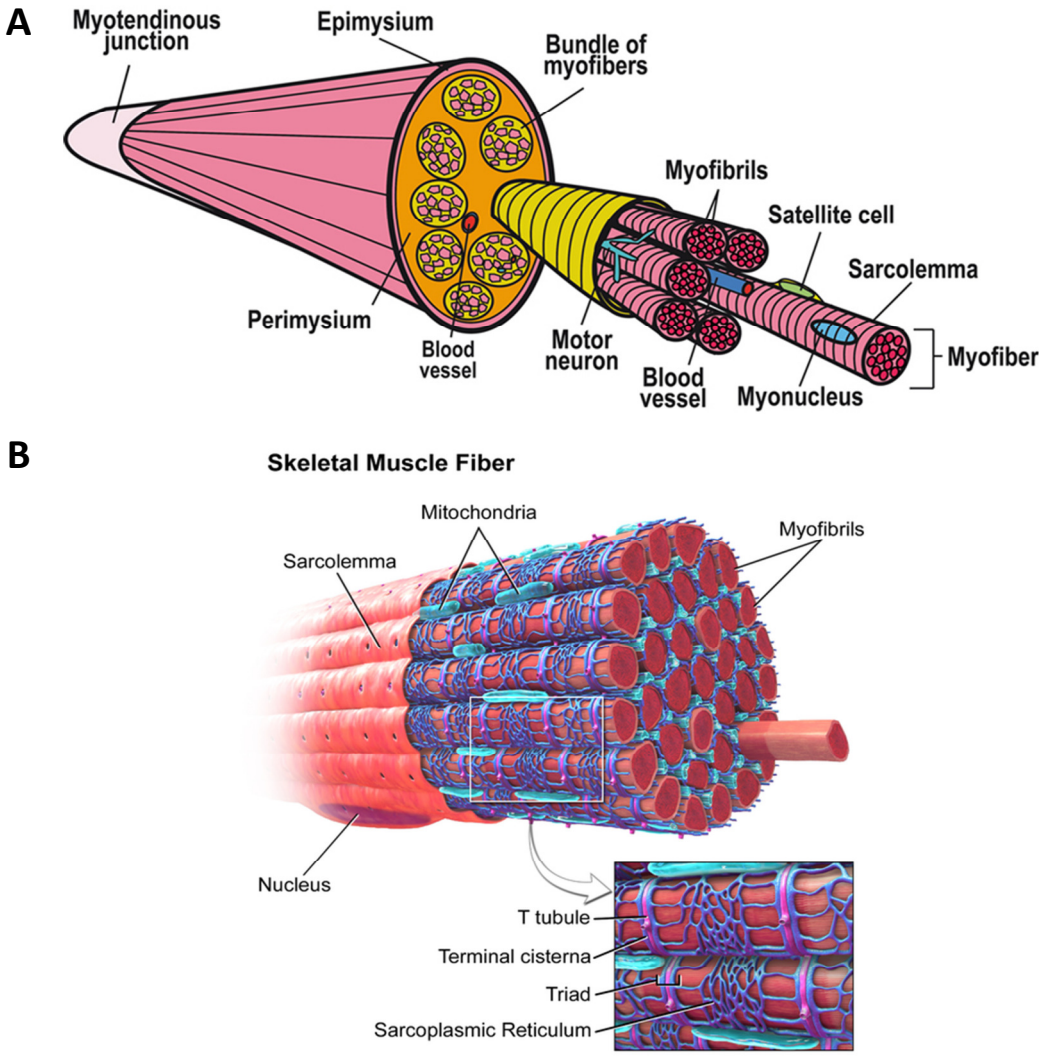

Figure 1.1: The structure of skeletal muscle. A, cartoon showing the basic structure of skeletal muscle, source (Scime, Caron et al. 2009). B, a 3-dimentional rendering of an individual skeletal muscle fibre source (www.wikipedia.org).

1.1.2 Function

The basic structural unit of vertebrate skeletal muscle is the muscle fibre, a single multinucleated cell capable of shortening to produce mechanical force and thereby providing the basis of vertebrate locomotion. A neuronal action potential initiates the contraction of skeletal muscle, via axons that innervate muscle fibres at the neuromuscular junction (Reger 1958). At the neuromuscular junction, the muscle fibre and nerve form a synaptic cleft, which allows for the propagation of an action potential through the nerve and into the muscle via the motor end plate (Martini 2001). Arrival of an action potential at the neuromuscular junction

induces the exocytotic release of acetylcholine from the axon terminal, which migrates across the cleft to bind receptors at the motor end plate, the result of which is increased permeability of the membrane to sodium ions. The influx of sodium ions (Na^+) generates an action potential in the fibre that propagates across the membrane surface and through the t-tubule system, this occurs with an almost equal and immediate efflux of potassium ions (K^+) (Martini 2001). The influx of sodium ions initiates the release of Ca^{2+} from the terminal cisternae of the sarcoplasmic reticulum, which binds troponin, freeing the contractile apparatus and allowing actin/myosin cross-bridges to form for muscle contraction to proceed (Huxley 1971). Uncoupling of the actin myosin cross-bridges is an ATP dependant process, and on activation, the head of the myosin molecule pivots, a motion known as the 'power stroke' and ADP is released along with a free phosphate molecule. To disengage the cross-bridge requires the binding of another ATP molecule, which generates the energy required to break the cross-bridge in addition to re-cocking the myosin head for the cycle to start again (Martini 2001). Thus muscle activity is closely linked to the metabolic status of the cell.

1.1.3 Muscle fibre type

Mammalian skeletal muscle is composed of a number of different fibre types, the proportions of which define fast and slow twitch skeletal muscle. Identification of the different fibre types has been carried out using a number of techniques. Most commonly, fibre types are classified based on the myosin heavy chain (MHC) isoform(s) they express. Four major fibre types have been identified in the adult skeletal muscles of small mammals using the MHC classification system, with additional isoforms identified in embryonic, foetal and in the head muscles (Schiaffino and Reggiani 1996; Pette and Staron 2000). The four main fibre types are; slow type I, which are suggested to originate from the primary fibres formed during myogenesis in the embryo, and fast type IIA, B and X. Functionally, these MHC isoforms have been correlated with shortening velocity. Studies indicate that type IIB fibres have the fastest shortening velocity, with IIX, IIA and I progressively slower. Different muscle fibre-types also display different metabolic profiles, primarily in terms of preferred energy substrate. In general, type I fibres are considered oxidative, with type II fibres becoming progressively

more glycolytic in the following order: type IIA<X<B (Schiaffino and Reggiani 2011). Embryonic, foetal and adult cell populations contain myoblasts that have the capacity to form various fibre types. For example, clonal cultures of embryonic chicken and mouse are heterogeneous with respect to their MHC profile (Cho, Webster et al. 1993). This suggests that myoblasts may be committed to a specific fibre type and this commitment is retained in the progeny cells. However, studies on clonal human myoblasts, demonstrated that all cultures, although heterogeneous in their MHC profile, had the ability to express 'slow' MHC during differentiation. This work also highlighted that extrinsic factors, such as innervation, growth factors the existing muscle structure are likely to play a role in the acquisition of muscle fibre type (Cho, Webster et al. 1993). In addition to fibres expressing a single MHC isoform, intermediate fibres that co-express two or more MHC isoforms also exist. The MHC isoforms have been shown to form up to seven myofibre hybrids. Notably, type I, IIC (type I and IIA hybrid), IIA, IIAX (type IIA and IIX hybrid), IIX, IIB and possibly, a IIXB based on their staining characteristics for antibodies to different MHC proteins (Picard, Duris et al. 1998; Zhang, Koishi et al. 1998; Greenwood, Tomkins et al. 2009). This plasticity in muscle fibre type is largely controlled by the external environment, in response to various stimuli such as neuromuscular or hormonal alterations, mechanical loading/unloading and aging (Schiaffino and Reggiani 2011). In addition, calcium dependant signal transduction has been shown to play a significant role in the modulation of skeletal muscle fibre type (Tavi and Westerblad 2011).

1.1.3.1 Origin of skeletal muscle

The paraxial mesoderm in the embryo is the origin of vertebrate skeletal muscle. This tissue forms cellular spheres, termed somites (Christ and Ordahl 1995). In mice, somite formation begins at about 8 days *post coitum* as the paraxial mesoderm on either side of the neural tube and notochord becomes segmented in a co-ordinated craino-caudal sequence. The somites provide a cellular reservoir for the formation of a number of specialised tissues including vertebrae, cartilage, tendon, skin and the skeletal muscle of the body and limbs. As somite development proceeds, specialised areas of the somite develop to form the dermomyotome (dorsal part of the somite) the myotome (underlying and

formed from the dermomyotome) and the sclerotome (dorsal part of the somite) (Buckingham, Bajard et al. 2003). Formation of these specialised regions requires the co-ordinated action of an array of genes. For the development of skeletal muscle development, important roles have been ascribed to the Pax3, MyoD and Mrf4 transcription factors in initial myotome formation, with Sonic hedgehog, Wnt and bone morphogenic protein signalling involved in the further segregation of the dermomyotome into epaxial (responsible for the formation of the back muscle) and hypaxial (responsible for the formation of diaphragm, body wall and limb muscle) regions (Buckingham, Bajard et al. 2003; Tzahor, Kempf et al. 2003; Le Grand and Rudnicki 2007). There is heterogeneity in the populations of precursor cells present in these different spatial regions of the developing dermomyotome (Yokoyama and Asahara 2011), which is thought to define the distinct populations of myogenic precursors.

1.1.3.2 Muscle progenitors in the developing embryo

One clearly distinct population of muscle precursors are the Pax3 positive cells that develop in the ventrolateral lip of the dermomyotome. These cells undergo an epithelial to mesenchymal transition before delaminating and migrating to form the limb buds in the developing embryo (Buckingham 2007). Once this Pax3 positive population has migrated into the limb, expression of Pax3 is reduced as the MRF family (discussed later) and associated transcription factors are induced to execute the myogenic program. The migration of progenitor cells into the limb bud requires a network of transcription factors (SIX1, SIX4, Eya1, Eya2, Myf5, Pax3 and Pitx3), in addition to genes with an ascribed role in the migration of the precursors (lbx1, c-met, CXCR4, HGF). Deletion of any of these genes impairs myogenesis in the limb buds (Buckingham, Bajard et al. 2003; Yokoyama and Asahara 2011).

Most pertinent to this thesis, is a second population of muscle precursors that are present in, but are not necessarily derived from the central dermomyotome. These cells express the transcription factor Pax7 and not necessarily Pax3, are mitotically active and devoid of MRF expression. They persist throughout embryonic development and enter the myotome compartment as the preceding central dermomyotome disintegrates during development. Progenitor cells expressing Pax7 activate the myogenic program via the induction of Myf5

expression. This stimulates a second wave of myogenesis, providing additional cells to incorporate with existing primary muscle fibres during foetal development. A number of studies have identified this population as being responsible for the formation of the satellite cell pool in post-natal muscle, with ~80% of satellite cells expressing Pax7 and Myf5 with or without Pax3 (Buckingham, Bajard et al. 2003; Buckingham 2007).

Satellite cells are defined based on their unique anatomical location between the basal lamina and the sarcolemma of multinucleated fibres. They are considered the major contributors to post-natal muscle growth and regeneration (Mauro 1961). They are also the major source of primary myoblasts isolated using enzymatic techniques (Rosenblatt, Lunt et al. 1995; Allen, Temm-Grove et al. 1997; Partridge 1997). In mice, satellite cells are first seen in the limb muscles during mid- to late-gestation (embryonic day 15 in mice). In new-born mice, approximately 30% of the sub-laminar nuclei in muscles are satellite cells. However, this percentage decreases with age as the adult size of muscles is reached, and at two months of age, the contribution of satellite cell nuclei to all sub-laminar nuclei is less than 5% (Gibson and Schultz 1983). Satellite cells have distinguishing morphological characteristics, such as a relatively high nuclear-to-cytoplasmic ratio and increased nuclear heterochromatin and few organelles (Hawke and Garry 2001). In adults, satellite cells are normally in a state of mitotic quiescence. However, a range of stimuli can activate satellite cells, which induces the cells to re-enter the cell cycle to participate in myogenesis. These stimuli include muscle stretch, voluntary exercise, various forms of injury and electrical stimulation (Appell, Forsberg et al. 1988; Rosenblatt, Yong et al. 1994; Schultz and McCormick 1994). Activation of satellite cells induces myogenic gene expression and the myoblasts, termed myogenic precursor cells, differentiate and then fuse with existing myofibres or each other to form new or replacement myofibres (Sabourin and Rudnicki 2000). The absolute number of (quiescent) satellite cells stays relatively constant during adult life, and with repeated cycles of degeneration and regeneration (Gibson and Schultz 1983; Schultz and Jaryszak 1985; Morlet, Grounds et al. 1989; Schultz 1996). This suggests that self-renewal maintains the satellite cell pool (Zammit and Beauchamp 2001), although other studies have demonstrated that other stem cell pools, for example pericytes, are

able to contribute to the satellite cell pool (Dellavalle, Maroli et al. 2011), and thus myogenesis.

1.1.4 MRFs and control of myogenesis

Myogenesis is an incremental process initiated with the commitment of a muscle precursor to the myogenic lineage. Once committed, myoblasts proliferate, differentiate into post-mitotic myocytes and finally fuse to form multinucleated myotubes, a process dependant on regulation of the cell cycle (see 1.1.5). This myogenic process is essentially the same in the embryo, post-natal muscle or *in vitro*, with the notable exception that the post-natal and *in vitro* precursors are, primarily, muscle satellite cells. Muscle-specific transcription factors control each stage of myogenesis, acting as the terminal effectors for multiple signalling cascades. These key transcription factors are responsible for the timely execution and maintenance of the myogenic program and have been well investigated and reviewed (Kuang, Kuroda et al. 2007; Knight and Kothary 2011). Figure 1.2 outlines the key transcription factors involved in regulating myogenesis, and the stage of myogenesis in which they act.

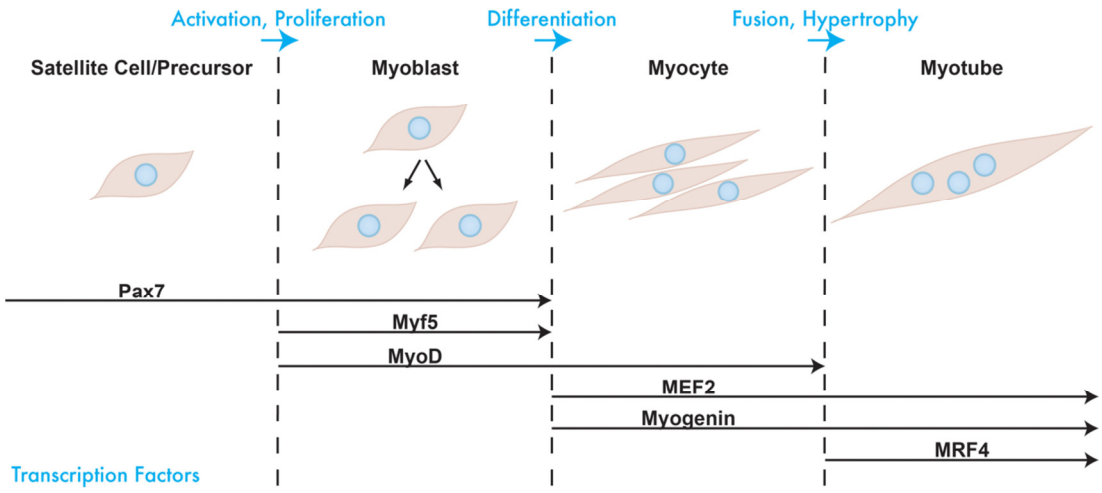

Figure 1.2: The key transcription factors involved in myogenesis. This figure depicts the key transcription factors involved in the regulation of myogenesis and indicates the stages of myogenesis at which they play a critical role. Figure taken from (Knight and Kothary 2011).

Much of our knowledge of the process of myogenesis has come from the use transgenic models in which the roles of specific transcription factors have been defined. In addition, the use of cultured myoblasts has contributed to the understanding of the signalling events that regulate myogenesis (Sharples and Stewart 2011). The regulation of myogenesis relies on the ability of specific transcription factors to commit cells to the myogenic lineage, and to coordinate extra and intra-cellular signals to regulate the timely and stage-specific induction of transcripts responsible for the execution and maintenance of the myogenic program. The following section will focus on the major transcription factors that regulate myogenesis, including the myogenic regulatory factors (MRFs), Pax7 and the MEF2 family.

The MRFs are members of the basic helix-loop-helix (bHLH) superfamily. These transcription factors play critical roles in the specification, proliferation, differentiation and maintenance of the myogenic lineage. The MRF family of transcription factors consists of four members, MyoD, Myf5, myogenin and MRF4 (Braun, Buschhausen-Denker et al. 1989; Edmondson and Olson 1989; Rhodes and Konieczny 1989; Wright, Sassoon et al. 1989). Each shares structural similarities, containing both the DNA binding domain and the dimerisation domain (responsible for hetero-dimerisation) (Lassar, Buskin et al. 1989; Murre, McCaw et al. 1989; Arnold and Braun 1996). The most well defined mechanism of MRFs induced gene regulation is the ability of the MRFs to bind the ubiquitously expressed E proteins through their bHLH motif. The resulting heterodimer(s) interact with specific DNA sequences known as E-boxes. The consensus E-box sequence is 5'-CANNTG-3' where N is any nucleotide. E-boxes are present in the promoters of numerous muscle specific genes and convey the ability to regulate gene expression in an MRF dependant manner (Arnold and Braun 1996; Sabourin and Rudnicki 2000). *In vivo* studies using knock-out models of the individual MRFs have provided great insight into specific MRF function, demonstrating a hierarchical relationship between the MRFs. Both MyoD and Myf5 are considered to be the primary MRFs with roles in myogenic determination, as evidenced by their functional and necessary roles in the establishment of epaxial (paraspinal and intercostal) and hypaxial (limb and muscle wall) muscle lineages, respectively, in the embryo (Arnold and Braun

1996; Yokoyama and Asahara 2011). Mice with both MyoD and Myf-5 deleted, are born completely devoid of skeletal muscle and die shortly after birth. The secondary MRFs, myogenin and MRF4 are thought to have critical roles in myogenic differentiation, with the most compelling evidence again from knock-out models. Myogenin null mice die shortly after birth and display a large reduction in the mass of skeletal muscle, with a greatly reduced density of myofibres and a lack of myosin heavy chain and actin, both of which are structural markers of muscle differentiation (Arnold and Braun 1996). Deletion of MRF4 suggests a role in supporting Myf5 expression and, as with myogenin, influencing the expression of structural myogenic genes (Arnold and Braun 1996).

Pax7 is an early transcription factor in the myogenic program and acts in concert with the MRFs to regulate myogenic gene expression. The importance of Pax7 to the myogenic program is best illustrated in the phenotype of the Pax7 null mouse. These animals have very few or no satellite cells (Seale, Sabourin et al. 2000) , with those that are present characterised as prone to apoptosis, having cell cycle defects and demonstrate an impaired ability to both execute the myogenic program, and recruit stem cells to the myogenic lineage (Seale, Sabourin et al. 2000; Relaix, Montarras et al. 2006; Lu, Cummins et al. 2008). Although at birth, Pax7 null animals appear normal, the postnatal growth of skeletal muscle is severely compromised and these animals die 2-3 weeks after birth (Lu, Cummins et al. 2008). One of the nine members of the Pax gene family, Pax7 contains a paired DNA binding domain and a homeodomain believed to regulate both DNA-protein and protein-protein interactions (Chi and Epstein 2002; Buckingham and Relaix 2007). The critical role for Pax7 in the specification of the myogenic lineage, is thought to be mediated through the regulation of both MyoD and Myf5 expression (Buckingham and Relaix 2007). Interestingly, it has also been reported that Pax7 can prevent the transcriptional activity of MyoD, thus preventing execution of the differentiation program. Pax7 has been shown to induce the expression of Id2 and Id3, direct inhibitors of MRF activity, as well as inducing the proteasome-dependant degradation of MyoD (Olguin and Pisconti 2012).

Activation of muscle specific genes is also dependent on the functional interactions between the MRF proteins and the MEF2 family of MADS box transcription factors. MEF2 transcription factors are able to activate MRF protein

activity, however, they are unable to regulate myogenic activity alone (Molkentin, Black et al. 1995). Thus, it has been proposed that these two families form regulatory networks with critical roles in myogenesis (Olson and Klein 1994). Four vertebrate MEF2 genes have been identified. Mef2A, Mef2B and Mef2D are expressed ubiquitously, and Mef2C is expressed specifically in muscle, brain and spleen (Breitbart, Liang et al. 1993; Leifer, Krainc et al. 1993; Martin, Miano et al. 1994). The MEF2 factors all contain a MADS domain that is involved in dimerisation and binding DNA, and a MEF2 specific domain that influences dimerisation and cofactor interactions (Molkentin, Firulli et al. 1996). MADS box transcription factors bind to conserved A/T rich DNA sequences in many muscle specific genes to regulate their function (Molkentin, Firulli et al. 1996).

The network of transcription factors that is described above, represent the major factors known to date that regulate myogenesis. As the control of myogenesis by this transcriptional network involves both the proliferation of myoblasts and their growth arrest to allow myoblast differentiation, their activity is also associated with control of the cell cycle.

1.1.5 The cell cycle

Control of the cell cycle is integral to the myogenic program, with significant roles in maintenance of proliferation as well as timely execution of the differentiation program. The following outlines mechanisms regulating the cell cycle program during myogenesis. Myogenesis involves the irreversible withdrawal of proliferating myoblasts from the cell cycle. This process involves the co-ordinated activation and control of muscle specific gene expression throughout myoblast proliferation, for cell cycle exit and for the formation of terminally differentiated myotubes (Lassar, Skapek et al. 1994). The cell cycle comprises of four stages; the DNA synthesis (S-phase) stage, mitosis (M-phase) and two gap phases (G_1 and G_2), which are between S- and M- phases. Cells can also exit the cell cycle at G_1 into a state of quiescence known as G_0 (Kitzmann and Fernandez 2001). It is thought that the first gap phase (G_1) plays a role in the decision to continue or withdraw from the cell cycle, and therefore, a number of the signalling pathways that regulate cell cycle progression are associated with the G_1 phase (Grana and Reddy 1995; Kitzmann and Fernandez 2001).

Cell signalling pathways involved in the the cell cycle have a wide range of targets, including the retinoblastoma protein (Rb), the cyclins, cyclin-dependent kinases (CDKs) and cyclin dependent kinase inhibitors (CKIs). The phosphorylation state of Rb serves as the major contributing factor in regulating exit from the cell cycle. Inactive (hyperphosphorylated) Rb results in progression of the cell cycle, and the transition from G_1 to S phase. In contrast, active (hypophosphorylated) Rb is thought to stall the cell cycle at the G_1 checkpoint. This is achieved through the binding to, and the inactivation of transcription factors responsible for the regulation of DNA synthesis (S-phase) genes, with E2F and DP1 genes providing good examples (Weinberg 1995; Wu, Zukerberg et al. 1995; La Thangue 1996; Dyson 1998). Control of the cell cycle by Rb involves the CDKs and their obligate partners, the cyclins. Figure 1.3 provides an overview of cell cycle regulation.

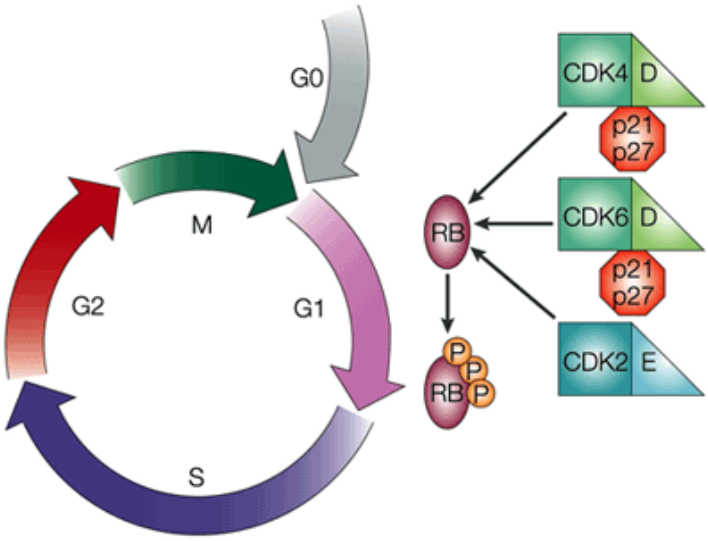

Figure 1.3: The eukaryotic cell cycle. The figure showns the distinct phases of the cell cycle: the first gap phase (G1), the DNA synthesis phase (S), the second gap phase (G2) and mitosis (M). Quiescent cells that exit the cell cycle are in the G0 phase. The progression through the cell cycle is regulated by the activity of the cyclin (triangles) and Cdk (squares) complexes, with complex activity also regulated by the Cdk inhibitors. Figure taken from (Coleman, Marshall et al. 2004).

The CKIs also play a major role in the control of the cell cycle. The CKIs are grouped into two families, based on their structure and target Cdks. The first family is the INK4 (inhibitors of Cdk4) family and includes; $p15^{INK4b}$, $p16^{INK4a}$, $p18^{INK4c}$ and $p19^{INK4d}$. The forced over-expression of INK4 family members results in a reduced rate of cell proliferation. They target both Cdk4 and 6, interfering with their binding to cyclin-D (Gu, Turck et al. 1993; Serrano, Hannon et al. 1993; Guan, Jenkins et al. 1994; Hannon and Beach 1994; Chen, Jackson et al. 1995; Grana and Reddy 1995; Hirai, Roussel et al. 1995). The second family is the Cip/Kip family, which and includes $p21^{CIP1/WAF1}$, $p27^{KIP1}$, and $p57^{KIP2}$ (el-Deiry, Tokino et al. 1993; Gu, Turck et al. 1993; Harper, Adami et al. 1993; Xiong, Hannon et al. 1993). The Cip/Kip family of proteins contain binding motifs that enable them to bind to both cyclin and CDK proteins. These complexes which are present during the G1 phase, are inhibited by p21, p27 and p57. In addition, this family also inhibits cyclin:Cdk interactions during DNA synthesis (Harper, Adami et al. 1993; Xiong, Hannon et al. 1993; Polyak, Kato et al. 1994; Lee, Reynisdottir et al. 1995). The association of Cdk4 with D-type cyclins is also thought to be promoted in a p21 dependant manner. This association occurs during periods of reduced p21 expression as seen in proliferating cells, conversely, an increased ratio of p21 to cyclin:Cdk results in the inactivation of cyclin:Cdk complexes (Zhang, Hannon et al. 1994; Sherr 1995; LaBaer, Garrett et al. 1997).

The MRFs and other regulatory proteins play a role in exit from the cell cycle. MyoD is critical to the differentiation process, controlling the activation of cell cycle machinery involved in cell cycle withdrawal. MyoD has been shown to bind to and facilitate the homodimerisation of the CKIs p21, p27 and p57. These interactions result in the inhibition of the specific Cdks and ultimately exit from the cell cycle (Reynaud, Leibovitch et al. 2000; Guo, Wang et al. 1995; Halevy, Novitch et al. 1995; Parker, Eichele et al. 1995; Martelli, Cenciarelli et al. 1994). MyoD has also been shown to bind and enhance the expression of Rb protein (through preventing Rb phosphorylation), and induce p21 expression in differentiating myoblasts, two mechanisms promoting exit from the cell cycle (Gu, Schneider et al. 1993; Zhang, Zhao et al. 1999). Thus, regulation of the cell cycle is critical for normal development and any defect in these mechanisms will

perturb myogenesis during foetal development, postnatal growth or in the regeneration of skeletal muscle in adults.

1.1.6 General signal transduction in muscle

At all stages of development, skeletal muscle responds to cues from an array of stimuli that includes: stretch, contraction, disuse, nutrient availability, pH, ion flow, growth factors, cytokines, mitogens, hormones, oxidative or heat stress, vitamins, toxins, and neuronal stimulation. In addition, skeletal muscle functions as an endocrine organ, secreting factors or 'myokines' that can elicit specific biological responses on muscle, or in other target tissues, this list includes: IL-6, 8 and 15, BDNF, irisin, follistatin like 1, FGF21, Leukaemia inhibitory factor, FGF-2, IGF-1 and Mstn (Pedersen and Febbraio 2008; Henriksen, Green et al. 2012). The architecture of skeletal muscle also plays a critical role in signal transduction, with muscle containing a number of specialised protein complexes and structures that play a critical role, including the neuromuscular junction, dystrophin sarcoglycan complex, caveolae, calthrin coated vesicles and t-tubules (Heydemann and McNally 2007; McMahon and Boucrot 2011; Staubach and Hanisch 2011; Takamori 2012). Specific signalling molecules are targeted to these discrete cellular locations, providing another means of regulating signal transduction, through the localisation of signalling intermediates.

The ability of skeletal muscle and myoblasts to transduce a biological signal relies heavily on activation of a vast array of receptors. These are located throughout the cell, and, importantly in the cell membrane. Cell membrane receptors can be broadly classified into five major groups: the G-protein coupled receptors (GPCRs), tyrosine kinase receptors, cytokine receptors, ion channels and the TGF-β receptors (Jameson and DeGroot 2010). Activation of receptors involves binding of a secreted or introduced extracellular ligand to a surface receptor which results in conformational change. For secreted ligands, binding to receptors can occur in, (1) an endocrine manner (e.g. insulin produced in the pancreas acting on skeletal muscle), (2) paracrine manner (e.g. the release of acetylcholine at the neuromuscular junction), or (3), an autocrine manner. The receptor complex then transmits the signal into the cell, which can have both immediate and/or longer term consequences and can involve conjoint or different second messenger cascades (Jameson and DeGroot 2010).

Pertinent to this thesis is signal transfer through the simple and reversible process of phosphorylation, as occurs following the binding of Insulin-like growth factor (IGF-1) to the insulin-like growth factor receptor, or the binding of Mstn to the activin receptor type IIB (ACTRIIB) (Joulia-Ekaza and Cabello 2007; Laviola, Natalicchio et al. 2007; Elkina, von Haehling et al. 2011). It is notable that phosphorylation independent mechanisms to mediate receptor signalling also exist. For example, the signalling of the notch family of proteins, where ligand binding results in the cleavage and release of an intracellular C-terminal portion of the receptor, nuclear localisation of this C-terminal portion has been shown to directly participate in gene transcription (Oswald, Tauber et al. 2001). The regulation of GPCR signalling provides another example, with the binding of a GPCR interacting protein GRK2 altering the interaction of the receptor with other signalling molecules to influence signal transduction (Ferguson 2007).

The control of phosphorylation dependant signal transduction lies with a vast array of protein kinases, with over 500 identified so far in mice and humans. Protein kinases perpetuate the signal of a given stimulus via phosphorylation of signalling intermediates. Protein kinases can alter the activity, location and stability of many cellular proteins, coordinating and adapting critical cellular processes, including proliferation, differentiation, specification, cell death, metabolism, transcription and translation, often in a tissue or lineage specific context (Manning, Whyte et al. 2002). The major role of protein kinases in mammalian skeletal muscle development and regeneration has been recently reviewed (Knight and Kothary 2011). Most pertinent to this thesis are the phosphorylation events in the TGF-β and p38 (mitogen activated protein kinase (MAPK)) cascades (as described specifically for Mstn signalling (see 1.1.7.3-4)), and the ERK (MAPK) and Phosphatidylinositide 3-kinase (PI3K)/AKT signal transduction cascades.

1.1.6.1 Extracellular regulated kinase (ERK) signalling

In myoblasts, the events leading to ERK1/2 phosphorylation via RTK activation are well defined, a good example being ligand activation of fibroblast growth factor receptor (FGFR4). Following the binding of FGF, FGFR4 auto phosphorylates, which leads to the recruitment of Src homology 2 (SH2) domain-containing proteins such as growth-factor receptor-bound 2 GRB2, the first step in

the formation of an adaptor complex. GRB2 interacts with the guanine-nucleotide exchange factor son of sevenless (SOS), the GRB2/SOS interaction allows activation of the plasma membrane bound GTPase, Ras. Ras activation requires SOS catalysed GTP exchange, with GTP bound Ras activating Raf and initiating the MAPK signal transduction cascade. In this pathway, Raf phosphorylates the MAP or ERK kinases (MEK), then ERK1/2. To date MEK1/2 are the only known activators of ERK1/2 (Knight and Kothary 2011). Thus, pharmacological inhibitors of the ERK pathway generally prevent the phosphorylation of MEK, which disrupts the downstream signal transduction cascade. Activation of ERK signalling influences multiple cellular processes including proliferation, differentiation, protein synthesis, mitochondrial function and the maintenance of the fast glycolytic muscle fibres (Roux, Shahbazian et al. 2007; Shi, Scheffler et al. 2008; Shi, Scheffler et al. 2009; Knight and Kothary 2011; Wortzel and Seger 2011). In addition, activation of the SOS/GRB-2/Ras/Raf/MEK pathway is common to other RTK, G protein-coupled receptors and the Na^+ K^+ ATPase (Schlessinger 2000; Hur and Kim 2002; Kotova, Al-Khalili et al. 2006).

1.1.6.2 Phosphatidylinositol-3 Kinase (PI3K)/AKT

The PI3K/AKT pathway has been studied in depth in skeletal muscle. Specifically, this pathway in conjunction with its downstream target mammalian target of rapamycin (mTOR) is a key regulator of growth and hypertrophy (Trendelenburg, Meyer et al. 2009). The principle activators of this pathway are insulin and IGF-1. The binding of IGF-1 to its receptor causes a conformational change in the receptor to induce the trans-phosphorylation and subsequent phosphorylation of insulin receptor substrate 1 (IRS-1). IRS-1 then activates the PI3K lipid kinases, which, in turn, phosphorylate phosphatidylinositol 4, 5 bisphosphate (PIP2) to produce phosphatidylinositol 3, 4, 5 triphosphate (PIP3). PIP3 then recruits and phosphorylates phosphatidylinositol-dependant-kinase (PDK1), which in turn phosphorylates the serine/threonine kinase AKT. AKT then targets numerous intracellular targets including: mammalian target of rapamycin (mTOR), glycogen synthase kinase 3 (glycogen synthesis) and the fork-head box family of transcription factors (involved in the regulation of muscle atrophy related genes). Pertinent to this thesis is the phosphorylation/activation of targets downstream of mTOR which include p70 S6 kinase (p70S6K), which, in

turn, phosphorylates the ribosomal protein S6 (rpS6). The phosphorylation of rpS6 is suggested to increase the translational efficiency of a class of mRNA transcripts containing an oligopyrimidine tract. The mTOR complex also phosphorylates and inactivates 4EBP1, a repressor of the translation initiation factor eIF4E. When growth factor and nutrients are limiting 4EBP1 is hypo-phosphorylated and is bound tightly with eIF4E which represses assembly of the translation initiation complex (Knight and Kothary 2011; Magnuson, Ekim et al. 2012). Thus, the downstream activation of the PI3K pathway can have a direct influence on the cellular protein synthesis machinery.

There is considerable crosstalk across signal transduction cascades, which involves specific intermediates. For example, ERK dependant activation of ribosomal S6 kinase (RSK) induces the phosphorylation of rpS6 on S234/236 following ERK activation. PI3K signalling has also been shown to induce rpS6 phosphorylation as mentioned earlier through p70S6K following activation by mTOR (Roux, Shahbazian et al. 2007; Won, Yang et al. 2012). This provides a mechanism for targeted crosstalk between MAPK and PI3K signal transduction, which converges on rpS6. Furthermore, crosstalk between MAPK and PI3K precedes the activation of ERK. For example, Grb2 possesses the ability to transduce signal down both MAPK and PI3K cascades (Won, Yang et al. 2012), an example of which is shown in Figure 1.3. Crosstalk through multiple signalling intermediates adds additional complexity to biological systems. This redundancy may play a substantial role in the ability of cells and tissues to ‘buffer’ a given stimulus, through preventing the saturation of a specific cascade. Regardless, signal transduction plays an indispensable role in all aspects of skeletal muscle function.

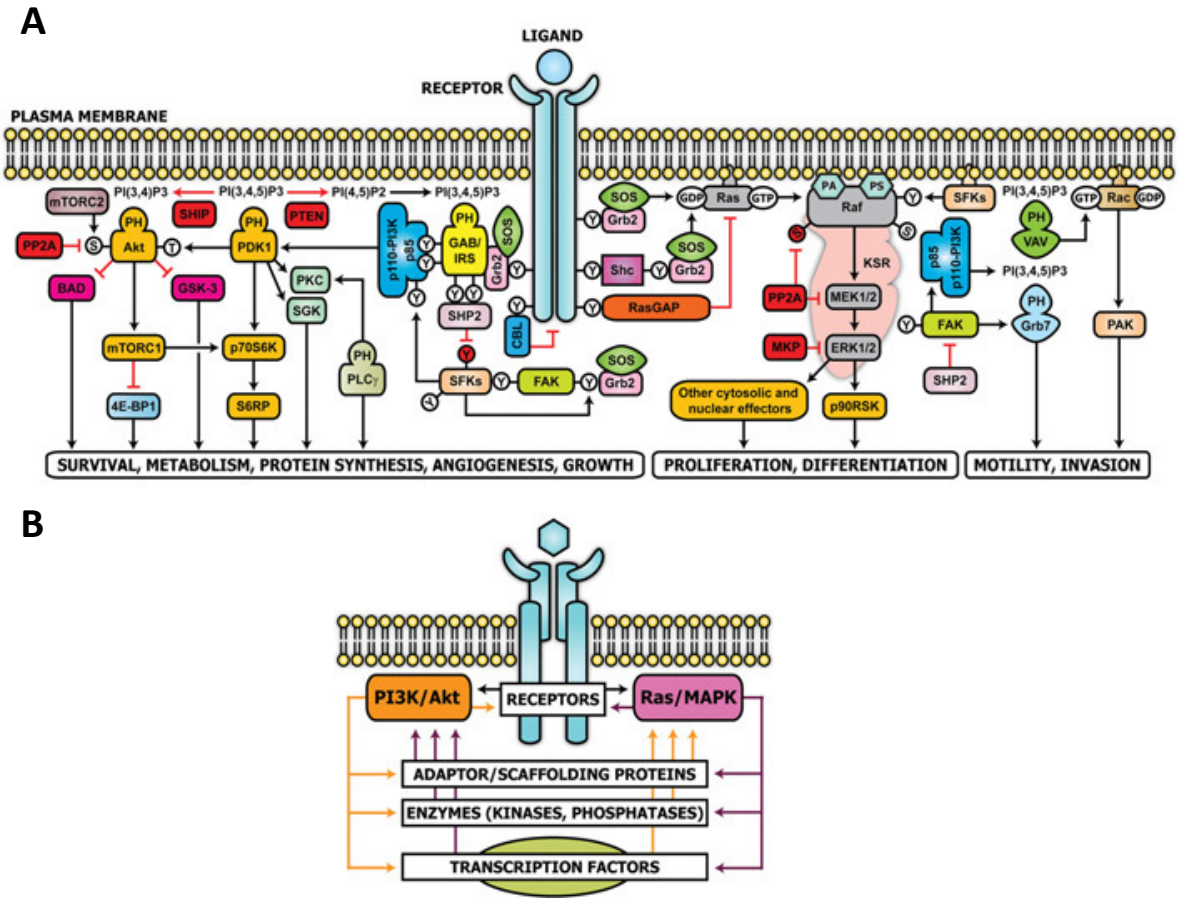

Figure 1.4: PI3K/AKT and MAPK crosstalk. A, Schematic diagram illustrating the how cross talk between PI3K/AKT and MAPK pathways can occur. 4E-BP1 (eukaryotic initiation factor 4E-binding protein 1), KSR (kinase suppressor of Ras), mTORC1 (mTOR–raptor (regulatory associated protein of mTOR) complex), mTORC2 (mTOR–rictor (rapamycin-insensitive companion of mTOR) complex), PA (phosphatidic acid), PI (phosphatidylinositol), PP2A (protein phosphatase 2A), PS (phosphatidylserine), S (serine), S6RP (S6 ribosomal protein), SGK (serum- and glucocorticoid-induced protein kinase), T (threonine), Y (tyrosine). B, pictorial illustration of how the PI3K/AKT (orange lines) and Ras/MAPK (purple lines) signal transduction may interact with each other, source (Aksamitiene, Kiyatkin et al. 2012).

1.1.7 Myostatin (Mstn)

The Mstn gene was identified in 1997 as growth and differentiation factor-8 (GDF-8), a new member of the transforming growth factor-β (TGF-β) superfamily (McPherron, Lawler et al. 1997). GDF-8 mRNA was found in developing and adult skeletal muscle, as well as the myotome compartment of the somites during early embryogenesis, this strongly suggested a role for GDF-8 in the development of skeletal muscle. Subsequently, the GDF-8 gene was inactivated by gene targeting in mice, wherein homozygous null mice display an increase in the mass of skeletal muscle, with an approximate 2-3 fold increase in the size of individual muscles (McPherron, Lawler et al. 1997). The increase in muscle size was attributed to a combination of muscle cell hyperplasia (increase in muscle fibre number) and hypertrophy (increase in muscle fibre size). These data strongly indicated that GDF-8 functioned specifically as a negative regulator of skeletal muscle growth. As a consequence, the authors named the new gene Mstn (McPherron, Lawler et al. 1997).

1.1.7.1 Mutations and phenotypes of Mstn.

Following its discovery, natural inactivating mutations in the Mstn gene have been characterised in cattle (Grobet, Martin et al. 1997), dogs (Mosher, Quignon et al. 2007), sheep (Clop, Marcq et al. 2006) and humans (Schuelke, Wagner et al. 2004). The hypermuscular phenotype is observed for all these natural mutations, with different inter- and intra-species mutations that act in different ways to inactivate Mstn. For example, in Belgian Blue cattle there is an 11bp deletion in the mature region of Mstn which generates a shift in the open reading frame and introduces a premature stop codon (Grobet, Martin et al. 1997; Kambadur, Sharma et al. 1997). Alternatively in Piedmontese cattle, a missense mutation that results in the substitution of a tyrosine for a critical cysteine, disrupts the folding, and the activity of the mature protein (Kambadur, Sharma et al. 1997; McPherron and Lee 1997). In Texel sheep, a mutation in the 3' UTR of the Mstn transcript generates a microRNA (miRNA) site, which results in the reduced translation of Mstn protein (Clop, Marcq et al. 2006). However, other mechanisms exist for regulating the extent of the hyper-muscular growth in addition to the absence of functional Mstn. In support, Lee et al 2004 have elegantly demonstrated that Mstn is not the only regulator of skeletal muscle

mass. They observed further increases in muscle mass of mice following the introduction of a follistatin transgene into a Mstn null background (Lee 2007). Similarly, studies in our laboratory have shown further increases in the muscle mass of Mstn null mice following introduction of an IGF-1 transgene (unpublished data).

1.1.7.2 Expression of Mstn

Mstn is expressed in embryonic, foetal and postnatal muscle cells, which supports a role for this protein in regulating many facets of myogenesis (McPherron, Lawler et al. 1997). The expression of Mstn has also been reported in heart muscle, adipose, liver, spleen, lung, kidney, and fibroblasts (Jiao, Yuan et al. 2011). Transcriptional regulation of Mstn has been reported to occur via a number of pathways. The Mstn promoter is rich in E-box motifs in a number of vertebrate species. MyoD and Myf5 have been shown to bind to E-box motifs and both have been shown to play a role in transactivation of the Mstn promoter (Ma, Mallidis et al. 2001; Spiller, Kambadur et al. 2002; Senna Salerno, Thomas et al. 2004). Other regulators include MAPK (ERK and p38) signalling, activated glucocorticoid receptor, tumour necrosis alpha, FoxO1 and the Smad transcription factors (Ma, Mallidis et al. 2001; Allen and Unterman 2007; Lenk, Schur et al. 2009; Bish, Morine et al. 2010). In addition, Mstn has also been shown to auto-regulate its own expression through a mechanism dependant on Smad7 (Forbes, Jackman et al. 2006).

1.1.7.3 Structure

Mstn shares features common to other members of the TGF-β superfamily, including a putative N-terminal secretion signal, a conserved C-terminal RXRR proteolytic processing site and nine conserved cystine residues in the C-terminal region, six of which are essential for forming a cystine knot structure and the dimerization of the mature protein (McPherron and Lee 1996; McPherron, Lawler et al. 1997). Processing of the precursor produces an N-terminal latency associated peptide (LAP) and the mature C-terminal dimer. Initially, it was thought that Mstn was predominantly secreted as an inactive latent complex consisting of dimeric LAP non-covalently linked to the C-terminal dimer. However, other studies have suggested that the predominant form of secreted Mstn is a full length dimer that is processed and cleaved in the

extracellular matrix (Anderson, Goldberg et al. 2008). Disassociation or cleavage leads to the release of the 'mature' C-terminal dimer as the 'biologically active' form of the protein (Lee and McPherron 2001; Thies, Chen et al. 2001; Hill, Davies et al. 2002; Zimmers, Davies et al. 2002; Hill, Qiu et al. 2003; Wolfman, McPherron et al. 2003; McFarlane, Langley et al. 2005; Miura, Kishioka et al. 2006). The complex has also been reported to bind its own N-terminal LAP in addition to other molecules modulating Mstn activity *in vitro*. These include, decorin, LTBP3, follistatin, follistatin-related gene (FLRG, follistatin like 3 or follistatin related peptide) and GDF-associated serum protein-1 (Thies, Chen et al. 2001; Haidet, Rizo et al. 2008; Kishioka, Thomas et al. 2008; Elkina, von Haehling et al. 2011).

1.1.7.4 Canonical signalling of Mstn

The magnitude of the hyper-muscular phenotype observed in Mstn null animals has led to numerous studies aimed at delineating the mechanism underlying this phenomenon. Canonical TGF-β signalling involves binding of the mature dimer to the type II receptor, then recruitment of a type one receptor to form the active receptor complex. Similarly, the mature Mstn dimer binds activin receptor type IIB (ACTRIIB), then recruits either Alk4 or 5 (the type I TGF-β receptors), both of which are serine/threonine kinases. The active receptor complex then phosphorylates Smad2 or 3 proteins which bind to a common Smad or co-Smad (Smad4), which shuttles the complex into the nucleus. In the nucleus, Smad2/3 interact with binding partners to regulate Smad-dependant gene transcription, while Smad4 is shuttled back to the cytoplasm to continue the cycle (Jayaraman and Massague 2000; Lee and McPherron 2001). In addition, the Smad proteins also bind to a growing list of other transcription factors. These include key regulators such as MyoD and MEF2 (Liu, Black et al. 2001; Quinn, Yang et al. 2001) (see 1.1.5.1). More recent studies have identified a role for the Smad proteins in regulating miRNA expression (Blahna and Hata 2012), which provides an additional mechanism for Smad-dependent gene regulation. A role for canonical Mstn signalling in the inhibition of myogenic differentiation has been described. Early reports identified the down regulation of the myogenic regulatory factors MyoD and Myf5 as having a major role. The proposed mechanism suggested that increased Smad3 phosphorylation and thus Smad3:MyoD,

complex, in the presence of Mstn was responsible (Langley, Thomas et al. 2002). In support, a later study reported Smad3 could associate with and repress the activity of MyoD (Liu, Black et al. 2001).

In vivo studies have demonstrated that Mstn regulates protein synthesis. Specifically, mice treated with antibodies to antagonise Mstn have increased phosphorylation of p70S6K and rpS6, suggesting increased protein synthesis following blockade of Mstn (Welle, Burgess et al. 2009). In addition, Mstn has been shown to inhibit the differentiation of human myoblasts via inhibition of the PI3K/AKT pathway. These studies demonstrated that reduced phosphorylation of AKT and the inhibition of differentiation required the activity of Smad2/3. Of interest, the reduction in the phosphorylation of AKT was reversed following the addition of IGF-1 via stimulation of the PI3K/AKT signalling pathway, without a change in the Mstn induced phosphorylation of Smad2/3. The authors suggested that IGF-1 signalling predominates over that of Mstn (Trendelenburg, Meyer et al. 2009). In support, Morissette et al reported that adenoviral over-expression of Mstn in C_2C_{12} myoblasts attenuates the IGF-1 induced phosphorylation of AKT (Morissette, Cook et al. 2009). These data suggest that there is a delicate balance between the stimulatory and inhibitory signals, with the phenotype reflecting the dominant signal.

1.1.7.5 Non-Smad signalling pathways

In addition to canonical signalling through Smad-dependant pathways, other signal transduction cascades have also been shown to play a role in the function of Mstn. These pathways are referred to as non-canonical pathways, the majority of which have been shown to work in conjunction with canonical signalling (Philip, Lu et al. 2005; Yang, Chen et al. 2006). Mstn inhibits the proliferation of myoblasts through induction of p21 (McFarlane 2003). The induction of p21 is coupled with a decrease in the activity of CDK2, which results in the accumulation of hypophosphorylated Rb, which blocks the transition from G1 to S phase (Thomas, Langley et al. 2000). In support, Seoane et al observed that Foxo and Smad signalling induces the expression of p21 in HaCat (human keratinocyte) cells (Seoane, Le et al. 2004), while Phillip et al (2005) proposed a Smad-independent activation of the p38 MAPK signalling cascade through the TGF-β activated kinase (TAK1), in conjunction with canonical signalling is

responsible for the reduced rate of proliferation (Philip, Lu et al. 2005). In addition, TAK1 activation by Mstn has been reported to stimulate IL-6 production in C_2C_{12} myoblasts (Zhang, Rajan et al. 2011).

Mstn induces the phosphorylation of ERK1 and 2, which, with p38 constitutes another branch of MAPK signalling (Yang, Chen et al. 2006). The events leading to the Mstn-induced phosphorylation of ERK require the activation of Ras (Yang, Chen et al. 2006). However, the subsequent steps are not yet known. It is likely that this cascade is similar to that observed for the FGF-induced activation of ERK through the Ras/Raf/MEK pathway (see 1.1.6.1). Interestingly, pharmacological inhibition of type 1 TGF-β receptors has been reported to prevent the activation of ERK1/2 by Mstn (Yang, Chen et al. 2006). Recent studies have highlighted a role for Mstn regulating the activity of the AMP-activated protein kinase has been described. Zhang *et al* propose that Mstn plays a role in the regulation of insulin signalling, through the regulation of AMPK activity in adipose and muscle tissue (Zhang, McFarlane et al. 2011). Figure 1.3 gives an overview of the signal transduction associated with the function of Mstn.

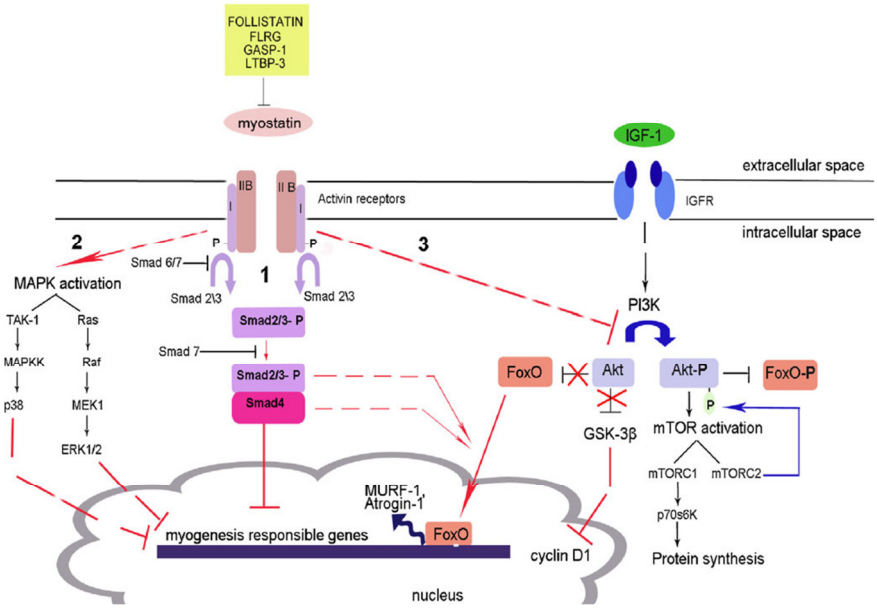

Figure 1.5: Overview of Mstn signalling. This figure shows the canonical (ACTRIIB binding and Smad activation) and non-conical (MAPK and PI3K/AKT/mTOR) branches of Mstn signalling. Arrows indicate activation, bars indicate an inhibition and dashed lines represent missing or unknown intermediate steps, source (Elkina, von Haehling et al. 2011).

1.1.7.6 Mstn and metabolism

Disruption of the Mstn gene causes phenotypic changes that support a role for Mstn in regulating metabolism. The shift in specific types of muscle fibres (increased glycolytic fibre content) and the reduction in the mass of fat observed in Mstn null animals (Shahin and Berg 1985; Lin, Arnold et al. 2002; McPherron and Lee 2002; Girgenrath, Song et al. 2005; Elashry, Otto et al. 2009; McPherron, Huynh et al. 2009; Wilkes, Lloyd et al. 2009; Matsakas, Mouisel et al. 2010), suggests that Mstn regulates metabolism in skeletal muscle. In support, treatment of WT myoblasts with Mstn maintains the expression of type I MHC (oxidative muscle), while down-regulating the expression of type II MHC (glycolytic muscle) (Wang, Yu et al. 2012). Interestingly, post-natal inhibition of Mstn regulates the hypertrophy of skeletal muscle fibres and not hyperplasia, suggesting that the hyperplasia that is associated with Mstn deficiency occurs before the neonatal period (Zhu, Hadhazy et al. 2000; Grobet, Pirottin et al. 2003; Whittemore, Song et al. 2003; Lee, Reed et al. 2005; Tang, Yan et al. 2007; Welle, Bhatt et al. 2007; Haidet, Rizo et al. 2008; Matsakas, Foster et al. 2009; Morine, Bish et al. 2010). Mstn is strongly implicated in the regulation of protein synthesis, Mstn null mice have an increased rate of synthesis of myofibrillar proteins (Welle, Bhatt et al. 2006), as do C_2C_{12} cells treated with antibodies or follistatin to block Mstn (Suryawan, Frank et al. 2006; Welle, Burgess et al. 2009).

The reduced mass of fat in Mstn null mice is accompanied by lower concentrations of circulating cholesterol, leptin and triglycerides as well as the content of triglycerides in the liver. This endocrine profile is consistent with increased insulin sensitivity and a reduced risk of insulin resistance (McPherron and Lee 2002; Guo, Jou et al. 2009). Beneficial effects of Mstn inactivation have been observed in murine models of obesity. In these studies, Mstn null animals were crossed with Agouti lethal yellow (A^y/a) or *ob/ob* mice, which reduced the mass of the fat pads, improved glucose tolerance (A^y/a) and reduced hyperglycaemia (*ob/ob*) (McPherron and Lee 2002). Resistance to the consequences of a high fat diet is a well-established feature of Mstn null mice. They have improved glucose tolerance and insulin sensitivity and show reduced

serum insulin, cholesterol, leptin and triglycerides compared to wild-type mice on the same high fat diet (McPherron 2010).

A number of studies have reported an increased sensitivity to insulin in Mstn null mice. Mstn null mice have increased glucose uptake in response to insulin and increased phosphorylation of AKT and IRS-1 in muscle and fat tissue in response to insulin (Shahin and Berg 1985; McPherron and Lee 2002; Guo, Jou et al. 2009; Wilkes, Lloyd et al. 2009). In addition, Mstn null mice fed a high fat diet from weaning have increased growth of skeletal muscle compared with null mice on a standard diet (Yang and Zhao 2006; Wilkes, Lloyd et al. 2009). These changes in the composition of both muscle and fat in Mstn null animals has made Mstn an attractive therapeutic target for a number of disorders, especially those involving muscle wasting and metabolic disorders such as obesity or diabetes.

More recently a role for Mstn in regulating the activity of the AMP-activated protein kinase has been described. AMPK responds to alterations in the ratio of AMP/ATP, which is considered a metabolic switch. Activated AMPK has been shown inhibit non-essential ATP-consuming processes such as, glycogen, fatty acid and protein synthesis, to conserve ATP, while promoting ATP production through the increased activation of catabolic processes. Thus, AMPK supports processes such as glucose transport, glycolysis and fatty acid oxidation (Hardie, Ross et al. 2012). Zhang *et al* propose that Mstn plays a role in the regulation of insulin signalling via regulating the activity of AMPK in muscle and fat (Zhang, McFarlane et al. 2011). However, the ability of Mstn to regulate AMPK activity is somewhat controversial as two independent studies have reported conflicting results on the activation status of AMPK and its downstream target ACC (Chen, Ye et al. 2010; Zhang, McFarlane et al. 2011). Specifically, both of these studies presented data on the phosphorylation AMPKα and its downstream target Acetyl-CoA carboxylase (ACC) in WT and Mstn null gastrocnemius muscle. Chen et al, show reduced AMPKα^{Thr172} and ACC^{Ser79} phosphorylation in the gastrocnemius of 15 week old female Mstn null mice on a standard diet (Chen, Ye et al. 2010). In contrast, Zhang et al show increased AMPKα (phosphorylation epitope not specified) and ACC^{Ser79} in 19 week old male Mstn null mice (Zhang, McFarlane et al. 2011). Thus, it seems that Mstn influences the activity of AMPK and its downstream target ACC, but, given what

looks to be differential regulation between male and female animals, the effect of Mstn on AMPK activity is not well understood.

1.2 Intermediary metabolism

This thesis will investigate the role of Mstn signalling in ovine myoblasts. Given the significant role that Mstn plays in metabolism, this section on ruminant and general intermediary metabolism has been included. The reactions constituting intermediary metabolism are similar in ruminants compared with monogastrics. However, they are partitioned quite differently between these two types of digestive physiologies. This is primarily due to the forage diet of ruminants and differences in the primary metabolites produced to fuel whole body metabolism. The major substrate for glucose production in ruminants is propionate, which provides up to 50% of glucose production through gluconeogenesis (Brockman RP 1986). Ruminants on a normal diet absorb very small amounts of carbohydrates, which is largely due to the fermentation of dietary carbohydrate in the rumen to short chain fatty acids, with the main fermentation products being acetate, propionate and butyrate (Brockman RP 1986). In essence, the primary function of metabolic regulation is to provide a constant concentration of glucose in the blood. For example, the brain relies almost exclusively on glucose for metabolic energy (Pappenheimer and Setchell 1973). Thus, gluconeogenesis is essential to maintain concentrations of glucose, a major consequence of this in ruminants being a net output of glucose from the liver. The major substrate of lipid metabolism differs in ruminant animals, with acetate, not glucose providing the major precursor for acetyl-CoA, which is required for the synthesis of fatty acids. In fact, the contribution of glucose to lipogenesis in ruminant mammary gland and liver is greatly reduced compared to that of the rat (Balmain, Folley et al. 1953; Hanson and Ballard 1967), with later studies showing this applies to all ruminant tissues (Ballard, Hanson et al. 1969). The reason for this difference is suggested to be a low activity of ATP-citrate lyase in ruminant tissues (Ballard, Hanson et al. 1969).

The major processes contributing to the dynamics of skeletal muscle metabolism revolve around the provision of mobility and the maintenance of what constitutes the largest store of mobile protein in the animal, with the activity of specific reactions controlling these differing between species and in an individual

depending on physiological state. In sheep held in confined laboratory conditions, skeletal muscle is reported to consume 8-19% of whole body energy requirements as measured by O_2 consumption (Lobley 1990). Broken down further, the major energy consuming processes in muscle are: posture and activity, protein turnover, ion transport, and substrate cycles. The specific contribution of these components is regulated by a number of physiological processes with age, nutrition, activity and hormonal regulation all playing a significant role (Lobley 1990). An example of the how O_2 consumption is partitioned in skeletal muscle is given in Figure 1.6, showing the contribution of specific processes to the energy expenditure in the muscle of the hind limb of lambs fed a maintenance diet.

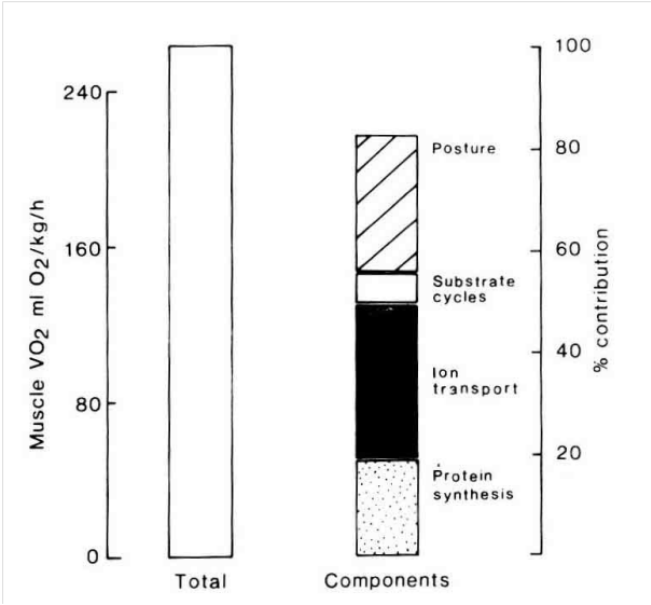

Figure 1.6**: Energy expenditure in the hind-limb of sheep.** The figure shows the relative contribution of the specific metabolic processes to energy (oxygen) consumption in the hindlimb of 35kg lambs fed a maintenance diet. Figure from (Lobley 1990).

In skeletal muscle, all energy required for cellular function is provided by the hydrolysis of ATP to ADP. When contractile activity is induced, the demand for energy in skeletal muscle is greatly increased. To counter the huge fluctuations in energy requirements, the fibres of skeletal muscle require fast and efficient methods of re-synthesising ATP. This is accomplished through three main mechanisms: creatine kinase activity, glycolysis and mitochondrial oxidative phosphorylation, with small amounts of ATP also generated by adenylate-kinase, which converts two ADP molecules to ATP and AMP (Schiaffino and Reggiani 2011).

1.2.1 Creatine kinase

Creatine kinase regenerates ATP using creatine as a high energy phosphate reserve. At rest, skeletal muscle produces an excess of ATP. This excess ATP is transferred to creatine to generate creatine phosphate. Although this system is extremely efficient at regenerating ATP, during sustained contraction it is rapidly exhausted within 20 s (Martini 2001; Schiaffino and Reggiani 2011).

Therefore, skeletal muscle must rely on other means of generating energy following the depletion of creatine phosphate reserves

1.2.2 Glycolysis

Glycolysis defines the intermediary metabolism reactions involved in ATP generation from glycogen or glucose to form lactate or pyruvate. This system is not as powerful as the creatine kinase system, but has a higher capacity for the generation of ATP. Glucose for fuelling glycolysis in skeletal muscle can be derived from multiple sources, which include the breakdown of glycogen reserves, active transport of circulating glucose and glucogenic amino acids. The major steps in glycolysis are illustrated in Figure 1.7, with pyruvate being the major end product. The metabolism of glucose to pyruvate generates a net yield of 2ATP per glucose molecule processed. The pyruvate derived from glycolysis has a number of intracellular fates; it can be reversibly converted to lactate (via lactate dehydrogenase), irreversibly converted to acetyl-CoA (pyruvate dehydrogenase) or used for gluconeogenesis to synthesise glucose for the repletion of glycogen reserves. Similarly, lactate shares a number of fates. Lactate can be converted back to pyruvate or secreted. Secretion of lactate from skeletal muscle is fibre-type dependant, wherein fast glycolytic fibres secrete more lactate than slow oxidative fibres. Secreted lactate is utilised by slow muscle fibres (cell-to-cell lactate shuttle hypothesis) or circulated to be processed back to glucose by the liver (the Cori cycle) (Martini 2001; Schiaffino and Reggiani 2011).

1.2.3 Mitochondrial metabolism.

Mitochondria further process acetyl-CoA produced from either glycolysis or the β-oxidation of fatty acids through the citric acid (TCA) cycle. Intermediate metabolites that fuel the TCA cycle are derived from multiple sources (e.g pyruvate, fatty acids and ketone bodies and amino acids) and these can enter the TCA cycle at a multiple number of entry points. The reactions and intermediates of the TCA cycle provide the basis of cellular respiration. Although only one net ATP molecule is generated per turn of the TCA cycle, the reducing power (in the form of H^+) generated by the reactions provides the major source of mitochondrial ATP production. The organic substrates of the TCA cycle reduce the co-enzymes NAD^+ and FAD to NADH and $FADH_2$, which provide the driving force for oxidative phosphorylation. In the inner mitochondrial membrane, NADH and

$FADH_2$ transfer their hydrogen atoms to other co-enzymes, such as flavin mononucleotide and co-enzyme Q. This results in the release of protons into the inter-membrane space of the mitochondria as the electrons are shuttled sequentially from coenzymes to the cytochromes of the electron transport chain. The sequential flow of electrons through the co-enzymes and cytochromes is stopped following terminal electron acception by oxygen and generation of H_2O. The gradient of H^+ generates or regenerates ATP as H^+ re-enter through the hydrogen ion channels in the inner mitochondrial membrane. Each pair of electrons removed from the TCA cycle by NAD^+ and FAD generate 3 and 2 molecules of ATP, respectively. Oxidative Phosphorylation is the least powerful method for the production of ATP, but has the highest generation capacity (Martini 2001; Schiaffino and Reggiani 2011).

1.2.4 Regulation of intermediary metabolism in skeletal muscle

The metabolic reactions that generate ATP in skeletal muscle are subject to control through physiological and endocrine mechanisms. Much of this control is imposed by regulating the abundance and/or the activity of key metabolic enzymes. The concentration of metabolites such as glucose, triglycerides, free fatty acids, as well as their metabolic intermediates also play a significant role in the control of metabolic activity in skeletal muscle. The flux of metabolities and their intermediates is altered in a fibre-type dependant manner, as illustrated in Figure 1.7, with type 1 fibres being more reliant on oxidative metabolism for the generation of energy. This is also reflected in the expression of both the metabolic enzymes and the different substrate transport proteins that provide a bias toward oxidative rather than glycolytic fuel. Situations that place skeletal muscle under stress, such as sustained contraction, infection, heat shock or starvation can profoundly alter metabolism (Bonaldo and Sandri 2013; Rhoads, Baumgard et al. 2013). Prolonged stress can also have detrimental consequences, because once the reserves of muscle glycogen are depleted, catabolic processes are activated to support the increased demand for energy. In skeletal muscle, this can cause a prolonged use of cellular protein as an energy source, which ultimately results in the atrophy of skeletal muscle (Bonaldo and Sandri 2013).

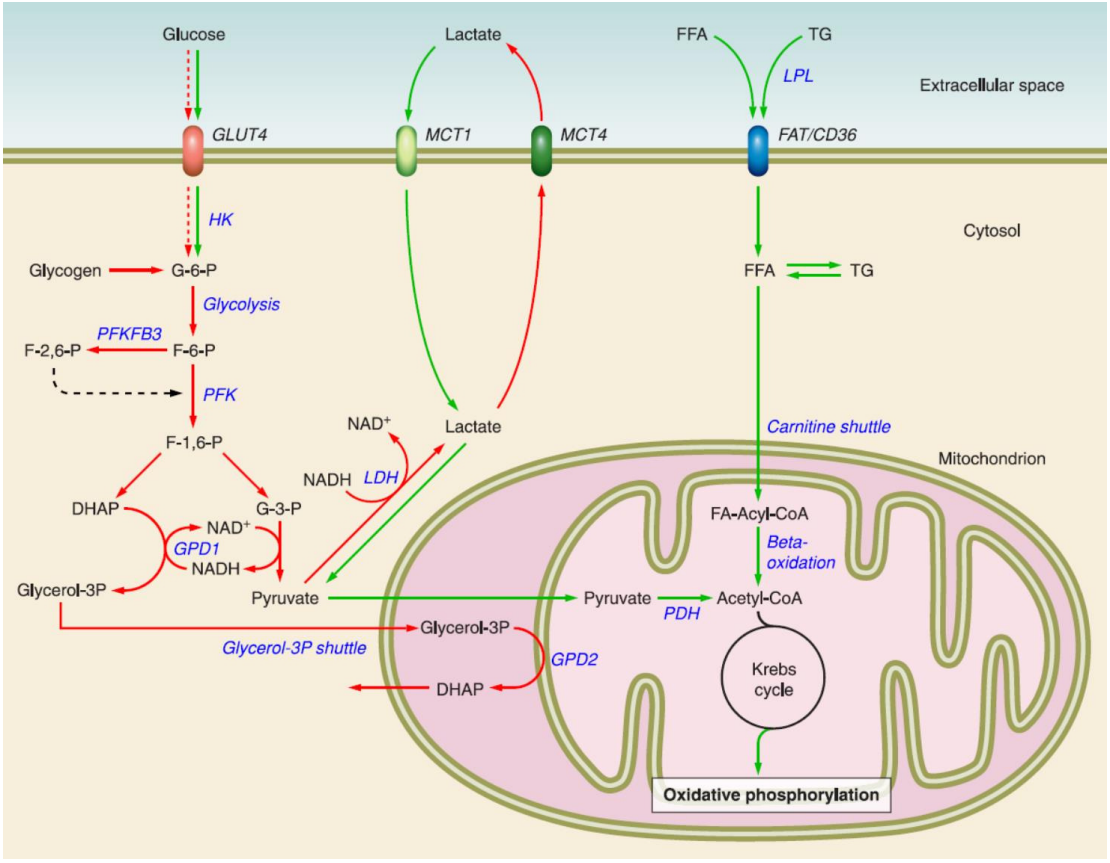

Figure 1.7: Intermediary Metabolism and fibre-type influences. Illustrating some of the key reactions and enzymes in the intermediary metabolism of skeletal muscle and how they are biased in different fibre types. The predominant pathways in slow or fast skeletal fibres are shown as green or red arrows, respectively. DHAP, dihydroxyacetone phosphate; GLUT4, glucose transporter 4; F-6-P, fructose-6-phosphate; FAT/CD36, fatty acid translocase; FFA, free fatty acids; F-1,6-P, fructose-1,6-bisphosphate; F-2,6-P, fructose-2,6-bisphosphate; G-3-P, glyceraldehyde-3-phosphate; G-6-P, glucose-6-phosphate; GPD1, glycerolphosphate dehydrogenase 1 (cytoplasmic); GPD2, glycerolphosphate dehydrogenase 2 (mitochondrial); HK, hexokinase; LDH, lactate dehydrogenase; MCT1, monocarboxilic acid transporter 1; MCT4, monocarboxylic acid transporter 4; PDH, pyruvate dehydrogenase; PFK, phosphofructokinase; PFKFB3, phosphofructokinasefructose bisphosphatase 3; TG, triglycerides. Figure from (Schiaffino and Reggiani 2011).

Hormonal changes and cytokine production can influence the metabolism of skeletal muscle. For example, insulin plays a major role in the uptake of glucose, glycogen synthesis and the regulation of protein synthesis (Jameson and DeGroot 2010). Skeletal muscle itself can function as an endocrine organ secreting 'myokines' that have the potential to influence whole body metabolism, with the post-exercise secretion of IL-6 providing a good example (Pedersen, Akerstrom et al. 2007). A more recent study identified 48 'myokines' whose secretion is regulated by contractile activity (Raschke, Eckardt et al. 2013). Interestingly this list included: Furin (the protease that cleaves full length Mstn (Anderson, Goldberg et al. 2008)), IGF binding protein 1 (modulator of IGF and insulin activity (Ruan and Lai 2010)), TGFβ1, FGFs (see 1.1.6.1) and interlukin family members, all of which have the potential to regulate skeletal muscle metabolism.

1.2.5 Signal transduction and metabolism

There are multiple signal transduction pathways involved in regulating the metabolism of skeletal muscle. The processes controlled by these pathways can regulate all aspects of glucose, lipid and protein metabolism. The signalling networks that are implicated in the regulation of skeletal muscle metabolism include PI3K/AKT/mTOR (protein synthesis and glucose metabolism), MAPK (glucose, protein and lipid metabolism) and the Ca^{2+} (muscle fibre-type specific) signalling pathways. The metabolic control that is imposed by these pathways is mediated through the activity of downstream signalling hubs, with AMPK and mTOR representing two major hubs that orchestrate the metabolic change in skeletal muscle. These two pathways act as 'energy sensing' mechanisms in skeletal muscle and other tissues, responding to physiological or endocrine signals to effect metabolic change.

AMPK is a heterotrimeric complex of α, β and γ subunits. In skeletal muscle activation of AMPK by a decreased AMP:ATP ratio or secreted factors such as IL6 (Kelly, Gauthier et al. 2009; Hardie, Ross et al. 2012). Activation of AMPK is a two-step process, firstly, binding of AMP to the γ-subunit induces a conformational change in the AMPK complex, and this allows upstream kinases to phosphorylate the α-subunit at threonine 172 to activate the complex. AMPK inhibits non-essential energy consuming processes such as protein and lipid

synthesis, to support the generation of ATP through increased catabolic processes (Hardie, Ross et al. 2012). For example, AMPK phosphorylates and inactivates acetyl-CoA carboxylase (ACC), an enzyme responsible for the conversion of acetyl-CoA to malonyl-CoA. Malonyl-CoA inhibits carnatine pamitoyltransferase, which transports fatty acids to the mitochondria, thus, providing a mechanism for increased fatty acid oxidation following the activation of AMPK (Ouchi, Shibata et al. 2005).

The mTOR hub revolves around the serine/threonine kinase activity of two distinct mTOR complexes TORC1 and TORC2 (Cornu, Albert et al. 2013). Like AMPK, mTOR signalling plays a major role in metabolism, this pathway can regulate cell growth and metabolism in response to cellular nutrient, oxygen and energy levels. The activity of mTOR is stimulated by a number of growth factors, including insulin and IGF-1 (Harris, Chi et al. 2006; Vary 2006). In addition, activation of AMPK has been shown to inhibit mTOR activity (Ning and Clemmons 2010). The regulation of mTOR activity plays a critical role in a number of the metabolic processes in skeletal muscle, with a good example being the ability of mTOR to directly influence the translational control of protein synthesis. This is achieved, in part, through modulation of the activity of 4EBP1 (Magnuson, Ekim et al. 2012). Thus the AMPK and mTOR complexes represent two critical control points in the signal transduction mediated changes of metabolism in skeletal muscle.

1.3 Mstn splice variant (MSV)

Mstn (see section 1.2) plays a significant role in regulating the mass of skeletal muscle mass. The expression of Mstn has been reported to be present in invertebrate species such as scallops, sea urchins and amphioxus, suggesting that Mstn in mammals arose from a common ancestral gene ~900 million years ago. The alternate splicing of the Mstn gene has been reported in bony fishes, and unpublished data from our laboratory has identified a cryptic intron in the third exon, which results in the generation of MSV in the Cetartiodactyl clade of mammals (Figure 1.6), including cattle, sheep, dolphins, pigs and alpaca. To date, the presence of MSV mRNA has been confirmed in cattle and sheep of different gestational and postnatal ages. The deduced polypeptide sequence of MSV contains an N-terminal domain of 256 amino acids, identical to that of Mstn and a

unique 65 amino acid C-terminal domain. This sequence is present in all organisms in the Cetartiodactyl clade, with the exception of alpacas, wherein the deletion of a single nucleotide in the C-terminal coding sequence codes for a premature stop codon (Jeanplong, Falconer et al. 2013).

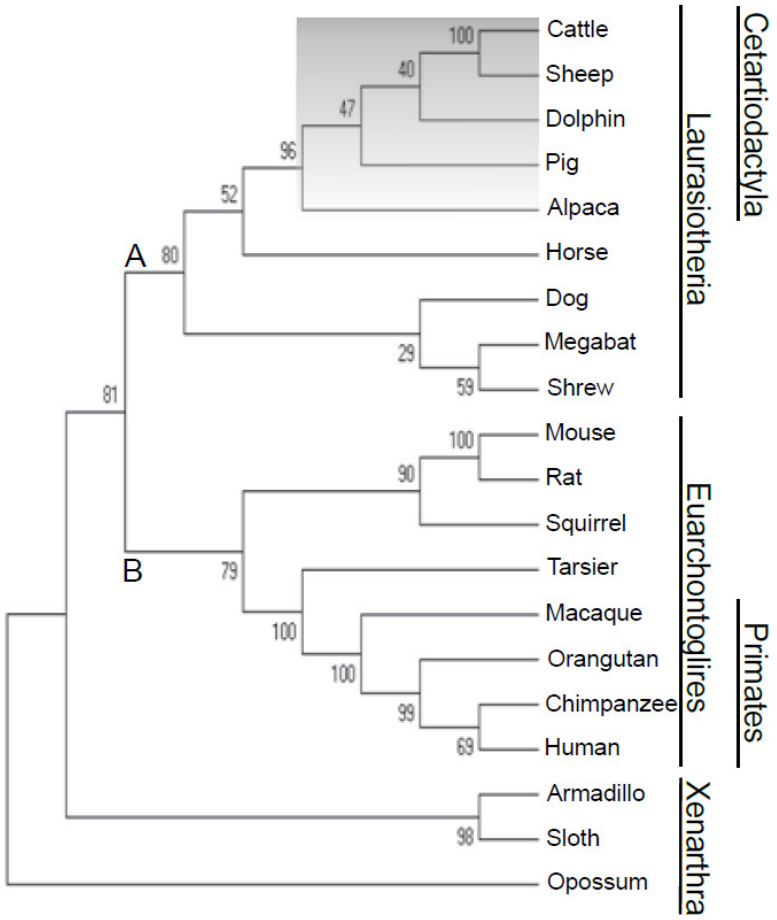

Figure 1.8: The Evolution of MSV. A phylogenetic topology plot showing the bootstrap consensus tree for a 1500 bp length of Mstn sequence from the start of exon 3 for a number of mammalian species (obtained from ensemble, www.ensembl.org). Numbers above each branch indicate the percent confidence for each division. Incomplete splicing motifs (dogs, shrews, rat), or indels (horses, megabats, mice) either change the ORF (megabats), or introduce premature stop codons (horses, mice). The gradient of shading reflects the postulate that MSV splicing became progressively fixed in the Cetartiodactyl clade (A), but may be present in primates (B), although efforts have failed to detect MSV in human tissue and it is not present in other species. Taken from (Jeanplong, Falconer et al. 2013).

Included in the C-terminal region of MSV is a consensus cleavage site for precursor convertases, suggesting that as with other TGF-β family members, MSV is cleaved to liberate a 47 amino acid c-terminal region. An in-silico analysis of the secondary structure of the C-terminal region of MSV suggests that this region forms two putative alpha-helices in sheep, cattle, dolphin and pig, but not in primates where a single alpha-helix is predicted. The function of MSV has been investigated, using a recombinant protein for the 47 amino acid c-terminal region produced in *E. coli*. This preparation induces the proliferation of C_2C_{12}, Belgian Blue (double-muscled cattle) and ovine myoblasts *in vitro*. In support, ovine myoblasts treated with MSV were shown to have an increased number of cells in S-phase, with an increased nuclear abundance of CDK2 and cyclin E, critical regulators of the G1-S transition of the cell cycle (see 1.1.5.2). Treatment of ovine myoblasts with MSV has also been shown to increase the expression of Myf5 transcript, which is consistent with the increased rate of proliferation. Furthermore, the expression of myogenin transcript is decreased, which indicates an inhibition of or delayed differentiation. Biacore analysis performed using MSV, demonstrated that MSV binds to both mature Mstn and its canonical receptor ACTRIIB with apparent high affinity with K_d values of 9.79×10^{-11} and 3.18×10^{-9}, respectively (Jeanplong, Falconer et al. 2013). Expression of MSV mRNA in foetal muscles from Belgian blue (double-muscled) and Friesian (wild-type) cattle at different gestational ages showed increased concentrations in the developing Belgian Blue foetus. Interestingly, the Mstn mutation in Belgian Blue cattle (an 11 base pair deletion in exon 3) is contained in the cryptic intron 3 sequence of the cattle Mstn gene, thus the alternate splicing of the sequence of MSV would not be affected. Despite the binding of MSV to both Mstn and its canonical receptor ACTRIIB, this binding does not appear to be able to directly antagonise Mstn function, because MSV could not repress the Smad dependant luciferase reporter activity induced by Mstn, suggesting that Mstn can still activate ACTRIIB in the presence of MSV. However, this does not rule out antagonism of Mstn *in vivo* by the N-terminal region of MSV, which contains almost the entire canonical LAP sequence of Mstn, which as mentioned earlier, has been previously shown to antagonise the function of mature Mstn (Thies, Chen et al. 2001). The inability of MSV to antagonise Mstn, coupled with its ability to increase the proliferation of myoblasts, strongly suggests that MSV may

signal through an alternate, as yet unidentified signalling cascade. Thus MSV appears to be a splice variant of Mstn, specific to the Cetartiodactyl clade of mammals. MSV can interact with Mstn and its receptor and in so doing may modulate activity of Mstn, via acting as an intra-genic regulator of the Mstn gene.

1.4 Scope and Aims

The scope of this thesis is to build on the previous work investigating the function of MSV. Previous studies suggested that MSV could play a role in the growth of skeletal muscle, especially in livestock species given that they are in the Cetartiodactyl clade (Jeanplong, Falconer et al. 2013). Thus, understanding the mechanisms associated with MSV function and how they compare to those associated with Mstn, could prove useful in identifying elite animals for the meat industry. In addition, one aspect of the biology of Mstn that had not been addressed in the context of MSV is a potential role in skeletal muscle metabolism.

Given the *in vitro* nature of these studies, the use of appropriate culture models was major consideration. Firstly, established protocols for isolating myoblasts (satellite cells) from sheep muscle, a tissue that contains endogenous MSV (Jeanplong, Falconer et al. 2013), provided an ideal model for investigating the signalling, gene expression and metabolic changes induced following the treatment of cultures with MSV. In addition, these could be compared to in parallel, with cultures treated with Mstn. Secondly, multiple studies have used C_2C_{12} myoblasts that stably over-express proteins to investigate the function of target genes. Although they do not express endogenous MSV like ovine myoblasts, C_2C_{12} myoblasts have been shown to respond to MSV treatment. Unlike primary cultures, C_2C_{12} myoblasts have the added advantage that they can be maintained in proliferation for multiple passages and differentiated for more than two weeks, allowing investigations that cannot be performed using the more transient primary cultures. Thus, stable cell lines were generated to provide an additional model for investigating the function of MSV. This was done with the aim of further validating the changes observed in the ovine myoblast studies. These investigations were carried out to test the hypothesis that: MSV signals independently of Mstn to regulate myogenesis, and the intermediary metabolism of myoblasts. Furthermore, the studies performed on C_2C_{12} myoblasts expressing MSV allowed initial testing of the hypothesis that, forced expression of MSV

influences myogenesis, intermediary metabolism and the abundance and/or phosphorylation of key molecules involved in the control of these processes. The aims of this thesis were to:

1. Identify the early signal transduction (1 hr post treatment) and transcriptional expression changes (6 hr post treatment) associated with recombinant Mstn and MSV treatment in ovine myoblasts.
2. Determine if MSV has a role in the intermediary metabolism of myoblasts.
3. Identify the signal transduction cascades involved in MSV function and how these diverge from those regulated by Mstn.

.

Chapter Two

2 Materials and Methods

2.1 Materials

Common laboratory chemicals and reagents were procured from BDH (Radnor, PA, United States of America), Roche (Basel, Switzerland), Sigma-Aldrich (St. Louis, MO, United States of America), BioRad (Hercules, CA, United States of America), Thermo Fisher Scientific (Waltham, MA, United States of America) and Life Technologies (Carlsbad, CA, United States of America). For specialised equipment and commercially available kits, the details are provided in the relevant Methods sections.

2.1.1 Enzymes

Enzymes were obtained from Roche, Life Technologies and Promega (Madison, WI, United States of America) as out lined in the relevant Methods sections.

2.1.2 DNA Plasmids and glycerol stocks

DNA plasmids used for these studies were the pET101D/-TOPO (Life Technologies), pcDNA3 (Life Technologies) and pGEM-T-easy (Promega) vectors. Glycerol stocks of transformed DH5α *E. coli* (Life Technologies) cells, were produced by diluting cultures in LB broth (Lennox Broth; Life Technologies) with 1:1 glycerol (BDH) before storage at -80°C. Plasmid DNA was isolated from stable transformants using either Quiagen mini- or maxi-prep plasmid isolation kits (Quiagen, Venlo, Limburg, Netherlands), according to manufacturer's instructions. Plasmid DNA isolated from bacterial transformants was re-suspended in H_2O and stored at -20°C.

2.1.3 Oligonucleotides (primers)

Oligonucleotides used in these studies were obtained from Life Technologies and Custom Science Ltd (New Zealand). Sequences of primers and the experiments they were utilised for, are listed in Table 2.1. All oligonucleotides were resuspended in 100 µL MQ H_20, with 1 µM and 10 µM primer stock solutions prepared from these parent solutions, all primer stocks were stored at -20°C. The design of specific primers for gene amplicons was performed using

Vector NTI (Life Technologies) software, to align RNA sequences from sheep and mouse, with primer design performed using Primer 3 software (Rozen and Skaletsky 2000).

Gene	Sense/Antisence	Sequence	Amplicon size (bp)
BHLH40	S	CAACTTTGGGTCACTTGGAA	188
	AS	TGTCTGGAAACCTGAGCAGA	
Ccl2	S	ACATGAAGTTCTCCGCTGCT	188
	AS	AGCTTCTTTGGGACACTTGC	
Ccl20	S	TGTCAGTGCTCTTGCTCCAC	211
	AS	GCTTGCTTCACCCACTTCTT	
CEBPα	S	GGCAACGACTTTGACTACCC	208
	AS	CTGCTTCGCTTCGTCCTC	
CTNND2	S	AAACCACCTCTGCCATCCTT	190
	AS	CCATCTTGTGATTGCCAGTG	
LDLRAD4	S	CTGGGTTCCCTGGTCTGTAA	202
	AS	GGGTGGATGCTCTGTAGTGG	
FGFR4	S	AGAGCAGCAGGAAGGAGATG	190
	AS	CCACAGCATAACCGCACA	
IL1A	S	CCTGGATACCTCGGAAACCT	183
	AS	GCTGATCTGGGCTTGATGAT	
IL6	S	TGGTGATGACTTCTGCTTTCC	189
	AS	GCCAGTGTCTCCTTGCTGTT	
OSR2	S	GCGTGGAATCAATGACCTTT	165
	AS	AGGACTCAGAAGCGGATGG	
PTX3	S	AACGTCGTCTCTCCAGCAAT	207
	AS	CAGCATGGTGAAGAGCTTGT	
ATP1B1	S	CTGGAACTCGGAGAAGAAGG	171
	AS	GCCACTCGGTCCTGATATGT	
p53	S	GCAACTACGGTTTCCGTCTC	195
	AS	TCATGTGCTCCAGCTTCTTG	
PDK3	S	ATGTGCCCTCACACCTCTTT	232
	AS	GCTAGGTCTCGGAGCAGTTG	

Table 2.1: Oligonucleotides used for qPCR analysis. Sequences for sense (S) and anti-sense (AS) oligonucleotides used for qPCR analysis. Sequences are shown in 5' to 3' orientation. Sequences were designed to amplify ovine target sequence, with the exception of ATP1B1 where a region that was conserved between mouse and ovine models was utilised for primer design.

2.1.4 Antibodies

Antibodies used for western blot analysis were purchased from multiple sources, the antibody catalogue number and the dilution used for western blot are outlined in brackets, with antibodies detecting phosphorylated protein denoted

(P-) and the phosphorylation epitope outlined in superscript where applicable. Antibodies were purchased from:

1. Developmental Studies Hybridoma Bank (DSHB, Iowa, United States of America): Pax7 monoclonal antibody.

2. Cell Signalling Technology (Danvers, MA, United States of America): Acetyl CoA Carboxylase (cs-3676, 1:2000), P-Acetyl CoA Carboxylase^{Ser79} (cs-3661, 1:3000), 4EBP-P$^{Thr37/46}$ (1:1000), rpS6 (cs-2217, 1:100000), P-rpS6$^{Ser\ 235/236}$ (cs-2211, 1:5000), p38 MAPK (cs-9212, 1:2000), P-p38 MAPK$^{Thr180/Tyr182}$ (cs-9211, 1:1000), CyclinE (cs-4132, 1:2000), PDK1 (cs-9211, 1:10000), P-PDK1^{Ser241} (cs-3061, 1:10000), P-Akt^{Ser473} (cs-4058, 1:1000), AMPK (cs-2532, 1:30000), P-AMPK^{Thr172} (cs-2535, 1:20000), p70s6K (cs-9027, 1:2000), P-p70s6K^{Thr389} (cs-9234s, 1:1000), with all antibodies derived from rabbit hosts.

3. Santa Cruz Biotechnology, Inc (Dallas, TX, United States of America): Myf-5 (sc-302, 1:3000), CDK2 (sc-163, 1:20000), Myogenin (sc-576, 1:10000), 4EBP1 (sc-6936, 1:2000), MRF4 (sc-784, 1:3000), P-AKT^{Thr308} (sc-16646, 1:30000), Smad2/3 (sc-6032, 1:3000), P-Smad2/3$^{Ser\ 423/425}$ (sc-11769, 1:10000), Mef2 (sc-313, 1:20000), ERK1/2 (sc-94, 1:50000), P-ERK1/2$^{Thr\ 202/204}$ (sc-16982, 1:10000), MyoD (sc-304, 1:3000), AKT (sc-8312, 1:10000), with the antibodies derived from rabbit hosts with the exception of Smad2/3 (Goat).

4. Dako (Glostrup, Denmark): Goat anti mouse-HRP (P0447, 1:5000), Goat anti-rabbit-HRP (P0448, 1:5000) and Rabbit anti-goat (P0160, 1:5000).

Antibodies utilised for other applications are outlined in the relevant method sections.

2.1.5 Mammalian cell lines

Mammalian cell lines used for this thesis include mouse C_2C_{12} myoblasts, Chinese hamster ovary (CHO) cells and Human embryonic kidney (HEK) 293 cells, with all of these cell lines sourced from ATCC (Manassas, VA, United States of America). Primary myoblasts were isolated in-house as described in the relevant method sections.

2.1.6 Cell Culture

Cell culture medium components were from Life Technologies (Dulbecco's Modified Eagle Medium (DMEM), chemical media, horse serum (H/S) and foetal bovine serum (FBS)) and Sigma-Aldrich (Phenol red, penicillin, streptomycin, ampicillin and geneticin). DMEM media with serum was supplemented with 7.22 nM phenol red, 1 x 10^5 U/L penicillin, and 100 mg/L streptomycin. Geneticin (500 µg/mL) was added to media used for the selection and maintenance of stably transfected cells. Chemical media was supplemented with 1 x 10^5 U/L penicillin, and 100 mg/L streptomycin. Cell lines were cultured at 37°C with an atmosphere of 5% CO_2 in a ThermoForma Series II, water jacketed CO_2 incubator (Thermo Fisher Scientific). Culture dishes were purchased from Thermo Fisher Scientific. Details for specialised cell culture components are outlined in the relevant methods sections.

2.2 Methods

2.2.1 Isolation of ovine myoblasts from late gestation foetal lambs

Primary myoblasts were cultured from the *semitendinosus* muscle of late gestation foetal lambs, based on previously described techniques (Allen, Temm-Grove et al. 1997; Partridge 1997; McCroskery, Thomas et al. 2003). Briefly, 5 g of muscle was excised, and then finely minced in sterile PBS (Thermo Fisher Scientific). The resulting slurry was centrifuged (1500 rpm for 1 min) to remove PBS. The muscle pellet was then resuspended in DMEM (no serum) that contained 0.2% collagenase type 1A (Sigma-Aldrich). The resulting slurry was incubated for 90 min with agitation at 37°C. Following centrifugation at 2500 rpm for 10 min, the collagenase solution was removed, fresh PBS was added and the digested muscle triturated to release attached myoblasts from muscle fibres. The resulting solution was then passed through a 100 µm cell strainer (Becton Dickinson (BD); Franklin Lakes, NJ, United States of America) to remove bulky muscle debris. The filtrate was then centrifuged at 2500 rpm for 10 min, and the supernatant removed. The resulting pellet was resuspended in growth media (DMEM with 20% FBS, 10% H/S). Cultures were then enriched for myoblasts by pre-plating on uncoated 10 cm cell culture plates (Thermo Fisher) for 3 h. Cultures were then transferred to 10 cm culture plates that were coated with 10% Matrigel (BD) in DMEM (no serum) and incubated in an atmosphere of 5% CO_2

at 37°C for a period of 48 h to allow for the attachment and proliferation of myoblasts. Once sufficient numbers of myoblasts were present, cultures were trypsinised and the myoblasts cryogenically frozen in freeze media (DMEM with 10% and 5% dimethyl sulfoxide (DMSO) (BDH)), and stored in liquid nitrogen for later use. A previous unpublished study in our laboratory demonstrated that ovine myoblasts isolated using this method yields cultures of high myogenic purity, with Pax 7 immunofluorescence demonstrating that approximately 90% of the cells isolated express this important myogenic marker.

2.2.2 Trypsinisation of myoblasts

The trypsinisation of all cell types was performed as follows: The culture medium was removed and the cells rinsed with sterile PBS (Thermo Fisher). Trypsin (Life technologies) was then added (0.25% solution in PBS) and the cells were incubated for 5-10 min at 37°C. Once the cells had detached, fresh media was added to inactivate the trypsin and resuspend the cultured cells. Cell density was established using a haemocytometer before re-plating for further culture.

2.2.3 Generation of a consistent ovine myoblast pool.

In order to generate a pool of myoblasts that would be consistent throughout the course of these studies, myoblasts from seven individual male animals were removed from cryostasis and allowed to proliferate for one passage (~72 h). The proliferating cells were then trypsinised, pooled and cryopreserved in freeze media (DMEM with 5% FBS and 5% DMSO (BDH)) in 1 mL aliquots that contained ~2 x 10^6 cells. Cells were then stored in liquid nitrogen and resurrected as experimentally required.

2.2.4 Culturing and treatment for microarray

Primary ovine myoblasts were resurrected and plated at a density of 15000 cells/cm^2 in DMEM with 10% FBS on 10 cm diameter culture plates. Following overnight attachment, myoblasts were given a media change and allowed to proliferate for a further 24 h. Cells were then subjected to a 6 h treatment (in triplicate) with either 660 ng/mL Mstn (R&D Systems, MN, United States of America), 3 µg/mL in house recombinant MSV or vehicle alone (control) before RNA was harvested using 2 mL TRIZOL® reagent (Life Technologies) per plate as per manufacturers instructions.

2.2.5 RNA isolation and reverse transcription.

RNA extraction from TRIZOL® (Life Technologies) samples was performed according to manufacturer's instructions. The concentration of isolated RNA samples was determined in duplicate using a Nandrop 1000 spectrophotometer. RNA samples were then diluted to a concentration 500 ng/mL and 2 µg (4 µL), of total RNA was used to synthesize cDNA with the superscript III (Life Technologies) reverse transcription kit as per manufactures instructions.

2.2.6 Agarose gel electrophoresis of RNA

RNA integrity was confirmed by running 1 µg of isolated RNA, on an agarose gel containing 1.2% agarose, 20 mM MOPS, and 0.66M formaldehyde. Prior to loading the RNA sample (made up to 5 µL total volume with DEPC water) was mixed with an equal volume of RNA loading dye (20 mM MOPS, 20% formaldehyde, 50% formamide, 5 mM EDTA, 0.04% bromophenol blue, 50 µg/mL ethidium bromide and 10% glycerol) and incubated at 65°C for 5 min, before loading. RNA was visualised under UV light using a Geldoc system (BioRad).

2.2.7 Microarray Analysis

Once the integrity of the purified RNA was confirmed, samples were sent to Auckland University for microarray analysis. Microarray analysis using 500 ng of total RNA was performed by the Microarray Facility (Centre for Genomics and Proteomics, University of Auckland). Analysis was performed by labelling isolated RNA with the Ambion Message Amp Premier 3' labelling kit using the GeneChip® Bovine Genome Array platform containing over 23000 bovine transcripts. Microarray data was supplied as data files, containing the intensity values for all array analysis performed. Two standard methods were employed to normalise the microarray data before analysis (AgR Bioinformatics/Math and Statistics Department). Affymetrix MicroArray Suite 5 (MAS.5) and Robust Multi-array Average (RMA) analysis were used to independently normalise the microarray data. RMA analysis was favoured due to the reduced data variation observed using this normalisation method. Following RMA analysis, the resulting normalised data had fold expression changes calculated for the following comparisons:

i. Control vs Mstn

ii. Control vs MSV

Following normalisation, P-values were calculated using an empirical Bayesian technique to shrink the standard errors towards a common value. A data set containing gene identifiers and corresponding expression values was uploaded into Ingenuity Pathway Analysis platform (www.ingenuity.com). Each identifier was mapped to its corresponding object in the Ingenuity® Knowledge Base. Cut-off values of a fold change of +/- 1.5 with a P-value of < 0.05 were imposed to identify molecules whose expression was significantly different between datasets. These molecules, called Network Eligible Molecules, were overlaid onto a global molecular network developed from information contained in the Ingenuity® Knowledge Base. Networks of Network Eligible Molecules were then algorithmically generated based on their connectivity. The results of each comparison were analysed using Ingenuity® Pathway Analysis (IPA: www.ingenuity.com) to provide extra information on the biological 'themes' of the data.

2.2.8 Polymerase chain reaction (PCR)

2.2.8.1 Standard PCR

Two different DNA polymerases were used during the course of these studies. Expand long polymerase (Roche) was used for the initial amplification of the MSV expression cassettes, where proof reading activity was required. For standard PCR where visualisation of PCR products was required Taq polymerase (Roche) was used. PCR reactions were performed in a PTC-0200 DNA Engine Peltier Thermal Cycler (BioRad). For PCR reactions 2 µL of template DNA was amplified in a 50 µL reaction mix containing: 5 µL of 10 x PCR buffer (as supplied for individual enzymes), 1 µL of dNTPs (Life Technologies), 1 µL of 10 µM sense and anti-sense primer, 1 µL of enzyme and 40 µL of PCR grade H_20. PCR cycling was performed as follows: 94°C for 1 min (denaturation), then 35 cycles of 94°C for 15 s, 55°C for 45 s (annealing) and 72°C for 2 min, then a final extension at 72°C for 5 min was performed. PCR products were visualised using agarose gel electrophoresis.

2.2.8.2 Quantitative real-time PCR (qPCR)

PCR was carried out with 2.5 µL of a 1:20 dilution (in PCR grade H_2O) of the reverse transcriptase reactions and 7.5 µL of master mix for each reaction (4.5 µL water, 0.5 µL of a 1 µM solution of forward and reverse primers and 2.0 µL FastStart DNA Master plus SYBR Green I reagent (Roche). A dilution series of pooled cDNA generated from the treated ovine myoblasts was used to establish a standard curve. PCR cycling was performed as follows: denaturation (95°C for 5 min), amplification (95°C for 5 s, 62°C for 10 s, 72°C for 20 s, with a single fluorescence measurement every cycle for 45 cycles), melt curve analysis (60-95°C with a heating rate of 0.1ºC/s with continuous fluorescence measurement) using a LightCycler 2.0 PCR machine (Roche Diagnostics). Arbitrary concentrations were calculated by the LightCycler software using the standard curve (Roche Diagnostics). Data for each sample were normalized to cDNA concentration in each parent RT reaction as determined using the Quant-it OliGreen ssDNA kit (Life Technologies) as per manufacturer's instructions. The PCR products were visualised using agarose gel electrophoresis to confirm the size and the specificity of the amplified products.

2.2.9 Agarose Gel Electrophoresis of DNA

Agarose gels contained 0.8-3% agarose or LMP agarose and were made in 1 X Tris-acetate-EDTA (TAE) buffer (0.4M Tris (base), 1.14% Glacial acetic acid and 1mM EDTA (pH 8)), with 100 ng/mL ethidium bromide. Electrophoresis was performed using an Owl electrophoresis system (Owl Separation Systems) containing 1 X TAE buffer. DNA samples were mixed with DNA loading dye and then loaded. Electrophoresis was performed at 30-100 V until the desired separation was achieved. DNA samples were visualised under UV light and photographed using the Gel Doc system (BioRad).

2.2.10 Methylene blue proliferation assay

For proliferation assays, a previously published photometric endpoint assay was used (Oliver, Harrison et al. 1989). Briefly, for each cell-type or treatment 1000 cells/well were seeded in 96 well cell culture plates using one plate per time-point. Following the specified proliferation period, the cells were fixed in 100µl of 10% formaldehyde in 0.9% saline per well and stored at room temperature prior to assay. For methylene blue assay, fixative was removed and,

100 µl of methylene blue stain was added to each well for 20 min at room temperature. After the removal of the staining solution, the cells were washed four times with 200 µl of 0.01M Borate buffer (pH, 8.5), followed by the addition of 200 µl of a 1:1 mixture of 0.1 M HCl and 70% ethanol to solubilise the cells and liberate the retained methylene blue stain. The absorbance of the wells was measured using a VersaMax tuneable microplate reader (Molecular Devices) at 655 nm, with the absorbance directly proportional to cell number.

2.2.11 Primary culture of mouse myoblasts

Primary myoblasts were cultured from the hind limb muscle of four week old wild-type and Mstn null mice. Muscle was excised then minced finely in sterile PBS (Thermo Fisher). The resulting slurry was then centrifuged (1500 rpm for 1 min) and PBS removed. The muscle pellet was then resuspended (5mL per mouse of DMEM (no serum) containing 0.2% collagenase type 1A (Sigma-Aldrich) and digested for 90 min with agitation at 37°C. Following centrifugation (2500 rpm for 10 min), the collagenase solution was removed, with fresh PBS ~12 mL per mouse added and the digested muscle triturated to release attached myoblasts from muscle fibres. The resulting solution was then passed through a 100 µm cell strainer (BD) to remove bulky muscle debris. The filtrate was then centrifuged (2500 rpm for 10 min, the supernatant removed and the resulting muscle pellet resuspended in growth media (DMEM/ 20% foetal bovine serum (FBS), 10% Horse serum (H/S). Cultures were then enriched for myoblasts by pre-plating on uncoated cell culture plates for 3 h. Cultures were then transferred to plates coated with matrigel (Beckton Dickenson) at a 1:10 dilution DMEM (no serum) and incubated in an atmosphere of 5% CO_2 at 37°C for 48 h to allow the attachment and proliferation of myoblasts. Once sufficient numbers of myoblasts were present, cultures were trypsinised, counted using a haemocytometer and re-plated for proliferation or differentiation studies.

2.2.12 Assessment of Na^+ K^+ ATPase β1 subunit transcript abundance in wild-type and Mstn null primary myoblasts.

For proliferation wild-type and Mstn null primary myoblasts were plated at a density of 15000 cells/cm^2 and left to attach overnight, following 24 h proliferation cells were harvested with TRIZOL® reagent for subsequent RNA

isolation. For differentiation studies myoblasts were seeded at a density of 25000 cells/cm^2 and allowed to attach overnight. Following overnight incubation at 37°C with 5% CO_2 cultures were switched to differentiation media (DMEM + 2% H/S) and incubated for a further 48 h, before TRIZOL® reagent (Life Technologies) was used to harvest cultures for RNA extraction.

2.2.13 Na^+ K^+ ATPase ATP hydrolysis assay

The method for measuring NKA dependant ATP hydrolysis was based on the technique described by Hatou et al (Hatou, Yamada et al. 2010). For these studies, ovine myoblasts were seeded at a density of 15000 cells/cm^2 in 24 well plates in DMEM with 10% FBS. Following overnight attachment cells were given a media change (DMEM + 5% FBS) and incubated for a further 24 h. The sub confluent cultures were then treated with R & D Mstn (100 ng/mL), MSV (3 µg/mL), insulin (100 nM) or vehicle alone (control) and harvested after 1, 6, 12 and 24 h intervals. Culture medium was then removed from cell monolayers, and ultrapure distilled water (150 µL) was added to each well. The culture plate was then placed in liquid nitrogen for 10 s (to freeze cultures), and 150 µL of lysis buffer (80 mM histidine, 20 mM KCl, 6 mM $MgCl_2$, 2 mM EGTA, 2 µg/mL alamethicin (Sigma-Aldrich), 30 µM digitonin (Sigma-Aldrich), and 200 mM NaCl at pH 7.4) was added to each well. Half of the wells from each treatment (N=6), were then incubated with 20 µL of 15 mM ouabain (final concentration, 1 mM) or vehicle alone (H_2O) for 30 min at 37°C. Finally, 10 µL of 300 mM ATP (final concentration, 10 mM) was added and the reaction mixtures were incubated for an additional 30 min at 37°C. The ATP hydrolysis reaction was terminated by the addition of 75 µL of 50% trichloroacetic acid to each well. The contents of each well were then centrifuged at 3000rpm for 10 minutes at room temperature. The resultant supernatants were diluted 50-fold with ultrapure distilled water, and 25 µL of the diluted samples were added to tubes containing 100 µL ammonium molybdate reagent (BiomolGreen; ENZO Life Sciences, Farmingdale, NY, United States of America), with phosphate content determined by measurement of absorbance at 640nm. Phosphate solutions of 0 to 40 µM diluted in Lysis buffer were used to generate a standard curve. Hydrolysed ATP values were normalised to protein concentration of the reaction mixtures as determined using the bicinchoninic acid assay (2.2.17). The Na^+, K^+-ATPase activity was calculated as

the difference in hydrolysed phosphate between cells exposed to ouabain and those not and was expressed as millimoles of ATP hydrolysed per mg of protein (per hour).

2.2.14 Production of recombinant MSV

The production of MSV was performed as follows, Origami B *E. coli* (Merck Millipore, Darmstadt, Germany) cells that were transformed with the pET100/D TOPO vector containing the putative mature sheep MSV sequence (aa 275-321) were used for the expression of MSV. Recombinant protein was purified with the use of the MSV N-terminal histidine tag and Ni-NTA resin (Life Technologies), according to the Life Technologies native purification protocol. Purified recombinant protein was dialysed against two changes of dialysis buffer (20 mM TRIS-HCl pH 7.0, 150 mM NaCl) at 4°C overnight. Protein concentration was determined using the bicinchoninic acid protein assay (2.2.17).

2.2.15 Recombinant protein purification using Polymyxin or Triton X-114

Purification of MSV with Affi-Prep® Polymyxin Matrix (BioRad) was performed as per manufacturer's instructions by incubating 500 µL of 1 mg/mL MSV per mL Polymyxin (binding capacity 5 mg/mL endotoxin) with constant stirring at 4°C in a 1.5 mL tube. Mixtures were incubated overnight at 4°C with constant stirring, samples were the centrifuged (14000 x g for 10 min) and the supernatant recovered as purified recombinant protein. Triton X-114 purification was performed by adding Triton X-114 to the protein preparation at a final concentration of 1%. The mixture was then incubated at 4°C for 30 min with constant stirring to ensure a homogenous solution. The sample was then transferred to a 37°C water bath, incubated for 10 min, and centrifuged at 14000 x *g* for 10 min at 25°C. The upper aqueous phase containing the protein was carefully removed and subjected to Triton X-114 phase separation for at least three further cycles. Protein concentration was then assessed with the bicinchoninic acid assay (2.2.19). All samples had endotoxin concentration assessed using the Lonza LAL Kinetic QCL kit (Lonza, Basel Switzerland).

2.2.16 Isolation of cellular protein

Protein was isolated from cultured myoblasts as follows. Following treatment, 300-500µL of low salt lysis buffer (10 mM Hepes-NaOH (pH 7.9), 10

mM MgCl, 5 mM KCl, 0.1 mM EDTA, 0.5 % IGEPAL (Sigma-Aldrich), 2mM vanadate, 2mM NaF, MQ H_20 to 25 mL, with half a Complete protease inhibitor tablet (Roche)) was added to each plate or well. Cells were then scraped off the culture surface and the resulting lysates were transferred to individual 1.5 ml tubes before freezing at -80°C. Cell lysates were later thawed and repeatedly passed through a 29-gauge needle before centrifuging at 14000 x *g* for 5 min at 4°C to pellet cell debris and the supernatant was taken as a total cell lysate. Alternatively, if enrichment of cytoplasmic and nuclear components was required, cells were initially triturated after thawing with a 100 µL pipette tip and incubated on ice for 15 min, lysates were then centrifuged at 14000 x *g* for 3 min at 4°C to pellet cell nuclei. The resulting supernatant was removed and stored separately as the cytoplasmic fraction. The pellet was then resuspended in 250 µL high salt lysis buffer (20 mM Hepes-NaOH (pH 7.9), 1.5 mM M MgCl, 500 mM NaCl, 0.2 mM EDTA, 25% Glycerol, 2 mM vanadate, 2 mM NaF, MQ H_20 to 25 mL, with half a Complete protease inhibitor tablet (Roche)) and repeatedly passed through a 29-gauge needle (BD) before incubating on ice for 30 min with intermittent flicking. The lysate was then centrifuged at 14000 x *g* for 3 min at 4°C and the supernatant retained. The supernatant was then loaded into an Amicon® Ultra 3K centrifugal filter (Merck Millipore) and spun at 4500 x *g* for 30 min to reduce the salt concentration per unit protein. The portion remaining in the upper chamber (typically 170-200 µL) was retained as nuclear enriched lysate. Aliquots (30 µL) of each type of lysate were diluted 1:1 in MQ H_2O to determine the concentration of the protein (see 2.2.19) and the remaining lysates were diluted 2:1 with 3x Laemmli buffer (final con 10% glycerol, 5% β-mercaptoethanol, 2% SDS, 60 mM Tris (pH 6.8)). Lysates were boiled for 5 min then stored at -20°C in 100 µL aliquots for subsequent western blot analysis.

2.2.17 Determination of protein concentration

The concentration of protein samples was determined using the bicinchoninic acid protein assay (Sigma-Aldrich). Protein lysates were diluted 1:1 with MQ H_20 and 25 µL was added to 200 µL of a 50:1 mix of bicinchoninic acid solution and Copper (II) Sulphate Pentahydrate 4% solution (Sigma-Aldrich). BSA standards (25 µL of 0 to 2 mg/mL solutions) were used to generate a standard curve. Assay mixtures were incubated in duplicate at 37°C on 96 well

plates (Thermo Scientific) for 30 min before OD_{562} for each sample was determined using a VERSAmax^{TM} tunable microplate reader (Molecular Devices, Sunnyvale, CA, United States of America) to estimate protein concentration.

2.2.18 SDS Polyacrylamide Gel Electrophoresis and Membrane Transfer

SDS polyacrylamide gel electrophoresis (SDS-PAGE) was performed using 10-15% polyacrylamide gels. Typically 5 to 15 µg of protein pre-mixed and boiled in Laemmli buffer (3 x solution; 30% glycerol, 15% β-mercaptoethanol, 6% SDS, 180 mM Tris (pH6.8) and a few grains of bromophenol blue) was thawed and loaded into the gels. Electrophoresis of the proteins was performed using 1 x running buffer (25 mM Tris base, 200 mM glycine, 0.1% SDS) at ~45 mA per gel until the bromophenol blue band reached the bottom of the gel. Following electrophoresis, proteins were transferred from the gel to nitrocellulose or PVDF membrane (Bio-Rad) by electro-blotting at 30 V overnight at 4°C. Following transfer, the membranes were stained with Ponceau Stain (0.05g Ponceau powder, 2.5 mL acetic acid, then up to 50 mL with H_20) and then rinsed in H_2O until bands were clearly defined, to confirm proteins had been uniformly transferred to the membrane.

2.2.19 Western blot analysis

Membranes were blocked in BSA blocking solution (Tris Buffered Saline-Tween (TBST) buffer (50 mM Tris (pH 7.6), 150 mM NaCl, 0.1% Tween 20), plus 1% PEG-4000, 1% PVP-10, 0.3% BSA and 0.01% Thimerosal) for at least 1 hr at room temperature and then incubated with primary antibody diluted in BSA blocking solution overnight at 4°C (see 2.1.4 for antibody dilutions). Membranes were then washed in TBST for 5 min (x5), then incubated with species specific horseradish peroxidise conjugated antibodies (Dako) (1:5000 in BSA blocking solution) for 1 h at room temperature. The TBST washes were then repeated before subjecting the membrane to Western Lightning™ Chemiluminescence Reagent Plus (Perkin-Elmer, Waltham, MA, United States of America), chemiluminescence was then visualised by exposure to XAR film (Kodak, Rochester, NY, United States of America), or using the ImageQuant LAS 4000 system (GE Healthcare; Little Chalfont, Buckinghamshire, United Kingdom). Developed films were scanned on a calibrated densitometer (GS-800, BioRad) and Quantity One software (Bio-Rad) used for the densitometry analysis of both

visualisation methods. Ponceau staining and visualisation was used to confirm equal loading and transfer of protein samples. The use of housekeeping genes such as tubulin, GAPDH and actin was not employed. The reasoning here was that these housekeeping genes are involved in pathways that have been shown to be influenced by treatment with Mstn, for example GAPDH in glycolysis and actin and tubulin in cell growth and differentiation. Thus comparing the abundance of western targets based on total protein loading was preferred. In addition, data obtained using this method for quantifying protein abundance has being published in numerous peer reviewed publications, with (Alway, Degens et al. 2002; Quadrilatero, Bombardier et al. 2010; Baseler, Dabkowski et al. 2013; Ilori, Blount et al. 2013) providing examples.

2.2.20 MSV over-expression

2.2.20.1 Restriction endonuclease digestion

For restriction endonuclease digests, up to 10 µg of plasmid DNA was digested with 0.5-2 µL (3-20 U) of the appropriate enzyme. Digests were performed in 1 x restriction endonuclease buffer, with digest volumes between 30 and 50 µL. Reactions were carried out at 37°C for at least 2 hours. DNA electrophoresis (2.2.9) was then used to characterise the digest and isolate DNA if required for subsequent manipulation.

2.2.20.2 DNA Ligations

Two types of ligation were used for the generation of the MSV expression constructs. Firstly the p-GEM-T easy system (Promega) was used to clone PCR products according to manufacturers protocol. Briefly, a 4-6 fold molar excess of insert DNA was used for cloning into the pGEM-T easy vector. The 10 µL ligation mix consisted of 1 x rapid ligation buffer, 50 ng pGEM-T easy vector, the appropriate volume of DNA insert and 0.3 Weiss units/µL of T4 DNA ligase. Ligations were incubated overnight at 4°C. Secondly, for the generation of MSV expression plasmids (Life Technologies), EcoRI digested insert (MSV) and vector (pcDNA3 (Invitrogen)) at a ratio of ~4:1, respectively, were combined for the ligation reaction, that was composed of 1 x ligation buffer (Roche, Basel, Switzerland) and 1U T4 DNA polymerase (Roche). Reactions were incubated overnight at 4°C.

2.2.20.3 Transformation of competent cells

Transformation of DH5α competent *E. coli* (Life Technologies) cells was performed by the addition of 2-5 µL of ligation mixture to 50 µL of competent cells. This mix was incubated on ice for 30 min and then heat shocked at 42°C for 30-45 s. Cells were then cooled on ice for 2 min, after which, 450 µL of LB media was added. Transformed cells were then incubated with agitation for 1 h before plating 100-500 µL on to LB agar plates containing 50 µg/mL ampicillin (Life Technologies).

2.2.20.4 Cloning of Full-length MSV

Initially, MSV expression cassettes were PCR amplified using the previously generated pET101/D-MSV vector as the PCR template (Frank Jeanplong, Developmental Biology Group, AgResearch Ruakura, New Zealand). This vector contained full-length MSV with a mutated stop codon upstream of the sequence coding for V5 and histidine epitopes. PCR amplification of the MSV cassettes for cloning into the pcDNA3 vector was performed using the Expand Long Template high fidelity PCR System (Roche). Custom synthesis of two reverse primers allowed the generation of both C-terminal tagged (C-MSV 5'- GGAATTCCTTTGTTAGCAGCCGGATCAAACTCA-3') and non-tagged (MSV 5'-GGAATTCCTTCGAATTGAGCTCGCCCTATTTCAT-3') MSV cassettes. Reverse primers also contained sequence coding a 5' EcoRI restriction enzyme sequence, to allow the subsequent cloning of the MSV expression cassettes into the pcDNA3 vector. The primer sequence for MSV R (non-tagged) contained a single nucleotide mutation (A in the MSV reverse primer sequence) to generate a correctly placed stop codon in the amplified MSV ORF. The C-MSV primer sequence was designed to include the V5 and histidine sequences thus, maintaining the mutated stop codon in the original template sequence. The T7 forward priming site, located in the pET101/D vector, upstream of the MSV ORF sequence used as the forward primer in the amplification of both MSV cassettes, which was upstream of an EcoRI restriction site. Following PCR amplification, reactions had standard Taq polymerase added for 5 min at 72°C to allow A tailing of the PCR products for their subsequent cloning into pGEM-T easy. PCR products were then purified by running on a low melting point agarose gel, with the MSV expression cassettes then excised and purified using the

Wizard DNA purification system (Life Technologies) as per manufacturers instructions. MSV cassettes were then TA cloned into the p-GEM T-easy vector (Promega) and the resulting ligation transformed into DH5α competent cells. EcoRI (Life Technologies) restriction digests were then used to identify positive transformants and to purify the MSV and C-MSV cassettes. Purified MSV cassettes were then ligated into EcoRI digested pcDNA3 vector using T4 DNA ligase (Roche), to generate the pcDNA3-MSV and pcDNA3-C-MSV expression constructs. Confirmation of the orientation of the MSV constructs were confirmed using restriction enzyme digestion in the first instance (data not shown). Secondly, clones displaying the expected restriction fragment sizes were DNA sequenced to confirm the integrity of MSV sequence (Allan Wilson Centre Genome Service; Massey University, Palmerston North, New Zealand). The DNA Sequence alignment of the pcDNA3/MSV and C-MSV constructs was performed using freely available online software (www.justbio.com), with the MSV construct sequences aligned to the predicted DNA and translated protein sequence of ovine MSV (GenBank accession number: DL465814.1).

2.2.20.5 Transfection and generation of MSV over-expressing cell lines

To generate stable (C_2C_{12}, HEK293 and CHO) MSV expressing cell lines, cells were transfected with the plasmids carrying the MSV expression cassettes or empty pcDNA3 vector using Lipofectamine 2000 reagent (LF2000, Life Technologies) according to the manufacturer's protocol. Briefly for each individual transfection 12 µg of plasmid DNA in 1.5 mL DMEM (no serum) was mixed with 40 µL of LF2000 in 1.5 mL DMEM (no serum), the resulting mixture was added drop-wise to 7 mL of culture media (DMEM with 10% FBS) in a 10 cm culture dish that contained sub-confluent cultures of the cell type to be transfected. Following a 24 h incubation period, the culture media was changed and cell lines were developed by selection in DMEM with 10% FBS containing 500 µg/mL geneticin. Cells were the passaged as required until full neomycin resistance was acquired (~3 weeks of culture). Cells were the cryogenically stored for later use, with passage number kept consistent for all experiments and cells continually maintained in the presence of 500 µg/mL geneticin. Geneticin concentration was chosen based on similar studies performed previously (McFarlane, Hennebry et al. 2008). Clonal C_2C_{12} cell lines were developed from

the initially transfected C_2C_{12} cell pool. Clonal selection was achieved by seeding neomycin resistant C_2C_{12} cells from MSV, C-MSV and pcDNA3 pools at 1000 cells per plate in 10 cm culture dishes. Cells were allowed to proliferate under continued geneticin selection until individual clonal colonies were of sufficient size to remove cells. Cells scraped from individual colonies were seeded in individual culture dishes. Clonal cultures were then expanded until sufficient cells were available for cryogenic storage of individual clonal cell lines.

2.2.21 Mitochondrial activity (EZ4U) assay

Cultured C_2C_{12} myoblasts expressing MSV were seeded in 96 well plates (Thermo Fisher) at 1000 cells per well. Cells were cultured in growth media (DMEM with 10% FBS) and allowed to attach overnight at 37°C with 5% CO_2. Mitochondrial activity (EZ4U assay; Biomedica, Wein, Divischgasse, Austria) was determined following overnight attachment (T0) and after 24, 48 and 72 h of proliferation. The EZ4U assay was performed as per manufacturer's instructions, with EZ4U reagent added (20 µL per well) and cells incubated for 2 h hour, before measuring OD_{450} (EZ4U) and OD_{620} (reference/background).

2.2.22 C_2C_{12} (MF20 fluorescence) differentiation assay

The expression of Myosin heavy chain is a well-established marker of myoblast differentiation. Traditional methods for investigating myoblast differentiation involve manual counting of cell nuclei within and excluded from differentiated myotubes. To assess the extent of differentiation in C_2C_{12} myoblasts, a fluorescence assay was developed to determine the relative abundance of myosin heavy chain and cell nuclei during differentiation. Initially, standardisation was performed to ensure that fluorescent data correlated well with the expression of myosin heavy chain and the abundance of cell nuclei. To determine if the myosin:DAPI fluorescence ratio could give an indication of the extent of myoblast fusion, an initial study was conducted using a previous model in which the inhibition of myoblast differentiation has been observed following Mstn treatment (see Appendix 1). For differentiation assay studies cells were seeded at a density of 25000 cells/cm^2 in multiple 96 well Optilux™ plates (BD) and allowed to attach overnight before the addition of differentiation media (DMEM + 2% H/S), which was designated time zero. Plates were then fixed periodically during differentiation (typically every 24 h) with ethanol, glacial

acetic acid and formaldehyde in a 20:2:1 ratio, respectively for 30 s, before rinsing with PBS. Wells then had 150µL PBS added and cells were then stored at 4°C until the differentiation assay was performed.

Fluorescent staining was the used to assess the abundance of myosin heavy chain and nuclei in fixed samples. Initially cells were permeabilised with 150 µL 0.1% Triton X (Sigma-Aldrich) in PBS per well for 10 min at room temperature, before rinsing with PBS. Next, 200 µL of blocking solution (PBS containing 0.35% Carrageenan λ (Sigma-Aldrich) and 10% Normal Sheep Serum (NSS, isolated in house) was added to each well and cells incubated at room temp for 2 h. Blocking solution was removed and 200 µL of MF20 myosin heavy chain (MF20 (DSHB)) or negative control (mouse IgG) antibody, diluted at 1:200 (in PBS with 0.35% Carrageenan λ and 5% NSS) was added to each well, plates were then incubated overnight at 4°C. Antibody solution was then removed and cells were rinsed 5 times for 5 min with PBS and gentle agitation at room temperature. Secondary antibody, anti-mouse Alexa Fluor® 488 conjugate (Life Technologies) was then added at a 1:500 dilution in PBS with 0.35% Carrageenan λ and 5% NSS) and plates incubated at room temperature in the dark for 1 h. Cells were then rinsed 5 times for 5 min with PBS, before addition of 4',6-diamidino-2-phenylindole (DAPI (Life Technologies)) at 1 µg/mL in PBS for 10 min. After three final 5 min PBS washes, 100 µL of PBS was then added to each well before the fluorescence was measured for (MF20 (Alexa Fluor 488®, (excitation 485nm, emission 528nm) and DAPI (excitation 360nm, emission 460nm) using a Synergy™ 2 multi-detection microplate reader and Gen5 software (BioTek Instruments Inc; Winooski, VT, United States of America). The average background fluorescence for MF20 (negative control) and DAPI (empty wells) were subtracted from the individual well values before analysis.

2.2.23 Statistical analysis

All data, with the exception of the microarray dataset were analysed by ANOVA, using GenStat v13 software (VSN International Ltd, Hemel Hempstead, United Kingdom). Post-hoc student's t-tests were used to generate P-values for *in vitro* comparisons. Data presented are mean +/- the standard error of the mean (S.E.M).

Chapter Three

3 Microarray

3.1 Introduction

Following the discovery of MSV, a number of studies in our laboratory have focused on a functional interaction between Mstn and MSV. Initial investigations lead to the postulate that MSV was an antagonist of Mstn. This was supported by *in vitro* studies, which showed that recombinant MSV could induce the proliferation of myoblasts, bind Mstn and its receptor and inhibit the Mstn induced phosphorylation of Smad 2/3. However, the signal transduction events, and the gene expression changes associated with MSV treatment were not well understood. In particular, and as stated in section 1.4, investigating how MSV signalling differed from that of Mstn was a major aim of this thesis. To address this aim, the first experiment in this thesis employed microarray analysis to directly compare the genes regulated by recombinant MSV and Mstn in ovine myoblasts.

In the past 10 years, significant advances have been made in the use of microarray analyses to investigate and compare changes in gene expression. Furthermore, the advent of analysis packages like Ingenuity Pathways Analysis (IPA) allows a much more in-depth look at the 'biological themes' of data sets, based on the observed gene expression changes. The only disadvantage is that the IPA analysis is based on findings in human, mouse and rat models. Thus, molecules in a microarray data set from another species (e.g. sheep as used for these studies) are included for analysis if they can be linked to orthologous genes in the IPA database (Ingenuity® Systems, www.ingenuity.com). In support for its use in this context, a number of sheep studies have cited the use of IPA for the analysis of micro array data (Bonnet, Bevilacqua et al. 2011; Burgess, Greer et al. 2012).

The Ingenuity® knowledge database is continually updated with new tools and scientific findings to assist with the analysis of data. Over the course of these studies, IPA analysis of the microarray data obtained for this chapter was repeated several times. This ensured that firstly, data obtained was kept up to date, and

secondly, that any new additions to the IPA analysis software that would assist in the interpretation of this data set, were included. The addition of the upstream activator analysis module provides a good example of how this approach was of benefit (3.2.3). This software enables a prediction of the upstream events regulating the expression changes in a microarray data set. This is based on which gene(s) are regulated, and the direction of change as referenced against findings in the Ingenuity database.

3.2 Results

Microarray analysis was performed on RNA isolated from primary ovine myoblasts treated for 6 h with recombinant Mstn, MSV or vehicle alone (control) prior to extraction of RNA. Each treatment was performed in triplicate, resulting in 9 RNA samples to be sent to Auckland University for microarray analysis (2.2.8). The raw microarray data was subjected to RMA (Robust Multichip Average) analysis by Paul Maclean (AgResearch, Bioinformatics Maths and Stats). The resulting normalised data was used to determine relative transcript levels for the following comparisons:

1. Mstn vs. Control
2. MSV vs. Control

The results of each comparison were analysed using IPA to provide extra information on the 'biological themes' of the data.

3.2.1 Top biological functions associated with Mstn and MSV gene expression predicted with IPA core analysis.

The data presented in this section summarises the biological functions associated with Mstn or MSV treatment in primary ovine myoblasts, as assessed using IPA.

A summary of the top biological functions predicted using IPA included three classes: diseases and disorders, molecular and cellular functions and physiological system development and function. Table 3.1 and 3.2 give a summary of the top biological functions associated with Mstn and MSV treatment, respectively. Consistent themes between Mstn and MSV datasets were, the regulation of genes involved in the inflammatory response, cellular movement,

cell growth and regulation, cell to cell signalling, cell to cell interaction and cell death and survival.

3.2.2 Top molecules

As an example of the changes in gene expression observed following analysis of the microarray data, Table 3.3 and 3.4 lists top ten up, and down-regulated genes following treatment with Mstn and MSV, respectively.

3.2.3 IPA Upstream Regulator analysis

The upstream regulator analysis was not available when the microarray data was assessed in the first instance. Following the release of this analysis module, the microarray data set was periodically re-analysed. This allowed the capture of any new information that IPA could provide on the upstream pathways regulating the changes in gene expression. The upstream regulator analysis assigns two statistical measures for each potential regulator in the IPA database, the overlap P-value and the activation z-score. The overlap P-value calls potential upstream regulators based on a significant overlap between data set genes and their known transcriptional targets. The activation z-score is used to infer the activation status of the upstream regulator based on the significant pattern match of up or down-regulation of the target genes in the dataset (Ingenuity® Systems, www.ingenuity.com). The data presented here were obtained following the most recent analysis of the microarray data set (May 2013).

IPA analysis identified a number of potential upstream regulators. The top 20 for each treatment are shown in Table 3.5 and 3.6 for Mstn and MSV, respectively. Presented in the table is the upstream regulator, its fold change (if contained in the array) and its predicted activation state based on the activation z-score (a z-score higher than 2 predicts activation (positive values) or inhibition (negative values)). The notes column contains the bias term, a biased dataset is one in which there are more up- than down-regulated genes or vice versa. In these cases the P-value for the overlap is the main determinant for significance of an upstream regulator (Ingenuity® Systems, www.ingenuity.com).

3.2.4 Selection and Validation of metabolic targets

As outlined in section 1.4, one of the aims of this thesis was to determine if MSV plays a role in intermediary metabolism. To confirm the integrity of the

microarray data, three potential metabolic targets of recombinant Mstn and(or) MSV that were differentially expressed were selected for further analysis. These were p53 (increased 1.56 fold by MSV), Pyruvate dehydrogenase kinase 3 (PDK3) (increased 1.55 fold by MSV) and the β1 subunit of the Na^+-K^+-ATPase (increased 2.13 fold by Mstn and decreased 1.84 fold by MSV). To validate the changes observed following microarray analysis, qPCR was performed on cDNA reverse transcribed from the same RNA pool. All targets investigated reflected the above expression values that were obtained following the microarray analysis (Figure 3.1).

3.2.5 Confirmation and removal of endotoxin present in recombinant MSV

When first analysing the microarray data using IPA, a number of genes were differentially expressed that suggested caution in interpreting the data. In particular, a number of gene expression changes associated with recombinant MSV treatment, were also linked to the presence of endotoxin (Ingenuity® Systems, www.ingenuity.com). This was concerning, as some of the experimental studies presented later, which investigated the signal transduction events regulated by Mstn and MSV had already been performed (Chapter 4), before the extent of the problem was realised and addressed. The Mstn preparation used for this analysis (R&D Systems) has certified as having low concentrations of endotoxin (<0.1 EU/μg). However the concentration of endotoxin in the recombinant MSV preparation used for these studies (produced in *E. coli*) was an unknown. Therefore steps were taken to ensure this preparation was endotoxin free. This was primarily due to the confounding biological effect endotoxin would have on my myoblast cultures. The following section details the experimental steps take to address the concerns regarding the presence of endotoxin in the MSV preparation used for my studies.

Table 3.1. Mstn vs. Control top biological functions		
Diseases and Disorders		
Name	**P-value range**	**# Molecules**
Connective Tissue Disorders	3.16E-06 - 5.41E-03	9
Inflammatory Disease	3.16E-06 - 7.21E-03	11
Skeletal and Muscular Disorders	3.16E-06 - 5.41E-03	14
Inflammatory Response	9.46E-06 - 7.21E-03	9
Neurological Disease	1.89E-05 - 5.41E-03	11
Molecular and Cellular Functions		
Name	**P-value range**	**# Molecules**
Cellular Movement	1.08E-07 - 7.21E-03	16
Cellular Growth and Proliferation	4.62E-07 - 7.21E-03	22
Cellular Development	5.01E-07 - 7.21E-03	19
Cell-To-Cell Signalling and Interaction	3.14E-05 - 7.21E-03	9
Cell Cycle	4.71E-05 - 7.21E-03	7
Physiological System Development and Function		
Name	**P-value range**	**# Molecules**
Skeletal and Muscular System Development and Function	5.01E-07 - 7.21E-03	11
Endocrine System Development and Function	2.39E-06 - 5.41E-03	3
Nervous System Development and Function	2.39E-06 - 5.76E-03	5
Tumor Morphology	5.94E-06 - 7.21E-03	8
Cell-mediated Immune Response	9.46E-06 - 7.21E-03	7

Table 3.2. MSV vs. Control top biological functions		
Diseases and Disorders		
Name	**P-value range**	**# Molecules**
Inflammatory Response	1.53E-16 - 2.32E-05	45
Cancer	2.73E-15 - 2.19E-05	70
Cardiovascular Disease	4.51E-14 - 8.70E-06	36
Organismal Injury and Abnormalities	4.02E-13 - 1.76E-05	38
Immunological Disease	6.92E-13 - 7.21E-06	33
Molecular and Cellular Functions		
Name	**P-value range**	**# Molecules**
Cellular Movement	1.04E-16 - 2.32E-05	51
Cell Death and Survival	1.89E-14 - 2.27E-05	56
Cellular Growth and Proliferation	1.49E-13 - 2.01E-05	60
Cell-To-Cell Signalling and Interaction	5.41E-12 - 2.18E-05	40
Cellular Function and Maintenance	8.60E-12 - 1.90E-05	48
Physiological System Development and Function		
Name	**P-value range**	**# Molecules**
Cardiovascular System Development and Function	6.94E-22 - 2.19E-05	46
Organismal Development	6.94E-22 - 2.18E-05	46
Hematological System Development and Function	4.62E-15 - 2.32E-05	48
Immune Cell Trafficking	4.62E-15 - 2.32E-05	35
Organismal Survival	5.70E-15 - 2.31E-05	52

Table 3.1 and 3.2: Top biological functions influenced by Mstn or recombinant MSV treatment. IPA core analysis was used to identify the top biological functions associated with Mstn (Table 3.1) and MSV (Table 3.2) treatment of ovine myoblasts. Analysis covered three broad categories: Diseases and disorders, Molecular and cellular functions and Physiological system development and function. The P-value range and the number of differentially expressed molecules, associated with their respective function are also presented.

Table 3.3. Top molecules regulated by Mstn			
Up	**Full gene name**	**Fold change**	**P-value**
BHLHE40	Basic helix-loop-helix family member e40	2.20	9.95E-04
CCL2	Chemokine (C-C motif) ligand 2	2.15	4.23E-06
ATP1B1	ATPase, Na+/K+ transporting, beta 1 polypeptide	2.13	2.31E-08
LDLRAD4	Low density lipoprotein receptor class A domain containing 4	1.89	1.49E-06
CCL20	Chemokine (C-C motif) ligand 20	1.87	1.20E-04
IL6	Interleukin 6	1.87	3.91E-06
IL1A	Interleukin 1, alpha	1.77	3.11E-06
TCF7	Transcription factor 7	1.72	2.16E-06
FAM101B	Family with sequence similarity 101, member B	1.72	3.10E-05
TGFB3	Transforming growth factor, beta 3	1.72	3.15E-05
Down	**Full gene name**	**Fold change**	**P-value**
FGFR4	Fibroblast growth factor receptor 4	-1.66	3.87E-06
KLF2	Kruppel-like factor 2	-1.61	5.59E-05
OSR2	Odd-skipped related 2	-1.60	1.36E-06
CTNND2	Catenin (cadherin- associated protein), delta 2	-1.56	4.66E-05
ATP2B1	ATPase, Ca2+ transporting, plasma membrane 1	-1.54	1.38E-03
PTX3	Pentraxin 3, long	-1.46	1.08E-03
CEBPA	CCAAT/enhancer binding protein (C/EBP), alpha	-1.42	6.81E-03
USP7	Ubiquitin-specific-processing protease 7	-1.39	2.05E-02
CPEB1	Cytoplasmic polyadenylation element binding protein 1	-1.38	1.25E-04
EPAS1	Endothelial PAS domain protein 1	-1.37	3.66E-03

Table 3.4. Top molecules regulated by MSV			
Up	**Full gene name**	**Fold change**	**P-value**
Saa3	Serum amyloid A1	32.85	8.69E-14
CCL20	Chemokine (C-C motif) ligand 20	17.55	7.68E-11
CCL2	Chemokine (C-C motif) ligand 2	7.30	4.43E-10
CXCL2	Chemokine (C-X-C motif) ligand 2	7.24	2.89E-08
CASP4	Caspase 4, apoptosis-related cysteine peptidase	4.96	7.86E-12
CHST9	Carbohydrate (N-acetylgalactosamine 4-0) sulfotransferase 9	4.47	1.21E-07
PTX3	Pentraxin 3, long	4.34	7.17E-09
RND1	Rho family GTPase 1	4.24	1.40E-07
ICAM1	Intercellular adhesion molecule 1	3.51	4.16E-08
IL6	Interleukin 6	3.46	5.70E-09
Down	**Full gene name**	**Fold change**	**P-value**
TGFB2	Transforming growth factor, beta 2	-2.38	2.88E-05
GYKL1	Glycerol kinase-like 1	-2.07	5.86E-08
MAP1B	Microtubule-associated protein 1B	-1.84	5.56E-04
ATP1B1	β1 subunit of the Na^+-K^+-ATPase	-1.84	1.93E-07
JUN	Jun oncogene	-1.75	9.92E-04
Chn2	Chimerin (chimaerin) 2	-1.71	3.65E-06
LRRC17	Leucine rich repeat containing 17	-1.69	1.30E-05
ATF3	Activating transcription factor 3	-1.66	6.67E-07
DAB2	Disabled homolog 2, mitogen-responsive phosphoprotein	-1.65	2.38E-05
FOXP2	Forkhead box P2	-1.61	7.95E-05

Table 3.3 and 3.4: Top Molecules differentially expressed following recombinant Mstn or MSV treatment. Shown here, are the top 10 up or down-regulated genes identified following treatment with Mstn (Table 3.3) or MSV (Table 3.4). The respective fold change (compared to control) and P-values are also presented.

Table 3.5: Predicted upstream regulators of recombinant Mstn. The table presented summarises the top 20 predicted upstream regulators (Ingenuity® Systems, www.ingenuity.com), for the gene expression changes associated with Mstn treatment in ovine myoblasts Regulators are ranked based on activation z-score. Also presented are the predicted activation state of the upstream regulator, the associated P-value (p-value of overlap), the number of target molecules downstream of the activator and the number of target molecules consistent with activation state (i.e. direction of regulation is consistent with predicted activation state. In the notes column the bias term appears, simply a biased data set is on that contains more up than down-regulated genes or vice versa.

Table 3.5. Predicted Upstream regulators of Mstn

Upstream Regulator	Fold Change	Molecule Type	Predicted Activation State	Activation z-score	Notes	p-value of overlap	# of target molecules	# of target molecules consistant with activation state.
PD98059		chemical - kinase inhibitor	Inhibited	-2.786	bias	1.33E-06	6	8
WNT3A		cytokine	Activated	2.588	bias	1.93E-08	7	7
TGFB1	1.060	growth factor	Activated	2.586		2.24E-05	11	9
IL1B	1.111	cytokine	Activated	2.566	bias	2.34E-05	8	7
E. coli B5 lipopolysaccharide		chemical	Activated	2.550	bias	1.12E-07	7	7
lipopolysaccharide		chemical drug	Activated	2.430	bias	2.81E-06	12	10
Cg		complex	Activated	2.423	bias	7.83E-06	6	6
NFkB (complex)		complex	Activated	2.396	bias	2.39E-05	7	6
F2	1.065	peptidase	Activated	2.345	bias	2.53E-06	6	6
FGF1	1.119	growth factor	Inhibited	-2.236		9.09E-07	8	5
STAT4	-1.098	transcription regulator	Activated	2.207	bias	2.20E-05	5	5
CD40LG	-1.105	cytokine	Activated	2.200	bias	3.44E-04	5	5
cycloheximide		chemical reagent	Activated	2.195		2.39E-04	5	5
poly rI:rC-RNA		chemical reagent	Activated	2.190	bias	3.52E-04	5	5
NR3C1	1.149	ligand-dependent nuclear receptor	Inhibited	-2.187		3.61E-04	5	5
Salmonella lipopolysaccharide		chemical toxicant	Activated	2.177	bias	7.39E-06	5	5
TLR3	-1.055	transmembrane receptor	Activated	2.162	bias	2.92E-05	5	5
OSM	1.017	cytokine	Activated	2.145		1.26E-03	5	5
TNF	1.167	cytokine	Activated	2.098	bias	1.80E-08	14	10
phorbol myristate acetate		chemical drug	Activated	2.041	bias	5.85E-04	7	6

Table 3.6: Predicted upstream regulators of recombinant MSV. The table presented summarises the top 20 predicted upstream regulators (Ingenuity® Systems, www.ingenuity.com) for the gene expression changes associated with MSV treatment in ovine myoblasts, regulators are ranked based on activation z-score. Also presented are the predicted activation state of the upstream regulator, the associated P-value (p-value of overlap), the number of target molecules downstream of the activator and the number of target molecules consistent with activation state (i.e. direction of regulation is consistent with predicted activation state. In the notes column the bias term appears, simply a biased data set is on that contains more up than down-regulated genes or vice versa.

Table 3.6. Predicted Upstream regulators of MSV

Upstream Regulator	Fold Change	Molecule Type	Predicted Activation State	Activation z-score	Notes	p-value of overlap	# of target molecules	# of target molecules consistant with activation state.
TNF	1.108	cytokine	Activated	5.400	bias	2.26E-31	52	44
IL1B	1.131	cytokine	Activated	4.791	bias	2.77E-33	43	36
NFkB (complex)		complex	Activated	4.787	bias	2.83E-27	34	28
lipopolysaccharide		chemical drug	Activated	4.467	bias	7.78E-23	45	34
RELA	1.026	transcription regulator	Activated	4.286	bias	9.58E-28	29	22
CHUK	1.154	kinase	Activated	4.078	bias	2.63E-20	20	18
MYD88	-1.002	other	Activated	3.981	bias	4.15E-18	19	17
IL1A	1.855	cytokine	Activated	3.891	bias	7.20E-23	22	20
poly rI:rC-RNA		chemical reagent	Activated	3.857	bias	1.35E-20	25	20
TICAM1		other	Activated	3.749	bias	3.75E-16	15	15
IL1		group	Activated	3.671	bias	1.30E-15	19	17
STAT1		transcription regulator	Activated	3.515	bias	1.90E-13	16	13
E. coli B5 lipopolysaccharide		chemical - endogenous non-mammalian	Activated	3.496	bias	1.99E-18	20	18
IKBKB	1.084	kinase	Activated	3.469	bias	1.36E-28	27	22
prostaglandin E2		chemical - endogenous mammalian	Activated	3.426		1.33E-17	20	18
IL17A	-1.160	cytokine	Activated	3.341	bias	1.88E-15	15	14
TLR4	1.128	transmembrane receptor	Activated	3.325	bias	2.51E-17	20	14
IFNG	1.086	cytokine	Activated	3.273	bias	8.84E-19	36	26
peptidoglycan		chemical - endogenous non-mammalian	Activated	3.250	bias	2.68E-12	11	11
Tlr		group	Activated	3.232	bias	5.94E-12	11	11

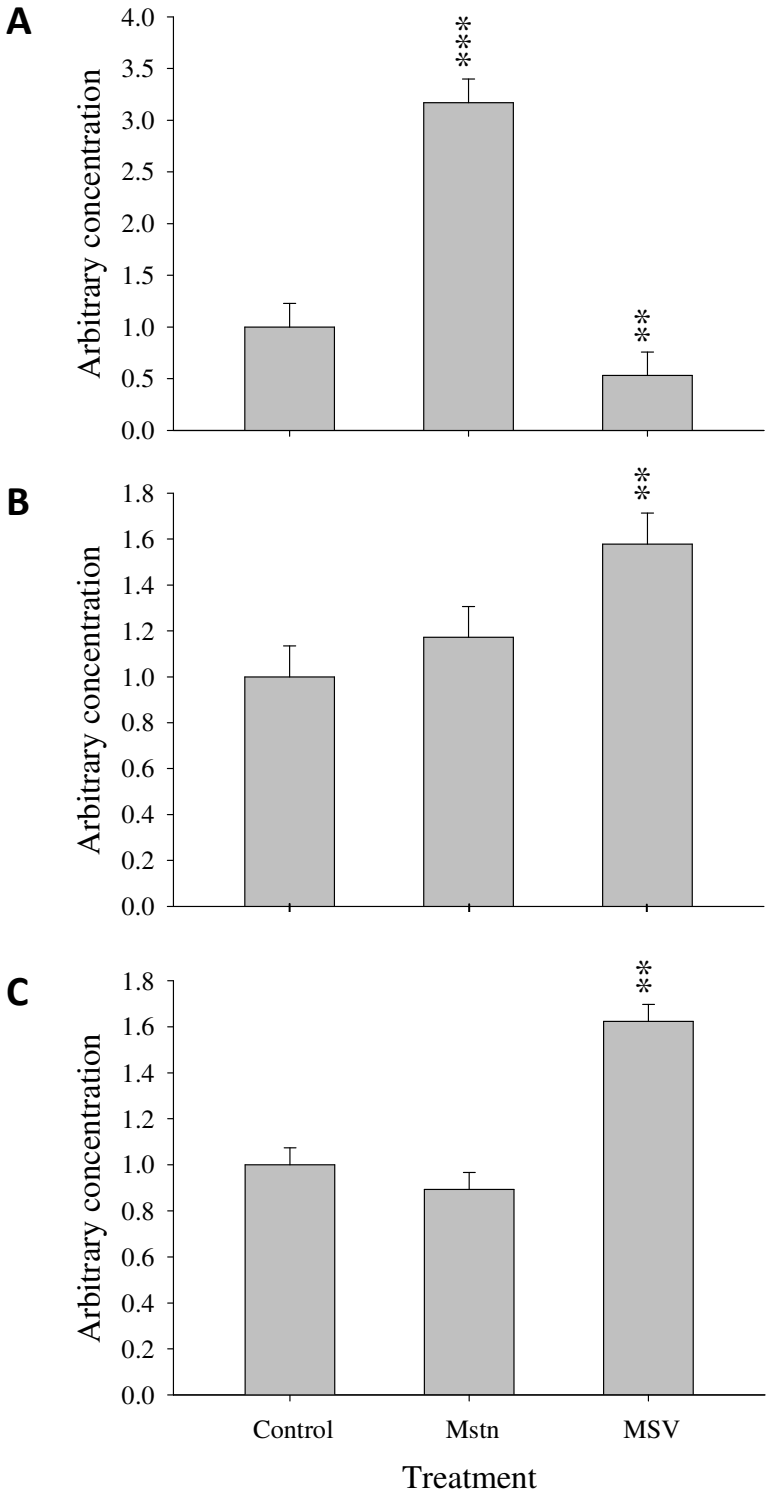

Figure 3.1: Confirmation of microarray differential expression. Concentrations of Na^+-K^+-ATPase (A), PDK3 (B) and p53 (C) mRNA, quantified using qPCR, were determined in microarray samples following treatment with recombinant Mstn, MSV or vehicle alone (control). Data presented are mean +/- SEM, asterisks denote significant differences from controls (vehicle), (**P<0.01, *** P<0.001), n=3 for each treatment. Concentrations were normalised to vehicle alone (control) values following adjustment to oligreen (total cDNA) values.

3.2.5.1 Concentration of endotoxin in the recombinant MSV preparation

Given the potential confounding influence that endotoxin may have in my myoblast cultures, the concentrations of endotoxin in the MSV preparation was assessed. Endotoxin was measured using the Lonza Limulus Amebocyte Lysate (LAL) Kinetic QCL kit (Cat# 50-650U). The assay data demonstrated that the MSV preparation contained a significant amount of endotoxin ~36470 EU (endotoxin units) /mL, which equated to ~300ng/mL of endotoxin in a 3 µg/mL MSV treatment.

3.2.5.2 Low concentrations of LPS stimulate ovine but not C_2C_{12} myoblast proliferation.

Once the presence of endotoxin was confirmed, my major concern was that the bioactivity associated with MSV, could in fact be due to contamination with endotoxin. Thus, it was prudent to assess the effect of endotoxin on both ovine and C_2C_{12} myoblasts using the methylene blue proliferation assay. Purified endotoxin (LPS) had a biphasic effect on the proliferation of ovine myoblasts. In these cells, concentrations of LPS between 1 ng and 10 µg/mL significantly increased myoblast proliferation, while higher concentrations inhibited myoblast proliferation (Figure 3.2). The C_2C_{12} cells exhibited a different response profile to the ovine myoblasts, with no response to lower LPS concentrations (<100 ng/mL), but high concentrations (1-300 µg/mL) significantly inhibited proliferation (Figure 3.2).

3.2.5.3 Purification of MSV

Once the presence of endotoxin had been confirmed in the MSV preparation, its removal became a primary focus. Two well described methods for the removal of endotoxin were used to address this problem. They were the use of a Polymyxin affinity resin (BioRad) and a detergent based phase separation using Triton X-114 (Sigma-Aldrich) as previously described (Liu, Tobias et al. 1997). The latter, was shown to be the most effective method for endotoxin removal. Purification of MSV was performed using these two methods (2.2.15), with the efficacy of each method validated using the Lonza LAL QCL kit. As shown in Figure 3.3, Polymyxin reduced the amount of endotoxin in the MSV preparation by approximately 75%. In contrast, Triton X-114 removed all traces of endotoxin from the MSV preparation. Both methods reduced the amount of protein in the

MSV preparation, with recoveries as assessed by BCA assay (2.2.19) of ~94% and 76% for polymyxin and Triton X-114 respectively (data not shown).

3.2.6 Proliferation of ovine and C_2C_{12} myoblasts with LPS free MSV

To determine the effect of MSV on the proliferation of myoblasts following Polymyxin or Triton X-114 purification, ovine and C_2C_{12} myoblasts were subjected to treatment with both treated and non-treated MSV. Proliferation was assessed using the methylene blue proliferation assay. For the ovine myoblasts, treated and non-treated LPS was included as an internal control for the purification process. As shown in Figure 3.3, ovine myoblasts had a significant increase in proliferation following exposure to untreated LPS (~20 %), and MSV (~25 %), at 100ng/mL and 10μg/mL, respectively ($P<0.001$). Treatment of ovine myoblasts with Polymyxin treated LPS and MSV also increased proliferation by ~18 % ($P<0.001$) and 25 % ($P<0.01$), respectively. In contrast, Triton X-114 treatment removed the proliferative response associated with both LPS and MSV in ovine myoblasts. For C_2C_{12} myoblasts, only MSV was tested, as previous data (Figure 3.1) had shown that proliferation is not increased in response to LPS. Untreated MSV increased the proliferation of C_2C_{12} cells by ~27 % ($P<0.001$), using 10 μg/mL of MSV. Similarly, polymyxin treated MSV induced an ~ 27% increase in proliferation ($P<0.001$). Triton X-114 treated MSV also stimulated the proliferation of C_2C_{12} myoblasts, with the largest increase of ~27% ($P<0.01$) observed at 3 μg/mL MSV.

3.2.7 MSV regulation of microarray targets differentially regulated by Mstn

The data obtained from the microarray analysis for ovine myoblasts treated with MSV was compromised by the presence of LPS in the MSV preparation. Thus, the Mstn component of this study provided the only reliable dataset following microarray analysis. In an effort to determine if genes that were differentially expressed following treatment with Mstn, were also altered by Triton X-114 treated MSV, five of the top up or down-regulated transcripts influenced by Mstn (as identified from the microarray analysis (Table 3.3)) were assessed using qPCR. Of the 10 targets selected, qPCR data was obtained for 7, with 3 primer sets yielding multiple unspecific PCR products following qPCR (data not shown) as thus, unreliable analysis. For the remaining targets qPCR analysis (Figure 4.13) showed that none of the targets initially thought to

regulated by MSV were altered following exposure to an endotoxin free preparation.

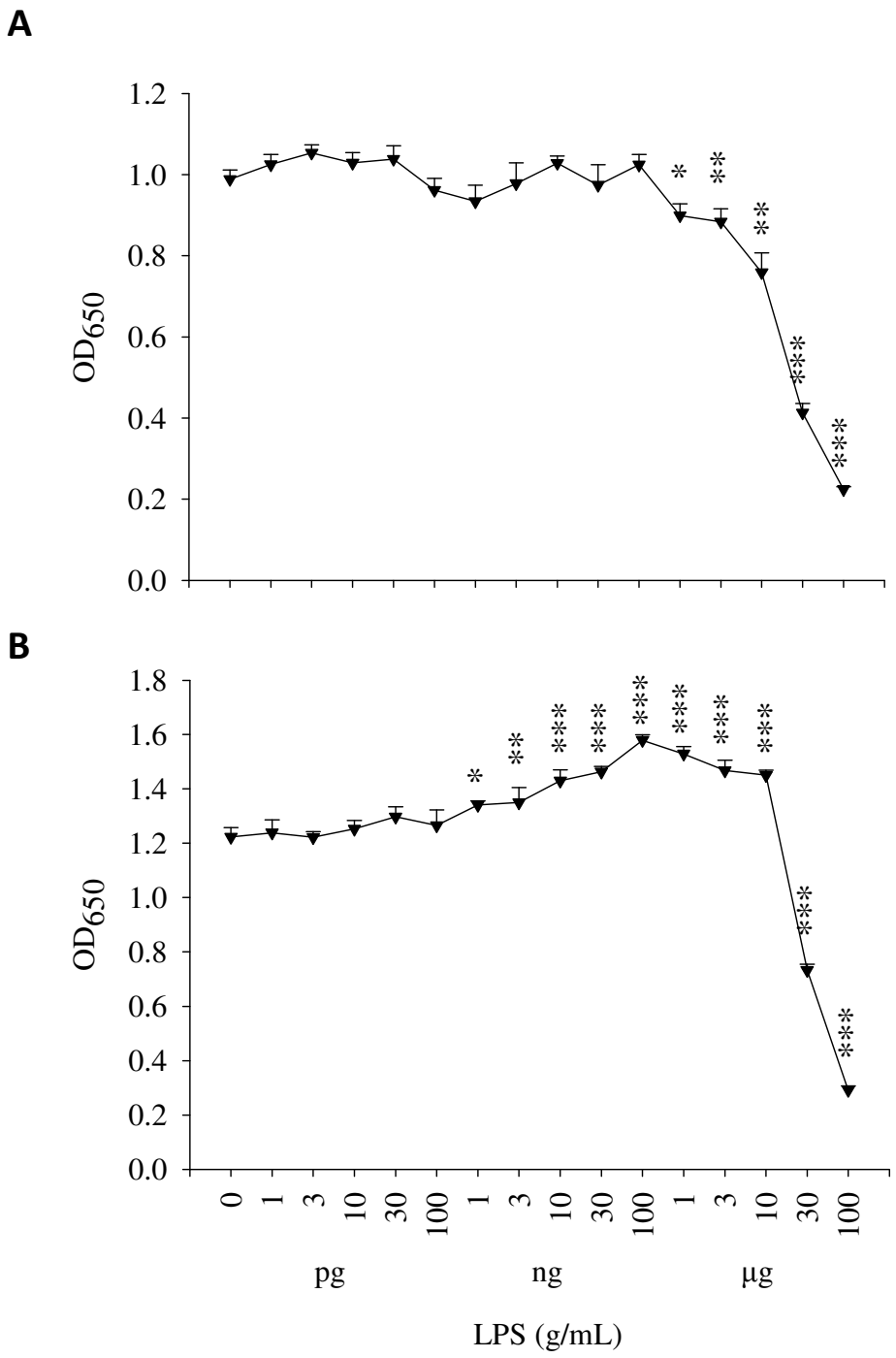

Figure 3.2: Effect of LPS on the proliferation ovine and C_2C_{12} myoblasts. Myoblasts were cultured in the presence of increasing concentrations of LPS. Proliferation was determined using the methylene blue proliferation assay at an OD of 650nM for C_2C_{12} (A) and ovine (B) cultures after 48h of proliferation. Data presented are mean +/- SEM, asterisks denote significant differences from vehicle controls at each LPS concentration (*P<0.05, **P<0.01, *** P<0.001). N=6 replicates per LPS concentration.

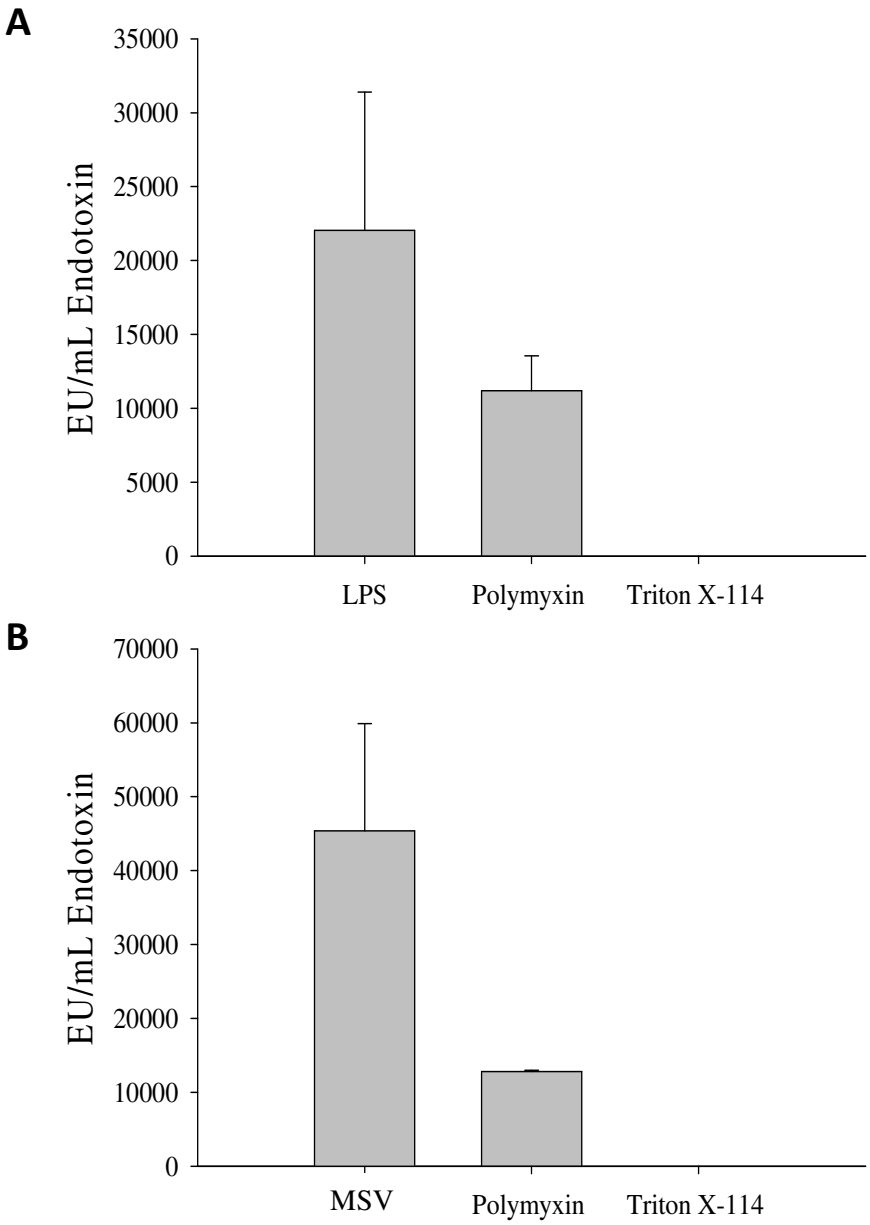

Figure 3.3: The concentrations of Endotoxin following purification of recombinant MSV or LPS solutions. Endotoxin concentration of untreated and polymyxin or Triton X-114 treated LPS (A) or MSV (B) solutions, was determined using the LAL assay. Samples were assayed in duplicate, with the untreated LPS solution at a concentration of 1 mg/mL. Data presented are mean **+/-** SEM.

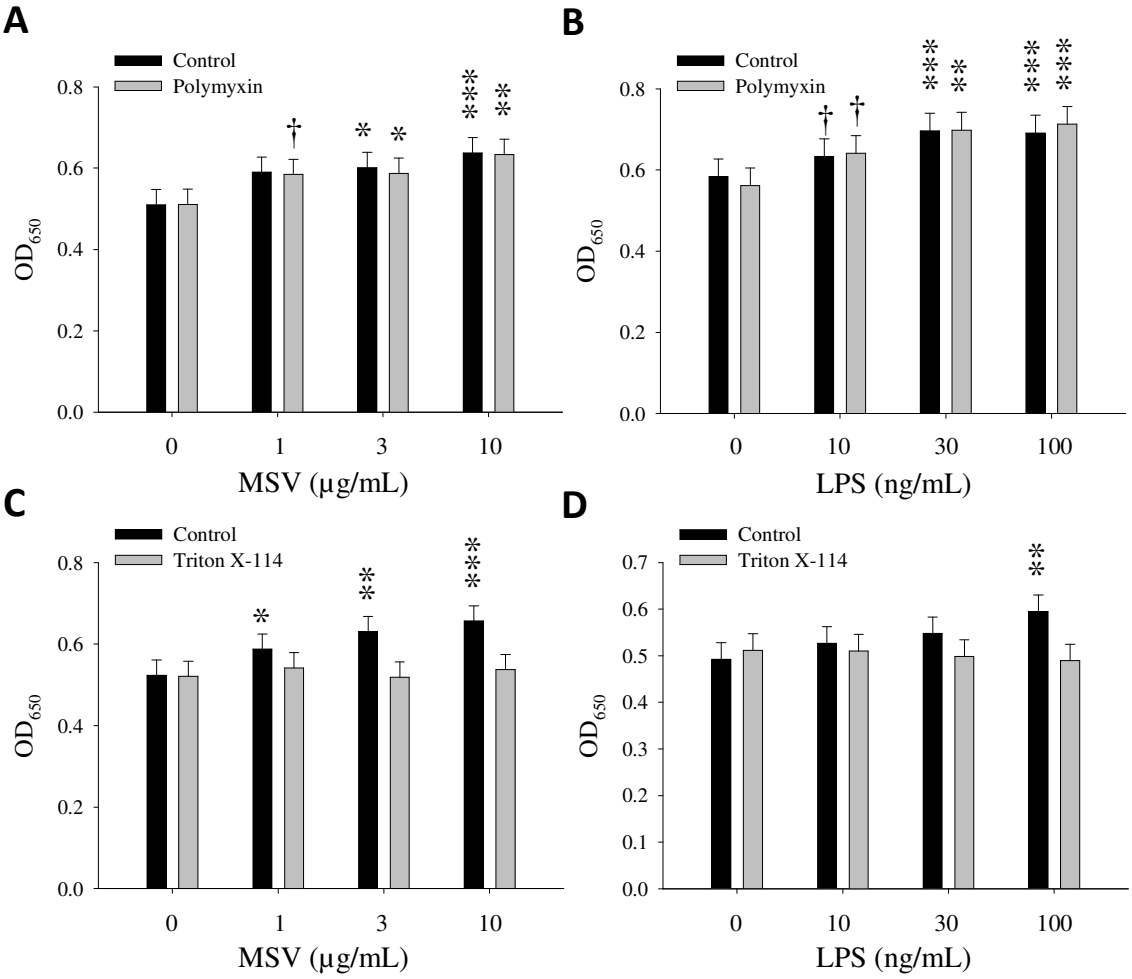

Figure 3.4: Proliferation of Ovine myoblasts exposed to MSV and LPS that was treated with Polymyxin or Triton X-114. Myoblasts were cultured in the presence of increasing concentrations of untreated or treated LPS or MSV. Proliferation was determined after 48 h of culture using the methylene blue proliferation assay at an OD of 650nM. This was done for MSV and LPS treated with Polymyxin, (A) and (B) respectively and MSV and LPS treated with Triton X-114, (C) and (D) respectively. Data presented are mean +/- SEM, asterisks denote significant differences from vehicle controls at each concentration of LPS or MSV (†P<0.1, *P<0.05, **P<0.01, *** P<0.001). N=8 replicates per concentration of LPS or MSV.

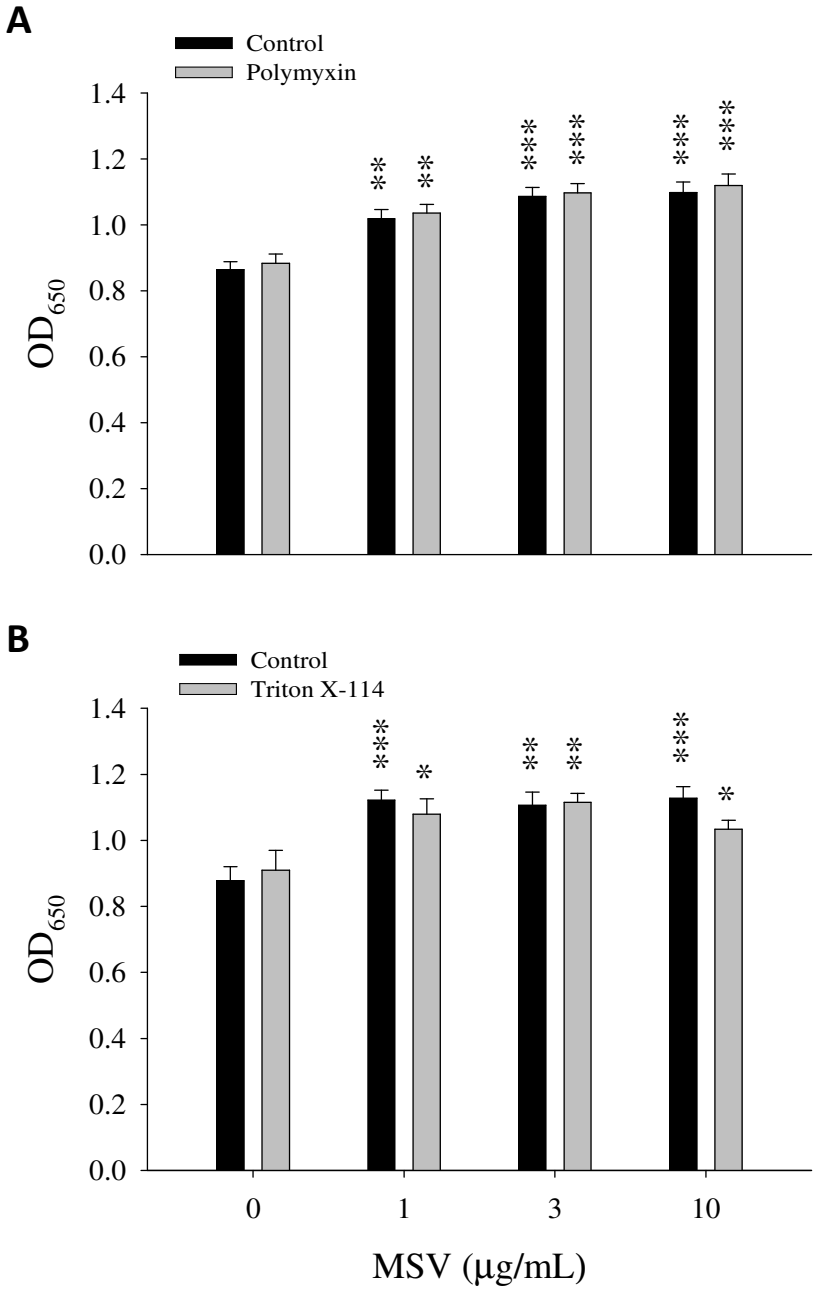

Figure 3.5: Proliferation of C_2C_{12} myoblast exposed to MSV that was treated with Polymyxin or Triton X-114. Myoblasts were cultured in the presence of increasing concentrations of treated or non-treated MSV. Proliferation was determined after 48 h of culture using the methylene blue proliferation assay at an OD of 650nM. This was done for MSV treated with Polymyxin, (A), and MSV treated with Triton X-114 (B). Data presented are mean +/- SEM, asterisks denote significant differences from vehicle controls (0) at each LPS or MSV concentration (†P<0.1, *P<0.05, **P<0.01, *** P<0.001). N=8 replicates per LPS or MSV concentration.

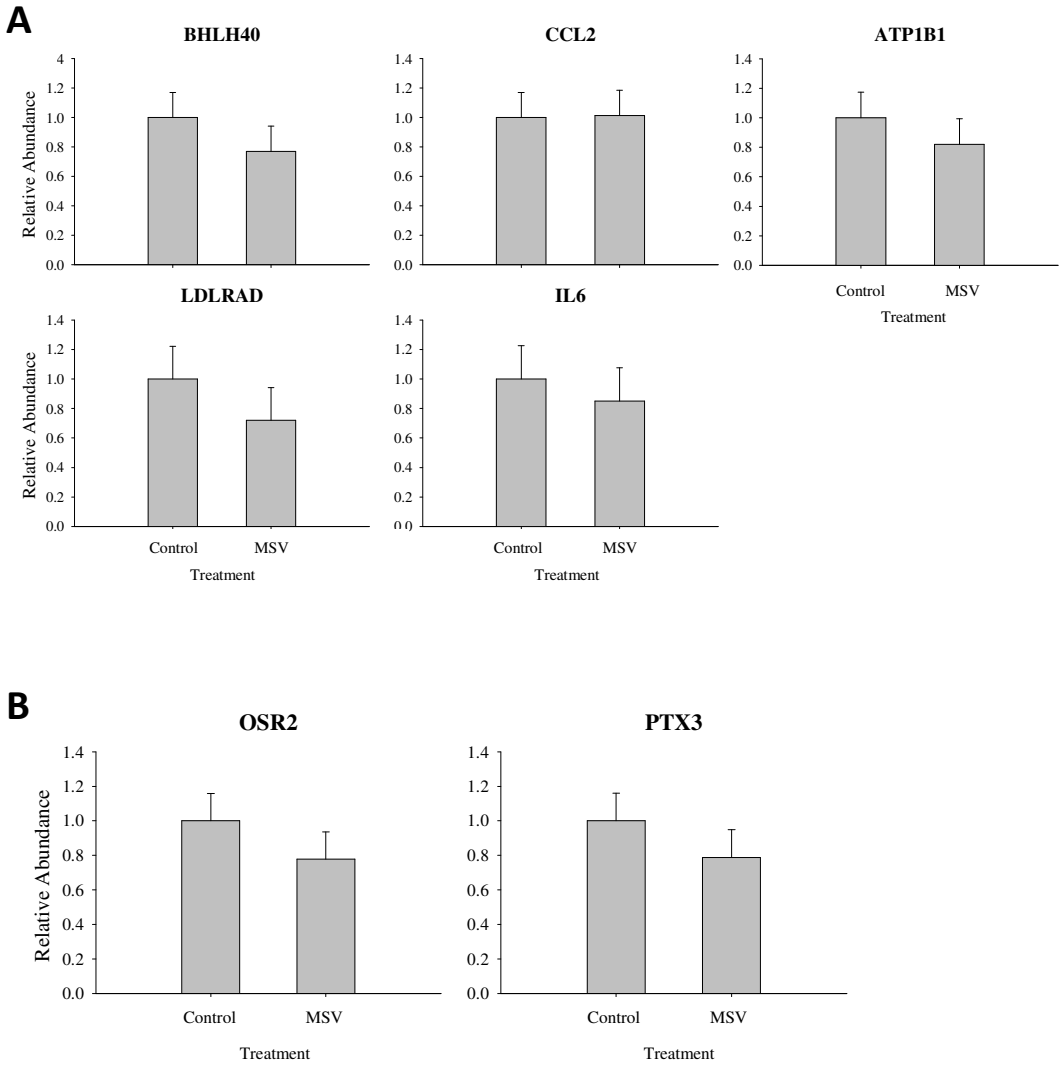

Figure 3.6: Effect of Triton-X 114 treated MSV on a selection of the top Mstn regulated transcripts (microarray) in ovine myoblasts. Using qPCR 7 of the top transcripts regulated by Mstn (from microarray analysis) were assessed in ovine myoblasts following treatment with 3 µg/mL MSV for 6 h. Shown in (A), transcripts that were increased following treatment with Mstn and in (B) decreased following treatment with Mstn (as evidenced by microarray data). Relative abundance was calculated by normalising values for MSV treatment to those of controls, with n=3 for each treatment.

3.3 Discussion

Using microarray and IPA analyses, the changes in gene expression associated with Mstn and MSV treatment in ovine myoblasts was investigated. Both proteins induced significant gene expression changes after a 6 h treatment, and the integrity of the microarray data was confirmed by the validation of the metabolic targets using qPCR. With the use of IPA, the top biological functions associated with Mstn treatment appeared consistent with Mstn function. These included the regulation of genes involved in skeletal muscle disorders, cellular growth and proliferation, cellular development, the cell cycle and skeletal and muscular system development and function. The response to MSV on the other hand did not display any top biological functions associated with skeletal muscle. Rather, MSV induced changes in gene expression that had a greater connectivity with inflammatory responses, with three functions similar to those identified for Mstn (cellular movement, cellular growth and proliferation and the inflammatory response). Identification of the inflammatory response as a top biological function was a concern with 45 genes up-regulated by MSV vs. 9 for Mstn. Therefore, the purity of the MSV preparation was questioned. This was due primarily to the fact that it had been produced in *E. coli*, and no prior steps were taken to ensure it was LPS free. This was not a concern with the commercial Mstn preparation, which is produced in a eukaryotic system and has certified low concentrations of endotoxin (<0.1 EU/µg protein). Upon investigating the top 10 genes up-regulated by MSV treatment, 8 have been previously shown to be regulated by LPS as opposed to 4 in the Mstn top 10 (Ingenuity® Systems, www.ingenuity.com). Interestingly, IPA upstream regulator analysis predicted LPS as an upstream regulator for both datasets, with MSV regulating 34 out of 45 and Mstn 10 out 12 identified LPS target genes from their respective data sets, in a manner consistent with LPS as an upstream activator. However, there were key differences in this analysis indicating that the regulation of Mstn targets occurred via different mechanisms. Importantly, the MSV data set also identified Toll like receptor 4 (TLR4), the LPS receptor, as an upstream regulator. In addition, TGFβ1, a close relative of Mstn, was identified as an upstream regulator in the Mstn but not the MSV data set. This is of particular importance, as activation of this pathway can regulate 7 of the 10 LPS target genes (referred to above) identified in the Mstn analysis, with the remaining three not influenced by MSV treatment in this analysis (data not

shown), illustrating that the changes induced following exposure to Mstn are consistent with TGF-β treatment.

Following my discovery that recombinant MSV preparations were likely to be contaminated with endotoxin, the extent of this problem had to be investigated. This required firstly determining if endotoxin could regulate the proliferation of myoblasts and, secondly, the removal of endotoxin from the MSV preparation. LPS significantly increased the proliferation of ovine myoblasts at concentrations consistent with those observed in the MSV preparation using the LAL assay. This had significant consequences on my interpretation of the microarray data. With no clear way to discriminate between an LPS and/or an MSV dependent target, the Mstn data was the only reliable portion of this analysis. As the differential regulation of the β1 subunit of the Na^+-K^+-ATPase by both Mstn and MSV containing LPS (Figure 3.1) had been confirmed, this target was selected for further investigation from the Mstn perspective (Chapter 5). This and other Mstn targets would be investigated following treatment with MSV, once an endotoxin free preparation was available. To determine if the purified MSV preparation influenced the transcription of Mstn targets identified from the microarray analysis, primers for qPCR were designed to amplify top molecules regulated by Mstn. Purified MSV did not alter the transcription of any of the top molecules influenced by Mstn that were investigated in this study.

Following the determination of the endotoxin concentration present in the MSV preparation, its removal became a strong focus. The use of Polymyxin resin and Triton X-114 phase separation were used as established methods for the removal endotoxin from bacterially produced recombinant proteins. Polymyxin reduced the concentration of endotoxin present in the MSV preparation by ~75%, but not enough to warrant its use as a purification method. Purification with Triton X-114 reduced endotoxin content to undetectable levels. However, this method introduced a caveat for ongoing studies using this preparation. This is due to residual Triton X-114 remaining in the preparation, which could potentially alter protein folding, have bioactivity of its own or interfere with the MSV contained in this preparation. This was addressed by including dialysis buffer and LPS solutions that had also been subjected to Triton X-114 as controls where appropriate. Given that concentration of endotoxin in the Triton X-114 purified

MSV was zero, this method was chosen to purify MSV for further investigations. It is noteworthy here that purification with Polymyxin was performed with a single incubation with MSV, while Triton X-114 involved 4 phase separations (see 2.2.16). Thus, it is possible that a refined Polymyxin protocol could yield similar results to that of Triton X-114. However, concerns regarding the use of Triton X-114 were lessened from other studies reporting that proteins treated with Triton X-114 maintain bioactivity in binding as well as physiological studies (Liu, Tobias et al. 1997; Magalhaes, Lopes et al. 2007). Furthermore, residual Triton X-114 is reported to be less than 0.018% (Aida and Pabst 1990).

The proliferative response was the first bioassay used to determine if the LPS free MSV had retained its bioactivity. Interestingly, proliferation assays showed that the MSV preparation could still stimulate $C_2C_{12,}$ but not ovine myoblast proliferation as previously shown (unpublished data). This was done in parallel with a purified LPS preparation to ensure the Triton X-114 procedure yielded endotoxin free and biologically inactive medium. The species specific response to the MSV, suggests that there may be differing mechanisms that convey the function of MSV in myoblasts. Alternatively, primary ovine myoblasts may be more sensitive to residual Triton X-114 as compared to the immortalised C_2C_{12} cells. Importantly, this resulted in a purified MSV preparation that could be used for signal transduction and metabolic studies in ovine myoblasts.

Chapter Four

4 The effect of Mstn and MSV on signal transduction in ovine myoblasts.

4.1 Introduction

The signal transduction mechanisms that Mstn induces, give this molecule the ability to regulate gene transcription in myoblasts and to ultimately play a major functional role in the growth and development of skeletal muscle (see 1.1.7.4-6). The binding of mature Mstn to activin type IIB receptors activates a number of signal transduction cascades, in conjunction with non-canonical signalling, these events culminate in the inhibition of myoblast proliferation, reduced synthesis of protein and ultimately reduced myogenesis. Given that recombinant MSV can interact directly with Mstn and with the type IIB activin receptor (Jeanplong, Falconer et al. 2013), It was anticipated that MSV would influence or block signal transduction pathways activated by Mstn. Therefore the aim of the studies in this chapter was to determine the pathways through which MSV signals in ovine myoblasts in comparison to those known for Mstn.

One of the major setbacks faced while conducting the experiments in this chapter, was the presence of endotoxin in the MSV preparation. As detailed in the previous chapter we had success in removing this contaminant from the MSV preparation. Unfortunately, this was not before ovine myoblasts had been treated for the first signalling experiment presented in this chapter. Therefore, data are presented for the signalling pathways activated by Mstn in the first experiment. Then, data are presented for MSV, following the treatment of myoblasts with a preparation that was free of endotoxin. This allowed comparison of the signal transduction pathways as influenced following treatment with Mstn or MSV. In addition, the generation of stable C_2C_{12} myoblasts expressing MSV provided a eukaryotic model for investigating MSV function and signalling, while circumventing the issues associated with the use of recombinant protein, and is presented in Chapter 6.

4.2 Results

4.2.1 Mstn signalling in ovine myoblasts

To identify the early signalling events associated with the presence of Mstn on, cytoplasmic and nuclear enriched protein lysates were isolated following a 1 h treatment of ovine myoblasts. Western blot analysis was used to determine the relative abundance of multiple intracellular targets. These included the major transcription factors that control myogenesis, signalling molecules in the TGF-β, MAPK and PI3K signalling cascades and targets involved in regulation of the cell cycle and cellular metabolism.

4.2.1.1 Myogenic transcription factors

Previous studies have identified a role for Mstn in the regulation of transcription factors with well-established roles in myogenesis (1.1.7). To determine if Mstn altered the abundance of major myogenic transcription factors, the relative abundance of MyoD, Myf5, MRF4, myogenin, Pax7 and Mef2 was determined using western blot analysis. As shown in Figure 4.1, cytoplasmic lysates isolated from myoblasts treated with Mstn had an increased abundance of MyoD (~1.3 fold, $P<0.05$) and MRF4 (~1.6 fold, $P<0.01$), with a decrease in the abundance of Myf5 (~0.65 fold, $P<0.05$). No change was observed in the abundance of Myogenin, Mef2 or Pax7. Mstn also increased the abundance of MyoD (~1.7 fold, $P<0.01$), Mef2 (~3 fold, $P<0.01$) and Pax7 (~5.2 fold, $P<0.05$) in nuclear enriched lysates, with no changes observed in the abundance of MRF4, Myogenin or Myf5 (Figure 4.2).

4.2.1.2 Canonical Mstn signalling

To confirm that canonical Mstn signalling was induced in ovine myoblasts treated with Mstn, the relative abundance of total and phosphorylated Smad 2/3 was determined. There was no change in the abundance or phosphorylation of Smad 2 or 3 in cytoplasmic lysates (Figure 4.3). Consistent with the data from cytoplasmic lysates, there was no change in the abundance of total Smad 2 or 3 in nuclear enriched lysates. However, as shown in Figure 4.3 (B, F), treatment with Mstn increased the abundance of phosphorylated Smad 2 (~1.8 fold, $P<0.05$) in nuclear enriched lysates, while phosphorylated Smad 3 was not detected in this study.

4.2.1.3 PI3K/AKT Signalling

Mstn has a well-established role in regulating the activity of the PI3K/AKT signalling cascade (1.1.7.5). To establish if the Mstn treatment of ovine myoblasts altered the abundance or the phosphorylation of molecules in the PI3K/AKT signalling cascade, the abundance and phosphorylation of AKT and its major upstream kinase PDK1 were assessed. As shown in Figure 4.4, treatment with Mstn decreased total cytoplasmic AKT (~0.9 fold, $P<0.05$), had no effect on the phosphorylation of AKT at threonine (T) 308, but increased the phosphorylation of AKT at serine (S) 473 (~1.7 fold, $P<0.001$). Total PDK1 was increased by Mstn treatment (~1.2 fold, $P<0.05$) with no change in the phosphorylation of PDK1. In nuclear enriched lysates (Figure 4.5), Mstn treatment increased both total AKT and phosphorylated of AKT^{S473} (~2 fold, $P<0.05$ and ~1.6 fold, $P<0.05$, respectively), with no change observed in the phosphorylation of AKT^{T308}. Finally, treatment with Mstn did not alter the abundance or the phosphorylation of PDK1 in nuclear enriched lysates.

4.2.1.4 MAPK signalling

Mstn has been previously shown to signal through MAPK signalling pathways, targeting both ERK and p38 MAPK signalling intermediates (see section 1.1.7.5). To determine if Mstn signals through these MAPK pathways in ovine myoblasts, the abundance and phosphorylation of these molecules was determined in cytoplasmic and nuclear enriched lysates. In cytoplasmic lysates, Mstn treatment did not alter the abundance of total ERK1, ERK2 or p38. In contrast, as shown in Figure 4.6, Mstn treatment altered the phosphorylation of these molecules, with increases observed in the phosphorylation of ERK1 (~1.4 fold, $P<0.001$), ERK 2 (~1.7 fold, $P<0.001$, respectively), and p38 (~2 fold, $P<0.01$). Data from nuclear enriched lysates (Figure 4.7) were more variable, with an increase in the abundance of total ERK1 (~2 fold, $P<0.05$), and a tendency towards increased ERK2 and p38 (~1.5 fold, $P<0.1$ and ~4.4 fold, $P<0.1$, respectively). In terms of the phosphorylation of MAPK intermediates, only the phosphorylation of ERK2 was increased in nuclear enriched lysates (~1.6 fold, $P<0.05$), with no change in the abundance of phosphorylated ERK1, and no detection of phosphorylated p38.

4.2.1.5 Metabolic targets

Although it is clear that Mstn plays a functional role in metabolism of skeletal muscle (see 1.1.7.6), the early signal transduction events through which Mstn initiates metabolic change, especially in ruminant myoblasts, is not well understood. Thus, the ability of Mstn to regulate the abundance and phosphorylation of major effectors of metabolic change in skeletal muscle was investigated. Included for analysis were AMPK and its downstream effector ACC. This system has been shown to be influenced by Mstn and play a major role in the control of cellular metabolism (Chen, Ye et al. 2010; Zhang, McFarlane et al. 2011). Also included in this section are 4EBP1, rpS6 and p70S6K (an upstream kinase that plays a role in the phosphorylation of rpS6 and 4EBP1). These molecules play a role in the regulation of protein synthesis, a major point of control for cellular metabolism. In addition, the phosphorylation of these molecules can be influenced through both the PI3K and/or MAPK signalling pathways (Roux, Shahbazian et al. 2007). Mstn treatment did not alter the abundance or the phosphorylation of AMPK or its downstream target ACC in cytoplasmic lysates (Figure 4.8). Mstn treatment did not alter the abundance, but increased the phosphorylation of rpS6 (~1.3 fold, $P<0.05$), Mstn also increased 4EBP1 (~1.6 fold, $P<0.01$), with no change in the phosphorylation of 4EBP1 in cytoplasmic lysates (Figure 4.8). Finally, Mstn treatment did not alter the abundance p70S6K, but increased the phosphorylation of p70S6K at threonine (T) 389 (~1.8, $P<0.01$) in cytoplasmic lysates (Figure 4.8). Mstn treatment had a tendency to increase the abundance of rpS6 (~1.9 fold, $P<0.1$) and increased the phosphorylation of rpS6 (~1.5 fold, $P<0.05$) in nuclear enriched lysates (Figure 4.9). Mstn did not alter the abundance, but increased the phosphorylation of 4EBP1 (~1.9 fold, $P<0.01$). Mstn tended to increase the abundance of p70S6K (~2 fold, $P<0.1$), and increased phosphorylation of p70S6K at T389 (~2 fold, $P<0.05$) in nuclear enriched lysates. The abundance of AMPK and ACC were not determined in nuclear enriched lysates.

4.2.1.6 Cell cycle

Mstn has been shown to regulate the expression of the cell cycle regulators Cyclin E and Cdk2 in muscle precursor cells (Langley, Thomas et al. 2004). Thus, the relative abundance of Cyclin E and Cdk2 was assessed to establish if

treatment with Mstn altered the abundance of these cell cycle regulators in ovine myoblasts. As shown in Figure 4.10, Mstn did not alter the abundance of cyclin E or Cdk2 in cytoplasmic lysates. In nuclear enriched lysates Cyclin E was unchanged, while Cdk2 was increased (~1.6 fold, $P<0.05$) following Mstn treatment (Figure 4.10).

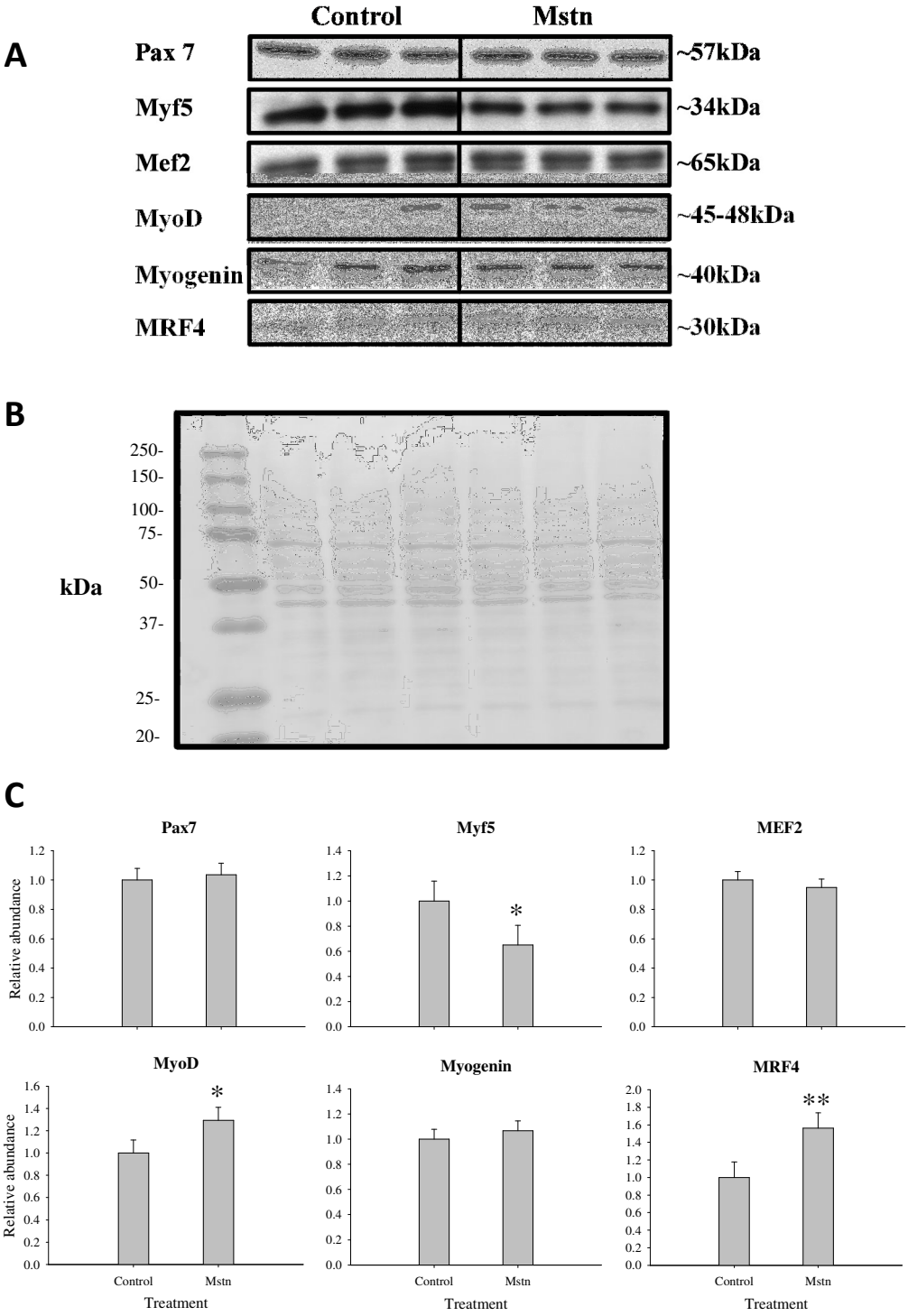

Figure 4.1: Abundance of myogenic transcription factors in the cytoplasmic lysates of ovine myoblasts treated with Mstn. For western blot analysis, cytoplasmic lysates were isolated from ovine myoblasts treated with vehicle (controls) or 100 ng/mL of Mstn for 1 h. Isolated protein (10 µg per sample) was run on a SDS/PAGE gel and blotted onto nitrocellulose. Immunoblots were performed for the depicted proteins (A), with representatives (n=3) shown. Blots were then exposed to autoradiographic film to capture the chemiluminescent signal. Equal loading of protein samples was assessed using Ponceau stain, with a representative blot shown in (B). The optical density of individual bands was obtained using a GS800 scanning densitometer and Quantity One software (BioRad). Relative abundance (C) was calculated by normalising the density values obtained from the cells treated with Mstn to those of their control counterparts. Normalised data presented are mean +/- SEM, asterisks denote significant differences between ovine myoblasts treated with Mstn and controls, with: *P<0.05, **P<0.01, n=6 replicates per treatment.

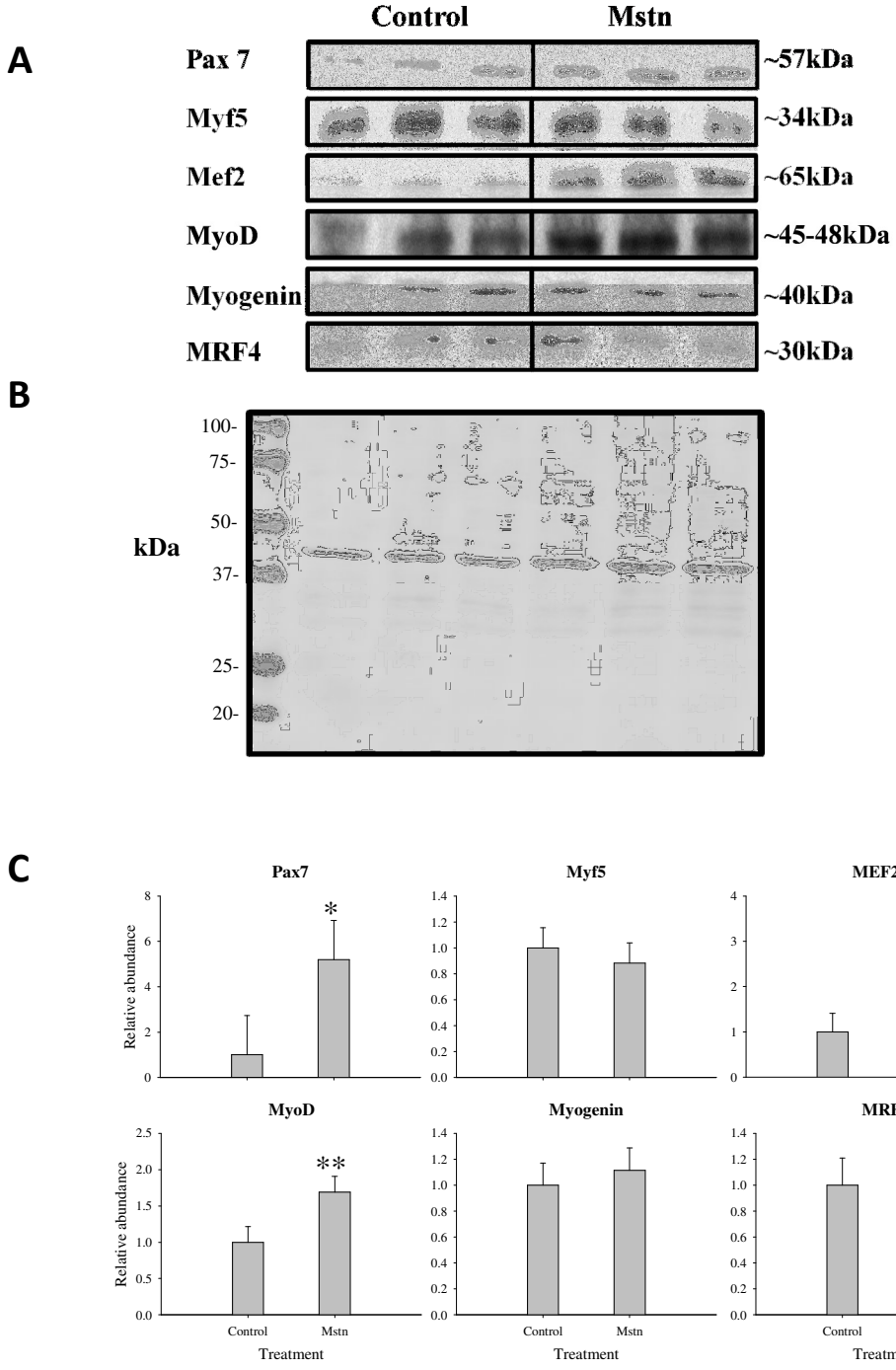

Figure 4.2: Abundance of myogenic transcription factors in the nuclear enriched lysates of ovine myoblasts treated with Mstn. For western blot analysis, nuclear enriched lysates were isolated from ovine myoblasts treated with vehicle (controls) or 100 ng/mL of Mstn for 1 h. Isolated protein (5 µg per sample) was run on a SDS/PAGE gel and blotted onto nitrocellulose. Immunoblots were performed for the depicted proteins (A), with representatives (n=3) shown. Blots were then exposed to autoradiographic film to capture the chemiluminescent signal. Equal loading of protein samples was assessed using Ponceau stain, with a representative blot shown in (B). The optical density of individual bands was obtained using a GS800 scanning densitometer and Quantity One software (BioRad). Relative abundance (C) was calculated by normalising the density values obtained from the cells treated with Mstn to those of their control counterparts. Normalised data presented are mean +/- SEM, asterisks denote significant differences between ovine myoblasts treated with Mstn and controls, with: *P<0.05, **P<0.01, n=6 replicates per treatment.

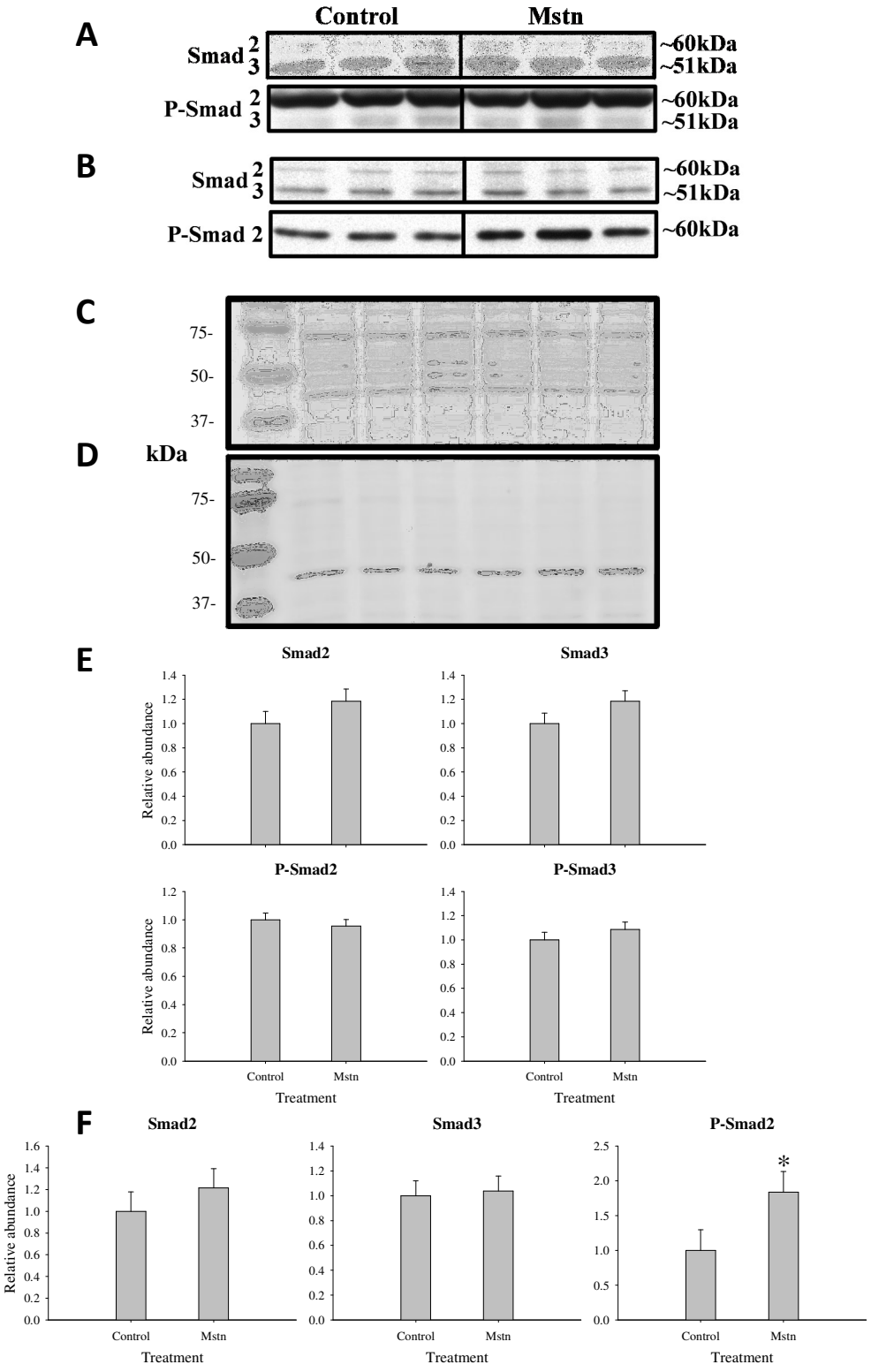

Figure 4.3: Abundance of Smad2/3 transcription factors in the cytoplasmic and nuclear enriched lysates of ovine myoblasts treated with Mstn. For western blot analysis, 10 µg of cytoplasmic, or 5 µg of nuclear enriched lysate that was isolated from ovine myoblasts treated with vehicle (control) or 100 ng/mL of Mstn for 1 h, was run on SDS/PAGE gels and blotted onto nitrocellulose. Immunoblots were performed for the depicted proteins, with representatives (n=3) shown for cytoplasmic (A) and nuclear enriched lysates (B). Blots were then exposed to autoradiographic film to capture the chemiluminescent signal. Equal loading of protein samples was assessed using Ponceau stain, with a representative blot shown for cytoplasmic (C), and nuclear enriched (D) lysates. The optical density of individual bands was obtained using a GS800 scanning densitometer and Quantity One software (BioRad). Relative abundance was calculated by normalising the density values obtained from the cells treated with Mstn to those of their control counterparts for cytoplasmic (E) and nuclear enriched (F) lysates. Normalised data presented are mean +/- SEM, asterisks denote significant differences between ovine myoblasts treated with Mstn and controls, with: *P<0.05, n=6 replicates per treatment.

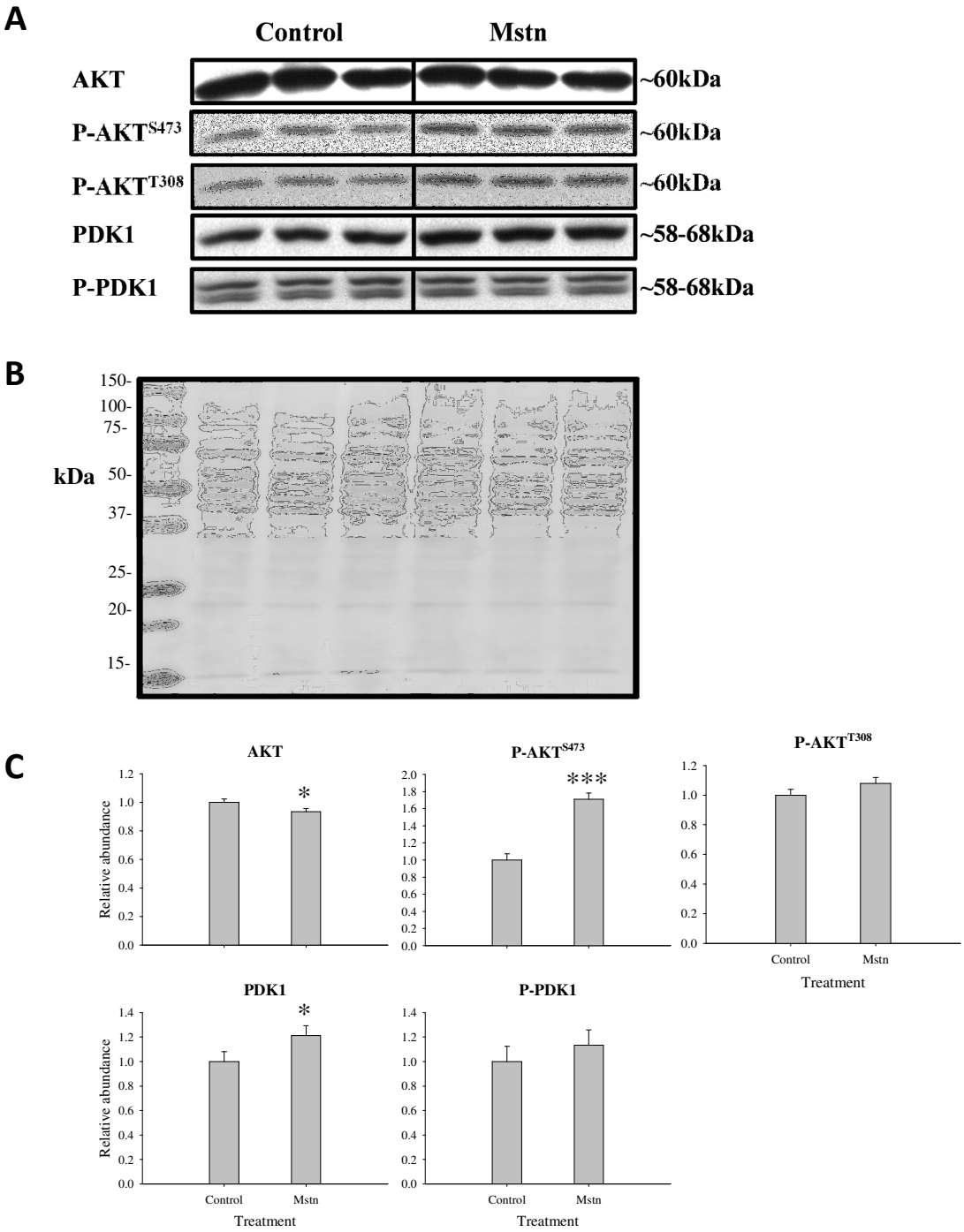

Figure 4.4: Abundance of PI3K/AKT targets in the cytoplasmic lysates of ovine myoblasts treated with Mstn. For western blot analysis, cytoplasmic lysates were isolated from ovine myoblasts treated with vehicle (controls) or 100 ng/mL of Mstn for 1 h. Isolated protein (10 µg per sample) was run on a SDS/PAGE gel and blotted onto nitrocellulose. Immunoblots were performed for the depicted proteins (A), with representatives (n=3) shown. Blots were then exposed to autoradiographic film to capture the chemiluminescent signal. Equal loading of protein samples was assessed using Ponceau stain, with a representative blot shown in (B). The optical density of individual bands was obtained using a GS800 scanning densitometer and Quantity One software (BioRad). Relative abundance (C) was calculated by normalising the density values obtained from the cells treated with Mstn to those of their control counterparts. Normalised data presented are mean +/- SEM, asterisks denote significant differences between ovine myoblasts treated with Mstn and controls, with: *P<0.05, ***P<0.001, n=6 replicates per treatment.

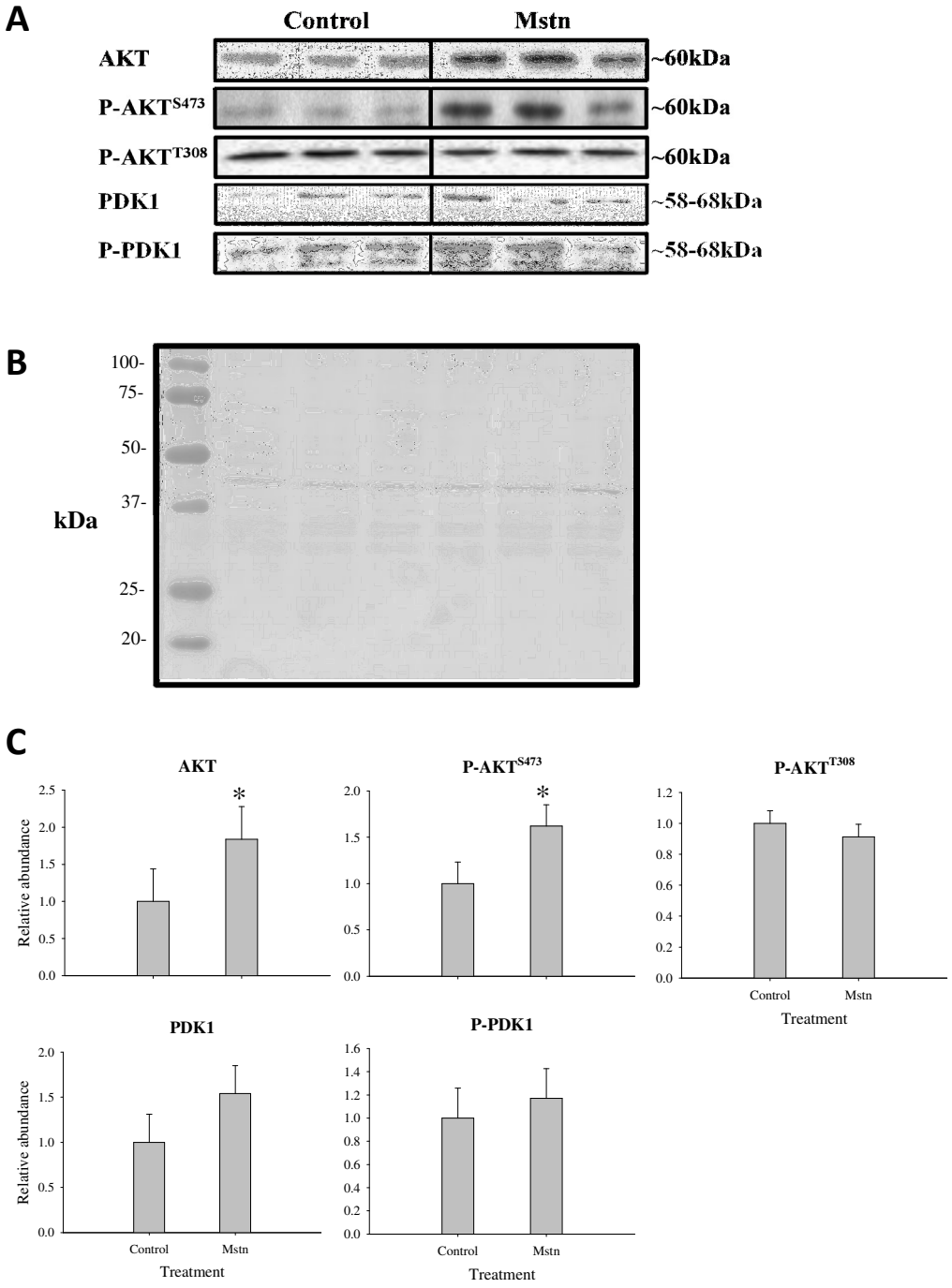

Figure 4.5: Abundance of PI3K/AKT targets in the nuclear enriched lysates of ovine myoblasts treated with Mstn. For western blot analysis nuclear enriched lysates were isolated from ovine myoblasts treated with vehicle (controls) or 100 ng/mL of Mstn for 1 h. Isolated protein (5 µg per sample) was run on a SDS/PAGE gel and blotted onto nitrocellulose. Immunoblots were performed for the depicted proteins (A), with representatives (n=3) shown. Blots were then exposed to autoradiographic film to capture the chemiluminescent signal. Equal loading of protein samples was assessed using Ponceau stain, with a representative blot shown in (B). The optical density of individual bands was obtained using a GS800 scanning densitometer and Quantity One software (BioRad). Relative abundance (C) was calculated by normalising the density values obtained from the cells treated with Mstn to those of their control counterparts. Normalised data presented are mean +/- SEM, asterisks denote significant differences between ovine myoblasts treated with Mstn and controls, with: *P<0.05, n=6 replicates per treatment.

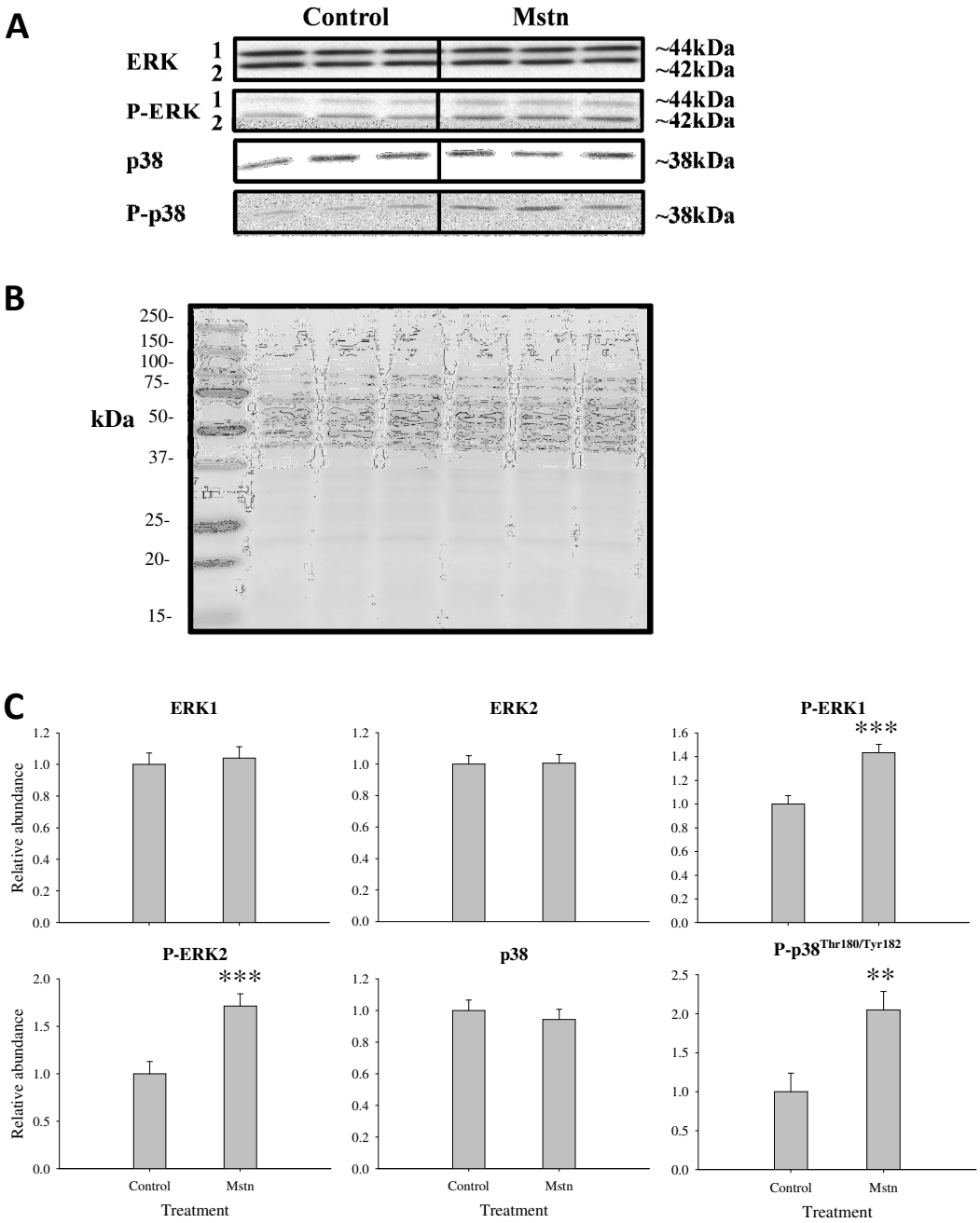

Figure 4.6: Abundance of MAPK targets in the cytoplasmic lysates of ovine myoblasts treated with Mstn. For western blot analysis, cytoplasmic lystates were isolated from ovine myoblasts treated with vehicle (controls) or 100 ng/mL of Mstn for 1 h. Isolated protein (10 µg per sample) was run on a SDS/PAGE gel and blotted onto nitrocellulose. Immunoblots were performed for the depicted proteins (A), with representatives (n=3) shown. Blots were then exposed to autoradiographic film to capture the chemiluminescent signal. Equal loading of protein samples was assessed using Ponceau stain, with a representative blot shown in (B). The optical density of individual bands was obtained using a GS800 scanning densitometer and Quantity One software (BioRad). Relative abundance (C) was calculated by normalising the density values obtained from the cells treated with Mstn to those of their control counterparts. Normalised data presented are mean +/- SEM, asterisks denote significant differences between ovine myoblasts treated with Mstn and controls, with: **P<0.01, ***P<0.001, n=6 replicates per treatment.

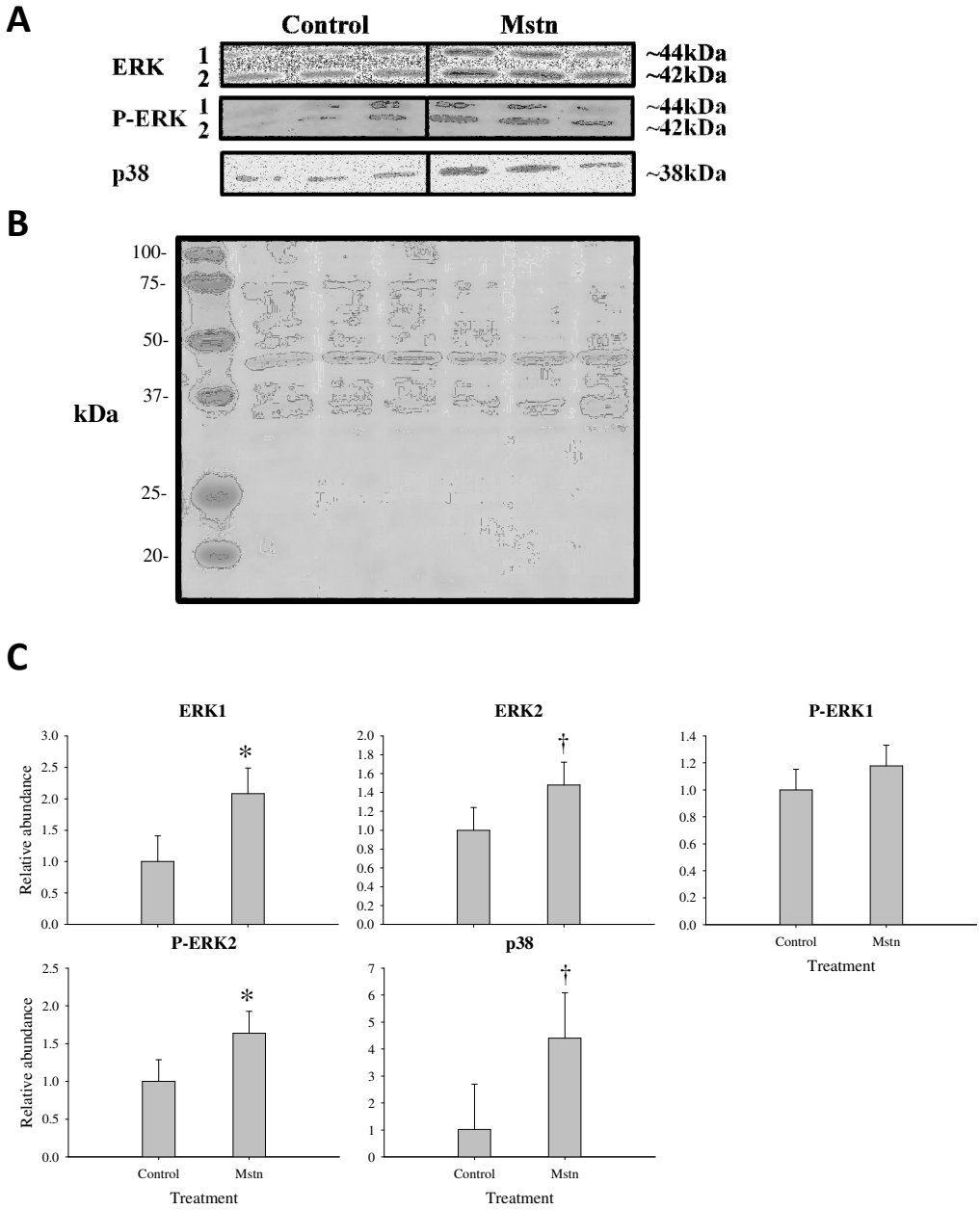

Figure 4.7: Abundance of MAPK targets in the nuclear enriched lysates of ovine myoblasts treated with Mstn. For western blot analysis nuclear enriched lysates were isolated from ovine myoblasts treated with vehicle (controls) or 100 ng/mL of Mstn for 1 h. Isolated protein (5 µg per sample) was run on a SDS/PAGE gel and blotted onto nitrocellulose. Immunoblots were performed for the depicted proteins (A), with representatives (n=3) shown. Blots were then exposed to autoradiographic film to capture the chemiluminescent signal. Equal loading of protein samples was assessed using Ponceau stain, with a representative blot shown in (B). The optical density of individual bands was obtained using a GS800 scanning densitometer and Quantity One software (BioRad). Relative abundance (C) was calculated by normalising the density values obtained from the cells treated with Mstn to those of their control counterparts. Normalised data presented are mean +/- SEM, asterisks denote significant differences between ovine myoblasts treated with Mstn and controls, with: †P<0.1, *P<0.05, n=6 replicates per treatment.

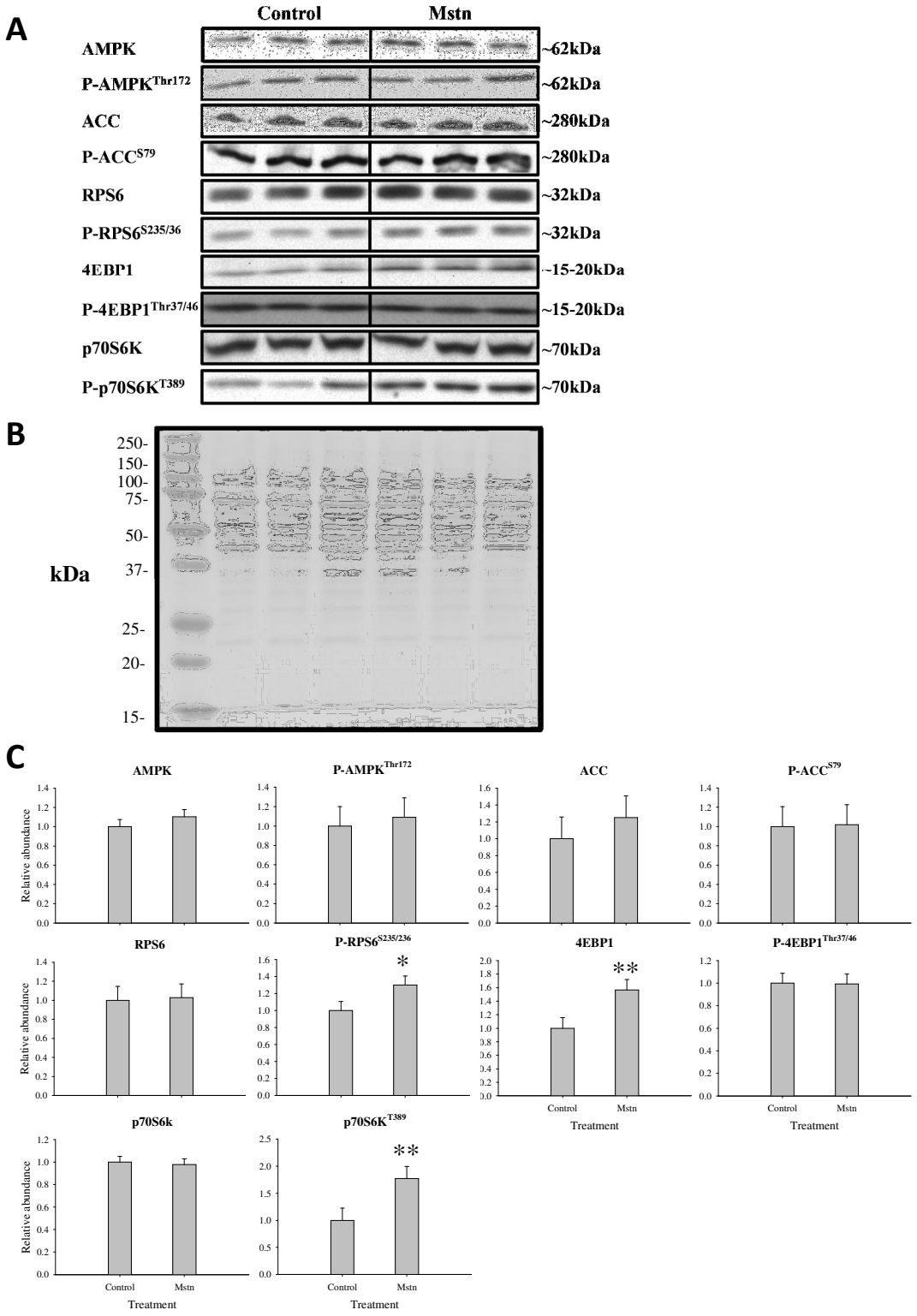

Figure 4.8: Abundance of metabolic targets in the cytoplasmic lysates of ovine myoblasts treated with Mstn. For western blot analysis, cytoplasmic lysates were isolated from ovine myoblasts treated with vehicle (controls) or 100 ng/mL of Mstn for 1 h. Isolated protein (10 µg per sample) was run on a SDS/PAGE gel and blotted onto nitrocellulose. Immunoblots were performed for the depicted proteins (A), with representatives (n=3) shown. Blots were then exposed to autoradiographic film to capture the chemiluminescent signal. Equal loading of protein samples was assessed using Ponceau stain, with a representative blot shown in (B). The optical density of individual bands was obtained using a GS800 scanning densitometer and Quantity One software (BioRad). Relative abundance (C) was calculated by normalising the density values obtained from the cells treated with Mstn to those of their control counterparts. Normalised data presented are mean +/- SEM, asterisks denote significant differences between ovine myoblasts treated with Mstn and controls, with: *P<0.05, **P<0.01, n=6 replicates per treatment.

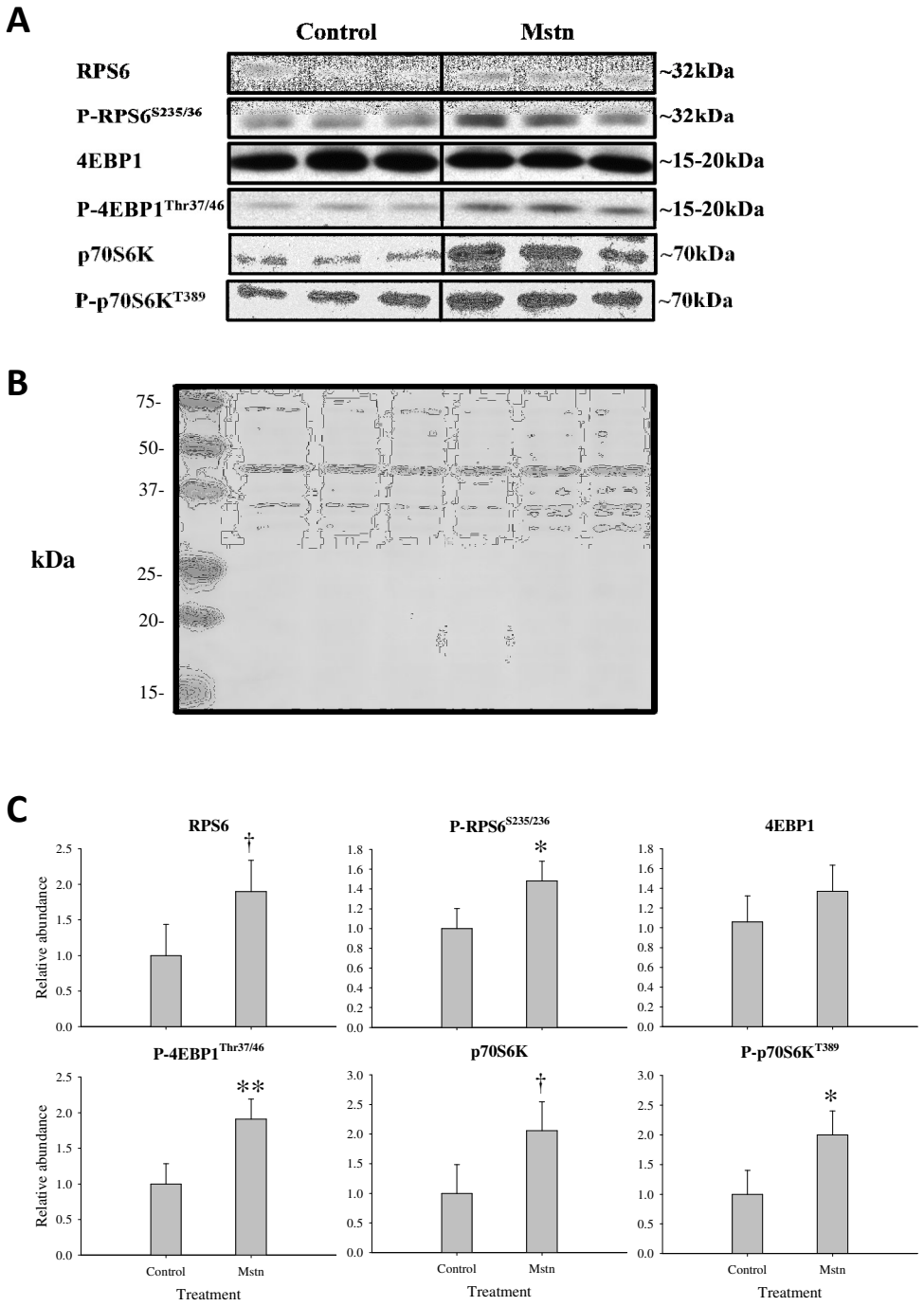

Figure 4.9: Abundance of metabolic targets in the nuclear enriched lysates of ovine myoblasts treated with Mstn. For western blot analysis nuclear enriched lysates were isolated from ovine myoblasts treated with vehicle (controls) or 100 ng/mL of Mstn for 1 h. Isolated protein (5 µg per sample) was run on a SDS/PAGE gel and blotted onto nitrocellulose. Immunoblots were performed for the depicted proteins (A), with representatives (n=3) shown. Blots were then exposed to autoradiographic film to capture the chemiluminescent signal. Equal loading of protein samples was assessed using Ponceau stain, with a representative blot shown in (B). The optical density of individual bands was obtained using a GS800 scanning densitometer and Quantity One software (BioRad). Relative abundance (C) was calculated by normalising the density values obtained from the cells treated with Mstn to those of their control counterparts. Normalised data presented are mean +/- SEM, asterisks denote significant differences between ovine myoblasts treated with Mstn and controls, with: †P<0.1, *P<0.05, **P<0.01, n=6 replicates per treatment.

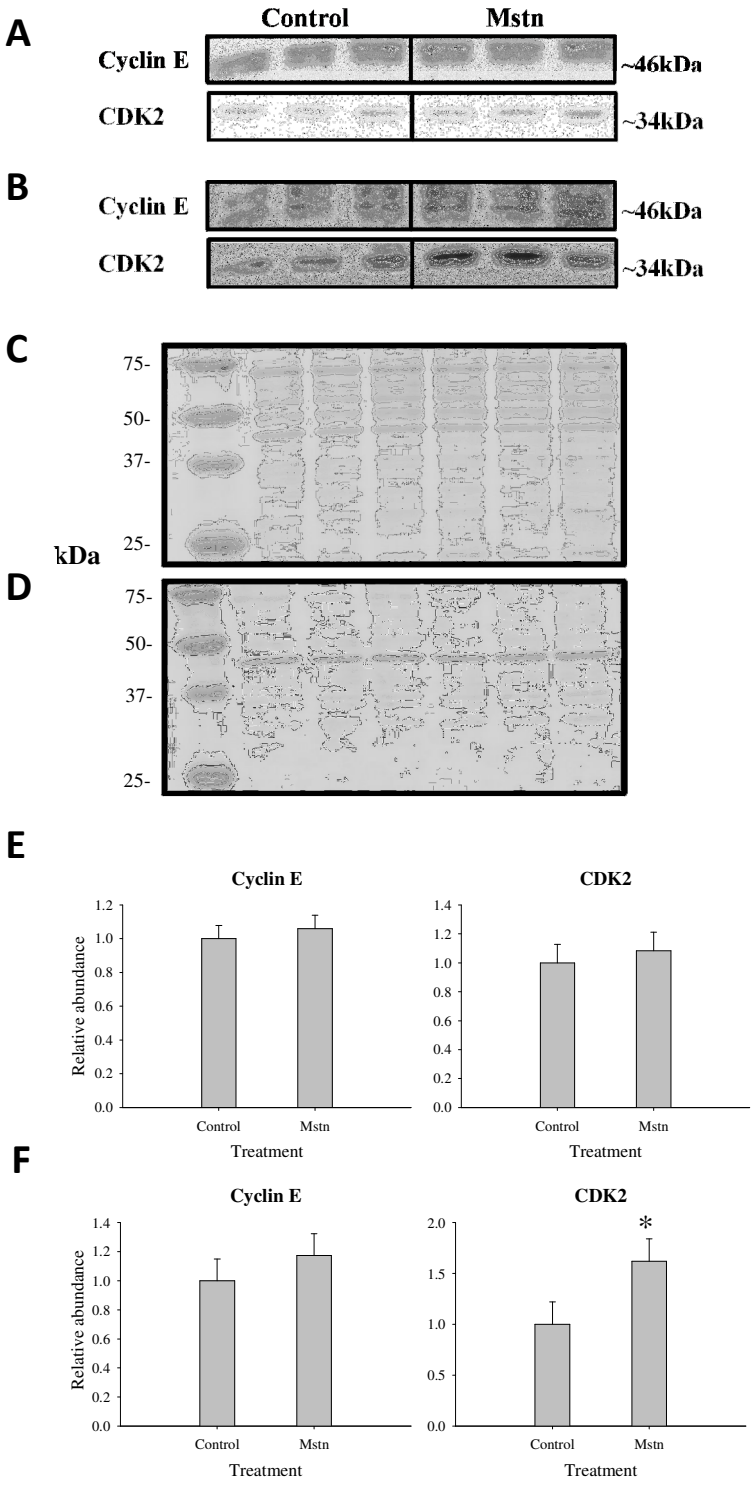

Figure 4.10: Abundance of the cell cycle regulators cyclin E and CDK2 in the cytoplasmic and nuclear enriched lysates of ovine myoblasts treated with Mstn. For western blot analysis, 10 µg of cytoplasmic, or 5 µg of nuclear enriched lysate that was isolated from ovine myoblasts treated with vehicle (control) or 100 ng/mL of Mstn for 1 h, was run on SDS/PAGE gels and blotted onto nitrocellulose. Immunoblots were performed for the depicted proteins, with representatives (n=3) shown for cytoplasmic (A) and nuclear enriched lysates (B). Blots were then exposed to autoradiographic film to capture the chemiluminescent signal. Equal loading of protein samples was assessed using Ponceau stain, with a representative blot shown for cytoplasmic (C), and nuclear enriched (D) lysates. The optical density of individual bands was obtained using a GS800 scanning densitometer and Quantity One software (BioRad). Relative abundance was calculated by normalising the density values obtained from the cells treated with Mstn to those of their control counterparts for cytoplasmic (E) and nuclear enriched (F) lysates. Normalised data presented are mean +/- SEM, asterisks denote significant differences between ovine myoblasts treated with Mstn and controls, with: *P<0.05, n=6 replicates per treatment.

4.2.2 MSV signalling in ovine myoblasts

Once the use of Triton X-114 was validated as a suitable method for the removal of LPS, the signalling of the purified MSV protein was investigated. One caveat, introduced through the use of Triton X-114 was the presence of residual detergent in the preparation, which is reported to be less than 0.018% (Aida and Pabst 1990). Thus, in control treatments, dialysis buffer that was also subjected to Triton X-114 treatment, was added to control ovine myoblast media at equivalent volumes to those used for the addition of MSV. The abundance of a targeted subset of the genes was investigated in whole cell lysates using western blot analysis. The targeted molecules representing a subset of those investigated following the treatment of ovine myoblasts with Mstn as described above.

4.2.2.1 Myogenic transcription factors

As shown above (4.2.1.1) the myogenic transcription factors MRF4 and Myf5 were altered in ovine myoblasts in response to treatment with Mstn. In, addition Mstn treatment also induced the phosphorylation of Smad2. Thus, the ability of MSV to regulate the abundance of these transcription factors and the phosphorylation of Smad2/3 was investigated. As shown in Figure 4.11, treatment with MSV increased the abundance of Myf5 (~2.4 fold, $P<0.01$), while the abundance of MRF4 was not altered. Treatment with MSV also increased the abundance of total Smad2 and Smad3 proteins (~1.4 fold, $P<0.05$ and ~1.3 fold $P<0.05$, respectively), with no change observed in the phosphorylation of Smad2 and no detection of phosphorylated Smad3.

4.2.2.2 PI3K, MAPK and metabolic targets

As shown above, Mstn treatment of ovine myoblasts influences signalling components involved the PI3K and MAPK signalling cascades, in addition to metabolic targets that are controlled by the activation of these pathways. Thus, the ability of MSV to regulate the phosphorylation of AKT (S473) and ERK1/2 was investigated, with the abundance and the phosphorylation of 4EBP1 and the phosphorylation of rpS6 also assessed in this study. As shown in Figure 4.12 (A) treatment with MSV had a tendency to increase the phosphorylation of AKT (~1.5 fold, $P<0.1$), while no change was observed in the phosphorylation of ERK1 or 2. Treatment with MSV also increased the abundance and phosphorylation of 4EBP1

(~3.5 fold, $P<0.05$, ~1.8 fold, $P<0.01$, respectively), while the phosphorylation of rpS6 was not altered.

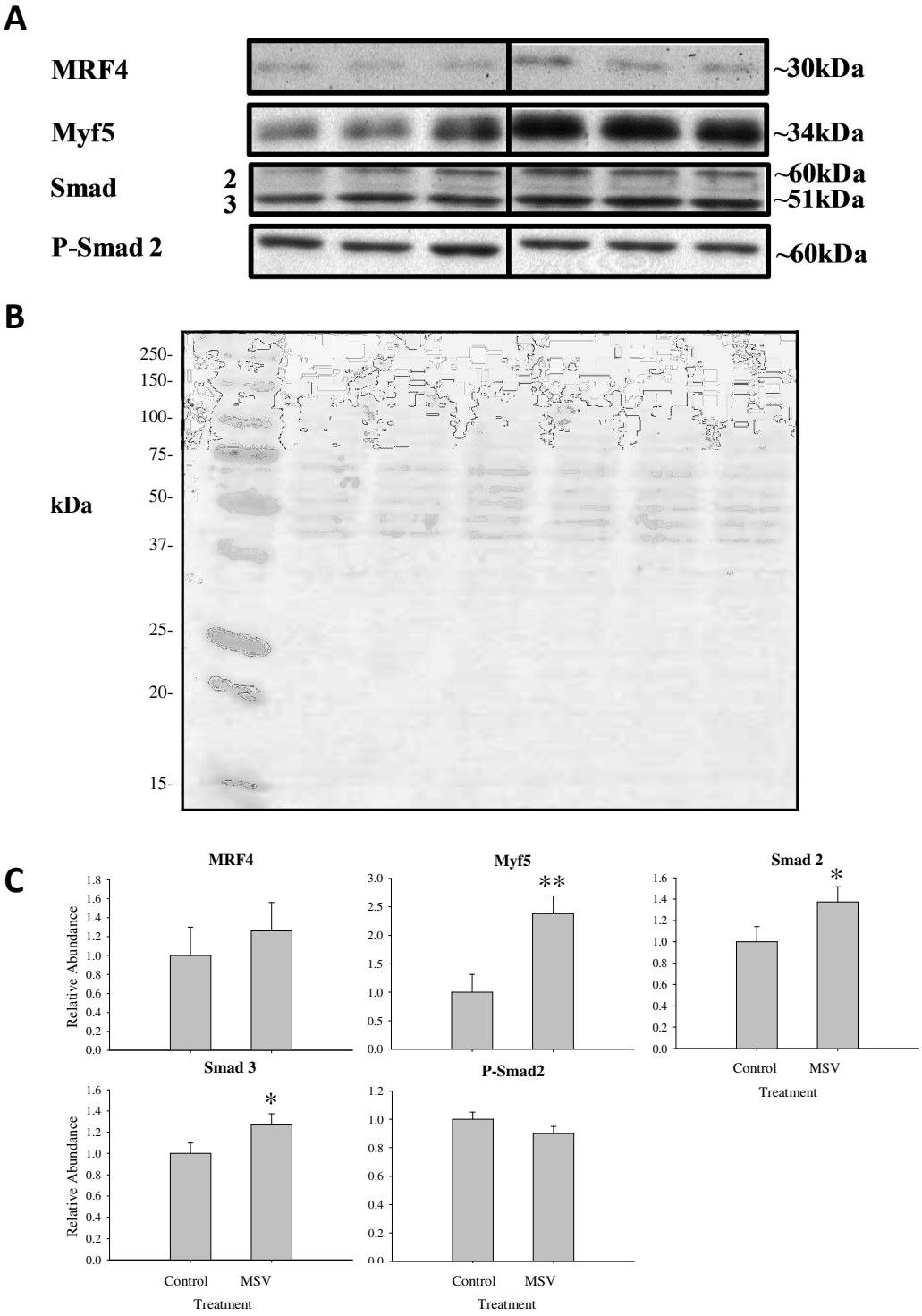

Figure 4.11: Abundance of myogenic transcription factors in ovine myoblasts treated with MSV. For western blot analysis whole cell lysates were isolated from ovine myoblasts treated with vehicle (controls) or 3 µg/mL of recombinant MSV for 1 h. Isolated protein (10 µg per sample) was run on a SDS/PAGE gel and blotted onto nitrocellulose. Immunoblots were performed for the depicted proteins (A), and the blots were then exposed to autoradiographic film to capture the chemiluminescent signal. Equal loading of protein samples was assessed using Ponceau stain, with a representative blot shown in (B). The optical density of individual bands was obtained using a GS800 scanning densitometer and Quantity One software (BioRad). Relative abundance (C) was calculated by normalising the density values obtained from the cells treated with MSV to those of their control counterparts. Normalised data presented are mean +/- SEM, asterisks denote significant differences between ovine myoblasts treated with MSV and controls, with: *P<0.05, **P<0.01, n=3 replicates per

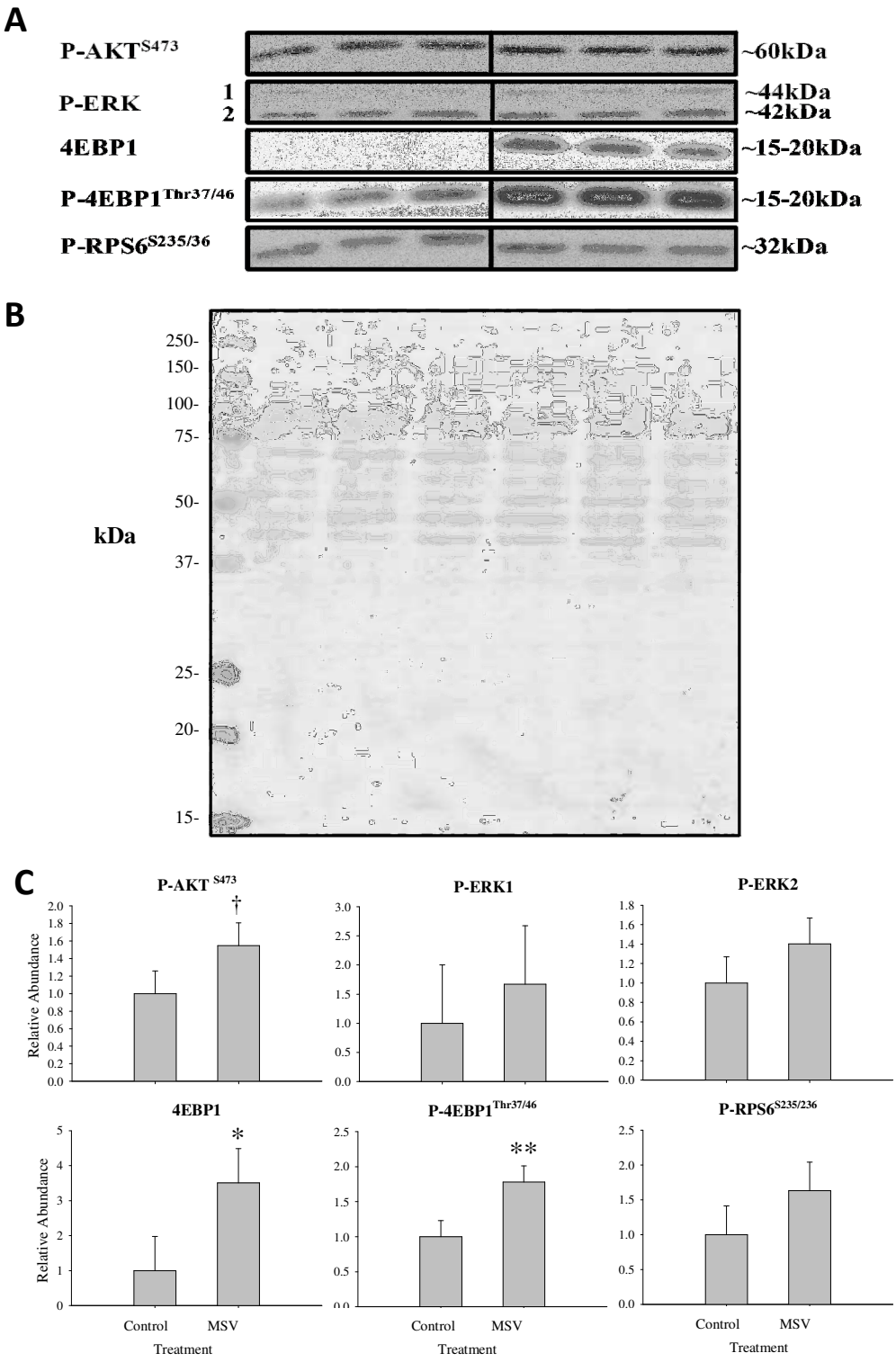

Figure 4.12: Abundance of PI3K/AKT, MAPK and metabolic targets in ovine myoblasts treated with MSV. For western blot analysis whole cell lysates were isolated from ovine myoblasts treated with vehicle (controls) or 3 µg/mL of recombinant MSV for 1 h. Isolated protein (10 µg per sample) was run on a SDS/PAGE gel and blotted onto nitrocellulose. Immunoblots were performed for the depicted proteins (A), and the blots were then exposed to autoradiographic film to capture the chemiluminescent signal. Equal loading of protein samples was assessed using Ponceau stain, with a representative blot shown in (B). The optical density of individual bands was obtained using a GS800 scanning densitometer and Quantity One software (BioRad). Relative abundance (C) was calculated by normalising the density values obtained from the cells treated with MSV to those of their control counterparts. Normalised data presented are mean +/- SEM, asterisks denote significant differences between ovine myoblasts treated with MSV and controls, with: †P<0.1,*P<0.05, **P<0.01, n=3 replicates per treatment.

4.3 Discussion

The studies undertaken in this chapter investigated the early signalling events regulated by Mstn and MSV in ovine myoblasts. The majority of previous studies describing the signalling events that are regulated by Mstn, have focused primarily on human or mouse cells and tissues (Trendelenburg, Meyer et al. 2009; Elkina, von Haehling et al. 2011). Those studies elucidated a number of the critical signalling events that are regulated by Mstn and play a role in the growth and development of skeletal muscle. These include ability of Mstn to influence signalling events involved in the synthesis and degradation of protein, the control of cell proliferation and differentiation, and in the control of energy metabolism. Therefore, previous work investigating the signalling of Mstn provided a list of candidate targets for investigation in the current studies. In an effort to maximise the information gained from this study, the cell lysates from the ovine myoblasts treated with Mstn were fractionated. This allowed the analysis of cytoplasmic and nuclear enriched lysates, with the aim of providing further insight into the localisation of target molecules following Mstn treatment. There is a caveat here, in that the nuclear enriched lysates are also likely to contain membrane bound proteins, which are solubilised during the isolation procedure. This point is particularly important in the signalling context, given that a number of signal transduction molecules can interact either directly or in complex with the cell membrane. Thus, the data presented here needs to be interpreted with that in mind.

Transcription factors that have defined roles in myogenesis were the first candidate genes that were investigated in this study. These transcription factors represent key molecules involved in the regulation of myoblast growth and indeed, myogenesis (see 1.1.4). Treatment with Mstn induced changes in the abundance of five out of the six myogenic transcription factors investigated in this study. In cytoplasmic lysates, Mstn treatment increased the abundance of MyoD, MRF4 and decreased the abundance of Myf5, while nuclear enriched lysates showed increases in MyoD, Mef2 and Pax7. The down-regulation of Myf5, and increased Mef2 is consistent with earlier reports (Langley, Thomas et al. 2002; Hennebry, Berry et al. 2009). Here, Langley et al, showed that Mstn decreased the expression of Myf5 in proliferating C_2C_{12} myoblasts following a 72 h of

treatment, an observation that the authors link to the decreased myogenesis observed following the treatment of differentiating myoblasts with Mstn for the same time period. However, the treatments with Mstn investigated in that study were much longer that those investigated here, with the current studies focusing on the early signalling events influenced by Mstn. With regard to Mef2, one of my earlier studies demonstrated that the expression of Mef2 is higher in the nuclear extracts of myoblasts, and the muscle isolated from WT vs $Mstn^{-/-}$ mice (Hennebry, Berry et al. 2009). In that study we proposed that increased nuclear Mef2, associated with the presence Mstn plays a role in the regulation of fibre-type specific genes, through the regulation of muscle-specific gene transcription. This idea is consistent with later, independent studies investigating the differentiation of mouse myoblasts, where treatment with Mstn has been shown to promote the expression of structural muscle genes that are associated with the slow muscle phenotype (Wang, Yu et al. 2012).

More difficult to explain here, is the increased abundance of MRF4 in cytoplasmic lysates and, of Pax7 and MyoD in nuclear enriched lysates. Previous studies investigating the role of Mstn in the regulation of these transcription factors have shown that Mstn decreases rather than increases their levels of expression. This is especially true for MyoD and Pax7, where other studies have clearly demonstrated that Mstn reduces the abundance of these factors (Langley, Thomas et al. 2002; McFarlane, Hennebry et al. 2008). In fact, in a recent study in ovine myoblasts, where siRNA targeting Mstn was used, decreases in the expression of MyoD transcript at 48, 72 and 96 h of differentiation were observed (Liu, Li et al. 2012). However, as with MEF 2 and Myf5, there is a lack of studies investigating the response of these major myogenic transcription factors following a short interval of treatment with Mstn. One aspect of the current study that may be of major importance, is the ability of Mstn to target these transcription factors in or, perhaps, to specific cellular compartments. This is particularly evident in the increased expression of MyoD, Mef2 and Pax7 found in nuclear enriched lysates and in the reduced abundance of cytoplasmic Myf5. In support, the microarray data shows a reduced abundance of MyoD transcript following 6 h of Mstn treatment (~1.3 fold, $P<0.01$, data not shown). Thus, these data extend our knowledge on the effect of Mstn on these key myogenic transcription factors,

detailing aspects of their early responses to Mstn treatment differ from those observed following prolonged exposure to Mstn.

A potential explanation for these discrepancies may lie with the interactions of the myogenic transcription factors, with molecules whose activity is altered following Mstn treatment. For example, the role of the Smad and Mef2 transcription factors in addition to p38 are likely to play pivotal role. Interactions between MyoD and Smad 3 have been described (Liu, Black et al. 2001; Langley, Thomas et al. 2002), and between Mef2 and Smad 2 proteins (Quinn, Yang et al. 2001). Mef2 has also been shown to interact with the MRF family members to regulate the transcription of muscle specific genes, an interaction that is independent of DNA binding activity (Molkentin, Black et al. 1995). In addition, the MyoD:Pax7 ratio has been shown to be important for myogenic fate decisions, including the proliferation and differentiation of myoblasts in addition to the induction of cellular quiescence. Although studies suggest that there is no direct interaction between MyoD and Pax7, immunoprecipitation experiments suggest they complex with each other through common intermediates to regulate myogenesis (Olguin, Yang et al. 2007; Olguin and Pisconti 2012). Furthermore, the activity of p38, a well-established target of Mstn, has been shown to be important in the control of MyoD, MEF2 and Pax7 activity (Knight and Kothary 2011). Thus, these observations clearly demonstrate an altered distribution of key myogenic transcription factors following a short interval of Mstn treatment, that occurs in parallel with modulation of the activity of key signalling pathways that regulate the activity of key myogenic transcription factors. Indeed, further investigations will be required to elucidate the specific nature of these interactions and how they control the activity of the myogenic transcription factors.

To establish the early effects of exposure to Mstn on components of the PI3K/AKT signalling cascade (see 1.1.6.2), the abundance and phosphorylation of PDK1 and AKT in the protein lysates from ovine myoblasts was investigated. Consistent with no change in the phosphorylation status of PDK1, the phosphorylation of AKT^{T308} was not altered following Mstn treatment. Unexpectedly, Mstn treatment induced the phosphorylation of AKT^{S473}, with increases observed in both cytoplasmic and nuclear enriched lysates. The increase in the phosphorylation of AKT^{S473}, was accompanied by a decrease in the

abundance of cytoplasmic AKT, with a corresponding increase in the abundance of AKT observed in nuclear enriched lysates. These data conflict with previous literature regarding the effect of Mstn on AKT phosphorylation and also suggest that Mstn treatment alters the distribution of AKT within the cell. Previous studies have reported that Mstn inhibits the phosphorylation of AKT, specifically, reducing the phosphorylation of AKT^{S473} in human myoblasts (Trendelenburg, Meyer et al. 2009). Again, the timeframes of these observations in previous studies is the major point of difference with the data presented here. Alternatively, these data may highlight points of difference in Mstn signalling between myoblasts isolated from ruminant vs monogastric species.

In the previous myoblast study that reported reduced phosphorylation of AKT^{S473}, following treatment with the same Mstn preparation, AKT phosphorylation was assessed 24 h after the addition of Mstn (Trendelenburg, Meyer et al. 2009). Therefore, an initial increase in the phosphorylation of AKT^{S473} would have been missed. In addition, other observations from the current study support the increase in the phosphorylation of AKT^{S473}. Firstly, the phosphorylation of p38 MAPK was induced following treatment with Mstn, presumably through TAK1 as reported in other myoblast models and in fibroblasts (Philip, Lu et al. 2005; Li, Kollias et al. 2008; Zhang, Rajan et al. 2011). AKT and p38 have being shown to associate with each other in human neutrophils and vascular smooth muscle cells with the later study demonstrating that p38 recruits the MAPKAPK-2 kinase to phosphorylate AKT specifically at S473 (Rane, Coxon et al. 2001; Taniyama, Ushio-Fukai et al. 2004). Furthermore Li et al reported that Mstn induces the phosphorylation of AKT^{S473} in fibroblasts, an increase that is blocked by the pharmacological blockade of p38 (Li, Kollias et al. 2008). Interestingly, a recent study demonstrated that specific phosphorylation of AKT at S473, targets AKT for ubiquitination and subsequent proteasomal degradation (Wu, Ouyang et al. 2011). In this study the authors also show that this mechanism is independent of the phosphorylation of AKT at T308, which has also been show to target the degradation of AKT through independent mechanisms. This provides a plausible explanation for the increased phosphorylation of AKT^{S473} observed in this study. In addition, they support a mechanism involving MAPK signalling, through which AKT may be targeted for degradation following

exposure to Mstn. Thus, these early observations may represent the starting point of the reduced activity of AKT that is observed following longer periods of exposure to Mstn.

The treatment of ovine myoblasts with Mstn also altered the abundance and the phosphorylation of additional components of the MAPK signalling cascade in conjunction with p38. Treatment with Mstn altered both the abundance and the phosphorylation of ERK1 and 2 in ovine myoblasts. The ERKs represent major intermediates for the MAPK signalling cascade, with their activity influenced by a an array of growth factors and mitogens (Knight and Kothary 2011). ERK signalling has also being shown to play a crucial role in the control of the proliferation and differentiation of myoblasts (Knight and Kothary 2011). Others have reported that Mstn activates ERK signalling to inhibit both the proliferation and the differentiation of C_2C_{12} myoblasts (Yang, Chen et al. 2006). Unfortunately, the mechanistic details of cellular events downstream of ERK1/2 in myoblasts, have remained elusive (Knight and Kothary 2011). Thus, the data presented here confirm that Mstn regulates the abundance and phosphorylation of ERK1/2 in ovine myoblasts.

The metabolic role of Mstn in skeletal muscle has been the focus of a number of studies. Genetic ablation of Mstn in mice has been shown to improve tolerance to diets high in fat (McPherron and Lee 2002), to increase protein synthesis (Welle, Burgess et al. 2009) and, reports have also proposed a role for Mstn in the regulation of glucose metabolism (Chen, Ye et al. 2010). Thus, the effect of Mstn treatment on some of the key signalling molecules involved in the regulation of these processes was investigated. Firstly, the ability of Mstn to alter the abundance and the phosphorylation of AMPK and its downstream target ACC were investigated. No changes in the abundance or the phosphorylation of AMPK or ACC were observed following treatment with Mstn. Previous studies have shown that Mstn increased the phosphorylation of AMPK and ACC in HeLa cells, and observed differences in the phosphorylation of these molecules between WT and Mstn null mice (Chen, Ye et al. 2010; Zhang, McFarlane et al. 2011). In the HeLa cells these changes were observed following a 6 h treatment with *E. coli* derived Mstn, at concentrations (750-1500ng/mL) that are orders of magnitude higher than those that used for the current study (Chen, Ye et al. 2010). Thus, the

treatment time and the Mstn concentration, or the nature of the Mstn preparation are likely explanations for the lack of AMPK and ACC activation observed here.

Also investigated was the abundance and phosphorylation of rpS6, 4EBP1 and p70S6K, all of which are molecules with established roles in cellular growth and the regulation of protein synthesis (Magnuson, Ekim et al. 2012). Mstn treatment altered the abundance and phosphorylation of all three of these molecules. The increased abundance of 4EBP1 in cytoplasmic lysates is interesting. 4EBP1 has a well-defined role in the inhibition of cap-dependant translation, binding in complex to the translation initiation factor eIF4E, to inhibit translation. This inhibition of translation is reversed following the phosphorylation dependant dissociation of 4EBP1 (Magnuson, Ekim et al. 2012). Thus, increased cytosolic 4EBP1 should result in decreased cap-dependant translation (Choo, Yoon et al. 2008), consistent with a role for Mstn in the reduction of protein synthesis. The reason for increased phosphorylation of 4EBP1 in nuclear enriched lysates is unclear. However, this does suggest that the distribution of 4EBP1 within the cell plays a role in the changes induced following Mstn treatment.

Treatment with Mstn also induced changes in rpS6, primarily through increased phosphorylation. The consequences of rpS6 phosphorylation are not well understood, with conflicting data on a direct link between the phosphorylation of rpS6 and protein synthesis (Meyuhas 2008). However, Mouse embryonic fibroblasts with a knock-in, phosphorylation inactive form of RPS6 show increased synthesis of protein and an accelerated rate of growth. Thus, in these cells rpS6 phosphorylation is refractory to protein synthesis, which would be consistent with the function of Mstn and the increased phosphorylation of rpS6 observed in this study. The last metabolic target investigated was p70S6K, this kinase has been shown to regulate multiple downstream targets, including 4EBP1 and rpS6 via preceding activation through both the PI3K/AKT and MAPK pathways. Treatment with Mstn stimulated the phosphorylation of p70S6K at T389, a phosphorylation site regulated through the mTOR complex. Interestingly, the phosphorylation of p70S6K through mTOR can occur following activation of the PI3K/AKT and MAPK pathways (Magnuson, Ekim et al. 2012). Importantly the mTOR/p70S6K pathway plays a role in the control of both the

phosphorylation of rpS6 and 4EBP1, with rpS6 being a direct substrate for p70S6K and, 4EBP1 a target of mTOR (Magnuson, Ekim et al. 2012). Given the absence of signalling through PDK1 that was observed in this study, it is likely that the increased phosphorylation of p70S6K at T389 is a result of mTOR activation, with the MAPK signalling observed following Mstn treatment a likely candidate for the activation of this pathway. Previous studies investigating the effect of Mstn on the phosphorylation of p70S6K, have shown that extended periods of exposure to Mstn reduced the phosphorylation of p70S6K (Trendelenburg, Meyer et al. 2009). Thus, as with AKT, the early effects of Mstn on this molecule may differ from those observed following extended periods of Mstn treatment.

The ability of Mstn to alter the abundance of the cell cycle regulators cyclin E and CDK2 was also assessed. Previous studies have shown that treatment with Mstn reduces the abundance of this factor, with this linked to the reduced proliferation associated with Mstn treatment (Langley, Thomas et al. 2004). In the current study, an increase in the abundance of CDK2 in nuclear enriched lysates was the only difference observed in the abundance of these key cell cycle regulators. Interestingly, over-expression of Mstn has been shown to increase the abundance of CDK2 transcript in sheep fibroblasts (Lu, Ren et al. 2012). Thus, similar to the increases observed in the phosphorylation of AKT, other models support the data observed in these studies.

In addition to investigating the signalling of Mstn, the signalling events induced by MSV were also investigated in this chapter. The range of targets investigated following MSV treatment was reduced, this was done for a number reasons. Firstly, to focus on molecules that had been altered following Mstn treatment. Secondly, although LPS had been removed, there were still concerns regarding the proper folding of MSV following LPS removal with Triton X-114. Finally, with the successful generation of C_2C_{12} myoblasts stably expressing MSV (Chapter 6), a decision between further studies investigating MSV signalling or a more substantial investigation of C_2C_{12} cells expressing MSV had to be made. As the C_2C_{12} cells provided the most robust model for further investigating the function of MSV, a larger study in this model was preferred (see Chapter 6).

Initially, the abundance of members of the MRF family were investigated. In contrast to Mstn treatment, ovine myoblasts exposed to MSV showed an increased abundance of Myf5, showing that the regulation of Myf5 is differentially regulated by Mstn and MSV. The consequence of this increase is uncertain, although Myf5 is thought to play an important role in the expansion of myogenic precursors, in addition to working in concert with other myogenic transcription factors to regulate myogenesis (Rudnicki, Schnegelsberg et al. 1993; Knight and Kothary 2011). The ability of MSV to regulate canonical signalling of Mstn was assessed, with the abundance and phosphorylation of Smad 2/3 determined following MSV treatment. Interestingly MSV increased the abundance of both Smad 2 and 3, while no change was observed in Smad phosphorylation. The effect of the increased Smad 2 and 3 induced by MSV is unclear, but demonstrates that MSV influences the content of key molecules involved in canonical Mstn and thus TGF-β signalling. However, an increased abundance of total Smad2 and 3 may have implications for canonical Mstn signalling pathways. Studies have shown that the ratio of phosphorylated:total Smad may be important in determining Smad activity, thus increased abundance of total Smad2/3 may reduce Smad activity or, alternatively, this response may constitute a positive feedback mechanism to counter reduced Smad activity.

Treatment with Mstn altered components of the PI3K and MAPK signalling pathways. Thus, the ability of MSV to alter components of these pathways was investigated. Treatment with MSV had a tendency to increase the phosphorylation of AKT at S473, thus, the phosphorylation of AKT represents a potential target for MSV signalling. No change was observed in the phosphorylation of ERK1/2, thus the function of MSV does not appear to involve the regulation of this major intermediate of MAPK signalling. Metabolic targets were also investigated following MSV treatment. As with Mstn treatment MSV induced an increase in the abundance of 4EBP1, MSV also increased the phosphorylation of 4EBP1. Thus, both Mstn and MSV regulate the abundance and activity of 4EBP1, highlighting a target with an important role in protein synthesis that is targeted by both Mstn and MSV.

In summary, the data presented in this chapter shows that treatment of ovine myoblasts with Mstn alters the abundance and the phosphorylation of

targets involved in signal transduction across multiple pathways. In addition, Mstn altered the abundance of myogenic transcription factors that play important roles in the regulation of myogenic gene expression, in addition to the abundance and the phosphorylation of metabolic targets involved in the control of protein synthesis. Consistent with previous studies, Mstn increased the phosphorylation of components in the MAPK, and Smad signalling pathways. In addition, the data obtained from this short interval of Mstn treatment also conflicted with earlier reports, especially with regard to the phosphorylation of AKT and 4EBP1, and the abundance of the major myogenic transcription factors Pax7 and MyoD. The current data extend the knowledge of these early events controlled by Mstn, demonstrating that the initial signalling events differ from those observed following longer periods of exposure to Msn. The early signalling events regulated by MSV were also investigated in this chapter. Common molecules targeted by both Mstn and MSV were the Smads, 4EBP1, phosphorylated AKT (S473) and the myogenic regulatory factor Myf5. Thus, these targets provide potential convergence points for Mstn and MSV signalling in the regulation of myogenesis and protein synthesis and provide a starting point for the further investigations of MSV signalling, in a myoblast model expressing MSV (see Chapter 6).

Chapter Five

5 Mstn regulates the expression of the β1 subunit of the Na^+- K^+ -ATPase through a Smad dependant mechanism.

5.1 Introduction

This chapter follows on from the identification that the β1 subunit of the Na^+-K^+-ATPase is a downstream target of Mstn (Chapter 3). The following section gives an overview of what is known about the Na^+-K^+-ATPase.

The Na^+-K^+-ATPase complex was discovered in 1957 by Jens Christian Skou, a discovery that would some 40 years later see him awarded the Nobel Prize in chemistry. The Na^+-K^+-ATPase complex belongs to the P-type ATPase family and is expressed in the plasma membrane of all mammalian cells. The Na^+-K^+-ATPase complex mediates coupled cellular export of $3Na^+$ and import of $2K^+$ ions against their electrochemical gradients in an ATP dependant process (Skou 1957; Clausen 2003). The maintenance and control of ionic gradients by the Na^+-K^+-ATPase complex is crucial for many biological processes including: early embryonic development, cell volume regulation, transport of metabolites (e.g. glucose and amino acids), stimulation of glycolysis, H^+ and Ca^{2+} transport and maintaining the electrical activity of muscle and nerve (Devarajan, Gilmore-Hebert et al. 1992; James, Wagner et al. 1999; Madan, Rose et al. 2007; Doi and Iwasaki 2008). In fact, the ion transport controlled by this complex is indispensable for maintaining the contractility of skeletal muscle (Clausen 2003).

The Na^+-K^+-ATPase complex consists of three subunits, an essential hetero-dimer of an α and β-subunit, which constitutes the functional body of the complex, and a regulatory γ-subunit (FXYD) protein. The Na^+-K^+-ATPase α and β subunits are expressed in various isoforms and, to date four α isoforms (α_1-α_4), three β isoforms (β_1-β_3), and seven FXYD family members have been identified. The α_1 and β_1 isoforms are ubiquitously expressed, while other α, β and γ isoforms have a more tissue specific profile (Tokhtaeva, Clifford et al. 2012). The Na^+-K^+-ATPase complex in skeletal muscle is comprised predominantly of α_1-α_2/β_1-β_2 hetero-dimers with FXYD1 (phospholemma) the only γ-subunit identified in muscle (Kristensen and Juel 2010). In skeletal muscle, there are three cellular

pools of the Na^+-K^+-ATPase, which reside within the sarcolemma, t-tubules and an intracellular component(s) that lacks a precisely defined location (Clausen 2003). Interestingly, a recent study identified a functional Na^+-K^+-ATPase complex in the nuclear membrane of HEK 293 cells, a site not yet studied in skeletal muscle, which in conjunction with sub-sarcolemmal vesicles and triad junctions, provide potential locations for this unidentified intracellular pool (Clausen 2003; Galva, Artigas et al. 2012).

In terms of specific subunit functionality, the α-subunit contains the major trans-membrane region of the Na^+-K^+-ATPase complex, harbouring ten trans-membrane domains, which include the ion and the cardiotonic steroid binding sites. The alpha subunit contains three distinct cytoplasmic domains, the actuator, the nucleotide binding and the phosphorylation domains. These domains control specific aspects of ATPase function including, ion flow, ATP binding and interaction with a growing list binding partners, a list that includes insulin, the nicotinic acetylcholine receptor, CD36 (fatty acid transporter) and Src kinase (Heiny, Kravtsova et al. 2010; Oubaassine, Weckering et al. 2012; Kennedy, Chen et al. 2013; Reinhard, Tidow et al. 2013). The β-subunit is composed of a short cytoplasmic N-terminal tail, a single trans-membrane helix and a highly glycosylated extracellular domain. The β subunit has been shown to influence Na^+-K^+-ATPase K^+ affinity and plays a crucial role in the trafficking of the α_1/β_1 complex and subsequent insertion in the plasma membrane (Clifford and Kaplan 2008). A role for the β_1 subunit in mediating cell-cell interactions and a critical role in early embryonic development have also been described (Madan, Rose et al. 2007).

Na^+-K^+-ATPase ion transport is specifically inhibited by cardiotonic steroids (CTS), through their interaction with the α subunit. Members of the CTS family include the plant derived, digitalis drugs ouabain and digoxin as well as the vertebrate derived aglycones, bufalin and marinobufagenin. Both ouabain and marinobufagenin have been reported in humans as circulating endogenous hormones (Reinhard, Tidow et al. 2013). CTS have been used for decades as positive inotropic agents to treat congestive heart failure. Initially, this choice of treatment was attributed to the ability of CTS to increase intracellular Ca^{2+}. However, it was later demonstrated that CTS treatment not only improves cardiac

contractility, but also induced hormone like effects, independent of changes in intracellular ion concentrations (Xie and Askari 2002). These effects include the initiation of signal transduction cascades, and the modulation of a number of cellular processes including: cardiomyocyte growth and hypertrophy, increased protein synthesis, altered gene expression and perturbation of cell to cell interactions (Xie and Askari 2002). These investigations led to the postulate that the Na^+-K^+-ATPase complex has a role in signal transduction, in addition to its critical role in regulating Na^+-K^+ transport (Xie and Askari 2002). Importantly, the CTS ouabain influences both the signal transduction and ion flow functions of the Na^+-K^+-ATPase, and involves the direct interaction of ouabain with the α subunit of the Na^+-K^+-ATPase (Kometiani, Li et al. 1998; Laursen, Yatime et al. 2013). The specificity of ouabain for the Na^+-K^+-ATPase was highlighted in a recent study that solved the structure of ouabain bound to the α_1 subunit of the Na^+-K^+-ATPase (Laursen, Yatime et al. 2013). In fact, after decades of research on the Na^+-K^+-ATPase, the use of ouabain as a selective inhibitor of the 'ion flow' function of the Na^+-K^+-ATPase complex remains the primary method for determining specific Na^+-K^+-ATPase activity. Indeed, subsequent studies have revealed a significant role for Na^+-K^+-ATPase induced signal transduction in major intracellular cellular signalling cascades that include MAPK, Phospholipase C and PI3K (Yuan, Cai et al. 2005; Kotova, Al-Khalili et al. 2006; Zhang, Zhang et al. 2008). Many of the mechanisms governing these effects are not fully elucidated. In addition, a significant role for the β subunit cannot be discounted with its role in the trafficking of the Na^+-K^+-ATPase complex and its interaction with an upstream regulator of MAPK signalling (Src), providing good examples (Bhullar, Clough et al. 2007; Clifford and Kaplan 2008).

A number of factors have been shown to regulate the activity and abundance of the Na^+-K^+-ATPase complex in skeletal muscle, a list that includes: exercise, calcitonins, epinephrine, β2- agonists, insulin, IGF-1, amylin, AMPK, glucose concentration and PGC-1α (Benziane, Bjornholm et al. 2009; Ingwersen, Kristensen et al. 2011; Benziane, Bjornholm et al. 2012; Rivelli, Amaiden et al. 2012). The primary stimulus for muscle Na^+-K^+-ATPase activity is the increase in the concentration of intracellular Na^+ ($[Na^+]_i$) that is induced by electrical stimulation. Myofibre-type specific responses for Na^+-K^+-ATPase have been

described, with Na^+-K^+-ATPase activity in type I muscle fibres being more sensitive to increased $[Na^+]_i$ than that of type II fibres (Juel 2009). Interestingly, the fibre-type specific differences are not accounted for by differences in the abundance of the Na^+-K^+-ATPase complex. However, fibre-type dependant differences in the abundance of the Na^+-K^+-ATPase β subunits have been observed in rat skeletal muscle with a greater abundance of Na^+-K^+-ATPase β1 subunits in 'slow' oxidative than 'fast' glycolytic muscle, with the opposite being true for the β2 subunit (Fowles, Green et al. 2004). These differences illustrate the importance of the other mechanisms that regulate the activity and concentration of the Na^+-K^+-ATPase complex in skeletal muscle. In addition, a role for TGF-β in the regulation of both the abundance of α and β subunits in addition to the activity of the Na^+-K^+-ATPase has been described (Tang, Wang et al. 1995; Rajasekaran, Huynh et al. 2010). However, reports have not yet demonstrated a role for TGF-β dependant regulation of specific Na^+-K^+-ATPase subunits in skeletal muscle. Given the critical role of the Na^+-K^+-ATPase complex in maintaining the contractile function of skeletal muscle and the signal transduction function of the Na^+-K^+-ATPase complex, its regulation by Mstn may constitute a critical aspect of Mstn function. Thus, the following chapter presents studies that further characterise the Mstn-dependant regulation of the Na^+-K^+-ATPase β1 subunit.

5.2 Results

5.2.1 Regulation of the Na^+- K^+-ATPase β1 subunit by Mstn.

To quantify the relative abundance of the Na^+-K^+ ATPase β1 subunit mRNA, and to confirm the differential expression that was observed in the microarray analysis, qPCR primers were designed that would amplify a 171bp amplicon spanning across exons 2, to 3 of the Na^+-K^+- ATPase β1 gene transcript. This region is conserved across human, murine, bovine and ovine species. Consistent with the microarray analysis, qPCR confirmed that, 6 h of Mstn treatment induced a ~3 fold ($P<0.01$) increase in the abundance of Na^+-K^+ ATPase β1 transcript (Figure 5.1) in the same pool of RNA from ovine myoblasts.

5.2.2 Regulation of the Na^+-K^+-ATPase β1 transcript in proliferating and differentiating ovine myoblasts is not a transient response.

Regulation of the Na^+-K^+-ATPase β1 subunit by Mstn has not been previously reported. To establish that the regulation of the Na^+-K^+-ATPase β1 subunit by Mstn was not a transient response, qPCR was used to assess the relative abundance of the Na^+-K^+-ATPase β1 subunit following prolonged Mstn treatment. This was performed on both proliferating and differentiating ovine myoblasts, cultured in the presence of Mstn. The Mstn dependant induction of Na^+-K^+-ATPase β1 transcript was sustained in proliferating myoblasts following 48 h of Mstn treatment (2-fold, $P<0.01$). The increase in concentrations of β1 subunit mRNA was also observed in myoblast cultures differentiated for 48 h in the presence of Mstn (1.4-fold, $P<0.01$), as shown in Figure 5.2.

5.2.3 Na^+- K^+-ATPase activity plays a role in ovine myogenesis.

5.2.3.1 Proliferation

To establish if the Na^+-K^+-ATPase plays a role in the control of proliferation in ovine myoblasts, myoblast cultures were incubated in the presence ouabain throughout proliferation. Proliferation was assessed using the Methylene blue proliferation assay (see 2.2.5). In proliferating myoblasts, ouabain treatment at low concentrations (100 pM-10 nM) produced small, but, significant increases in the proliferation of ovine myoblasts after 24 h in culture, see Figure 5.3. Treatment with ouabain at 300pM induced the greatest increase in proliferation (~15%, $P<0.001$). This increase was not observed following 48 h of proliferation, with reduced methylene blue staining observed in the pico-molar range for this time-point. Treatment with Ouabain at concentrations higher than 30nM, reduced the proliferative capacity of primary ovine myoblasts ($P<0.001$), with concentrations of ouabain higher than 300nM for at 24 and 48 h yielding OD_{650} values below their 12 and 24 h counterparts.

5.2.3.2 Differentiation

To establish if the Na^+-K^+-ATPase complex plays a role in regulating the differentiation of ovine myoblasts, differentiating myoblasts were incubated in the presence of ouabain. The extent of differentiation was assessed using the MF20 antibody to identify when myosin heavy chains appear. Ouabain consistently

increased the differentiation of ovine myoblasts at a concentration of 10nM (Figure 5.4) at 12 h (~2.8 fold, $P<0.001$), 24 h (~2.1 fold, $P<0.001$) and 48 h (~1.4 fold, $P<0.001$). In contrast, very low concentrations of ouabain (1-30pM) reduced differentiation, with a ouabain concentration of 30pM giving the greatest reduction in this range (~0.76 fold, $P<0.001$). The treatment of differentiating cultures with ouabain concentrations at 30nM and above severely compromised the expression of myosin heavy chain ($P<0.001$).

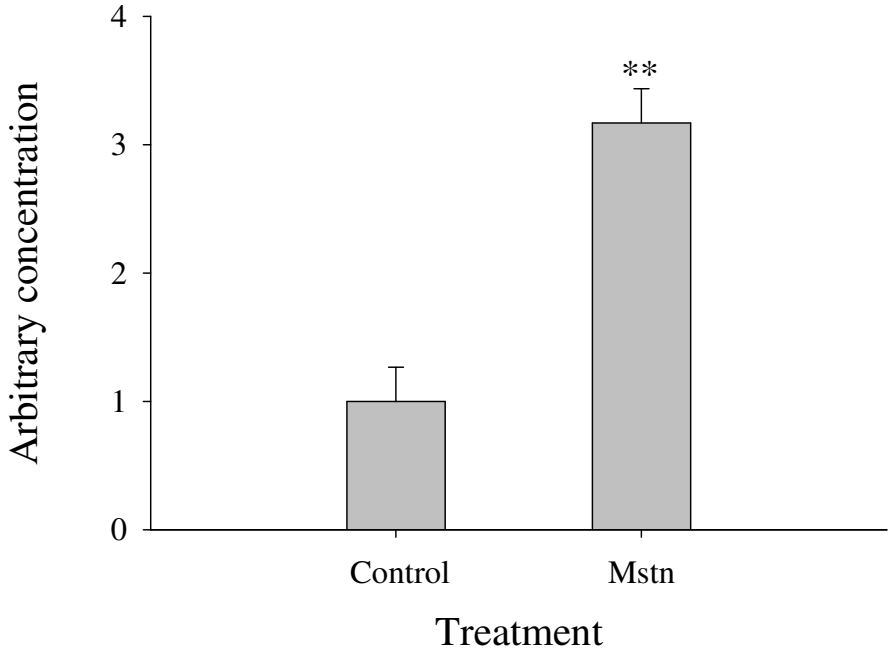

Figure 5.1: Concentrations of Na^+-K^+- ATPase β1 subunit mRNA in Mstn treated ovine myoblasts. Microarray RNA samples were used for qPCR analysis, with myoblasts treated with Mstn (600ng/ml) or vehicle alone (control) for 6 h. Data presented are mean +/- SEM, asterisks denote a significant difference from control, with: **P<.001), n=3 for each treatment. Concentrations were normalised control values following adjustment to oligreen (total cDNA) values.

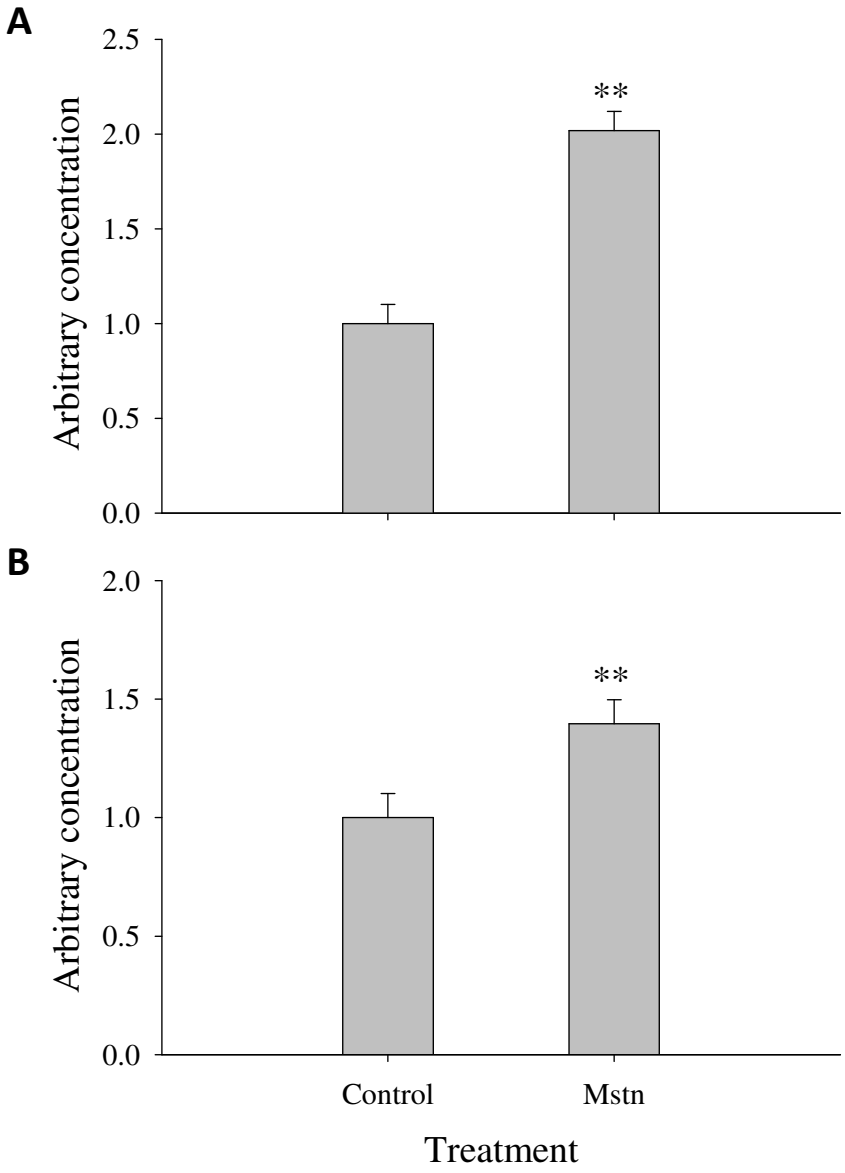

Figure 5.2: Na^+-K^+-ATPase β1 subunit expression in ovine myoblasts. The arbitrary concentrations (mean +/- SEM) of Na^+-K^+-ATPase β1 subunit mRNA, as determined by qPCR in proliferating (A) or differentiating (B) ovine myoblasts treated in the presence or absence of 100ng/mL Mstn or vehicle alone (control) for 48 h. Data presented are mean +/- SEM, asterisks denote a significant difference from control (** $P<0.01$), n=3 for each treatment. Concentrations were normalised to vehicle alone (control) values following adjustment to oligreen (total cDNA) values (2.2.1.4)

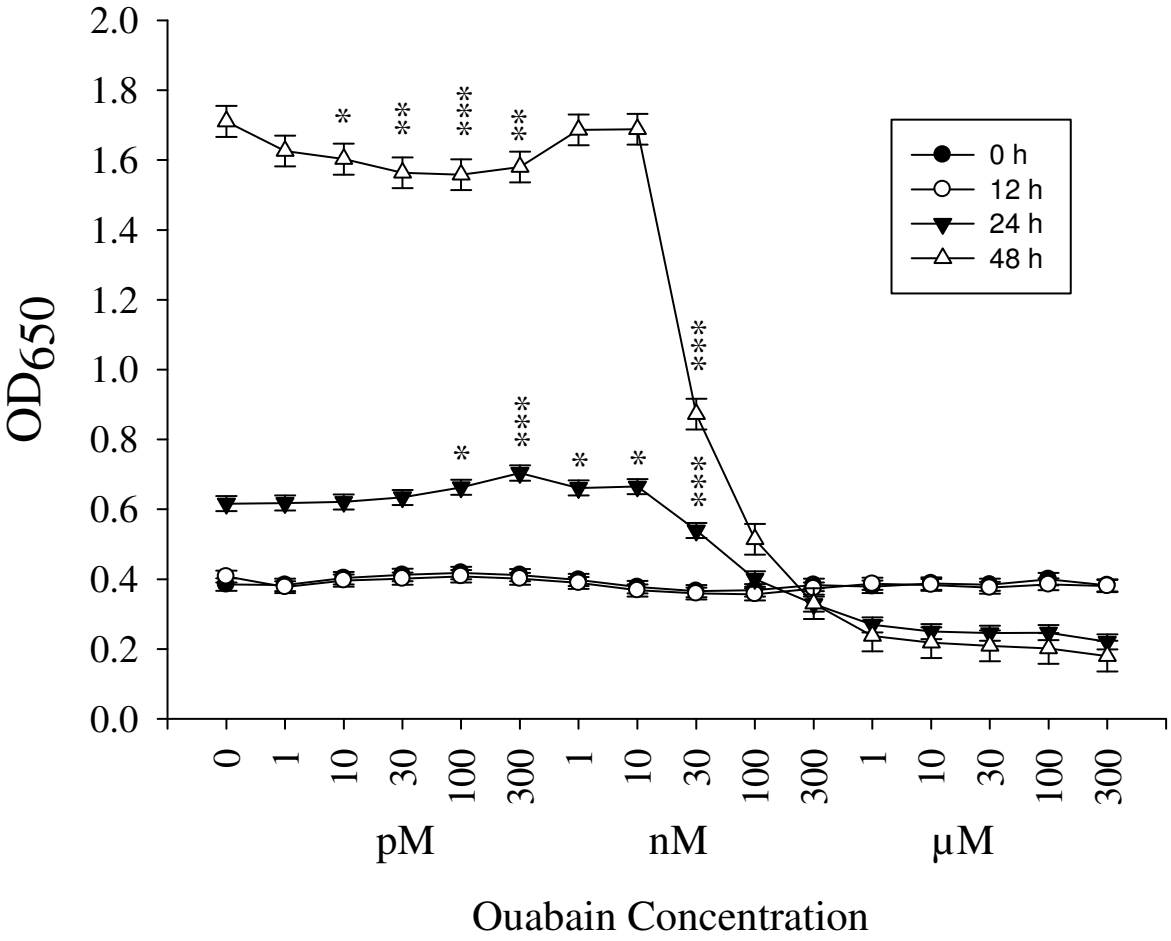

Figure 5.3: The effect of ouabain on ovine myoblast proliferation. Ovine myoblasts were cultured in the presence of increasing concentrations of ouabain, and proliferation was determined using the methylene blue assay and read at an optical density (OD) of 650nm. Data presented are mean +/- SEM, asterisks denote significant differences from vehicle controls at each concentration of ouabain: *P<0.05, **P<0.01, *** P<0.001, n=6 replicates per concentration.

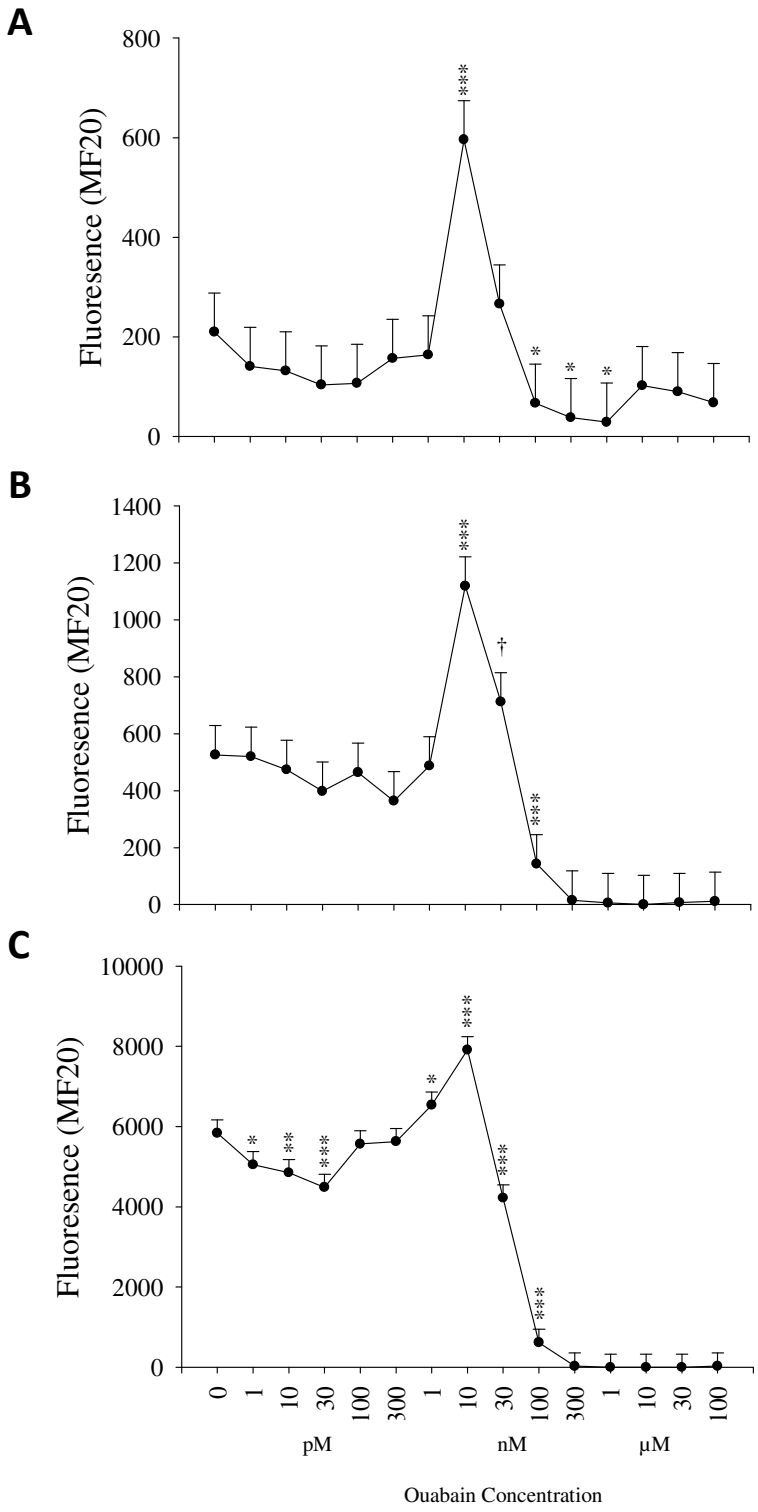

Figure 5.4: The effect of ouabain on the induction of myosin heavy chain in differentiating ovine myoblasts using the MF20 antibody. The relative expression of MF20 in ovine myoblast cultures differentiated in the presence of increasing concentrations of ouabain for 12 h (A), 24 h (B) and 48 h (C), as determined by measuring the intensity of MF20 fluorescence (2.2.22). Data presented are mean +/- SEM, the dagger and asterisks denote significant differences from vehicle alone: †P<0.1, *P<0.05, **P<0.01, ***P<0.001, n=6 replicates per concentration.

5.2.4 Mstn dependent regulation of the Na^+- K^+-ATPase β1 subunit occurs through a canonical Smad mechanism.

To identify signal transduction cascades involved in the Mstn dependant regulation of the Na^+-K^+-ATPase β1 transcript, proliferating ovine myoblasts were treated with Mstn for 6 h in the presence or absence of inhibitors for the MAPK, PI3K/AKT and ALK/Smad signal transduction cascades (Figure 4.5). The inhibitors of the MAPK and PI3K/AKT cascades did not alter the concentration of Na^+-K^+-ATPase β1 transcripts. In contrast, inhibition of ALK/Smad signalling reduced the concentration of β1 transcript (~0.4 fold, $P<0.01$). Co-treatment of myoblasts with Mstn and inhibitors showed that Mstn retained the ability to increase Na^+-K^+-ATPase β1 transcript abundance following the pharmacological blockade of both MAPK and PI3K/AKT pathways, (~2.3 fold, $P<0.01$) and (~2.1 fold, $P<0.01$) respectively, vs inhibitor alone. In contrast, Mstn could not induce the transcription of Na^+-K^+-ATPase β1 in the presence of the ALK/Smad inhibitor.

5.2.5 The effect of Mstn on Na^+- K^+-ATPase activity in vitro.

The hydrolysis of ATP inhibited by ouabain was assessed as a proxy for Na^+-K^+-ATPase activity at 1, 6, 12 and 24 h post Mstn or insulin treatment. Insulin was included as a positive control. Treatment of ovine myoblasts with Mstn had a tendency to reduce the hydrolysis of ATP inhibited by ouabain, with reductions at 1 h (28%, $P<0.1$), 6 h (62%, $P<0.1$) and 12 h (50%, $P<0.1$) post addition of Mstn. Unexpectedly, reduced ATP hydrolysis inhibited by ouabain at 1 h (78%, $P<0.01$), 6 h (76%, $P<0.01$) and 12 h (70%, $P<0.01$) was observed following insulin treatment. At 24 h post treatment there were with no significant changes in hydrolysis of ATP inhibited by ouabain in the presence of Mstn or insulin.

5.2.6 Na^+- K^+-ATPase β1 transcript is differentially expressed in the skeletal muscles and myoblasts of WT and Mstn-null mice.

To determine if the Na^+-K^+-ATPase β1 subunit was differentially expressed in muscles and myoblasts lacking functional Mstn, *gastrocnemius* muscles and primary myoblasts, isolated from wild-type (WT) and Mstn null mice, were used to assess the concentration of the β1 subunit transcript. Consistent with ovine myoblasts, *gastrocnemius* muscles of WT mice had

significantly higher concentrations of Na^+-K^+-ATPase β1 transcript (Figure 5.7) than their Mstn null counterparts (~1.8 fold, $P<0.05$). In contrast, primary WT myoblasts had reduced concentrations of Na^+-K^+-ATPase β1 subunit message (Figure 5.7) compared with their Mstn null counterparts in both proliferating and differentiating conditions (~2.2 fold, $P<0.01$, and ~4.2 fold, $P<0.01$), respectively.

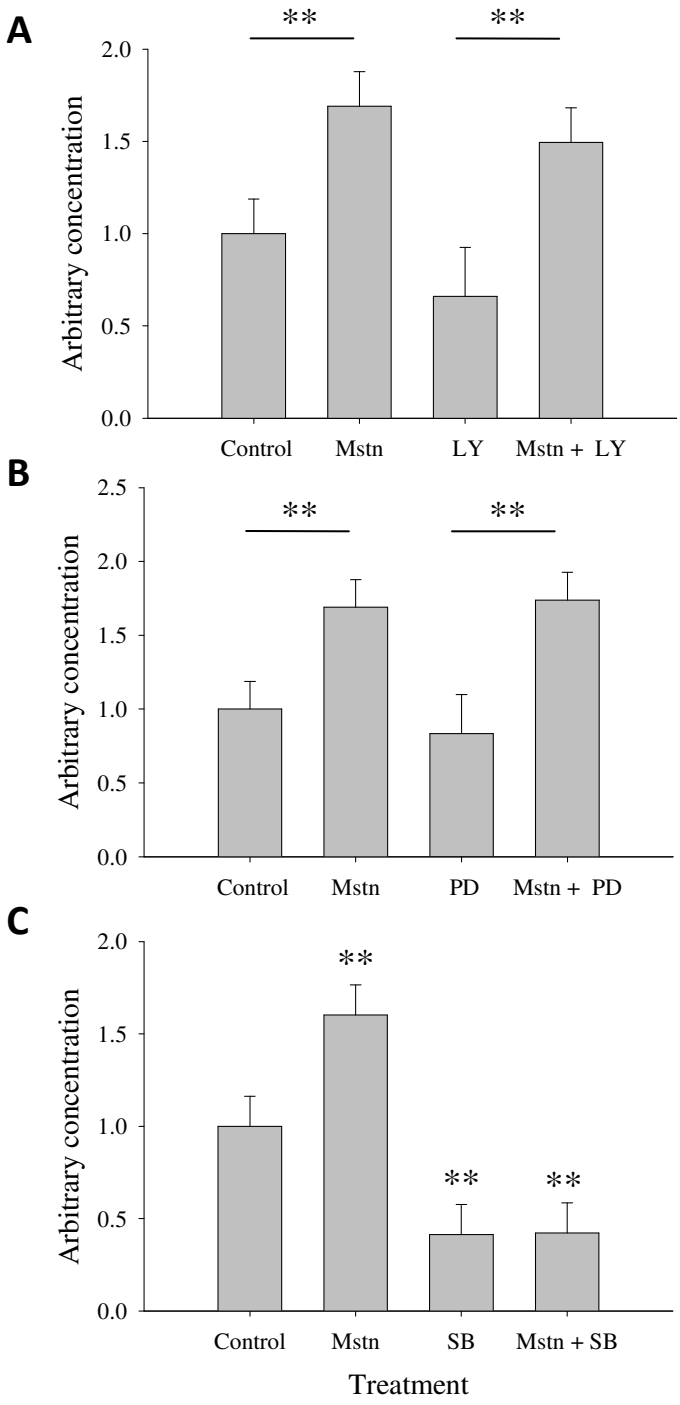

Figure 5.5: Mstn regulates the Na^+-K^+-ATPase β1 subunit through a Smad dependant mechanism. The relative abundance of Na^+-K^+-ATPase β1 subunit transcript in proliferating ovine myoblasts was assessed using qPCR. This was done in the presence or absence of Mstn and (A), PI3K/AKT (LY294002 (LY), 10μM), (B), MAPK (PD98059 (PD), 10μM) and (C), ALK/Smad (SB431542 (SB), 1μM) pharmacological inhibitors. Data presented are mean +/- SEM, asterisks denote significant differences from controls (**P<0.01), n=6 replicates per treatment. Concentrations were normalised to vehicle alone (control) values following adjustment to oligreen (total cDNA) values (2.2.1.4).

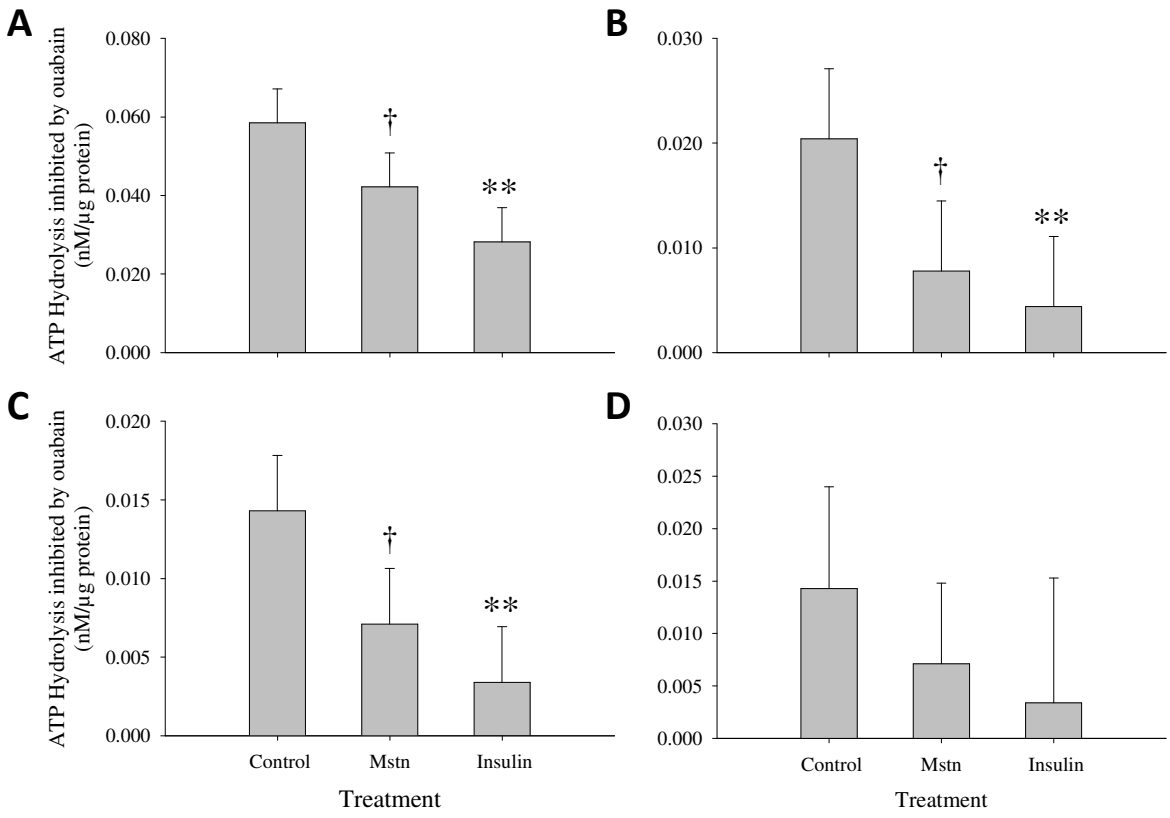

Figure 5.6: The effect of Mstn on the hydrolysis of ATP inhibited by ouabain (an assay of Na^+-K^+-ATPase activity) in ovine myoblasts. Activity of the Na^+-K^+-ATPase was determined in myoblast cultures treated with Mstn (100ng/mL), insulin (100nM) or vehicle alone (control). The reduction in ATP hydrolysis induced by ouabain for each treatment was used to calculate the ouabain inhibitable (OI) portion of ATP hydrolysis at 1 h (A), 6 h (B), 12 h (C) and 24 h (D) post Mstn or insulin treatment. Data presented are mean +/- SEM, asterisks denote significant differences from vehicle alone (control) values, †$p<0.1$, **$p<0.01$). n=6 replicates per treatment.

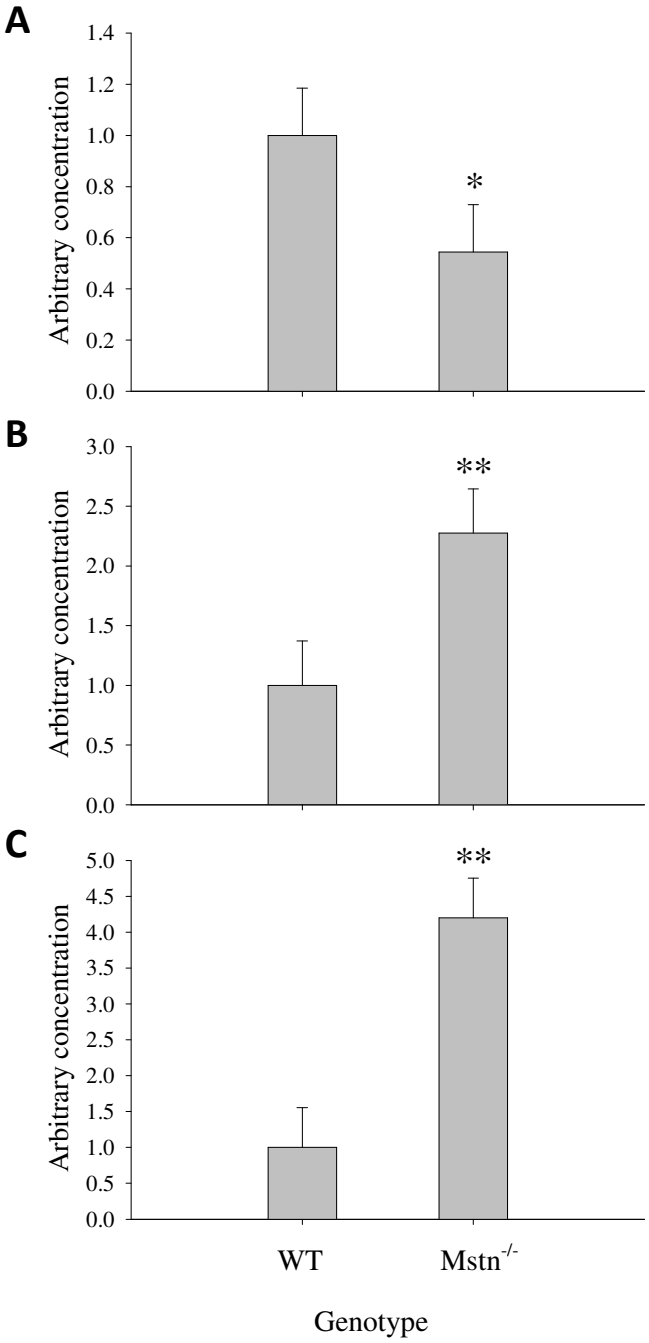

Figure 5.7: The Na^+-K^+-ATPase β1 subunit transcript is differentially expressed in skeletal muscles and myoblasts derived from WT and Mstn null mice. An arbitrary concentration of Na^+-K^+-ATPase β1 transcript was determined using qPCR in WT and $Mstn^{-/-}$ gastrocnemius muscle (A), proliferating myoblasts (B), and differentiating myoblasts (C). Data presented are mean +/- SEM, asterisks denote significant differences from WT (*$p<0.05$, **$p<0.01$). n=6 replicates per genotype for muscle and n=3 for myoblast cultures. Concentrations were normalised to vehicle alone (control) values following adjustment to oligreen (total cDNA) values.

5.3 Discussion

Mstn plays a major role in the regulation of skeletal muscle mass and a number of signalling pathways and downstream targets have now been identified (for review see (Elkina, von Haehling et al. 2011)). In the current study the Na^+-K^+-ATPase β1 subunit was identified as a transcriptional target of Mstn. Furthermore this regulation is dependent on canonical ALK/Smad signalling. Microarray analysis provided the first indication that the Na^+-K^+-ATPase β1 transcript was regulated by Mstn. This was subsequently confirmed using qPCR in both proliferating and differentiating ovine myoblasts treated with Mstn for 48 h. These data further demonstrated that Na^+-K^+-ATPase β1 transcript is not transiently regulated, but is sustained during extended periods of myoblast proliferation and differentiation.

To determine if Na^+-K^+-ATPase plays a functional role in myoblast proliferation or differentiation, the effect of ouabain was assessed in myoblasts during proliferation and differentiation. These studies demonstrated that the Na^+-K^+-ATPase complex plays a role in both the proliferation and differentiation of ovine myoblasts. An increased rate of cell proliferation following ouabain treatment has been previously described in a number of cell types, including: myocardial cells, smooth muscle cells, astrocytes, and renal proximal tubule cells (Nguyen, Wallace et al. 2007). The proliferative response seen here with low concentrations of ouabain (100pM-10nM) is consistent with other studies (Nguyen, Wallace et al. 2007) where proliferation is associated with the signal transduction rather than the ion flow function of the Na^+-K^+-ATPase (Xie and Askari 2002). However, the increases in proliferation observed at 24 h, were not seen following 48 h of proliferation. The reason for this discrepancy is not clear, but could be an artefact due to the spontaneous fusion of the myoblast cultures as they reach confluence at the later time points. After differentiation, myotubes absorb less methylene blue stain than proliferating myoblasts (unpublished observations). Treatment of myoblast cultures with high concentrations of ouabain (>30nM) significantly impaired myoblast proliferation, which illustrates the importance of the ion flow controlled by Na^+-K^+-ATPase in the maintenance of the proliferative phenotype. The inhibitory and most likely toxic action of high concentrations of ouabain on myoblast differentiation observed here, have been

previously described in cultured rat and mouse myoblasts (Pauw and Hermann 1994). Of particular interest here, were the changes observed in the expression of myosin heavy chain, following treatment with ouabain. Treatment with low concentrations of ouabain, suggested that the signal transduction function of the Na^+-K^+-ATPase can influence the early steps involved in the execution of the differentiation program. In support, previous studies have reported a stimulatory effect of ouabain on the hypertrophic gene expression in rat cardiomyocytes (Kometiani, Li et al. 1998), in addition to a role in facilitating the cardiac differentiation of mouse embryonic stem cells (Lee, Ng et al. 2011). As with proliferation, differentiating myoblasts were refractory to high concentrations of ouabain, which is most likely due the toxicity of ouabain at high concentrations and, illustrate the importance of the ion flow function of the Na^+-K^+-ATPase for myogenesis.

After establishing that Mstn regulates the β1 subunit of the Na^+-K^+-ATPase, identifying the signal transduction cascade responsible for this action became a strong focus. These studies revealed that Mstn signalled via the canonical Alk/Smad pathway, but not through PI3K or MAPK pathways to regulate the β1 subunit. This was evidenced by the inability of PI3K or MAPK blockade to influence the Mstn dependant regulation of the β1 subunit transcript. Interestingly, the pharmacological inhibition of ALK/Smad alone significantly reduced the concentration Na^+-K^+-ATPase β1 subunit, which implies this pathway is of major importance in the regulation of the Na^+-K^+-ATPase β1 subunit in myoblasts. Therefore, this mechanism may not be exclusive to Mstn and may be common to other members of the TGF-β super-family, conveying the ability to regulate β1 transcript in both muscle, and potentially, other tissues.

In an effort to determine if Mstn also regulates Na^+-K^+-ATPase activity, the hydrolysis of ATP inhibited by ouabain was assessed in proliferating ovine myoblasts treated with Mstn over a 24 h period. A trend to reduce the ouabain inhibitable hydrolysis of ATP was observed following Mstn treatment for 1, 6 and 12 h. Therefore, Mstn may directly regulate the activity of the Na^+-K^+-ATPase. Interestingly, insulin treatment also reduced ouabain inhibitable ATP hydrolysis. This was an unexpected finding given that insulin was included as positive control and was expected to stimulate the activity of the Na^+-K^+-ATPase (Omatsu-Kanbe

and Kitasato 1990; Al-Khalili, Kotova et al. 2004; Hatou, Yamada et al. 2010). However, other studies in rat skeletal muscle have demonstrated that insulin treatment can increase the activity of the Na^+-K^+-ATPase, as assessed by ^{86}Rb uptake, without altering the ouabain binding affinity of the Na^+-K^+-ATPase (McKenna, Gissel et al. 2003). Alternatively, it cannot be discounted that insulin may differentially affect the activity of the Na^+-K^+-ATPase in these cells compared with other cell types. the effect of insulin on Na^+-K^+-ATPase activity in ovine myoblasts has not being previously reported

To support a role for Mstn in the regulation of the Na^+-K^+-ATPase β1 subunit, the concentration of the β1 transcript was quantified in WT and Mstn null *gastrocnemius* muscles and myoblasts. Consistent with Mstn increasing the concentration of β1 transcript, WT *gastrocnemius muscles* contained higher concentrations of β1 transcript. In contrast, the concentration of β1 transcript was higher in proliferating and differentiating Mstn null myoblasts. The reason for this discrepancy is unclear. It should be noted that the culture medium is common to both WT and Mstn null myoblasts, and with the numerous growth factors present in the culture medium a differential effect on the two genetic backgrounds cannot be discounted.

In conclusion, Mstn regulates the β1 subunit of the Na^+-K^+-ATPase transcript through a canonical signalling mechanism, and potentially, regulates the activity of the Na^+-K^+-ATPase in ovine myoblasts. However, it is likely that other TGF β family members also influence the expression of this subunit, with the ALK/Smad pathway common to this super-family. Given that the β1 subunit of the Na^+-K^+-ATPase is one of the most abundantly expressed isoforms in skeletal muscle (Murphy, Medved et al. 2008) and that it plays a significant role in the assembly and localisation of the functional Na^+-K^+-ATPase complex (Johar, Priya et al. 2012), its regulation by Mstn may play a significant role in myogenesis. Others have reported that TGF-β1, also a member of the TGF-β super-family, regulates the β1 subunit via a Smad dependant pathway in renal epithelial cells (Rajasekaran, Huynh et al. 2010). In support a much earlier study identified an effect of TGF- β treatment on Na^+-K^+-ATPase α and β transcript (isoform was not specified), and the activity of the Na^+-K^+-ATPase in proximal tubule cells (Tang, Wang et al. 1995). The β1 subunit has also been shown to be a target of the

MicroRNA-192 (Mladinov, Liu et al. 2013), a MicroRNA that has also been shown to be altered in response to TGF-β signalling (Hong, Li et al. 2013). Thus, the β1 subunit can be regulated by TGF-β signalling in at least two different tissues through Smad dependant pathways. These findings suggest that regulation of the Na^+-K^+-ATPase β1 subunit through TGF-β signalling constitutes a conserved mechanism that may prove to be important in the tissue specific regulation and activity of the Na^+-K^+-ATPase.

Chapter Six

6 Over-expression of MSV in C_2C_{12} myoblasts

6.1 Introduction

The production of eukaryotic proteins in prokaryotic systems such as *E. coli* has provided a valuable research tool, allowing the mass production of specific proteins to aid in the investigation of protein function. However, the use of prokaryotic systems for protein production has limitations that often depend on the nature of the expressed protein. This can include the incorrect folding of the expressed protein due to the absence of necessary chaperone proteins. In addition, bacterial contaminants such as LPS or bacterial proteins can be co-purified as contaminants in the recombinant preparation. The presence of incorrectly folded protein or bacterial contaminants can compromise protein function and potentially, introduce artefacts which confound bioactivity. Furthermore, methods for the removal of these contaminants can alter the yield and the function of the target protein. Therefore, the aim of the following chapter is to address the function of MSV in a murine myoblast line (C_2C_{12}) that expresses MSV. The use of this model allows the production of MSV in a eukaryotic cell line, with the advantage of avoiding the confounding issues associated with the production of this protein in *E. coli*. Thus, the hypothesis for these studies was that: The over-expression of MSV in C_2C_{12} myoblasts would alter the proliferation, differentiation and/or metabolic characteristics of these cells. In addition, that the over-expression of MSV would alter the abundance and/or the phosphorylation of signal transduction molecules involved in this processes.

With the aim of investigating the function of over-expressed MSV in C_2C_{12} myoblast proliferation, differentiation, metabolism and signal transduction, C_2C_{12} cell lines expressing full length ovine MSV (GenBank accession number: DL465814.1) were generated. One challenge faced in the generation of MSV expressing cell lines, was the detection of translated MSV protein. Thus, CHO and HEK293 cells expressing MSV were generated to provide additional models to confirm the translation of the expressed MSV protein. To provide an alternative means of detecting MSV, two over-expression constructs were generated, one containing the full length ovine MSV open reading frame (MSV) and one

containing full length MSV with in frame C-terminal V5 and histidine tags (C-MSV). The tagged construct provided a means of demonstrating that the over-expressed MSV transcript is translated into protein, with the caveat that the C-terminal tag may perturb the functionality of over-expressed MSV protein. Control cell lines were also generated using the pcDNA3 vector lacking the MSV expression cassettes.

6.2 Results

6.2.1 Sequence integrity of full length MSV constructs

The MSV expression cassettes were cloned into the pcDNA3 (Invitrogen) vector, containing an upstream CMV promoter and an independent neomycin resistance cassette. The integrity of the MSV sequence was confirmed using DNA sequencing (Massey University). Subsequent alignment of the DNA sequences (www.justbio.com) revealed two discrepancies at positions 435 and 600 of the predicted ovine MSV open reading frame. These corresponded to the third bases of codons 135 and 150 respectively. These mutations were subsequently identified as wobble bases, with the protein sequence coded for by the cloned MSV cassettes being identical to that of the predicted ovine MSV sequence. In addition, sequence data confirmed that the C-terminal V5 and histidine epitopes of the tagged MSV construct (C-MSV) were in-frame, with a correctly placed stop codon. Figure 6.1 outlines the DNA, and Figure 6.2 the translated protein alignment of the two MSV constructs as compared to the predicted sequence of ovine MSV (GenBank accession number: DL465814.1).

6.2.2 Confirmation of over-expression in transfected cell lines

Following transfection and neomycin selection, two approaches were used to confirm that the MSV transgene was being expressed. Reverse transcriptase PCR was used to confirm the presence of the MSV transcript in neomycin resistant C_2C_{12} cells from pooled and clonal cell lines. As seen in Figure 6.3 (A), the full-length MSV transcript was detected in pooled and clonal C_2C_{12} cell lines. MSV transcript was also detected in C-MSV stable cell lines. Furthermore, primers specific for C-MSV only amplified MSV in C-MSV myoblasts (Figure 6.3 (B)). To confirm that over-expressed MSV transcript was translated into protein, stable MSV, C-MSV expressing and control cell lines were cultured in

serum free chemically defined media (Invitrogen), and conditioned media was harvested following 72 hours of culture. In house antibodies raised against the C-terminal portion of MSV failed to detect MSV in the conditioned media from C_2C_{12}, CHO or HEK 293 cells expressing MSV or C-MSV (data not shown). However, western blot analysis of conditioned media from cells expressing C-MSV, showed the presence a V5 reactive band close to the expected molecular weight (~40kDa) of MSV, present in conditioned media from CHO and HEK293 cells (Figure 6.3 (C)), but not in C_2C_{12} cells. Thus, a further investigation of conditioned media from clonal C_2C_{12} cell lines that were derived from the original neomycin resistant C-MSV C_2C_{12} cell pool was performed. As shown in Figure 6.3 (D), conditioned media from some clonal C-MSV cell lines demonstrated a V5 reactive band of the same molecular weight as that observed in conditioned media from C-MSV HEK293 and CHO cells. This result gave me confidence that the presence of the MSV expression cassette resulted in the translation and secretion of MSV protein, albeit at low concentrations in the C_2C_{12} myoblasts. To reduce the variation that is associated with the use of clonal C_2C_{12} cell lines, the parent C_2C_{12} cell pool was preferred over individual clonal MSV expressing cell lines to continue investigating MSV function. Thus, remaining studies in this chapter investigated the differences between MSV expressing and control C_2C_{12} cell lines.

6.2.3 Proliferation of over-expressing cell lines

Given the well-established role of Mstn as a regulator of myoblast proliferation, it was hypothesised that the expression of MSV would influence the proliferative capacity of C_2C_{12} myoblasts. To assess a potential role for MSV in myoblast proliferation, stable MSV and control C_2C_{12} cultures were seeded on 96-well plates at a density of 1,000 cells per well and proliferation was assessed with the methylene blue proliferation assay. Cells were fixed at 24h intervals, over a 96h time-course to assess proliferation. As shown in Figure 6.4, myoblasts expressing MSV showed, small, but significant increases in proliferation following 48 h (10%, $P<0.001$) and 72 h (2.5%, $P<0.001$) of proliferation, with no changes in proliferation observed at earlier time-points.

6.2.4 Differentiation of over-expressing cell lines

Mstn has been shown to inhibit myoblast differentiation, thus it was hypothesised that the expression of MSV may enhance this process in myoblasts. To assess a potential role for MSV in myogenic differentiation, MSV and control C_2C_{12} cell lines were seeded at 25000 cells per well in growth media and left overnight before the addition of differentiation media (T0). Cells were then fixed at 24h intervals over a 96h differentiation time course. The extent of differentiation assessed using a myosin heavy chain fluorescence assay (2.2.22 and Appendix 1). As shown in Figure 6.4 (B), C_2C_{12} cells expressing MSV displayed significantly more MHC immunoreactivity at 48 h (1.9 fold, $P<0.01$), 72 h (1.8 fold, $P<0.001$) and 96 h (1.4 fold, $P<0.001$) of differentiation, as compared to control C_2C_{12} cells. In addition, the DAPI (Invitrogen) fluorescent DNA dye was used to detect nuclei in the same cells (Figure 6.4 (C)), with DAPI fluorescence increased at all time-points in cells expressing MSV (~1.5-1.8 fold, $P<0.001$). The MHC:DAPI ratio (i.e. MF20 expression per nuclei) was used to indicate the relative fusion of the differentiating cultures. As shown in Figure 6.4 (D) no difference was observed in the MHC:DAPI ratio between MSV and pcDNA3 cultures.

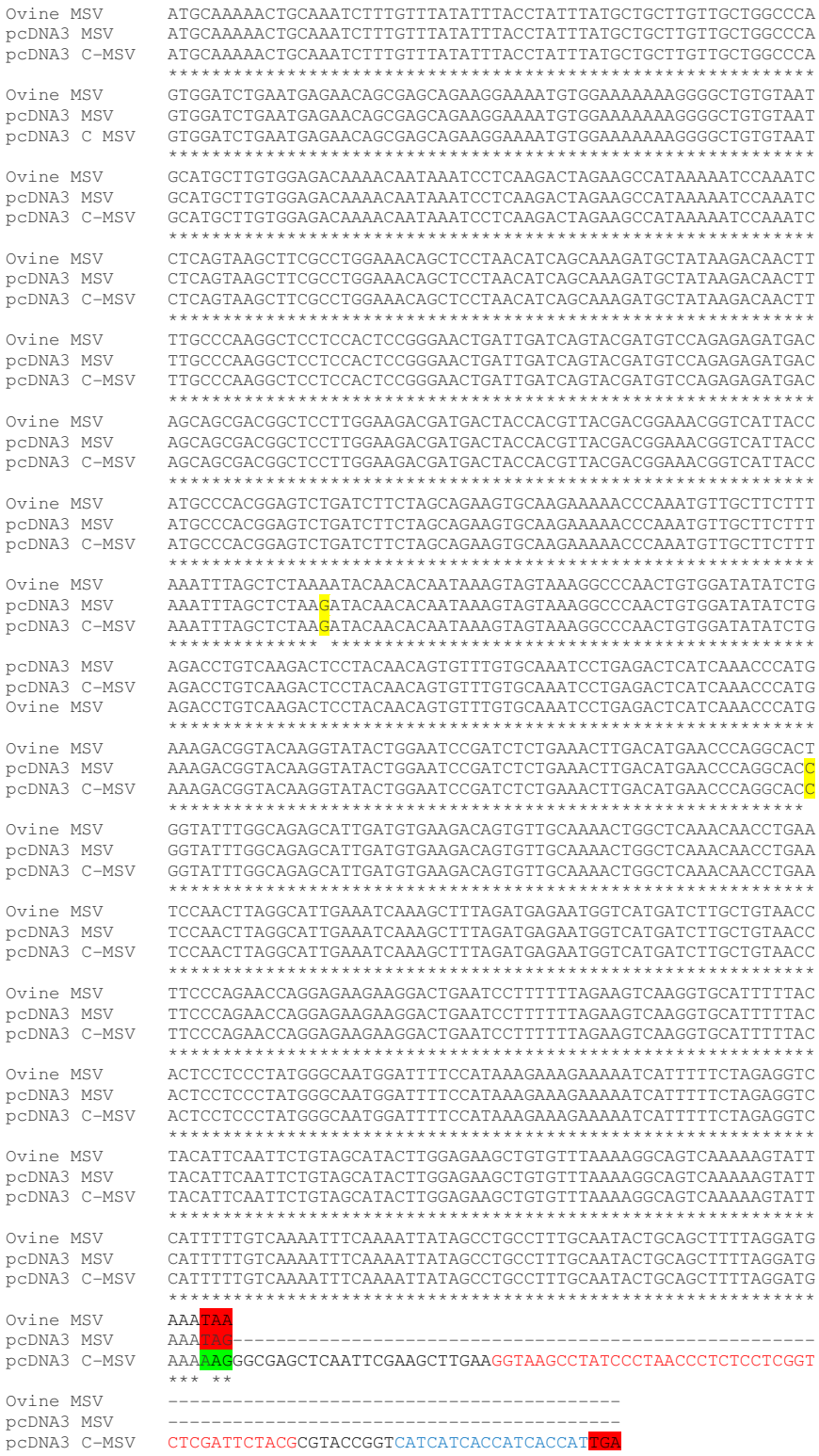

Figure 6.1: Sequence alignment of MSV expression cassettes. The MSV expression cassettes were sequenced and the predicted open reading frames of MSV (GenBank: DL465814.1), pcDNA3 MSV and pcDNA3 C-MSV were aligned. (www.justbio.com). Stars (⋆) indicate agreement between all three sequences for individual nucleotides. Highlighted are the mutations at nucleotides 435 and 600 (yellow), stop codons (red), the mutated stop of the C-MSV cassette (green). Also shown are the V5 sequence (red letters) and histidine tag sequence (blue letters).

```
Ovine MSV              MQKLQIFVYIYLFMLLVAGPVDLNENSEQKENVEKKGLCNACLWRQNNKSSRLEAIKIQI
MSV in pcDNA3          MQKLQIFVYIYLFMLLVAGPVDLNENSEQKENVEKKGLCNACLWRQNNKSSRLEAIKIQI
C-MSV in pcDNA3        MQKLQIFVYIYLFMLLVAGPVDLNENSEQKENVEKKGLCNACLWRQNNKSSRLEAIKIQI
                       ************************************************************

Ovine MSV              LSKLRLETAPNISKDAIRQLLPKAPPLRELIDQYDVQRDDSSDGSLEDDDYHVTTETVIT
MSV in pcDNA3          LSKLRLETAPNISKDAIRQLLPKAPPLRELIDQYDVQRDDSSDGSLEDDDYHVTTETVIT
C-MSV in pcDNA3        LSKLRLETAPNISKDAIRQLLPKAPPLRELIDQYDVQRDDSSDGSLEDDDYHVTTETVIT
                       ************************************************************

Ovine MSV              MPTESDLLAEVQEKPKCCFFKFSSKIQHNKVVKAQLWIYLRPVKTPTTVFVQILRLIKPM
MSV in pcDNA3          MPTESDLLAEVQEKPKCCFFKFSSKIQHNKVVKAQLWIYLRPVKTPTTVFVQILRLIKPM
C-MSV in pcDNA3        MPTESDLLAEVQEKPKCCFFKFSSKIQHNKVVKAQLWIYLRPVKTPTTVFVQILRLIKPM
                       ************************************************************

Ovine MSV              KDGTRYTGIRSLKLDMNPGTGIWQSIDVKTVLQNWLKQPESNLGIEIKALDENGHDLAVT
MSV in pcDNA3          KDGTRYTGIRSLKLDMNPGTGIWQSIDVKTVLQNWLKQPESNLGIEIKALDENGHDLAVT
C-MSV in pcDNA3        KDGTRYTGIRSLKLDMNPGTGIWQSIDVKTVLQNWLKQPESNLGIEIKALDENGHDLAVT
                       ************************************************************

Ovine MSV              FPEPGEEGLNPFLEVKVHFYTPPYGQWIFHKERKIIFLEVYIQFCSILGEAVFKRQSKSI
MSV in pcDNA3          FPEPGEEGLNPFLEVKVHFYTPPYGQWIFHKERKIIFLEVYIQFCSILGEAVFKRQSKSI
C-MSV in pcDNA3        FPEPGEEGLNPFLEVKVHFYTPPYGQWIFHKERKIIFLEVYIQFCSILGEAVFKRQSKSI
                       ************************************************************

Ovine MSV              HFCQNFKIIACLCNTAAFRMKX
MSV in pcDNA3          HFCQNFKIIACLCNTAAFRMKX
C-MSV in pcDNA3        HFCQNFKIIACLCNTAAFRMKKGELNSKLEGKPIPNPLLGLDSTRTGHHHHHHX
                       **********************
```

Figure 6.2: Predicted protein sequence from MSV expression cassettes. Protein sequences for MSV, pcDNA3 MSV and pcDNA3 C-MSV, derived from the respective nucleotide sequence for each, were aligned (www.justbio.com). Stars (*) indicate agreement between all three sequences for individual amino acids. Highlighted are the stop codons (red), and the V5 (red letters) and histidine tag (blue letters) epitopes.

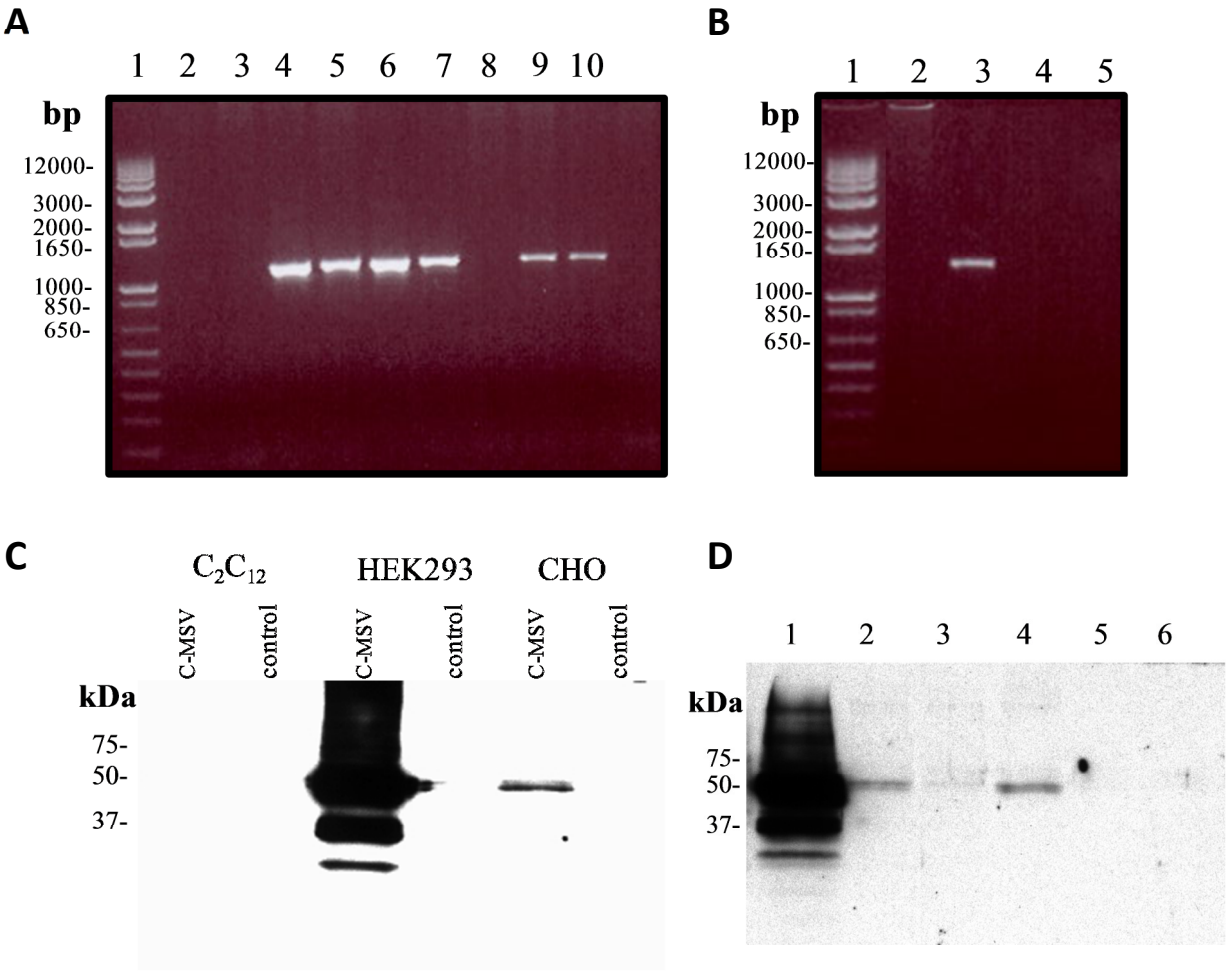

Figure 6.3: Confirmation of MSV over-expression. Firstly, the expression of MSV in C_2C_{12} pooled and clonal myoblasts was confirmed using PCR. The full MSV sequence was amplified from reverse transcribed cDNA, isolated from distinct neomycin resistant C_2C_{12} cell lines. (A) PCR amplification using primers specific for MSV (expected size, 1064bp), with: Lane 1, 1kb+ DNA ladder, 2, negative control, 3-7, MSV C_2C_{12} clones a-e, 8, control (pcDNA3 only) C_2C_{12} cell pool, 9, MSV C_2C_{12} pool and 10, C-MSV cell pool. (B) PCR amplification using primers specific for C-MSV (expected size, 1160bp), with Lane 1, 1kb+DNA ladder, 2, control C_2C_{12} cell pool, 3, C-MSV cell pool, 4, MSV C_2C_{12} pool and 5, negative control. Secondly, neomycin resistant cells transfected with C-MSV were cultured and used to condition chemical media for 72 h. Western blot analysis following SDS PAGE was performed on ~20 µL of conditioned media from each cell line tested. Anti V5 antibody was used to detect the C-terminal V5 tag of C-MSV, with the theoretical molecular weight of C-MSV ~40 kDa (www.justbio.com). (C), V5 immunoblot performed on C-MSV and control C_2C_{12}, HEK293 CHO cell pools. (D) Clonal analysis of C-MSV in C_2C_{12} cells, with Lane 1, C-MSV HEK293 cells (positive control), 2-5 C-MSV C_2C_{12} clones a-d, 6, control C_2C_{12} clonal cell line.

1.462423

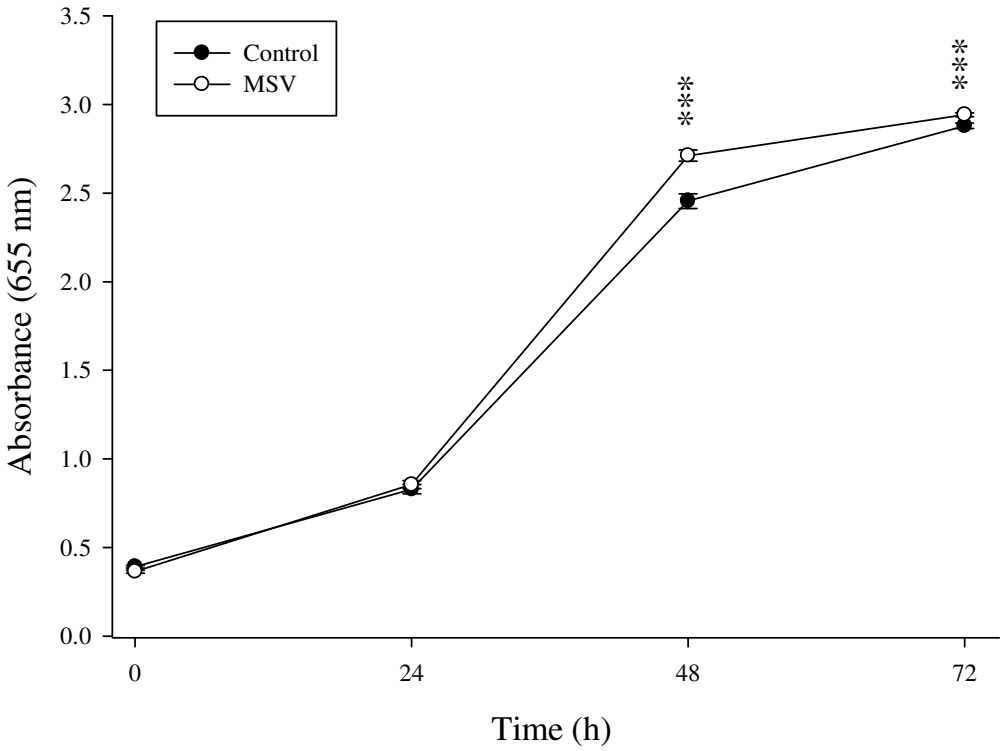

Figure 6.4: Proliferation of C_2C_{12} cells expressing MSV. Stable C_2C_{12} myoblasts expressing MSV or pcDNA3 (control), were cultured over a 72 h period in growth media to assess proliferation, with cells fixed at 24 h intervals. Proliferation was determined using the methylene blue assay and read at an optical density (OD) of 650nm. Data presented are mean +/- SEM, asterisks denote significant differences between MSV expressing and control cultures, with: **P<0.01, *** P<0.001, n=8 replicates per cell type.

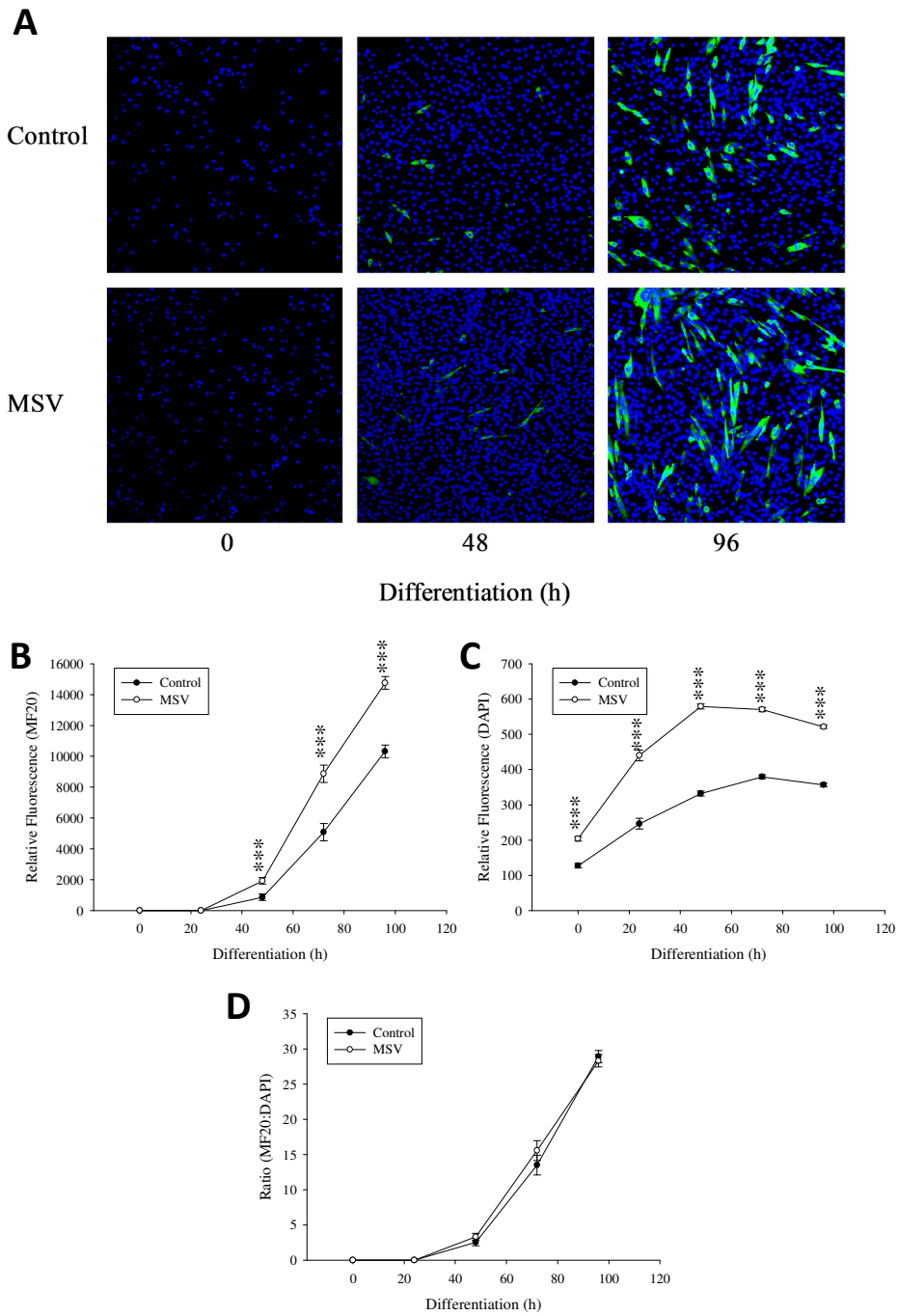

Figure 6.5: Differentiation of C_2C_{12} cells expressing MSV. Stable C_2C_{12} myoblasts expressing MSV or pcDNA3 (control), were cultured in differentiation media over a 96 h time-course. At 24 h intervals cells were fixed and assessed for relative DAPI (nuclei) and MF20 (myosin heavy chain) fluorescence. Shown in (A) are representative images of differentiating MSV and control cells at 0, 48 and 96 h of differentiation. Relative fluorescence values are shown for (B), MF20 (excitation 485nm, emission 528nm), (C), DAPI (excitation 360nm, emission 460nm) and (D) the MF20:DAPI ratio. Data presented are mean +/- SEM, asterisks denote significant differences between MSV and control cells at each time-point: *** P<0.001, n=12 replicates per cell-type per time-point.

6.2.5 Gene expression analysis in C_2C_{12} cells over-expressing MSV.

To establish if the expression of MSV in C_2C_{12} myoblasts affected the same signalling targets as those investigated earlier for Mstn (4.2.1), western blot analysis of whole cell lysates derived from MSV and control C_2C_{12} cultures was performed. Included in the analysis, were major transcription factors that control myogenesis, signal transduction molecules with crucial roles in the TGF-β, MAPK and PI3K cascades, and targets involved in metabolic regulation.

6.2.5.1 Regulation of myogenic transcription factors in MSV over-expressing cell lines

Mstn activates signalling pathways that regulate the expression of muscle specific transcription factors. To determine if the expression of MSV altered the abundance of key myogenic transcription factors, the relative abundance of Pax7, Mef2 and the MRF family of transcription factors (MyoD, Myf5, myogenin and MRF4) was assessed. Western analysis (Figure 6.5) showed that the expression of MSV increased the abundance of MyoD (1.3 fold, $P<0.05$), MRF4 (~1.3 fold, $P<0.05$) and myogenin (~1.3 fold, $P<0.05$). With no difference in the abundance of Pax7, Mef2 and Myf5 transcription factors between the MSV and control cell lines.

6.2.5.2 Canonical Mstn signalling in MSV over-expressing cell lines

To determine if the expression of MSV influenced cellular targets involved in Mstn signalling, the abundance and phosphorylation status of Smad 2 and 3 were investigated. As shown in Figure 6.6, C_2C_{12} cells expressing MSV had an increased abundance of Smad 3 protein (~1.6 fold, $P<0.05$), with no change in the abundance of Smad 2. In addition, phosphorylation of Smad 2 or 3 was not detected by western blot in this study (data not shown).

6.2.5.3 MAPK signalling in MSV over-expressing cell lines

To establish if the expression of MSV influenced components of the MAPK signalling cascade, the abundance and phosphorylation status of ERK 1, ERK 2 and p38 MAPK was investigated (Figure 6.7). In C_2C_{12} expressing MSV, no change was observed in the abundance of ERK 1 or 2. The expression of MSV tended to increase the phosphorylation of ERK1 (~1.3 fold, $P<0.1$), with no

change observed in the phosphorylation of ERK 2. Neither p38 MAPK, nor phosphorylated p38 were able to be detected in these lysates (data not shown).

6.2.5.4 PI3K/AKT signalling in MSV over-expressing cell lines

To determine if the expression of MSV altered components in the PI3K signalling cascade, the abundance and phosphorylation status of AKT and PDK1 were investigated. As shown in Figure 6.8, the expression of MSV increased the abundance of total AKT and phosphorylated AKT at S473 (~1.2 fold, $P<0.05$ and ~1.5 fold, $P<0.05$, respectively), but not the phosphorylation of AKT at T308. However, no changes in the abundance or phosphorylation of PDK1 were observed in C_2C_{12} myoblasts expressing MSV.

6.2.5.5 Metabolic Targets

Given that Mstn plays a role in regulating metabolism in skeletal muscle (1.1.7.6), the expression of MSV may alter similar metabolic targets to those regulated by Mstn. Key metabolic targets previously reported to be influenced by Mstn include, AMPK, ACC, rpS6 and 4EBP1. Therefore, the abundance and phosphorylation of these targets was assessed in C_2C_{12} cells expressing MSV (Figure 6.9). In comparison to control cells, C_2C_{12} cells expressing MSV tended to have higher abundance of total AMPK (~1.2 fold, $P<0.1$), with no change in the abundance of phosphorylated AMPK. The abundance and the phosphorylation of ACC (a downstream target of AMPK) was increased in cells expressing MSV (~1.3 fold, $P<0.05$ and, ~1.3 fold, $P<0.01$, respectively). The abundance of total rpS6 was increased in cells expressing MSV (~2.2 fold, $P<0.01$), with no change observed in the phosphorylation of rpS6 (data not shown). Finally, the abundance and the phosphorylation of 4EBP1 was increased in cells expressing MSV (~1.4 fold, $P<0.01$ and ~1.3 fold, $P<0.01$, respectively).

6.2.6 Metabolic capacity of over-expressing cell lines using the EZ4U assay

To assess if the increases in proliferation observed in myoblasts expressing MSV could be due to an increase in metabolic capacity, the EZ4U assay (ALPCO) was used to measure the metabolic capacity of C_2C_{12} cells expressing MSV. The EZ4U assay utilises the ability of functional mitochondria to metabolise tetrazolium salts, this yields coloured, soluble formazan derivatives. These can be quantified with the use of spectrophotometry, with the OD

proportional to the amount of formazan derivative formed and thus, the functionality of the cellular mitochondria. As shown in Figure 6.10, there was no difference in EZ4U activity at the start of the proliferation time-course (0 h) or following 24 h of proliferation. After 48 and 72 h of proliferation EZ4U activity was increased in myoblasts expressing MSV as compared with their control counterparts (~5.8%, $P<0.01$ and ~9.4%, $P<0.001$, respectively).

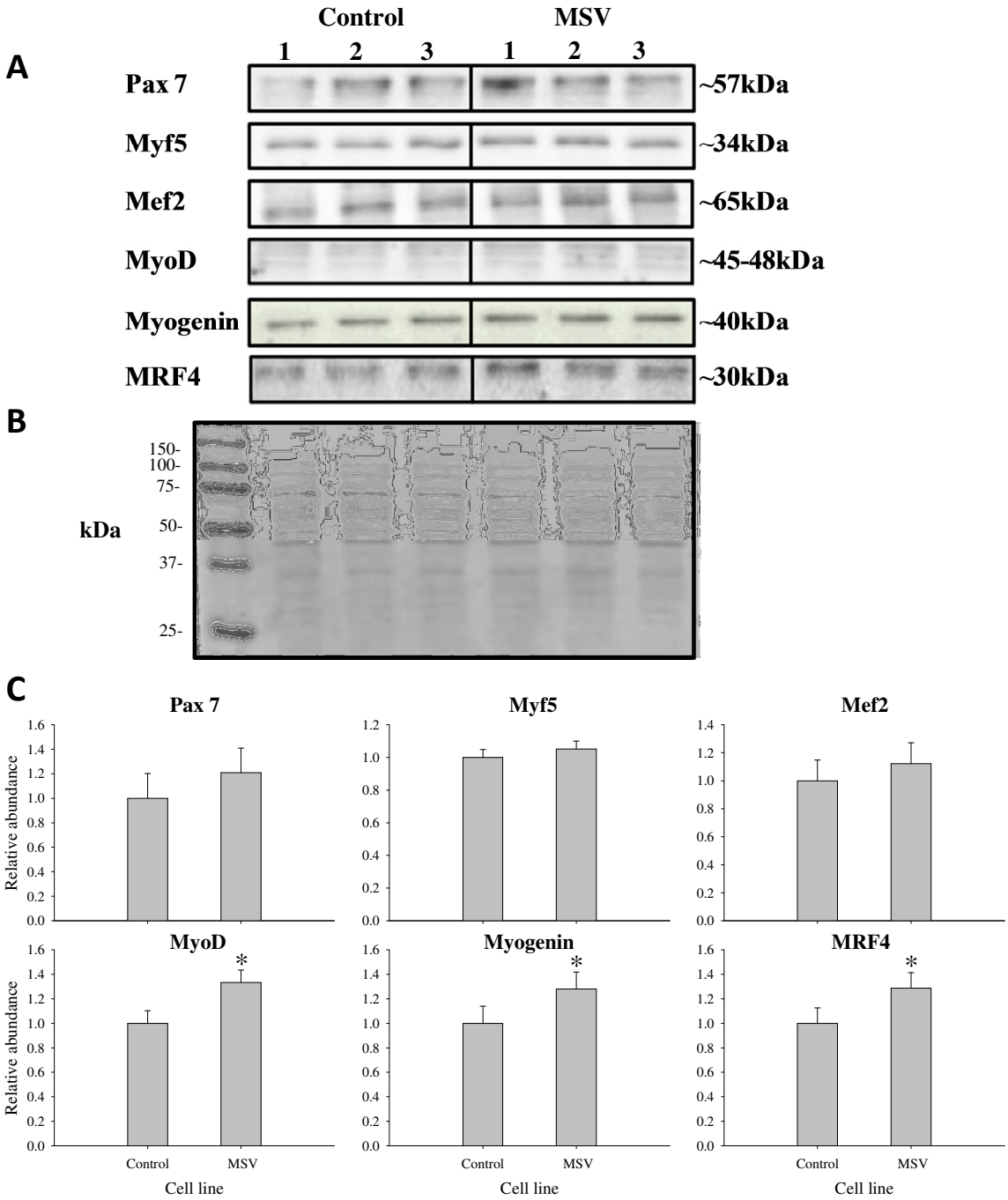

Figure 6.6: Abundance of myogenic transcription factors in C_2C_{12} cells expressing MSV. For western blot analysis, 10µg of whole cell lystates isolated from actively growing C_2C_{12} cells expressing MSV, and controls were run on a SDS/PAGE gel and blotted onto nitrocellulose. Immunoblots were performed for the depicted proteins (A), with the image capture performed using a LAS4000 imaging system (GE healthcare). Equal loading of protein samples was assessed using Ponceau stain, with a representative blot shown in (B). Density values were obtained using Quantity One software (BioRad), with the relative abundance calculated by normalising the density values obtained from MSV expressing cells to those of their control counterparts (C). Normalised data presented are mean +/- SEM, asterisks denote significant differences between MSV expressing and control C_2C_{12} cells, with: *$P<0.05$, n=3 replicates per cell type.

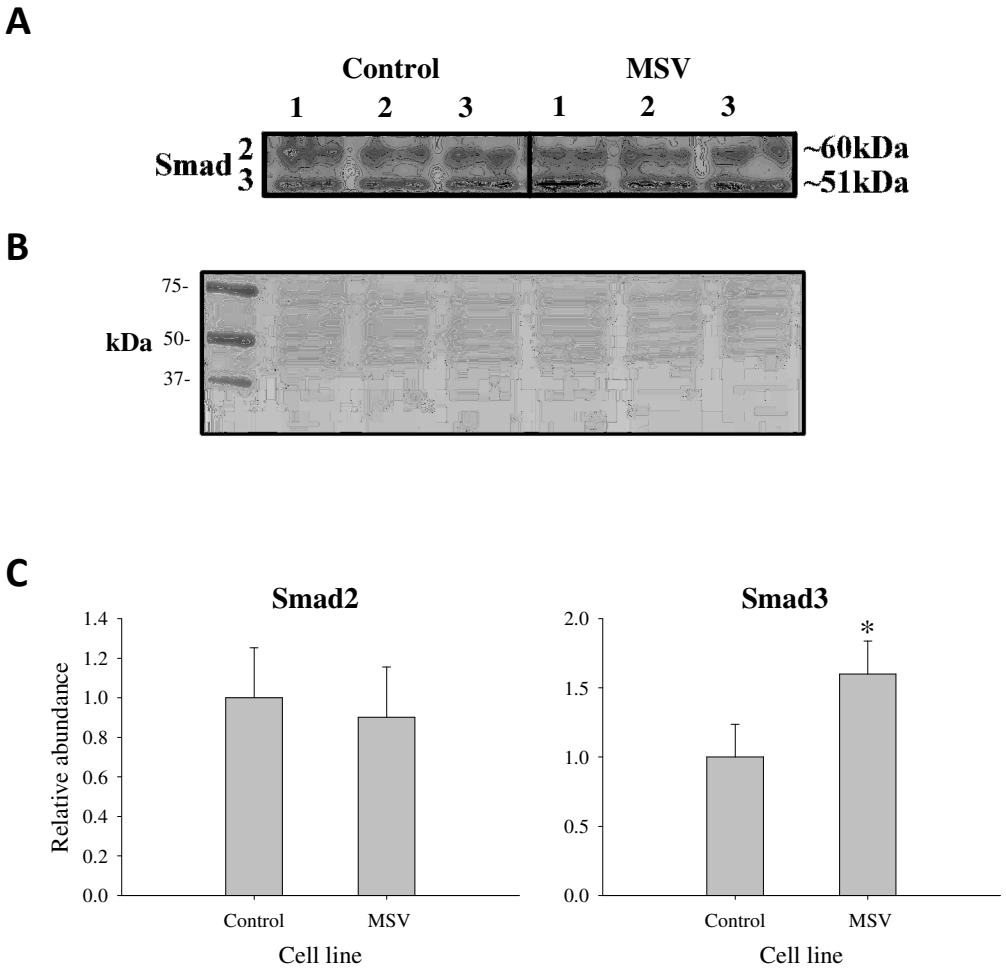

Figure 6.7: Abundance of the Smad transcription factors in C_2C_{12} cells expressing MSV. For western blot analysis, 10µg of whole cell lysates isolated from actively growing C_2C_{12} cells expressing MSV, and controls were run on a SDS/PAGE gel and blotted onto nitrocellulose. Immunoblots were performed for the depicted proteins (A), with the image capture performed using a LAS4000 imaging system (GE healthcare). Equal loading of protein samples was assessed using Ponceau stain, with a representative blot shown in (B). Density values were obtained using Quantity One software (BioRad), with the relative abundance calculated by normalising the density values obtained from MSV expressing cells to those of their control counterparts (C). Normalised data presented are mean +/- SEM, the asterisk denotes a significant difference between MSV expressing and control C_2C_{12} cells, with: *P<0.05, n=3 replicates per cell type.

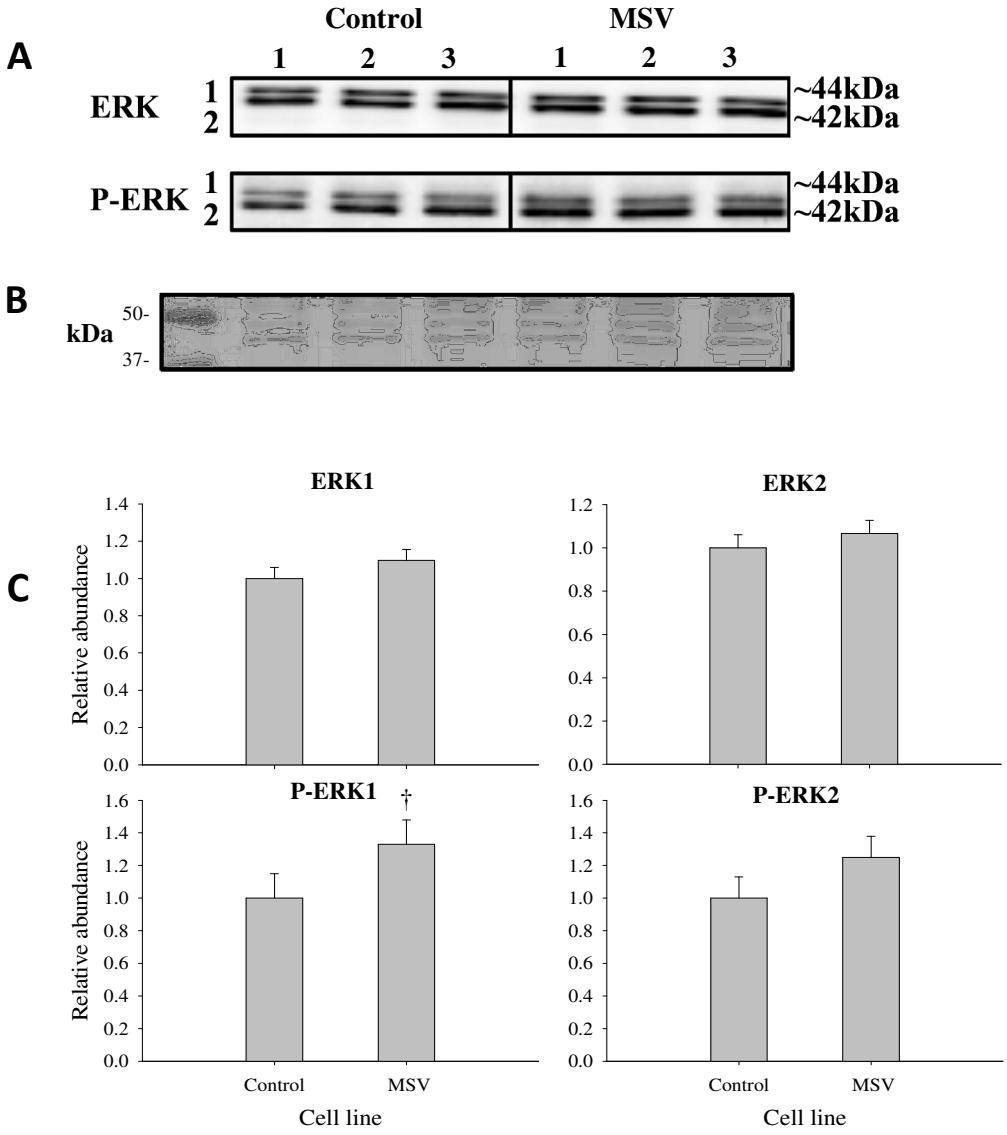

Figure 6.8: **Abundance of MAPK targets in C_2C_{12} cells expressing MSV.** For western blot analysis, 10µg of whole cell lysates isolated from actively growing C_2C_{12} cells expressing MSV, and controls were run on a SDS/PAGE gel and blotted onto nitrocellulose. Immunoblots were performed for the depicted proteins (A), with the image capture performed using a LAS4000 imaging system (GE healthcare). Equal loading of protein samples was assessed using Ponceau stain, with a representative blot shown in (B). Density values were obtained using Quantity One software (BioRad), with the relative abundance calculated by normalising the density values obtained from MSV expressing cells to those of their control counterparts (C). Normalised data presented are mean +/- SEM, The dagger denotes a trend between MSV expressing and control C_2C_{12} cells, with: †$P<0.1$, n=3 replicates per cell type.

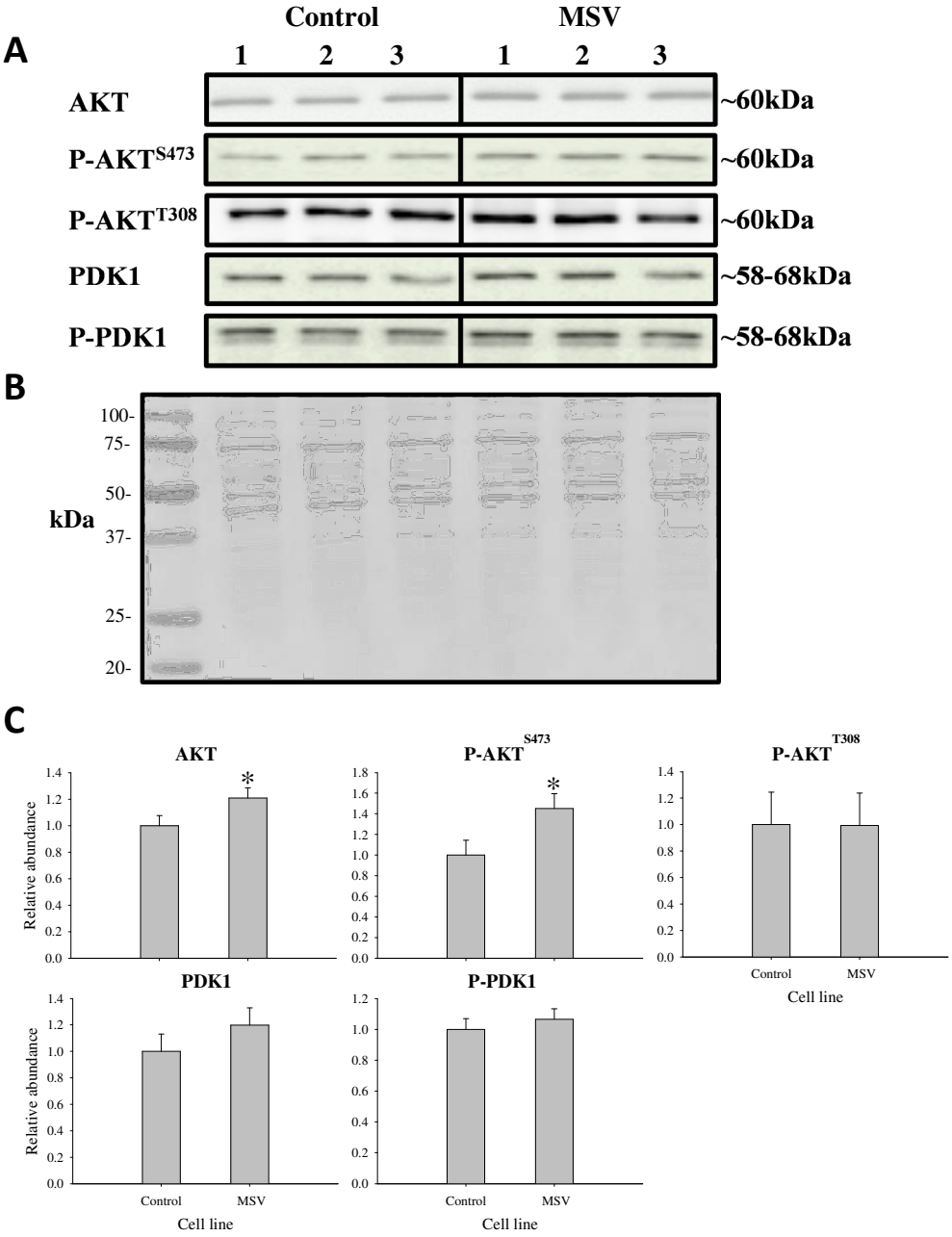

Figure 6.9: Abundance and phosphorylation of PI3K and AKT targets in C_2C_{12} cells expressing MSV. For western blot analysis, 10µg of whole cell lysates isolated from actively growing C_2C_{12} cells expressing MSV, and controls were run on a SDS/PAGE gel and blotted onto nitrocellulose. Immunoblots were performed for the depicted proteins (A), with the image capture performed using a LAS4000 imaging system (GE healthcare). Equal loading of protein samples was assessed using Ponceau stain, with a representative blot shown in (B). Density values were obtained using Quantity One software (BioRad), with the relative abundance calculated by normalising the density values obtained from MSV expressing cells to those of their control counterparts (C). Normalised data presented are mean +/- SEM, asterisks denote a significant difference between MSV expressing and control C_2C_{12} cells, with: *P<0.05, n=3 replicates per cell type.

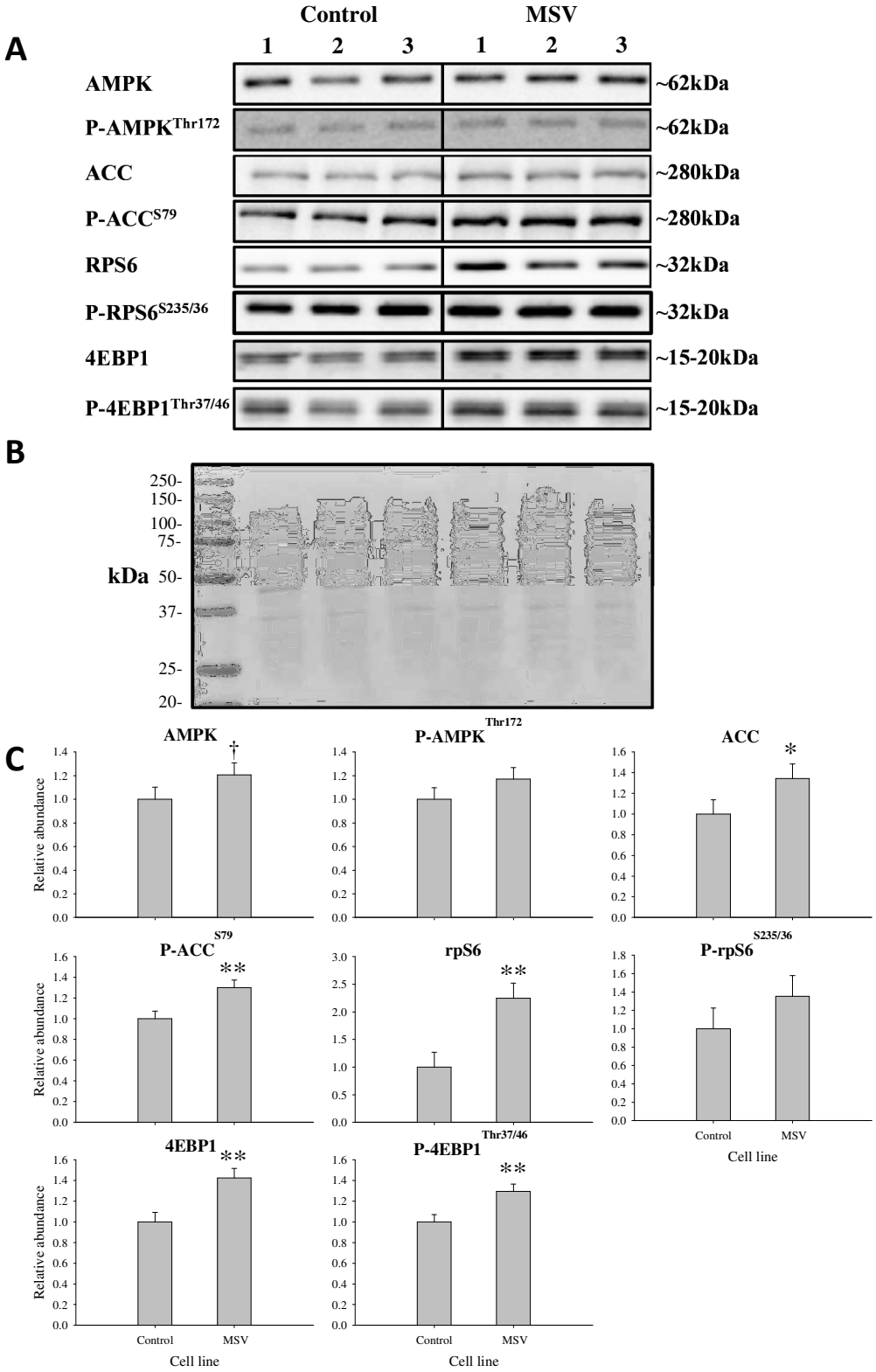

Figure 6.10: Abundance and phosphorylation of metabolic targets in C_2C_{12} cells expressing MSV. For western blot analysis, 10µg of whole cell lysates isolated from actively growing C_2C_{12} cells expressing MSV, and controls were run on a SDS/PAGE gel and blotted onto nitrocellulose. Immunoblots were performed for the depicted proteins (A), with the image capture performed using a LAS4000 imaging system (GE healthcare). Equal loading of protein samples was assessed using Ponceau stain, with a representative blot shown in (B). Density values were obtained using Quantity One software (BioRad), with the relative abundance calculated by normalising the density values obtained from MSV expressing cells to those of their control counterparts (C). Normalised data presented are mean +/- SEM, asterisks denote significant differences between MSV expressing and control C_2C_{12} cells, with: *P<0.05, *P<0.01, n=3 replicates per cell type.

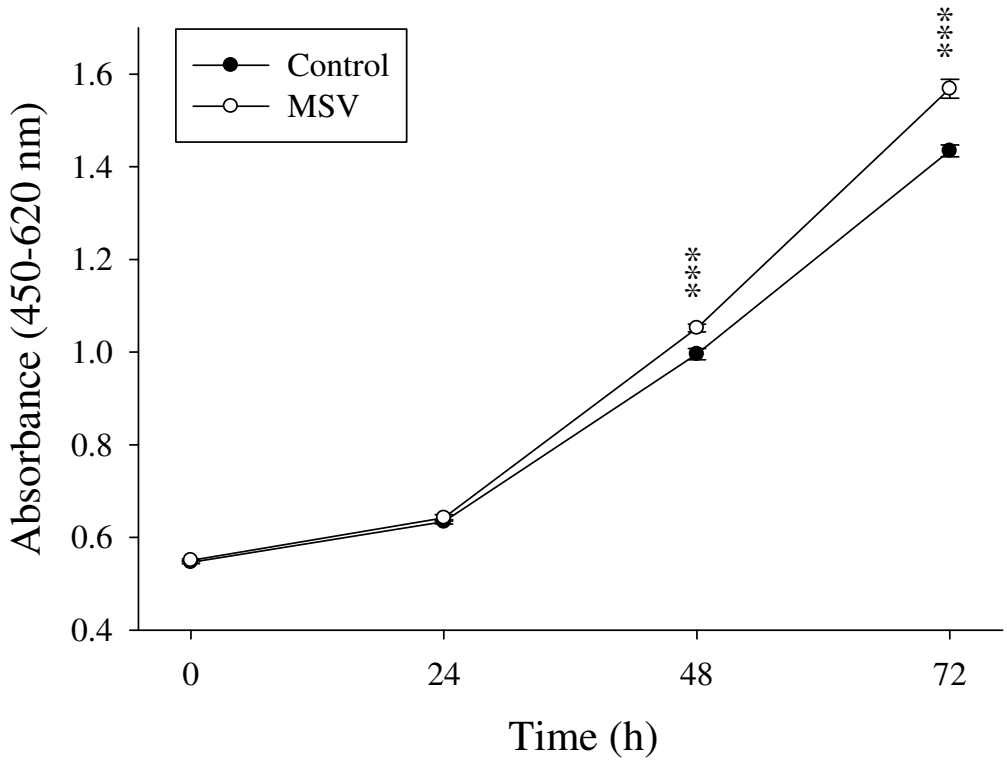

Figure 6.11: Metabolic activity of C_2C_{12} cells expressing MSV. The metabolic capacity of MSV expressing and control C_2C_{12} cells over a 72 h proliferation time course was assessed using the EZ4U assay every 24 h. EZ4U activity was determined following a 2 h incubation with EZ4U reagent. Absorbance was the measured at 450nm and background values at 650nM we subtracted. Data presented are mean +/- SEM, asterisks denote significant differences between MSV expressing and control C_2C_{12} cells, with: *P<0.05, *P<0.01, n=8 replicates per cell type

6.3 Discussion

Initial work for this chapter centred on the generation of the MSV over-expressing cell lines following the discovery of LPS in our MSV preparation. To circumvent this problem and to produce MSV in a eukaryotic cell line, expression constructs were generated that harboured the predicted full length open reading frame of ovine MSV. Two MSV expression cassettes were developed and over-expressed, one full length (start to stop codons) and one with sequence for C-terminal V5 and histidine epitopes (C-MSV). The C-MSV construct was generated primarily to allow detection of full length MSV protein using commercial antibodies, directed against the tagged epitopes. This proved valuable in establishing the presence of MSV protein in cells expressing MSV, as our own MSV antibodies could not detect over-expressed MSV in these cells. An important point here is that the antigens used for the production of our antibodies, were synthetic or recombinant peptides, targeting small portions of the predicted MSV sequence. Thus, one possible explanation is that the expressed full length MSV protein may disrupt the epitope recognised by the 'in-house' antibodies.

Construct specific PCR was used to confirm the expression of MSV and C-MSV transcript in C_2C_{12} cell lines. Western blot analysis of conditioned chemical media from C-MSV cell lines, confirmed that the over-expression of MSV transcript also resulted in the presence of MSV protein. Results from the expression studies demonstrated an anti-V5 reactive band close to the expected ~40kDa size, in neomycin resistant HEK293 and CHO cells. No smaller anti-V5 reactive bands were observed, that would indicate the presence of a cleaved C-terminal MSV product. Interestingly, western blot analysis did not detect the presence of a V5 reactive band in pooled C_2C_{12} C-MSV cells. This was surprising, given the presence of the C-MSV protein detected in the conditioned media from HEK293 and CHO cells and the readily detectable MSV message in C_2C_{12} cells expressing MSV. To determine if C_2C_{12} cells were expressing MSV, and translating the mRNA into protein, conditioned media from clonal cell lines, derived from the initial pool of neomycin resistant C_2C_{12} cells were subjected to western blot analysis. This allowed closer scrutiny of C-MSV expression in these cells, and allowed a determination to be made on whether the absence of C-MSV in the parent C_2C_{12} population was due to dilution, i.e. only a few clones

expressing C-MSV protein, or, if C-MSV is undetectable in C_2C_{12} cells expressing MSV. Analysis of conditioned media demonstrated the presence of a V5 reactive band of the expected size in some clonal cell lines expressing MSV. Thus, confirming the presence of translated protein in this model, albeit at concentrations substantially lower than those seen in HEK293 and CHO cell lines. The presence of C-MSV is conditioned media also confirmed that as with Mstn, MSV mRNA is translated and secreted from these cells. The reason for the low abundance of C-MSV protein in C_2C_{12} cells is unclear. However, given the readily detectable presence of the transcript in the C_2C_{12} cell lines, mechanisms may exist to regulate the abundance of this protein in C_2C_{12} myoblasts that are not present in HEK293 or CHO cells. A caveat to note here, is that the C-terminal tag of C-MSV (~31 amino acids) could interfere with functionality of the over-expressed protein. For this reason, my studies focused on the differences between MSV expressing and the control (pcDNA3) C_2C_{12} cell lines, once confirmation that MSV was translated in these cells was obtained. This was performed using the parent C_2C_{12} cell pool that expressed MSV, these were chosen preferentially over clonal MSV expressing cells to reduce the variation that would be introduced through the use of individual clonal cell lines.

Initially, the effect of MSV on the proliferation and differentiation of myoblasts expressing MSV was investigated. The methylene blue assay confirmed that C_2C_{12} cells expressing MSV have an increased rate of proliferation as compared to their control counterparts. Furthermore, an independent study in our laboratory also confirmed that the same C_2C_{12} cells expressing MSV display increased expression of nuclear cyclin E and CDK2, which provided a molecular basis for the increased rate of proliferation observed in MSV expressing C_2C_{12} cells (Jeanplong, Falconer et al. 2013).

Under differentiation conditions, MSV expressing cultures had an increased abundance of the MF20 differentiation marker throughout a differentiation time-course. Also apparent in this study, was the increased abundance of nuclei as assessed using DAPI fluorescence. It is important to note here, that prior to taking the first time-point, cells were incubated overnight in growth media. Thus, as cells were seeded at the same density, the differences in nuclear fluorescence (DAPI staining), that were observed at T0 in MSV expressing cultures is attributable to

an increased rate proliferation over this period. A potential explanation for the enhanced growth observed during the first 48 h of differentiation is the concentration of growth factors in the culture medium. Differentiation media contains horse serum (2%) as compared to growth media with foetal bovine serum (10%), thus, MSV may have more pronounced effect due to the reduced growth factor concentration in the differentiation media. The increased growth continued until the cells withdrew from the cell cycle to differentiate, which occurs at ~48 h post addition of differentiation media, as evidenced by the appearance of MF20 and plateau in nuclear fluorescence. Interestingly, the increases in both MF20 and DAPI occurred without an increase in the extent of myoblast fusion, as assessed using the ratio of MF20:DAPI. Thus, although the C_2C_{12} cells expressing MSV proliferate faster, and have more differentiated myotubes, the proportion of myoblasts forming myotubes remained constant.

As the studies in ovine myoblasts had focused on changes in gene expression under proliferation conditions, western blot analysis was performed on whole cell lysates isolated from proliferating cells expressing MSV and controls. The target molecules investigated for this study were the same as those investigated for Mstn (Chapter 4). Cells expressing MSV had increased abundance of MyoD, MRF4 and myogenin. These data indicate that the expression of MSV regulates the abundance of key myogenic transcription factors. In particular, the regulation of MyoD and myogenin are consistent with MSV functioning to block endogenous Mstn. Both of these factors have been implicated in the inhibition of myogenesis caused by Mstn in mouse and ovine myoblasts (Langley, Thomas et al. 2002; Joulia, Bernardi et al. 2003; Liu, Li et al. 2012). Changes in the abundance of myogenin and MRF4, are likely to play a role in the differentiation of the MSV expressing cells. However, the major focus of these studies was to gain a deeper understanding of the MSV-mediated mechanisms in proliferating myoblasts. Thus, this study confirmed that the expression of MSV can alter key myogenic transcription factors. Further studies will be required to understand the extent to which the increased expression of these factors may influence myogenesis.

To establish if the expression of MSV influenced the signalling of canonical Mstn, the abundance and phosphorylation status of Smad 2 and 3 was investigated. Western blot analysis showed an increased abundance of total

Smad3 in C_2C_{12} cells expressing MSV. No changes were observed in the abundance of Smad2 and no phosphorylated Smad 2 or 3 was detected in this study. Smad 3 has been shown to interact with binding partners such as MyoD and MEF2 (Liu, Black et al. 2001; Quinn, Yang et al. 2001), thus, increased Smad 3 may play a role in the regulation of myogenic gene expression in these cells. Alternatively, an independent study on C_2C_{12} cells expressing MSV that were co-transfected with a Smad reporter construct (CAGA luciferase assay), demonstrated reduced ability of Mstn to induce Smad dependant reporter activity in these cells as compared to control cells (Jeanplong, Falconer et al. 2013). This implies that the expression of MSV impairs signalling through the Smads, thus, the increased abundance of Smad 3 may reflect a negative feedback mechanism to counter a reduced ability to signal through this pathway in C_2C_{12} cells expressing MSV.

MAPK signal transduction has been shown to play a role in both Mstn signalling (Yang, Chen et al. 2006; Elkina, von Haehling et al. 2011), and signalling events involved in the proliferation and differentiation of muscle precursors (Knight and Kothary 2011). Thus, the effect of the expression of MSV on the abundance and phosphorylation of components of ERK and p38 MAPK signalling cascades was investigated. Cells expressing MSV had a tendency for an increased abundance of phosphorylated ERK1, with no changes were observed in the abundance of ERK1 or 2, and phosphorylated ERK2. The effect of this small changes is unclear, but suggest that the expression of MSV may influence components involved in MAPK signalling, a cascade that plays a major role in the regulation of myogenesis.

In numerous studies, Mstn has been shown to influence the PI3K/AKT signal transduction cascade. In muscle, Mstn has been shown to reduce signalling through this pathway, which provides a mechanism for the Mstn mediated inhibition of hypertrophy and protein synthesis (Trendelenburg, Meyer et al. 2009). Thus, the effect of the expression of MSV on the abundance and phosphorylation of components in the PI3K signal transduction cascade was determined. In cells expressing MSV, western blotting showed an increase in both total and phosphorylated AKT^{S473}, but not AKT phosphorylated at T308. The abundance and phosphorylation of PDK1 (a major upstream kinase of AKT) was

not affected by the expression of MSV. The increases in AKT and AKT^{S473} in cells expressing MSV could have major consequences on cellular targets and processes downstream of AKT, as discussed in the next section.

As described in Chapter 1 (1.1.6.2), the cellular targets downstream of AKT play an important role in the control of protein synthesis. What is becoming more apparent is the extensive cross talk between signal transduction cascades that converge on common targets to regulate the activity of molecules with important roles in controlling the protein synthesis machinery and other metabolic processes (Roux, Shahbazian et al. 2007; Magnuson, Ekim et al. 2012). The regulation of rpS6 and 4EBP1 phosphorylation provides a good example, as the activity of these molecules can be targeted by PI3K or alternatively MAPK signalling (Nawroth, Stellwagen et al. 2011).

It was unclear from the current study which specific upstream cascades control the abundance or the signalling activity (phosphorylation) of these molecules. In cells expressing MSV there was increased rpS6, with no change in the phosphorylation of rpS6. The rpS6 protein is thought to play a role in the synthesis of protein, although, the mechanistic details of this role have remained elusive. Knock-out studies in mouse embryonic fibroblasts, have shown that rpS6 plays a role in the regulation of cell size, cell proliferation and glucose homeostasis (Ruvinsky, Sharon et al. 2005), implying an important metabolic role for rpS6. Cells expressing MSV also showed increased abundance and phosphorylation of 4EBP1. The increased phosphorylation of 4EBP1 is consistent with the observed increase in the phosphorylation of AKT^{S473} in MSV expressing cells. The activity of 4EBP1, has also been shown to be regulated through the ERK dependant signalling cascade through a mechanism involving mTOR activity (Herbert, Tee et al. 2002). In this case this seems unlikely, given the small changes observed in ERK signalling in this model. Thus the increased phosphorylation of 4EBP1 is more likely to be a direct result of increased phosphorylation of AKT^{S473}. The increases in 4EBP1 and rpS6, support a role for MSV in the control of cellular protein synthesis.

Other metabolic targets investigated were AMPK and its downstream target ACC, both of which play a major role in the control of cellular metabolism.

AMPK is considered an energy sensor (see 1.2.5) and as such activation of AMPK can occur in response to a drop in cellular energy levels, or more precisely a rise in the ratio of AMP/ATP. Cytokines can also induce AMPK activation, with activation by IL6 providing a good example (Kelly, Gauthier et al. 2009). Over-expression of MSV had a tendency to increase the abundance of total AMPK but not its phosphorylation state. The majority of studies investigating AMPK function have focused on AMPK activation (phosphorylation) rather than the amount of total AMPK. Thus, the consequences of the increased AMPK observed here is unclear. Interestingly, studies using AMPK KO mice have shown that AMPK, in addition to its role as an energy sensor has a physiological role in the regulation of the activity of the 26S proteasome (Xu, Wang et al. 2012), with AMPK KO mice having increased 26S proteasomal activity. Thus, it could be speculated that increased AMPK may provide a greater signalling capacity through this pathway, or play a role in the synthesis versus the degradation of protein.

The increases observed in both ACC and phosphorylated ACC are extremely interesting, as ACC plays a major role in the control of lipid synthesis and is important in the control of mitochondrial fatty acid oxidation (Kim 1997). The Phosphorylation of ACC has been shown to inhibit its activity and thus, reduce lipid synthesis through reduced formation of malonyl-CoA, this results in an increase in fatty acids available for oxidative metabolism (Kim 1997). The current data suggest that MSV alters signalling of this hub, and that ACC may represent a major target for MSV action. The increase in the phosphorylation of ACC appears to be independent of its upstream activator AMPK, given that there was no change in the phosphorylation of AMPK in the MSV expressing C_2C_{12} cells. What is interesting here is that the increases in total and phosphorylated ACC were of a similar magnitude, thus the ratio of active to inactive ACC would remain constant. Thus, the capacity of the processes controlled by ACC should be increased. In the context of MSV in ruminants, this may be extremely significant as the expression of MSV may alter the capacity of fatty acid metabolism in a digestive system that is more reliant on fatty acids derived from the fermentation of forage as a primary energy source.

To further establish a role for MSV in influencing cellular metabolism, the EZ4U assay was used to establish if the mitochondrial activity of MSV over-expressing cultures was increased as compared to control C_2C_{12} cells. The increase in EZ4U activity observed following 48 h of proliferation is most likely a result of the increased number of cells observed at this time-point and is consistent with the data from the methylene blue proliferation assay. However, the differences in proliferation observed at 72 h (~2.5%) are surpassed by the increased EZ4U activity (~9.6%) observed at this time-point. A potential explanation for this difference would be an increased oxidative capacity in the cells expressing MSV. However, experiments specifically targeting the role of MSV in mitochondrial metabolism would be required to firmly establish a role for MSV in this context.

In summary, the over-expression of MSV in C_2C_{12} myoblasts provided a new model for the investigation of MSV function and supports the increased proliferation observed in C_2C_{12} myoblasts using recombinant protein produced in *E.coli*. These studies show that expression of MSV increases the rate of proliferation but not the extent of differentiation in C_2C_{12} myoblasts. Furthermore, MSV over-expression alters the abundance and phosphorylation of a number of proteins with important roles in myogenesis, protein synthesis and metabolism. In addition, based on the EZ4U assay data MSV may also promote oxidative metabolism, an idea that is consistent with the increases observed in the abundance and phosphorylation of ACC in C_2C_{12} cells expressing MSV. Thus, the data presented here support a role for MSV in promoting the proliferation of myoblasts. With the increased activation of AKT, the altered canonical components of Mstn signalling pathways and increased abundance of myogenic transcription factors representing some of the changes that culminate in the altered abundance and phosphorylation of molecules involved in intermediary metabolic pathways and the control of protein synthesis, and thus, provide evidence that support the reciprocal functions of MSV and Mstn.

Chapter Seven

7 Final discussion and future perspectives

The studies presented in this thesis investigate the effects of MSV on key molecules involved in signal transduction and consequently the regulation of myogenic and metabolic processes in myoblasts and how they relate to that of Mstn. Since the discovery of Mstn was published 16 years ago (McPherron, Lawler et al. 1997), numerous studies have focused on the mechanisms through which Mstn can have such a profound effect on the growth of skeletal muscle. The preceding research has shown that Mstn signals through the canonical TGF-β, MAPK and PI3K/AKT signal transduction cascades. Ultimately, the integration of the Mstn signal results in the regulation and control of key molecules involved in the control of myogenesis and in the control of cellular metabolism. Thus, previous studies investigating Mstn function provided a foundation for investigating the function of a novel Mstn splice variant (MSV). MSV is thought to be restricted to the Cetartiodactlya clade of mammals, with initial studies suggesting that MSV and Mstn may regulate myogenesis reciprocally. In support are the key findings that include the observation that the expression of MSV increases rather that decreases the proliferation of myoblasts, MSV binds to both Mstn and its canonical ACTR IIB receptor and that MSV inhibits canonical Mstn signalling (Jeanplong, Falconer et al. 2013). Therefore, the primary aim of this thesis was to what was to investigate the signal transduction function of MSV in myoblasts, and to identify how this differed from that of Mstn.

Initially, ovine myoblasts were used to investigate the gene expression (microarray analysis) and signal transduction events (western blot analysis) following administration of recombinant Mstn and MSV. This allowed me to identify potential links between the initial signalling events and the subsequent changes in gene transcription. In addition, C_2C_{12} cells that stably express MSV were developed to investigate the function of MSV. A diagrammatic representation of the molecules influenced by Mstn and MSV in these studies is presented in Figure 7.1.

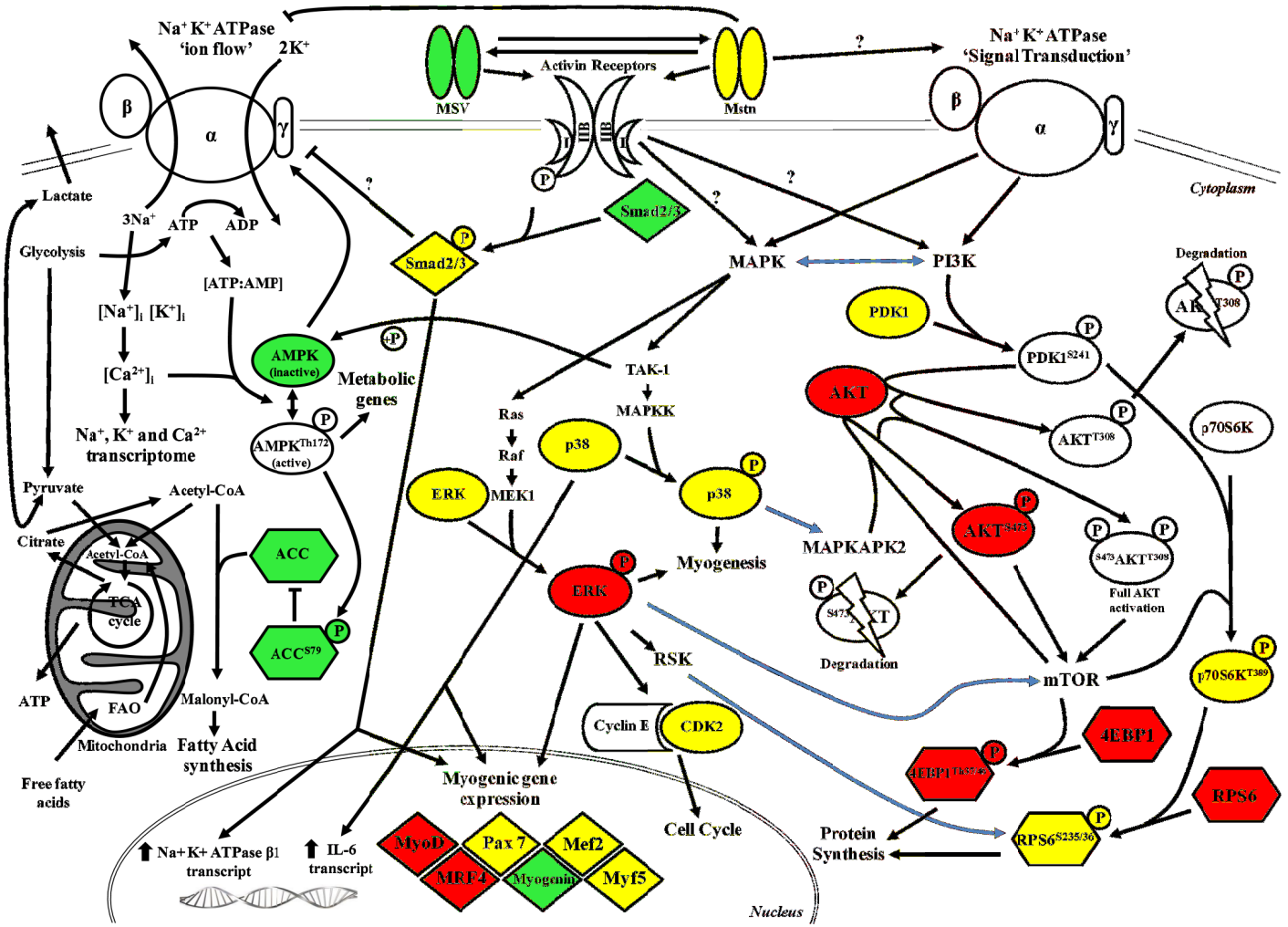

Figure 7.1: Summary of signalling pathways and molecules regulated by Mstn and MSV. Depicted above are the signalling pathways and molecules influenced by Mstn and MSV in the current studies. Colours indicate molecules regulated by Mstn (yellow), MSV (green) or both (red). Blue arrows represent points of crosstalk between the MAPK and PI3K/AKT pathways. Abbreviations: ACC (acetyl co-enzyme A carboxylase), ADP (adenosine diphosphate), AKT (v-akt murine thymoma viral oncogene homolog/protein kinase B), AMP (Adenosine monophosphate), AMPK (Adenosine monophosphate activated protein kinase), ATP (adenosine triphosphate), $[Ca^{2+}]_i$ (intracellular calcium concentration), 4EBP1 (4E-Binding Protein 1), ERK (extracellular regulated kinase), FAO (fatty acid oxidation), IL-6 (interleukin-6), $[K^+]_i$ (intracellular potassium concentration), MAPKAPK2 (mitogen activated protein kinase activated protein kinase 2), MAPKK (mitogen activated protein kinase kinase), Mef2 (myocyte enhancer factor-2), MEK1 (Mitogen activated protein kinase ERK kinase), Mstn (myostatin), MSV (myostatin splice variant), $[Na^+]_i$ (intracellular sodium concentration), p38 (p38 protein 38 kDa mitogen activated protein kinase), p70S6K (phosphoprotein 70 ribosomal protein S6 kinase), rpS6 (ribosomal protein S6), Smad (small mothers against decapentaplegic), mTOR (mammalian target of rapamycin), Ras (rat sarcoma), Raf (rapidly accelerated fibrosarcoma), TAK-1 (TGF-β activated kinase), and TCA (tricarboxylic acid/Krebs) cycle. Pathways based on interactions described in previous studies (Xie and Askari 2002; Ouchi, Shibata et al. 2005; Buchakjian and Kornbluth 2010; Knight and Kothary 2011; Wu, Ouyang et al. 2011; Zhang, Rajan et al. 2011). Targets investigated were transcription factors (diamonds), kinases (ovals) and metabolic targets (hexagons).

The microarray study identified a number of transcripts that were differentially expressed following treatment with Mstn. Some of the findings supported previous studies, for example the increased abundance of the IL6 transcript (Zhang, Rajan et al. 2011) and the decreased abundance of MyoD transcript (Liu, Li et al. 2012). In addition, a novel transcriptional target of Mstn, the β1 subunit of the Na^+-K^+-ATPase, was identified, and studies were carried out to understand the importance of regulating this complex (discussed later). The microarray data also had a significant impact on my approach to investigate the function of MSV. The IPA analysis of the microarray data, strongly suggested the presence of LPS in the MSV preparation. On confirmation, a method to eliminate LPS had to be established. Firstly, the removal off LPS from the MSV preparation using previously documented methods was investigated, with Triton X-114 phase separation (Liu, Tobias et al. 1997) proving to be the most effective method of removal. However, there were still doubts with regard to integrity of the recombinant protein, in particular with the protein folding and how the phase separation affected the MSV. Secondly, to circumvent the issues associated with the production of recombinant protein in *E.coli*, a C_2C_{12} myoblast line expressing MSV was generated, which provided an additional model to investigate the function of MSV.

Studies investigating the signal transduction events induced by Mstn and MSV in ovine myoblasts provided further insight into the signalling networks influenced by these molecules. Treatment with Mstn altered the abundance and/or the phosphorylation of a number of molecules in ovine myoblasts, as summarised in Figure 7.1. These included molecules in the canonical Smad pathway, the p38 and ERK MAPK signalling cascades and the PI3K/AKT pathway. In addition, the signalling events induced by Mstn, also resulted in the altered abundance of key myogenic transcription factors. These data also suggest that some of the early signalling events regulated following the addition of Mstn differ from those observed following long term exposure to Mstn. In particular, the increased phosphorylation of AKT^{S473} and $p70S6K^{T389}$ observed here are at odds with previous studies using human and mouse myoblasts (Trendelenburg, Meyer et al. 2009; Welle, Burgess et al. 2009). However, the increased phosphorylation of AKT^{S473} is consistent with a previous study in fibroblasts wherein Mstn

phosphorylates AKT through a mechanism that involves p38 MAPK, with increased phosphorylation of p38 also observed following Mstn treatment in this study. Further investigations may reveal that in fact the phosphorylation of AKT and p70S6K induced by Mstn may be a result of MAPK:AKT crosstalk through p38 or, alternatively, mTOR. In support of a p38 dependant mechanism, other studies have demonstrated that phosphorylation of AKT^{S473} is dependent on p38 in neutrophils and vascular smooth muscle cells (Rane, Coxon et al. 2001; Taniyama, Ushio-Fukai et al. 2004). The specific phosphorylation of AKT^{S473} following treatment with Mstn may represent a prerequisite step for the Mstn mediated inhibition of this pathway, which results in the specific ubiquitination and degradation of AKT, as described recently (Wu, Ouyang et al. 2011).

Investigation of MSV signalling in ovine myoblasts showed that MSV shared common targets with Mstn. These included Smad 2 and 3, Myf5, AKT and 4EBP1. The extent to which these were regulated by Mstn and MSV differed for individual molecules. The increased abundance of Smad 2 and 3 is likely to play a role in MSV function, with activity of the Smad pathway shown to be crucial for the effects of Mstn on p38, ERK and AKT activity (Yang, Chen et al. 2006; Trendelenburg, Meyer et al. 2009; Zhang, Rajan et al. 2011). In addition, MSV treatment increased the phosphorylation of AKT^{S473} and the abundance and phosphorylation of 4EBP1. Thus, canonical TGF-β signalling, the regulation of genes involved in protein synthesis and the myogenic regulatory factors were identified as points of potential convergence for the Mstn and MSV signals. This provided a starting point for further investigations of MSV signalling in C_2C_{12} myoblasts expressing MSV.

A drawback of the approach to investigate MSV signalling in C_2C_{12} cells that expressed MSV was the species difference between the cells used to investigate recombinant protein treatment (ovine) and MSV expression (mouse). In addition, alterations in the targets investigated here are the result of continuing exposure to over-expressed MSV, thus, comparisons to Mstn need to be made with this in mind. In ovine myoblasts that were treated with Mstn, the activation of canonical, p38 and ERK MAPK signalling demonstrated that, major aspects of Mstn function are conserved in these myoblasts (Yang, Chen et al. 2006; Trendelenburg, Meyer et al. 2009; Zhang, Rajan et al. 2011). Thus, based on

previous investigations showing that MSV is able to bind both Mstn, the Mstn receptor (Activin receptor type 2 B) and increases the rate of myoblast proliferation (Jeanplong, Falconer et al. 2013), it was reasoned that the majority of the pathways likely to be influenced by MSV, are conserved between these two myoblast models. Consistent with the treatment of ovine myoblasts with MSV, C_2C_{12} cells expressing MSV, had an increased abundance of Smad 3, had increased phosphorylation of AKT^{S473} and an increase in the abundance and phosphorylation of 4EBP1. This confirmed the overlapping nature of the function of Mstn and MSV in the regulation of these targets. In addition, the changes induced by the expression of MSV in the phosphorylation of AKT and 4EBP1 highlight a major point of difference between the previously characterised function of Mstn and that of MSV. The over-expression of Mstn has been shown to decrease the activity of AKT and its downstream targets, and indeed genetic ablation of Mstn increases the activity of these pathways (Welle, Bhatt et al. 2006; Trendelenburg, Meyer et al. 2009), these changes underpin the reduced synthesis of protein associated with the long-term exposure to, or the presence of active Mstn. In contrast, these pathways are increased in C_2C_{12} cells expressing MSV, which suggests that Mstn and MSV have reciprocal roles in the control of these targets and, potentially, the control of protein synthesis. Consistent with MSV opposing the function of Mstn, MSV expressing C_2C_{12} cells also had an increased rate of proliferation, and an increased abundance of the MyoD, MRF4 and myogenin.

Identifying a role for MSV in the regulation of intermediary metabolism represented an aim of these studies. The increased abundance and phosphorylation of Acetyl Co-enzyme A Carboxylase (ACC) observed in C_2C_{12} cells expressing MSV is likely to have an impact on metabolism. This enzyme represents a key molecular hub for the regulation of fatty acid metabolism, supporting a physiological role for MSV, The regulation of ACC could result in an altered fatty acid flux and/or an increased enzymatic capacity of ACC in C_2C_{12} cells expressing MSV. In addition, the increases in the mitochondrial activity assay (EZ4U) observed in these cells were disproportionate to the increases in proliferation demonstrated in these cells. This suggests that the expression of MSV modifies oxidative metabolism through increased mitochondrial number

and/or activity, which would be consistent with the increases observed in ACC. Based on previous studies, the full length MSV coding sequence is restricted to the Cetartiodactyla clade of mammals (Jeanplong, Falconer et al. 2013). Given, that the primary energy source for ruminants are fatty acids derived from the fermentation of forage, it is interesting to speculate that this splice variant may have evolved to promote growth in digestive systems more reliant on fatty acids as a source of metabolic fuel. Thus, the current data give the premise for future investigations centred on a role of MSV in the regulation of oxidative metabolism.

The microarray studies identified the Na^+-K^+ ATPase β1 subunit is a transcriptional target of Mstn. This was an unexpected finding, but is understandable given the significant overlap of processes regulated by the Na^+-K^+ ATPase complex and Mstn. Both play a role in the regulation of hypertrophy, proliferation of myocytes and the metabolism of skeletal muscle (James, Wagner et al. 1999; Xie and Askari 2002). In addition, a recent protein interaction study highlighted an interaction between Smad 2 and the Na^+-K^+ ATPase β1 subunit (Miyamoto-Sato, Fujimori et al. 2010), which supports the notion that TGF-β family members can signal via the Na^+-K^+ ATPase complex. In the current studies, I established that the Mstn dependant regulation of the Na^+-K^+ ATPase β1 subunit requires Smad activity. It is interesting to speculate that regulation of the Na^+-K^+ ATPase β1 transcript may be of critical importance to Mstn function. In support of this idea, the β1 subunit transcript was sensitive to the pharmacological blockade of the Smad pathway and the inhibition of this pathway antagonises multiple facets of Mstn function including its effects on canonical, MAPK and PI3K signalling (Philip, Lu et al. 2005; Yang, Chen et al. 2006; Trendelenburg, Meyer et al. 2009)

Data from these studies suggest that Mstn alters the function of the Na^+-K^+ ATPase on regulating the flow of ions. Interestingly, changes in the intracellular concentration of Na^+ and K^+ have recently been shown to regulate a plethora of transcriptional responses (Koltsova, Trushina et al. 2012) and to be important in the regulation of the intracellular concentration of calcium. Intracellular calcium plays a major role in the regulation of muscle fibre-type (Hogan, Chen et al. 2003), the distribution and activity of critical signalling molecules such as the ERKs (Chuderland, Marmor et al. 2008) and the activity of myogenic

transcription factors with Mef2 providing a good example (McKinsey, Zhang et al. 2002). Thus, control of the β1 subunit by Mstn provides a means to regulate multiple pathways controlled through the function of Na^+-K^+ ATPase in skeletal muscle. The chances of Mstn and the ATPase sharing so many common pathways is unlikely to be a coincidence and, further studies will be required to define how their function overlaps in the control of the growth and development of skeletal muscle.

7.1 Future perspectives

The studies outlined in this thesis give premise for further investigations from both the Mstn and MSV perspectives. For Mstn, the discovery of the link between Mstn and the sodium potassium Na^+-K^+-ATPase is intriguing. A more targeted study investigating the role of Mstn in the control of Na^+-K^+-ATPase activity and signal transduction would be very interesting. Conformation of a role for Mstn in the regulation of Na^+-K^+-ATPase activity, would confirm Mstn as a regulator of ion flow in skeletal muscle. Furthermore, investigating the overlapping nature of Mstn and Na^+-K^+-ATPase mediated signalling may reveal a close relationship between the signal transduction function of these two molecules. Also interesting in these studies is the regulation of IL-6 by Mstn, presumably through p38 as previously shown in C_2C_{12} myoblasts (Zhang, Rajan et al. 2011). The interest here centres around the release of IL6 released following bouts of exercise, with IL6 production important for glycogen repletion and the conservation of ATP (Pedersen, Akerstrom et al. 2007). To date there is no mechanism defined for the stimulation of IL-6. Interestingly, a recent study has identified the Furin protease, which is known to cleave Mstn (Anderson, Goldberg et al. 2008), as a myokine released following exercise (Raschke, Eckardt et al. 2013). Taking this a step further, does Mstn play a role in the post-exercise production of IL6, following Furin dependant extracellular cleavage. In support of this idea, it has been previously shown that mice with a loss of function Mstn mutation display decreased IL6 levels (Wilkes, Lloyd et al. 2009). Thus, a study in Mstn null mice, comparing IL6 production post exercise to that of wild-type controls could be very telling, and may reveal an important physiological mechanism of Mstn function.

In terms of MSV function, these studies highlighted a likely role for MSV in the control of oxidative metabolism and, in the control of protein synthesis. Further studies would be required to define a role for MSV in this context. Thus this initial study in C_2C_{12} mouse myoblasts would be well supported by data from an *in vivo* model of MSV over expression (which has been initiated in our lab). A role for MSV in supporting oxidative metabolism could be confirmed in this model, for example exposure to diets rich in oxidative fuel sources, such as a high fat diet could be used. If MSV does indeed influence oxidative metabolism there should be clear differences in the physiological response to a high fat diet, with parameters such as fat deposition and skeletal muscle growth likely to be influenced. Finally further studies investigating the interaction between Mstn and MSV would be valuable, the current data support the postulate that these molecules signal through common as well potentially independent pathways (see Figure 7.1). Thus, studies *in vitro* or *in vivo* that further define their specific roles, for example, in the context of Na^+-K^+-ATPase function, the regulation of protein synthesis and in the control intermediary metabolism would give valuable information on the specific physiological function of these two Mstn transcripts

In conclusion, the studies presented in this thesis further define the effect of MSV on signal transduction mechanisms that have major roles in myogenesis. In conjunction with the studies on Mstn signalling, they highlight specific signalling pathways that these molecules target and identify common targets with important roles in myogenesis and cellular metabolism. Furthermore, they establish that signalling through AKT is likely to represent a major point of divergence in the function and signalling of Mstn and MSV. Taking this further, it is interesting to speculate that MSV has evolved to permit increased growth in metabolic systems that rely on fatty acids derived from the fermentation of forage as a primary fuel source. These studies also show that in ovine myoblasts, some of the early signalling events induced by Mstn can differ from those imposed by long-term treatment or the over-expression of Mstn. In addition, these studies identified the β1 subunit of the Na^+ K^+ ATPase as a novel downstream transcriptional target of canonical Mstn signalling. Thus, these data extend the current knowledge on Mstn and MSV signalling, further highlighting the

conserved nature of Mstn function in ovine myoblasts and demonstrating that Mstn and MSV share common signalling targets to convey their distinct functions.

Appendix I

Development of a 96 well, MF20 (Myosin Heavy Chain) fluorescence assay to assess the differentiation of myoblasts.

Traditional methods for assessing the differentiation of myoblasts involve the immuno-histochemical staining of differentiated myotubes with antibodies that recognise a differentiation marker such as myosin heavy. The MF20 antibody provides a good example as it detects all forms of sarcomeric myosin (Bader, Masaki et al. 1982). A counter-stain such as haematoxylin is then used to allow the identification and quantification of nuclei. This method allows parameters such as the fusion index to be calculated through counting nuclei within myotubes and dividing this value by the total number of nuclei present, giving a percentage of the nuclei incorporated into myotubes as a fusion index. Thus, taking advantage of the fact that nuclei and myotubes can be stained using different fluorescent compounds, a fluorescence assay was established to track nuclei fluorescence with the 4',6-diamidino-2-phenylindole (DAPI; Life Technologies) nuclei stain, and MF20 immuno-fluorescence using the Alexa Fluor 488 fluorophore over a differentiation time course. The protocol for staining is described in materials and methods (2.2.22).

Initially, confirmation that the fluorescence of the DAPI stain was proportional to the number of cell nuclei present. This was performed by seeding C_2C_{12} myoblasts at different densities (from 0 (background) to 100000 cells per well) in 96 well Optilux™ (BD) plates (n=8 for each cell density). Following overnight attachment DAPI stain (1µg/mL in PBS) was used to stain nuclei and the fluorescence measured (excitation 360nm, emission 460nm) using a Synergy™ 2 multi-detection micro-plate reader and Gen5 software (BioTek Instruments). As shown below fluorescence measurements correlated well with the nuclei abundance, with readings reaching a plateau at about 75000 cells per well.

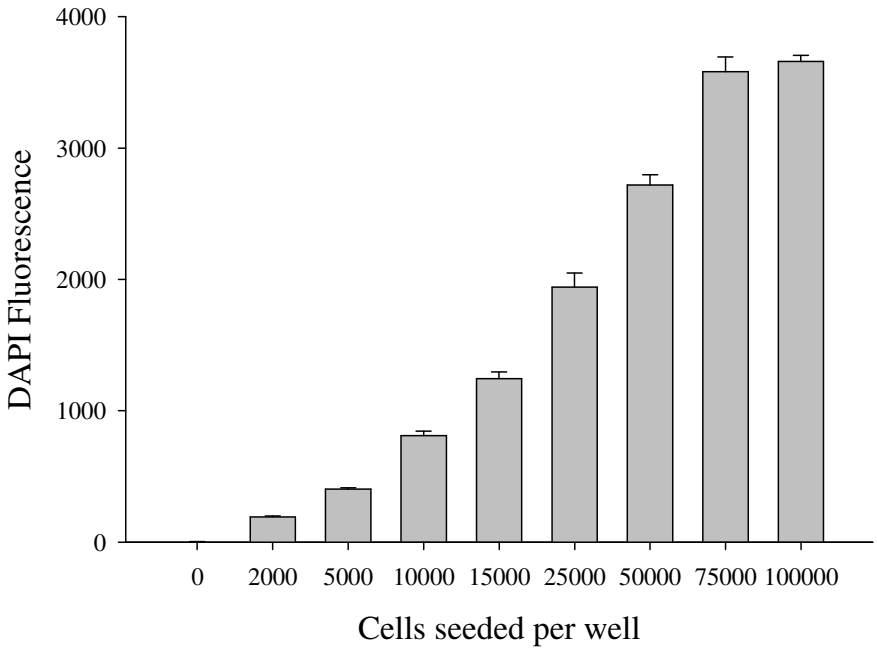

Following confirmation that relative abundance of nuclei could be quantified using this method, the MF20 immuno-staining protocol was standardised. This was done using a titration of the MF20 primary antibody to establish that the fluorescence measurements obtained using this assay were a result of specific antibody binding, with n=8 for each antibody dilution. Immuno-staining was performed on C_2C_{12} myoblasts that had been differentiated for 96 h. Bound MF20 antibody was detected using anti-mouse Alexa Flour 488 conjugate (Life Technologies) and fluorescence was measured with an excitation at 485nm and emission at 528nm. Shown below are the data for the MF20 antibody. The negative controls used were: no primary antibody (i.e. secondary only) or a non specific mouse IgG primary antibody (primary –ve). For subsequent experiments, the background values using the primary IgG negative control were subtracted from the MF20 fluorescent values.

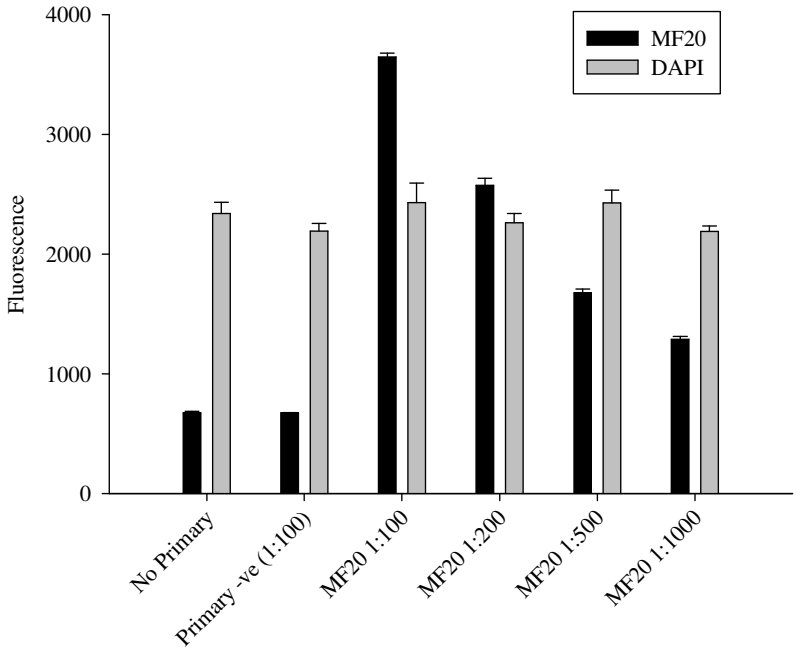

This result gave me confidence that the fluorescence measurements obtained following MF20 immuno-staining were a direct result of the proportion of myosin heavy chains, with the 1:200 dilution was used for all further fluorescent assays. In addition, DAPI values were reasonably consistent across the titration range, consistent with the equal number of cells seeded per well.

Although data obtained from this assay cannot be used to calculate an exact fusion index, the parameters could be used to indicate the extent of differentiation between cultures using the ratio of MF20:DAPI fluorescence. The reasoning here, is that as myoblasts progress through differentiation, cells exit from the cell cycle and the expression of myosin heavy chain increases as the myoblasts continue to fuse and differentiate. Thus, the ratio of myosin heavy chain to the amount of nuclei will increase as differentiation progresses, and differences in the extent of fusion would be indicated by alterations in this ratio. To confirm that this is indeed the case, C_2C_{12} myoblasts were differentiated in the presence or absence of 3μg/mL of recombinant Mstn for 96 h (n=8 for each treatment). Previous studies in our laboratory have shown that treatment of C_2C_{12} myoblasts with Mstn reduces the amount of fusion during myoblast differentiation (Langley, Thomas et al. 2002). As shown below, treatment with Mstn resulted in

reduced MF20 and DAPI fluorescence, consistent with Mstn inhibiting both the proliferation and differentiation of C_2C_{12} myoblasts (Thomas, Langley et al. 2000; Langley, Thomas et al. 2002).

Furthermore, consistent with reduced fusion of C_2C_{12} myoblasts in the presence of Mstn the ratio of MF20:DAPI was decreased following Mstn treatment (shown below), demonstrating that this ratio in indicative of the amount of fusion occurring in differentiating myoblast cultures.

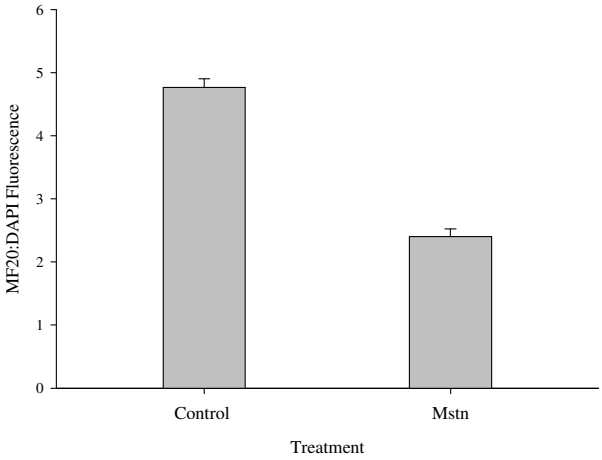

Although the fluorescence measurements described here do not provide an actual fusion index, this method allows the high throughput screening of multiple cell types or treatments in a 96 well format. In addition, if the MF20:DAPI ratio indicates differences in the fusion between cell types or treatments, microscope images with good contrast (as shown in Figure 6.5) can be captured to allow the manual calculation of the fusion index.

References

Aida, Y. and M. J. Pabst (1990). "Removal of endotoxin from protein solutions by phase separation using Triton X-114." J Immunol Methods **132**(2): 191-195.

Aksamitiene, E., A. Kiyatkin, et al. (2012). "Cross-talk between mitogenic Ras/MAPK and survival PI3K/Akt pathways: a fine balance." Biochem Soc Trans **40**(1): 139-146.

Al-Khalili, L., O. Kotova, et al. (2004). "ERK1/2 mediates insulin stimulation of Na(+),K(+)-ATPase by phosphorylation of the alpha-subunit in human skeletal muscle cells." J Biol Chem **279**(24): 25211-25218.

Allen, D. L. and T. G. Unterman (2007). "Regulation of myostatin expression and myoblast differentiation by FoxO and SMAD transcription factors." Am J Physiol Cell Physiol **292**(1): C188-199.

Allen, R. E., C. J. Temm-Grove, et al. (1997). "Skeletal muscle satellite cell cultures." Methods Cell Biol **52**: 155-176.

Alway, S. E., H. Degens, et al. (2002). "Potential role for Id myogenic repressors in apoptosis and attenuation of hypertrophy in muscles of aged rats." Am J Physiol Cell Physiol **283**(1): C66-76.

Anderson, S. B., A. L. Goldberg, et al. (2008). "Identification of a novel pool of extracellular pro-myostatin in skeletal muscle." J Biol Chem **283**(11): 7027-7035.

Appell, H. J., S. Forsberg, et al. (1988). "Satellite cell activation in human skeletal muscle after training: evidence for muscle fiber neoformation." Int J Sports Med **9**(4): 297-299.

Arnold, H. H. and T. Braun (1996). "Targeted inactivation of myogenic factor genes reveals their role during mouse myogenesis: a review." Int J Dev Biol **40**(1): 345-353.

Bader, D., T. Masaki, et al. (1982). "Immunochemical analysis of myosin heavy chain during avian myogenesis in vivo and in vitro." J Cell Biol **95**(3): 763-770.

Ballard, F. J., R. W. Hanson, et al. (1969). "Gluconeogenesis and lipogenesis in tissue from ruminant and nonruminant animals." Fed Proc **28**(1): 218-231.

Balmain, J. H., S. J. Folley, et al. (1953). "Relative ultilization of glucose and acetate carbon for lipogenesis by mammary gland slices, studied with tritium, 13C and 14C." Biochem J **53**(4): xxvi.

Baseler, W. A., E. R. Dabkowski, et al. (2013). "Reversal of mitochondrial proteomic loss in Type 1 diabetic heart with overexpression of phospholipid hydroperoxide glutathione peroxidase." Am J Physiol Regul Integr Comp Physiol **304**(7): R553-565.

Benziane, B., M. Bjornholm, et al. (2009). "AMP-activated protein kinase activator A-769662 is an inhibitor of the Na(+)-K(+)-ATPase." Am J Physiol Cell Physiol **297**(6): C1554-1566.

Benziane, B., M. Bjornholm, et al. (2012). "Activation of AMP-activated protein kinase stimulates Na+,K+-ATPase activity in skeletal muscle cells." J Biol Chem **287**(28): 23451-23463.

Bhullar, R. P., R. R. Clough, et al. (2007). "Ral-GTPase interacts with the beta1 subunit of Na+/K+-ATPase and is activated upon inhibition of the Na+/K+ pump." Can J Physiol Pharmacol **85**(3-4): 444-454.

Bish, L. T., K. J. Morine, et al. (2010). "Myostatin is upregulated following stress in an Erk-dependent manner and negatively regulates cardiomyocyte growth in culture and in a mouse model." PLoS One **5**(4): e10230.

Blahna, M. T. and A. Hata (2012). "Smad-mediated regulation of microRNA biosynthesis." FEBS Lett **586**(14): 1906-1912.

Bonaldo, P. and M. Sandri (2013). "Cellular and molecular mechanisms of muscle atrophy." Dis Model Mech **6**(1): 25-39.

Bonnet, A., C. Bevilacqua, et al. (2011). "Transcriptome profiling of sheep granulosa cells and oocytes during early follicular development obtained by laser capture microdissection." BMC Genomics **12**: 417.

Braun, T., G. Buschhausen-Denker, et al. (1989). "A novel human muscle factor related to but distinct from MyoD1 induces myogenic conversion in 10T1/2 fibroblasts." Embo J **8**(3): 701-709.

Breitbart, R. E., C. S. Liang, et al. (1993). "A fourth human MEF2 transcription factor, hMEF2D, is an early marker of the myogenic lineage." Development **118**(4): 1095-1106.

Brockman RP, L. B. (1986). "Hormonal regulation of metabolism in ruminants." Livestock Production science **14**(1986): 313-334.

Buchakjian, M. R. and S. Kornbluth (2010). "The engine driving the ship: metabolic steering of cell proliferation and death." Nat Rev Mol Cell Biol **11**(10): 715-727.

Buckingham, M. (2007). "Skeletal muscle progenitor cells and the role of Pax genes." C R Biol **330**(6-7): 530-533.

Buckingham, M., L. Bajard, et al. (2003). "The formation of skeletal muscle: from somite to limb." J Anat **202**(1): 59-68.

Buckingham, M. and F. Relaix (2007). "The role of Pax genes in the development of tissues and organs: Pax3 and Pax7 regulate muscle progenitor cell functions." Annu Rev Cell Dev Biol **23**: 645-673.

Burgess, S. T., A. Greer, et al. (2012). "Transcriptomic analysis of circulating leukocytes reveals novel aspects of the host systemic inflammatory response to sheep scab mites." PLoS One **7**(8): e42778.

Chen, J., P. K. Jackson, et al. (1995). "Separate domains of p21 involved in the inhibition of Cdk kinase and PCNA." Nature **374**(6520): 386-388.

Chen, Y., J. Ye, et al. (2010). "Myostatin regulates glucose metabolism via the AMP-activated protein kinase pathway in skeletal muscle cells." Int J Biochem Cell Biol **42**(12): 2072-2081.

Chi, N. and J. A. Epstein (2002). "Getting your Pax straight: Pax proteins in development and disease." Trends Genet **18**(1): 41-47.

Cho, M., S. G. Webster, et al. (1993). "Evidence for myoblast-extrinsic regulation of slow myosin heavy chain expression during muscle fiber formation in embryonic development." J Cell Biol **121**(4): 795-810.

Choo, A. Y., S. O. Yoon, et al. (2008). "Rapamycin differentially inhibits S6Ks and 4E-BP1 to mediate cell-type-specific repression of mRNA translation." Proc Natl Acad Sci U S A **105**(45): 17414-17419.

Christ, B. and C. P. Ordahl (1995). "Early stages of chick somite development." Anat Embryol (Berl) **191**(5): 381-396.

Chuderland, D., G. Marmor, et al. (2008). "Calcium-mediated interactions regulate the subcellular localization of extracellular signal-regulated kinases." J Biol Chem **283**(17): 11176-11188.

Clausen, T. (2003). "Na+-K+ pump regulation and skeletal muscle contractility." Physiol Rev **83**(4): 1269-1324.

Clifford, R. J. and J. H. Kaplan (2008). "beta-Subunit overexpression alters the stoicheometry of assembled Na-K-ATPase subunits in MDCK cells." Am J Physiol Renal Physiol **295**(5): F1314-1323.

Clop, A., F. Marcq, et al. (2006). "A mutation creating a potential illegitimate microRNA target site in the myostatin gene affects muscularity in sheep." Nat Genet **38**(7): 813-818.

Coleman, M. L., C. J. Marshall, et al. (2004). "RAS and RHO GTPases in G1-phase cell-cycle regulation." Nat Rev Mol Cell Biol **5**(5): 355-366.

Cornu, M., V. Albert, et al. (2013). "mTOR in aging, metabolism, and cancer." Curr Opin Genet Dev **23**(1): 53-62.

Dellavalle, A., G. Maroli, et al. (2011). "Pericytes resident in postnatal skeletal muscle differentiate into muscle fibres and generate satellite cells." Nat Commun **2**: 499.

Devarajan, P., M. Gilmore-Hebert, et al. (1992). "Differential translation of the Na,K-ATPase subunit mRNAs." J Biol Chem **267**(31): 22435-22439.
Doi, M. and K. Iwasaki (2008). "Na+/K+ ATPase regulates the expression and localization of acetylcholine receptors in a pump activity-independent manner." Mol Cell Neurosci **38**(4): 548-558.
Dyson, N. (1998). "The regulation of E2F by pRB-family proteins." Genes Dev **12**(15): 2245-2262.
Edmondson, D. G. and E. N. Olson (1989). "A gene with homology to the myc similarity region of MyoD1 is expressed during myogenesis and is sufficient to activate the muscle differentiation program." Genes Dev **3**(5): 628-640.
el-Deiry, W. S., T. Tokino, et al. (1993). "WAF1, a potential mediator of p53 tumor suppression." Cell **75**(4): 817-825.
Elashry, M. I., A. Otto, et al. (2009). "Morphology and myofiber composition of skeletal musculature of the forelimb in young and aged wild type and myostatin null mice." Rejuvenation Res **12**(4): 269-281.
Elkina, Y., S. von Haehling, et al. (2011). "The role of myostatin in muscle wasting: an overview." J Cachexia Sarcopenia Muscle **2**(3): 143-151.
Ezhevsky, S. A., H. Nagahara, et al. (1997). "Hypo-phosphorylation of the retinoblastoma protein (pRb) by cyclin D:Cdk4/6 complexes results in active pRb." Proc Natl Acad Sci U S A **94**(20): 10699-10704.
Fecchi, K., D. Volonte, et al. (2006). "Spatial and temporal regulation of GLUT4 translocation by flotillin-1 and caveolin-3 in skeletal muscle cells." FASEB J **20**(6): 705-707.
Ferguson, S. S. (2007). "Phosphorylation-independent attenuation of GPCR signalling." Trends Pharmacol Sci **28**(4): 173-179.
Forbes, D., M. Jackman, et al. (2006). "Myostatin auto-regulates its expression by feedback loop through Smad7 dependent mechanism." J Cell Physiol **206**(1): 264-272.
Fowles, J. R., H. J. Green, et al. (2004). "Na+-K+-ATPase in rat skeletal muscle: content, isoform, and activity characteristics." J Appl Physiol **96**(1): 316-326.
Galva, C., P. Artigas, et al. (2012). "Nuclear Na+/K+-ATPase plays an active role in nucleoplasmic Ca2+ homeostasis." J Cell Sci **125**(Pt 24): 6137-6147.
Gibson, M. C. and E. Schultz (1983). "Age-related differences in absolute numbers of skeletal muscle satellite cells." Muscle Nerve **6**(8): 574-580.
Girgenrath, S., K. Song, et al. (2005). "Loss of myostatin expression alters fiber-type distribution and expression of myosin heavy chain isoforms in slow- and fast-type skeletal muscle." Muscle Nerve **31**(1): 34-40.
Grana, X. and E. P. Reddy (1995). "Cell cycle control in mammalian cells: role of cyclins, cyclin dependent kinases (CDKs), growth suppressor genes and cyclin-dependent kinase inhibitors (CKIs)." Oncogene **11**(2): 211-219.
Greenwood, P. L., N. W. Tomkins, et al. (2009). "Bovine myofiber characteristics are influenced by postweaning nutrition." J Anim Sci **87**(10): 3114-3123.
Grobet, L., L. J. Martin, et al. (1997). "A deletion in the bovine myostatin gene causes the double-muscled phenotype in cattle." Nat Genet **17**(1): 71-74.
Grobet, L., D. Pirottin, et al. (2003). "Modulating skeletal muscle mass by postnatal, muscle-specific inactivation of the myostatin gene." Genesis **35**(4): 227-238.
Gu, W., J. W. Schneider, et al. (1993). "Interaction of myogenic factors and the retinoblastoma protein mediates muscle cell commitment and differentiation." Cell **72**(3): 309-324.
Gu, Y., C. W. Turck, et al. (1993). "Inhibition of CDK2 activity in vivo by an associated 20K regulatory subunit." Nature **366**(6456): 707-710.
Guan, K. L., C. W. Jenkins, et al. (1994). "Growth suppression by p18, a p16INK4/MTS1- and p14INK4B/MTS2-related CDK6 inhibitor, correlates with wild-type pRb function." Genes Dev **8**(24): 2939-2952.

Guo, K., J. Wang, et al. (1995). "MyoD-induced expression of p21 inhibits cyclin-dependent kinase activity upon myocyte terminal differentiation." Mol Cell Biol **15**(7): 3823-3829.

Guo, T., W. Jou, et al. (2009). "Myostatin inhibition in muscle, but not adipose tissue, decreases fat mass and improves insulin sensitivity." PLoS One **4**(3): e4937.

Haidet, A. M., L. Rizo, et al. (2008). "Long-term enhancement of skeletal muscle mass and strength by single gene administration of myostatin inhibitors." Proc Natl Acad Sci U S A **105**(11): 4318-4322.

Halevy, O., B. G. Novitch, et al. (1995). "Correlation of terminal cell cycle arrest of skeletal muscle with induction of p21 by MyoD." Science **267**(5200): 1018-1021.

Hannon, G. J. and D. Beach (1994). "p15INK4B is a potential effector of TGF-beta-induced cell cycle arrest [see comments]." Nature **371**(6494): 257-261.

Hanson, R. W. and F. J. Ballard (1967). "The relative significance of acetate and glucose as precursors for lipid synthesis in liver and adipose tissue from ruminants." Biochem J **105**(2): 529-536.

Hardie, D. G., F. A. Ross, et al. (2012). "AMPK: a nutrient and energy sensor that maintains energy homeostasis." Nat Rev Mol Cell Biol **13**(4): 251-262.

Harper, J. W., G. R. Adami, et al. (1993). "The p21 Cdk-interacting protein Cip1 is a potent inhibitor of G1 cyclin- dependent kinases." Cell **75**(4): 805-816.

Harris, T. E., A. Chi, et al. (2006). "mTOR-dependent stimulation of the association of eIF4G and eIF3 by insulin." EMBO J **25**(8): 1659-1668.

Hatou, S., M. Yamada, et al. (2010). "Role of insulin in regulation of Na+-/K+-dependent ATPase activity and pump function in corneal endothelial cells." Invest Ophthalmol Vis Sci **51**(8): 3935-3942.

Hawke, T. J. and D. J. Garry (2001). "Myogenic satellite cells: physiology to molecular biology." J Appl Physiol **91**(2): 534-551.

Heiny, J. A., V. V. Kravtsova, et al. (2010). "The nicotinic acetylcholine receptor and the Na,K-ATPase alpha2 isoform interact to regulate membrane electrogenesis in skeletal muscle." J Biol Chem **285**(37): 28614-28626.

Hennebry, A., C. Berry, et al. (2009). "Myostatin regulates fiber-type composition of skeletal muscle by regulating MEF2 and MyoD gene expression." Am J Physiol Cell Physiol **296**(3): C525-534.

Henriksen, T., C. Green, et al. (2012). "Myokines in myogenesis and health." Recent Pat Biotechnol **6**(3): 167-171.

Herbert, T. P., A. R. Tee, et al. (2002). "The extracellular signal-regulated kinase pathway regulates the phosphorylation of 4E-BP1 at multiple sites." J Biol Chem **277**(13): 11591-11596.

Heydemann, A. and E. M. McNally (2007). "Consequences of disrupting the dystrophin-sarcoglycan complex in cardiac and skeletal myopathy." Trends Cardiovasc Med **17**(2): 55-59.

Hezel, M., W. C. de Groat, et al. (2010). "Caveolin-3 promotes nicotinic acetylcholine receptor clustering and regulates neuromuscular junction activity." Mol Biol Cell **21**(2): 302-310.

Hill, J. J., M. V. Davies, et al. (2002). "The myostatin propeptide and the follistatin-related gene are inhibitory binding proteins of myostatin in normal serum." J Biol Chem **277**(43): 40735-40741.

Hill, J. J., Y. Qiu, et al. (2003). "Regulation of myostatin in vivo by GASP-1: a novel protein with protease inhibitor and follistatin domains." Mol Endocrinol.

Hirai, H., M. F. Roussel, et al. (1995). "Novel INK4 proteins, p19 and p18, are specific inhibitors of the cyclin D-dependent kinases CDK4 and CDK6." Mol Cell Biol **15**(5): 2672-2681.

Hogan, P. G., L. Chen, et al. (2003). "Transcriptional regulation by calcium, calcineurin, and NFAT." Genes Dev **17**(18): 2205-2232.

Hong, J. P., X. M. Li, et al. (2013). "VEGF suppresses epithelial-mesenchymal transition by inhibiting the expression of Smad3 and miR192, a Smad3-dependent microRNA." Int J Mol Med **31**(6): 1436-1442.
Hur, E. M. and K. T. Kim (2002). "G protein-coupled receptor signalling and cross-talk: achieving rapidity and specificity." Cell Signal **14**(5): 397-405.
Huxley, A. F. (1971). "The activation of striated muscle and its mechanical response." Proc R Soc Lond B Biol Sci **178**(50): 1-27.
Ilori, T. O., M. A. Blount, et al. (2013). "Urine concentration in the diabetic mouse requires both urea and water transporters." Am J Physiol Renal Physiol **304**(1): F103-111.
Ingwersen, M. S., M. Kristensen, et al. (2011). "Na,K-ATPase activity in mouse muscle is regulated by AMPK and PGC-1alpha." J Membr Biol **242**(1): 1-10.
James, J. H., K. R. Wagner, et al. (1999). "Stimulation of both aerobic glycolysis and Na(+)-K(+)-ATPase activity in skeletal muscle by epinephrine or amylin." Am J Physiol **277**(1 Pt 1): E176-186.
Jameson, J. L. and L. J. DeGroot (2010). Endocrinology : adult and pediatric. Philadelphia, Saunders/Elsevier.
Jayaraman, L. and J. Massague (2000). "Distinct oligomeric states of SMAD proteins in the transforming growth factor-beta pathway." J Biol Chem **275**(52): 40710-40717.
Jeanplong, F., S. J. Falconer, et al. (2013). "Discovery of a Mammalian splice variant of myostatin that stimulates myogenesis." PLoS One **8**(12): e81713.
Jiao, J., T. Yuan, et al. (2011). "Analysis of myostatin and its related factors in various porcine tissues." J Anim Sci **89**(10): 3099-3106.
Johar, K., A. Priya, et al. (2012). "Regulation of Na(+)/K(+)-ATPase by nuclear respiratory factor 1: implication in the tight coupling of neuronal activity, energy generation, and energy consumption." J Biol Chem **287**(48): 40381-40390.
Joulia-Ekaza, D. and G. Cabello (2007). "The myostatin gene: physiology and pharmacological relevance." Curr Opin Pharmacol **7**(3): 310-315.
Joulia, D., H. Bernardi, et al. (2003). "Mechanisms involved in the inhibition of myoblast proliferation and differentiation by myostatin." Exp Cell Res **286**(2): 263-275.
Juel, C. (2009). "Na+-K+-ATPase in rat skeletal muscle: muscle fiber-specific differences in exercise-induced changes in ion affinity and maximal activity." Am J Physiol Regul Integr Comp Physiol **296**(1): R125-132.
Kambadur, R., M. Sharma, et al. (1997). "Mutations in myostatin (GDF8) in double-muscled Belgian Blue and Piedmontese cattle." Genome Res **7**(9): 910-916.
Kelly, M., M. S. Gauthier, et al. (2009). "Activation of AMP-activated protein kinase by interleukin-6 in rat skeletal muscle: association with changes in cAMP, energy state, and endogenous fuel mobilization." Diabetes **58**(9): 1953-1960.
Kennedy, D. J., Y. Chen, et al. (2013). "CD36 and Na/K-ATPase-alpha1 form a proinflammatory signaling loop in kidney." Hypertension **61**(1): 216-224.
Kim, K. H. (1997). "Regulation of mammalian acetyl-coenzyme A carboxylase." Annu Rev Nutr **17**: 77-99.
Kishioka, Y., M. Thomas, et al. (2008). "Decorin enhances the proliferation and differentiation of myogenic cells through suppressing myostatin activity." J Cell Physiol **215**(3): 856-867.
Kitzmann, M. and A. Fernandez (2001). "Crosstalk between cell cycle regulators and the myogenic factor MyoD in skeletal myoblasts." Cell Mol Life Sci **58**(4): 571-579.
Knight, J. D. and R. Kothary (2011). "The myogenic kinome: protein kinases critical to mammalian skeletal myogenesis." Skelet Muscle **1**: 29.
Koltsova, S. V., Y. Trushina, et al. (2012). "Ubiquitous [Na+]i/[K+]i-sensitive transcriptome in mammalian cells: evidence for Ca(2+)i-independent excitation-transcription coupling." PLoS One **7**(5): e38032.

Kometiani, P., J. Li, et al. (1998). "Multiple signal transduction pathways link Na+/K+-ATPase to growth-related genes in cardiac myocytes. The roles of Ras and mitogen-activated protein kinases." J Biol Chem **273**(24): 15249-15256.

Kotova, O., L. Al-Khalili, et al. (2006). "Cardiotonic steroids stimulate glycogen synthesis in human skeletal muscle cells via a Src- and ERK1/2-dependent mechanism." J Biol Chem **281**(29): 20085-20094.

Kristensen, M. and C. Juel (2010). "Potassium-transporting proteins in skeletal muscle: cellular location and fibre-type differences." Acta Physiol (Oxf) **198**(2): 105-123.

Kuang, S., K. Kuroda, et al. (2007). "Asymmetric self-renewal and commitment of satellite stem cells in muscle." Cell **129**(5): 999-1010.

La Thangue, N. B. (1996). "E2F and the molecular mechanisms of early cell-cycle control." Biochem Soc Trans **24**(1): 54-59.

LaBaer, J., M. D. Garrett, et al. (1997). "New functional activities for the p21 family of CDK inhibitors." Genes Dev **11**(7): 847-862.

Langley, B., M. Thomas, et al. (2002). "Myostatin Inhibits Myoblast Differentiation by Down-regulating MyoD Expression." J Biol Chem **277**(51): 49831-49840.

Langley, B., M. Thomas, et al. (2004). "Myostatin inhibits rhabdomyosarcoma cell proliferation through an Rb-independent pathway." Oncogene **23**(2): 524-534.

Lapidos, K. A., R. Kakkar, et al. (2004). "The dystrophin glycoprotein complex: signaling strength and integrity for the sarcolemma." Circ Res **94**(8): 1023-1031.

Lassar, A. B., J. N. Buskin, et al. (1989). "MyoD is a sequence-specific DNA binding protein requiring a region of myc homology to bind to the muscle creatine kinase enhancer." Cell **58**(5): 823-831.

Lassar, A. B., S. X. Skapek, et al. (1994). "Regulatory mechanisms that coordinate skeletal muscle differentiation and cell cycle withdrawal." Curr Opin Cell Biol **6**(6): 788-794.

Laursen, M., L. Yatime, et al. (2013). "Crystal structure of the high-affinity Na+,K+-ATPase-ouabain complex with Mg2+ bound in the cation binding site." Proc Natl Acad Sci U S A **110**(27): 10958-10963.

Laviola, L., A. Natalicchio, et al. (2007). "The IGF-I signaling pathway." Curr Pharm Des **13**(7): 663-669.

Le Grand, F. and M. A. Rudnicki (2007). "Skeletal muscle satellite cells and adult myogenesis." Curr Opin Cell Biol **19**(6): 628-633.

Lee, M. H., I. Reynisdottir, et al. (1995). "Cloning of p57KIP2, a cyclin-dependent kinase inhibitor with unique domain structure and tissue distribution." Genes Dev **9**(6): 639-649.

Lee, S. J. (2007). "Quadrupling muscle mass in mice by targeting TGF-beta signaling pathways." PLoS One **2**(8): e789.

Lee, S. J. and A. C. McPherron (2001). "Regulation of myostatin activity and muscle growth." Proc Natl Acad Sci U S A **98**(16): 9306-9311.

Lee, S. J., L. A. Reed, et al. (2005). "Regulation of muscle growth by multiple ligands signaling through activin type II receptors." Proc Natl Acad Sci U S A **102**(50): 18117-18122.

Lee, Y. K., K. M. Ng, et al. (2011). "Ouabain facilitates cardiac differentiation of mouse embryonic stem cells through ERK1/2 pathway." Acta Pharmacol Sin **32**(1): 52-61.

Leifer, D., D. Krainc, et al. (1993). "MEF2C, a MADS/MEF2-family transcription factor expressed in a laminar distribution in cerebral cortex." Proc Natl Acad Sci U S A **90**(4): 1546-1550.

Lenk, K., R. Schur, et al. (2009). "Impact of exercise training on myostatin expression in the myocardium and skeletal muscle in a chronic heart failure model." Eur J Heart Fail **11**(4): 342-348.

Li, Z. B., H. D. Kollias, et al. (2008). "Myostatin directly regulates skeletal muscle fibrosis." J Biol Chem **283**(28): 19371-19378.

Lin, J., H. B. Arnold, et al. (2002). "Myostatin knockout in mice increases myogenesis and decreases adipogenesis." Biochem Biophys Res Commun **291**(3): 701-706.
Liu, C., W. Li, et al. (2012). "The critical role of myostatin in differentiation of sheep myoblasts." Biochem Biophys Res Commun **422**(3): 381-386.
Liu, D., B. L. Black, et al. (2001). "TGF-beta inhibits muscle differentiation through functional repression of myogenic transcription factors by Smad3." Genes Dev **15**(22): 2950-2966.
Liu, S., R. Tobias, et al. (1997). "Removal of endotoxin from recombinant protein preparations." Clin Biochem **30**(6): 455-463.
Lobley, G. E. (1990). "Energy metabolism reactions in ruminant muscle: responses to age, nutrition and hormonal status." Reprod Nutr Dev **30**(1): 13-34.
Lu, A., J. H. Cummins, et al. (2008). "Isolation of myogenic progenitor populations from Pax7-deficient skeletal muscle based on adhesion characteristics." Gene Ther **15**(15): 1116-1125.
Lu, J., H. Ren, et al. (2012). "Transcript characteristic of myostatin in sheep fibroblasts." J Cell Biochem **113**(8): 2652-2660.
Ma, K., C. Mallidis, et al. (2001). "Characterization of 5'-regulatory region of human myostatin gene: regulation by dexamethasone in vitro." Am J Physiol Endocrinol Metab **281**(6): E1128-1136.
Madan, P., K. Rose, et al. (2007). "Na/K-ATPase beta1 subunit expression is required for blastocyst formation and normal assembly of trophectoderm tight junction-associated proteins." J Biol Chem **282**(16): 12127-12134.
Magalhaes, P. O., A. M. Lopes, et al. (2007). "Methods of endotoxin removal from biological preparations: a review." J Pharm Pharm Sci **10**(3): 388-404.
Magnuson, B., B. Ekim, et al. (2012). "Regulation and function of ribosomal protein S6 kinase (S6K) within mTOR signalling networks." Biochem J **441**(1): 1-21.
Manning, G., D. B. Whyte, et al. (2002). "The protein kinase complement of the human genome." Science **298**(5600): 1912-1934.
Martelli, F., C. Cenciarelli, et al. (1994). "MyoD induces retinoblastoma gene expression during myogenic differentiation." Oncogene **9**(12): 3579-3590.
Martin, J. F., J. M. Miano, et al. (1994). "A Mef2 gene that generates a muscle-specific isoform via alternative mRNA splicing." Mol Cell Biol **14**(3): 1647-1656.
Martini, F. H. (2001). Fundamentals of Anatomy and Physiology. New Jersey, Prentice Hall International Inc.
Matsakas, A., K. Foster, et al. (2009). "Molecular, cellular and physiological investigation of myostatin propeptide-mediated muscle growth in adult mice." Neuromuscul Disord **19**(7): 489-499.
Matsakas, A., E. Mouisel, et al. (2010). "Myostatin knockout mice increase oxidative muscle phenotype as an adaptive response to exercise." J Muscle Res Cell Motil **31**(2): 111-125.
Mauro, A. (1961). "Satellite cell of skeletal fibers." Journal of Biophysical & Biochemistry Cytology **9**: 493-498.
McCroskery, S., M. Thomas, et al. (2003). "Myostatin negatively regulates satellite cell activation and self-renewal." J Cell Biol **162**(6): 1135-1147.
McFarlane, C. (2003). Regulation of p21 (CIP1/WAF1) by myostatin during myogenesis Masters, Waikato University.
McFarlane, C., A. Hennebry, et al. (2008). "Myostatin signals through Pax7 to regulate satellite cell self-renewal." Exp Cell Res **314**(2): 317-329.
McFarlane, C., B. Langley, et al. (2005). "Proteolytic processing of myostatin is auto-regulated during myogenesis." Dev Biol **283**(1): 58-69.
McKenna, M. J., H. Gissel, et al. (2003). "Effects of electrical stimulation and insulin on Na+-K+-ATPase ([3H]ouabain binding) in rat skeletal muscle." J Physiol **547**(Pt 2): 567-580.
McKinsey, T. A., C. L. Zhang, et al. (2002). "MEF2: a calcium-dependent regulator of cell division, differentiation and death." Trends Biochem Sci **27**(1): 40-47.

McMahon, H. T. and E. Boucrot (2011). "Molecular mechanism and physiological functions of clathrin-mediated endocytosis." Nat Rev Mol Cell Biol **12**(8): 517-533.
McPherron, A. C. (2010). "Metabolic Functions of Myostatin and Gdf11." Immunol Endocr Metab Agents Med Chem **10**(4): 217-231.
McPherron, A. C., T. V. Huynh, et al. (2009). "Redundancy of myostatin and growth/differentiation factor 11 function." BMC Dev Biol **9**: 24.
McPherron, A. C., A. M. Lawler, et al. (1997). "Regulation of skeletal muscle mass in mice by a new TGF-beta superfamily member." Nature **387**(6628): 83-90.
McPherron, A. C. and S. Lee (1996). "The transforming growth factor-b superfamily." *Growth Factors Cytokines Health Dis* **1B**: 357-393.
McPherron, A. C. and S. J. Lee (1997). "Double muscling in cattle due to mutations in the myostatin gene." Proc Natl Acad Sci U S A **94**(23): 12457-12461.
McPherron, A. C. and S. J. Lee (2002). "Suppression of body fat accumulation in myostatin-deficient mice." J Clin Invest **109**(5): 595-601.
Meyuhas, O. (2008). "Physiological roles of ribosomal protein S6: one of its kind." Int Rev Cell Mol Biol **268**: 1-37.
Miura, T., Y. Kishioka, et al. (2006). "Decorin binds myostatin and modulates its activity to muscle cells." Biochem Biophys Res Commun **340**(2): 675-680.
Miyamoto-Sato, E., S. Fujimori, et al. (2010). "A comprehensive resource of interacting protein regions for refining human transcription factor networks." PLoS One **5**(2): e9289.
Mladinov, D., Y. Liu, et al. (2013). "MicroRNAs contribute to the maintenance of cell-type-specific physiological characteristics: miR-192 targets Na+/K+-ATPase beta1." Nucleic Acids Res **41**(2): 1273-1283.
Molkentin, J. D., B. L. Black, et al. (1995). "Cooperative activation of muscle gene expression by MEF2 and myogenic bHLH proteins." Cell **83**(7): 1125-1136.
Molkentin, J. D., A. B. Firulli, et al. (1996). "MEF2B is a potent transactivator expressed in early myogenic lineages." Mol Cell Biol **16**(7): 3814-3824.
Morine, K. J., L. T. Bish, et al. (2010). "Systemic myostatin inhibition via liver-targeted gene transfer in normal and dystrophic mice." PLoS One **5**(2): e9176.
Morissette, M. R., S. A. Cook, et al. (2009). "Myostatin inhibits IGF-I-induced myotube hypertrophy through Akt." Am J Physiol Cell Physiol **297**(5): C1124-1132.
Morlet, K., M. D. Grounds, et al. (1989). "Muscle precursor replication after repeated regeneration of skeletal muscle in mice." Anat Embryol (Berl) **180**(5): 471-478.
Mosher, D. S., P. Quignon, et al. (2007). "A mutation in the myostatin gene increases muscle mass and enhances racing performance in heterozygote dogs." PLoS Genet **3**(5): e79.
Murphy, K. T., I. Medved, et al. (2008). "Antioxidant treatment with N-acetylcysteine regulates mammalian skeletal muscle Na+-K+-ATPase alpha gene expression during repeated contractions." Exp Physiol **93**(12): 1239-1248.
Murphy, R. M., J. P. Mollica, et al. (2009). "Plasma membrane removal in rat skeletal muscle fibers reveals caveolin-3 hot-spots at the necks of transverse tubules." Exp Cell Res **315**(6): 1015-1028.
Murre, C., P. S. McCaw, et al. (1989). "Interactions between heterologous helix-loop-helix proteins generate complexes that bind specifically to a common DNA sequence." Cell **58**(3): 537-544.
Nawroth, R., F. Stellwagen, et al. (2011). "S6K1 and 4E-BP1 are independent regulated and control cellular growth in bladder cancer." PLoS One **6**(11): e27509.
Nguyen, A. N., D. P. Wallace, et al. (2007). "Ouabain binds with high affinity to the Na,K-ATPase in human polycystic kidney cells and induces extracellular signal-regulated kinase activation and cell proliferation." J Am Soc Nephrol **18**(1): 46-57.
Ning, J. and D. R. Clemmons (2010). "AMP-activated protein kinase inhibits IGF-I signaling and protein synthesis in vascular smooth muscle cells via stimulation of

insulin receptor substrate 1 S794 and tuberous sclerosis 2 S1345 phosphorylation." Mol Endocrinol **24**(6): 1218-1229.
Olguin, H. C. and A. Pisconti (2012). "Marking the tempo for myogenesis: Pax7 and the regulation of muscle stem cell fate decisions." J Cell Mol Med **16**(5): 1013-1025.
Olguin, H. C., Z. Yang, et al. (2007). "Reciprocal inhibition between Pax7 and muscle regulatory factors modulates myogenic cell fate determination." J Cell Biol **177**(5): 769-779.
Oliver, M. H., N. K. Harrison, et al. (1989). "A rapid and convenient assay for counting cells cultured in microwell plates: application for assessment of growth factors." J Cell Sci **92**(Pt 3): 513-518.
Olson, E. N. and W. H. Klein (1994). "bHLH factors in muscle development: dead lines and commitments, what to leave in and what to leave out." Genes Dev **8**(1): 1-8.
Omatsu-Kanbe, M. and H. Kitasato (1990). "Insulin stimulates the translocation of Na+/K(+)-dependent ATPase molecules from intracellular stores to the plasma membrane in frog skeletal muscle." Biochem J **272**(3): 727-733.
Oswald, F., B. Tauber, et al. (2001). "p300 acts as a transcriptional coactivator for mammalian Notch-1." Mol Cell Biol **21**(22): 7761-7774.
Oubaassine, R., M. Weckering, et al. (2012). "Insulin interacts directly with Na(+)/K(+)ATPase and protects from digoxin toxicity." Toxicology **299**(1): 1-9.
Ouchi, N., R. Shibata, et al. (2005). "AMP-activated protein kinase signaling stimulates VEGF expression and angiogenesis in skeletal muscle." Circ Res **96**(8): 838-846.
Pappenheimer, J. R. and B. P. Setchell (1973). "Cerebral glucose transport and oxygen consumption in sheep and rabbits." J Physiol **233**(3): 529-551.
Parker, S. B., G. Eichele, et al. (1995). "p53-independent expression of p21Cip1 in muscle and other terminally differentiating cells [see comments]." Science **267**(5200): 1024-1027.
Partridge, T. A. (1997). "Tissue culture of skeletal muscle." Methods Mol Biol **75**: 131-144.
Pauw, P. G. and G. J. Hermann (1994). "Ouabain is a reversible inhibitor of myogenic fusion." In Vitro Cell Dev Biol Anim **30A**(1): 9-11.
Pedersen, B. K., T. C. Akerstrom, et al. (2007). "Role of myokines in exercise and metabolism." J Appl Physiol **103**(3): 1093-1098.
Pedersen, B. K. and M. A. Febbraio (2008). "Muscle as an endocrine organ: focus on muscle-derived interleukin-6." Physiol Rev **88**(4): 1379-1406.
Pette, D. and R. S. Staron (2000). "Myosin isoforms, muscle fiber types, and transitions." Microsc Res Tech **50**(6): 500-509.
Philip, B., Z. Lu, et al. (2005). "Regulation of GDF-8 signaling by the p38 MAPK." Cell Signal **17**(3): 365-375.
Picard, B., M. P. Duris, et al. (1998). "Classification of bovine muscle fibres by different histochemical techniques." Histochem J **30**(7): 473-479.
Polyak, K., J. Y. Kato, et al. (1994). "p27Kip1, a cyclin-Cdk inhibitor, links transforming growth factor-beta and contact inhibition to cell cycle arrest." Genes Dev **8**(1): 9-22.
Quadrilatero, J., E. Bombardier, et al. (2010). "Prolonged moderate-intensity aerobic exercise does not alter apoptotic signaling and DNA fragmentation in human skeletal muscle." Am J Physiol Endocrinol Metab **298**(3): E534-547.
Quinn, Z. A., C. C. Yang, et al. (2001). "Smad proteins function as co-modulators for MEF2 transcriptional regulatory proteins." Nucleic Acids Res **29**(3): 732-742.
Rajasekaran, S. A., T. P. Huynh, et al. (2010). "Na,K-ATPase subunits as markers for epithelial-mesenchymal transition in cancer and fibrosis." Mol Cancer Ther **9**(6): 1515-1524.
Rane, M. J., P. Y. Coxon, et al. (2001). "p38 Kinase-dependent MAPKAPK-2 activation functions as 3-phosphoinositide-dependent kinase-2 for Akt in human neutrophils." J Biol Chem **276**(5): 3517-3523.

Raschke, S., K. Eckardt, et al. (2013). "Identification and validation of novel contraction-regulated myokines released from primary human skeletal muscle cells." PLoS One **8**(4): e62008.
Reger, J. F. (1958). "The fine structure of neuromuscular synapses of gastrocnemii from mouse and frog." Anat Rec **130**(1): 7-23.
Reinhard, L., H. Tidow, et al. (2013). "Na(+),K (+)-ATPase as a docking station: protein-protein complexes of the Na(+),K (+)-ATPase." Cell Mol Life Sci **70**(2): 205-222.
Relaix, F., D. Montarras, et al. (2006). "Pax3 and Pax7 have distinct and overlapping functions in adult muscle progenitor cells." J Cell Biol **172**(1): 91-102.
Reynaud, E. G., M. P. Leibovitch, et al. (2000). "Stabilization of MyoD by direct binding to p57(Kip2)." J Biol Chem **275**(25): 18767-18776.
Rhoads, R. P., L. H. Baumgard, et al. (2013). "2011 AND 2012 EARLY CAREERS ACHIEVEMENT AWARDS: Metabolic priorities during heat stress with an emphasis on skeletal muscle." J Anim Sci **91**(6): 2492-2503.
Rhodes, S. J. and S. F. Konieczny (1989). "Identification of MRF4: a new member of the muscle regulatory factor gene family." Genes Dev **3**(12B): 2050-2061.
Rivelli, J. F., M. R. Amaiden, et al. (2012). "High glucose levels induce inhibition of Na,K-ATPase via stimulation of aldose reductase, formation of microtubules and formation of an acetylated tubulin/Na,K-ATPase complex." Int J Biochem Cell Biol **44**(8): 1203-1213.
Rosenblatt, J. D., A. I. Lunt, et al. (1995). "Culturing satellite cells from living single muscle fiber explants." In Vitro Cell Dev Biol Anim **31**(10): 773-779.
Rosenblatt, J. D., D. Yong, et al. (1994). "Satellite cell activity is required for hypertrophy of overloaded adult rat muscle." Muscle Nerve **17**(6): 608-613.
Roux, P. P., D. Shahbazian, et al. (2007). "RAS/ERK signaling promotes site-specific ribosomal protein S6 phosphorylation via RSK and stimulates cap-dependent translation." J Biol Chem **282**(19): 14056-14064.
Rozen, S. and H. Skaletsky (2000). "Primer3 on the WWW for general users and for biologist programmers." Methods Mol Biol **132**: 365-386.
Ruan, W. and M. Lai (2010). "Insulin-like growth factor binding protein: a possible marker for the metabolic syndrome?" Acta Diabetol **47**(1): 5-14.
Rudnicki, M. A., P. N. Schnegelsberg, et al. (1993). "MyoD or Myf-5 is required for the formation of skeletal muscle." Cell **75**(7): 1351-1359.
Ruvinsky, I., N. Sharon, et al. (2005). "Ribosomal protein S6 phosphorylation is a determinant of cell size and glucose homeostasis." Genes Dev **19**(18): 2199-2211.
Sabourin, L. A. and M. A. Rudnicki (2000). "The molecular regulation of myogenesis." Clin Genet **57**(1): 16-25.
Schiaffino, S. and C. Reggiani (1996). "Molecular diversity of myofibrillar proteins: gene regulation and functional significance." Physiol Rev **76**(2): 371-423.
Schiaffino, S. and C. Reggiani (2011). "Fiber types in mammalian skeletal muscles." Physiol Rev **91**(4): 1447-1531.
Schlessinger, J. (2000). "Cell signaling by receptor tyrosine kinases." Cell **103**(2): 211-225.
Schuelke, M., K. R. Wagner, et al. (2004). "Myostatin mutation associated with gross muscle hypertrophy in a child." N Engl J Med **350**(26): 2682-2688.
Schultz, E. (1996). "Satellite cell proliferative compartments in growing skeletal muscles." Dev Biol **175**(1): 84-94.
Schultz, E. and D. L. Jaryszak (1985). "Effects of skeletal muscle regeneration on the proliferation potential of satellite cells." Mech Ageing Dev **30**(1): 63-72.
Schultz, E. and K. M. McCormick (1994). "Skeletal muscle satellite cells." Rev Physiol Biochem Pharmacol **123**: 213-257.
Scime, A., A. Z. Caron, et al. (2009). "Advances in myogenic cell transplantation and skeletal muscle tissue engineering." Front Biosci (Landmark Ed) **14**: 3012-3023.

Seale, P., L. A. Sabourin, et al. (2000). "Pax7 is required for the specification of myogenic satellite cells." Cell **102**(6): 777-786.
Senna Salerno, M., M. Thomas, et al. (2004). "Molecular analysis of fiber-type specific expression of murine myostatin promoter." Am J Physiol Cell Physiol.
Seoane, J., H. V. Le, et al. (2004). "Integration of Smad and forkhead pathways in the control of neuroepithelial and glioblastoma cell proliferation." Cell **117**(2): 211-223.
Serrano, M., G. J. Hannon, et al. (1993). "A new regulatory motif in cell-cycle control causing specific inhibition of cyclin D/CDK4 [see comments]." Nature **366**(6456): 704-707.
Shahin, K. A. and R. T. Berg (1985). "Growth patterns of muscle, fat, and bone, and carcase composition of double muscled and normal cattle." Canadian Journal of Animal Science **65**: 279-293.
Sharples, A. P. and C. E. Stewart (2011). "Myoblast models of skeletal muscle hypertrophy and atrophy." Curr Opin Clin Nutr Metab Care **14**(3): 230-236.
Sherr, C. J. (1995). "D-type cyclins." Trends Biochem Sci **20**(5): 187-190.
Shi, H., J. M. Scheffler, et al. (2008). "Modulation of skeletal muscle fiber type by mitogen-activated protein kinase signaling." FASEB J **22**(8): 2990-3000.
Shi, H., J. M. Scheffler, et al. (2009). "Mitogen-activated protein kinase signaling is necessary for the maintenance of skeletal muscle mass." Am J Physiol Cell Physiol **296**(5): C1040-1048.
Skou, J. C. (1957). "The influence of some cations on an adenosine triphosphatase from peripheral nerves." Biochim Biophys Acta **23**(2): 394-401.
Spiller, M. P., R. Kambadur, et al. (2002). "The myostatin gene is a downstream target gene of basic helix-loop-helix transcription factor MyoD." Mol Cell Biol **22**(20): 7066-7082.
Staubach, S. and F. G. Hanisch (2011). "Lipid rafts: signaling and sorting platforms of cells and their roles in cancer." Expert Rev Proteomics **8**(2): 263-277.
Suryawan, A., J. W. Frank, et al. (2006). "Expression of the TGF-beta family of ligands is developmentally regulated in skeletal muscle of neonatal rats." Pediatr Res **59**(2): 175-179.
Takamori, M. (2012). "Structure of the neuromuscular junction: function and cooperative mechanisms in the synapse." Ann N Y Acad Sci **1274**: 14-23.
Tang, L., Z. Yan, et al. (2007). "Myostatin DNA vaccine increases skeletal muscle mass and endurance in mice." Muscle Nerve **36**(3): 342-348.
Tang, M. J., Y. K. Wang, et al. (1995). "Butyrate and TGF-beta downregulate Na,K-ATPase expression in cultured proximal tubule cells." Biochem Biophys Res Commun **215**(1): 57-66.
Taniyama, Y., M. Ushio-Fukai, et al. (2004). "Role of p38 MAPK and MAPKAPK-2 in angiotensin II-induced Akt activation in vascular smooth muscle cells." Am J Physiol Cell Physiol **287**(2): C494-499.
Tavi, P. and H. Westerblad (2011). "The role of in vivo Ca(2)(+) signals acting on Ca(2)(+)-calmodulin-dependent proteins for skeletal muscle plasticity." J Physiol **589**(Pt 21): 5021-5031.
Thies, R. S., T. Chen, et al. (2001). "GDF-8 propeptide binds to GDF-8 and antagonizes biological activity by inhibiting GDF-8 receptor binding." Growth Factors **18**(4): 251-259.
Thomas, M., B. Langley, et al. (2000). "Myostatin, a negative regulator of muscle growth, functions by inhibiting myoblast proliferation." J Biol Chem **275**(51): 40235-40243.
Tokhtaeva, E., R. J. Clifford, et al. (2012). "Subunit isoform selectivity in assembly of Na,K-ATPase alpha-beta heterodimers." J Biol Chem **287**(31): 26115-26125.
Trendelenburg, A. U., A. Meyer, et al. (2009). "Myostatin reduces Akt/TORC1/p70S6K signaling, inhibiting myoblast differentiation and myotube size." Am J Physiol Cell Physiol **296**(6): C1258-1270.

Tzahor, E., H. Kempf, et al. (2003). "Antagonists of Wnt and BMP signaling promote the formation of vertebrate head muscle." Genes Dev **17**(24): 3087-3099.
Vary, T. C. (2006). "IGF-I stimulates protein synthesis in skeletal muscle through multiple signaling pathways during sepsis." Am J Physiol Regul Integr Comp Physiol **290**(2): R313-321.
Wang, M., H. Yu, et al. (2012). "Myostatin facilitates slow and inhibits fast myosin heavy chain expression during myogenic differentiation." Biochem Biophys Res Commun **426**(1): 83-88.
Weinberg, R. A. (1995). "The retinoblastoma protein and cell cycle control." Cell **81**(3): 323-330.
Welle, S., K. Bhatt, et al. (2006). "Myofibrillar protein synthesis in myostatin-deficient mice." Am J Physiol Endocrinol Metab **290**(3): E409-415.
Welle, S., K. Bhatt, et al. (2007). "Muscle growth after postdevelopmental myostatin gene knockout." Am J Physiol Endocrinol Metab **292**(4): E985-991.
Welle, S., K. Burgess, et al. (2009). "Stimulation of skeletal muscle myofibrillar protein synthesis, p70 S6 kinase phosphorylation, and ribosomal protein S6 phosphorylation by inhibition of myostatin in mature mice." Am J Physiol Endocrinol Metab **296**(3): E567-572.
Whittemore, L. A., K. Song, et al. (2003). "Inhibition of myostatin in adult mice increases skeletal muscle mass and strength." Biochem Biophys Res Commun **300**(4): 965-971.
Wilkes, J. J., D. J. Lloyd, et al. (2009). "Loss-of-function mutation in myostatin reduces tumor necrosis factor alpha production and protects liver against obesity-induced insulin resistance." Diabetes **58**(5): 1133-1143.
Wolfman, N. M., A. C. McPherron, et al. (2003). "Activation of latent myostatin by the BMP-1/tolloid family of metalloproteinases." Proc Natl Acad Sci U S A **100**(26): 15842-15846.
Won, J. K., H. W. Yang, et al. (2012). "The crossregulation between ERK and PI3K signaling pathways determines the tumoricidal efficacy of MEK inhibitor." J Mol Cell Biol **4**(3): 153-163.
Wortzel, I. and R. Seger (2011). "The ERK Cascade: Distinct Functions within Various Subcellular Organelles." Genes Cancer **2**(3): 195-209.
Wright, W. E., D. A. Sassoon, et al. (1989). "Myogenin, a factor regulating myogenesis, has a domain homologous to MyoD." Cell **56**(4): 607-617.
Wu, C. L., L. R. Zukerberg, et al. (1995). "In vivo association of E2F and DP family proteins." Mol Cell Biol **15**(5): 2536-2546.
Wu, Y. T., W. Ouyang, et al. (2011). "mTOR complex 2 targets Akt for proteasomal degradation via phosphorylation at the hydrophobic motif." J Biol Chem **286**(16): 14190-14198.
Xie, Z. and A. Askari (2002). "Na(+)/K(+)-ATPase as a signal transducer." Eur J Biochem **269**(10): 2434-2439.
Xiong, Y., G. J. Hannon, et al. (1993). "p21 is a universal inhibitor of cyclin kinases." Nature **366**(6456): 701-704.
Xu, J., S. Wang, et al. (2012). "Regulation of the proteasome by AMPK in endothelial cells: the role of O-GlcNAc transferase (OGT)." PLoS One **7**(5): e36717.
Yang, J. and B. Zhao (2006). "Postnatal expression of myostatin propeptide cDNA maintained high muscle growth and normal adipose tissue mass in transgenic mice fed a high-fat diet." Mol Reprod Dev **73**(4): 462-469.
Yang, W., Y. Chen, et al. (2006). "Extracellular signal-regulated kinase 1/2 mitogen-activated protein kinase pathway is involved in myostatin-regulated differentiation repression." Cancer Res **66**(3): 1320-1326.
Yokoyama, S. and H. Asahara (2011). "The myogenic transcriptional network." Cell Mol Life Sci **68**(11): 1843-1849.
Yuan, Z., T. Cai, et al. (2005). "Na/K-ATPase tethers phospholipase C and IP3 receptor into a calcium-regulatory complex." Mol Biol Cell **16**(9): 4034-4045.

Zammit, P. and J. Beauchamp (2001). "The skeletal muscle satellite cell: stem cell or son of stem cell?" Differentiation **68**(4-5): 193-204.
Zhang, C., C. McFarlane, et al. (2011). "Myostatin-deficient mice exhibit reduced insulin resistance through activating the AMP-activated protein kinase signalling pathway." Diabetologia **54**(6): 1491-1501.
Zhang, H., G. J. Hannon, et al. (1994). "p21-containing cyclin kinases exist in both active and inactive states." Genes Dev **8**(15): 1750-1758.
Zhang, J. M., X. Zhao, et al. (1999). "Direct inhibition of G(1) cdk kinase activity by MyoD promotes myoblast cell cycle withdrawal and terminal differentiation." Embo J **18**(24): 6983-6993.
Zhang, L., V. Rajan, et al. (2011). "Pharmacological inhibition of myostatin suppresses systemic inflammation and muscle atrophy in mice with chronic kidney disease." FASEB J **25**(5): 1653-1663.
Zhang, L., Z. Zhang, et al. (2008). "Na+/K+-ATPase-mediated signal transduction and Na+/K+-ATPase regulation." Fundam Clin Pharmacol **22**(6): 615-621.
Zhang, M., K. Koishi, et al. (1998). "Skeletal muscle fibre types: detection methods and embryonic determinants." Histol Histopathol **13**(1): 201-207.
Zhu, X., M. Hadhazy, et al. (2000). "Dominant negative myostatin produces hypertrophy without hyperplasia in muscle." FEBS Lett **474**(1): 71-75.
Zimmers, T. A., M. V. Davies, et al. (2002). "Induction of cachexia in mice by systemically administered myostatin." Science **296**(5572): 1486-1488.